eman ta zabal zazu

Universidad del País Vasco

Euskal Herriko Unibertsitatea

Identification of ERBB4 and SOX1 role in central nervous system tumors. Implication in medulloblastoma and glioblastoma.

Juncal Aldaregia Fernandez

PhD Thesis

2020

Identification of ERBB4 and SOX1 role in central nervous system tumors. Implication in medulloblastoma and glioblastoma.

Juncal Aldaregia Fernandez

SUPERVISORS

Idoia Garcia Camino

Ander Matheu Fernandez

PhD Thesis

2020

(c) 2020 JUNCAL ALDAREGUIA FERNANDEZ

Abstract

Although in the recent decades the advances made in order to treat cancer have led to great improvements in terms of patient's survival, many cancer types present resistance to treatments, relapse, and metastasize, compromising patient's life. In addition, radiotherapy and chemotherapy high doses present serious side effects. Heterogeneity is one of the factors that causes tumor therapies resistance. It can be inter- and intratumor. Intertumoral heterogeneity, meaning the molecular and cellular differences between different tumors, interferes in establishing effective standard patient's treatments, thus increasing the need for personalized therapy. In turn, intratumor heterogeneity is due to the existence of a set of cancer stem cells (CSCs), responsible for tumor initiation, metastasis, recurrence and therapy resistance. Hence, the main challenge is finding targeted therapies to eliminate CSCs.

Dysregulation of genes related to embryonic development and essential in the maintenance of stem cells is critical for cancer malignant phenotype's development and progression. It is why in this thesis, we studied different molecular mechanisms involved in the regulation of stem cells and embryonic development in medulloblastoma (MB) and glioblastoma (GBM) tumorigenesis.

MB is the most common solid tumor in childhood, developed in the cerebellum. This tumor arises as a result of cerebellum development dysregulation. Although patient survival has increased up to 70-90 % in recent years, the high chemotherapy and radiotherapy doses required to eliminate the tumor cause serious permanent neurological sequelae, highlighting the urgent need to develop new therapeutic strategies. Due to intertumoral heterogeneity, these tumors are classified into different subgroups, according to the altered signaling pathways (WNT, SHH, Group 3 and Group 4). Moreover, MB tumors show a MB stem cells subpopulation (MBSCs), which cause both tumor recurrence and resistance to treatments.

Besides, GBM is the most common, aggressive and malignant adult brain tumor. Recent studies reveal several genetic mutations and molecular alterations that direct the tumorigenesis process. This implies different disease subgroups and the existence of

glioma stem cells (GSCs). Currently there is no effective treatment to treat this tumor and therefore no long-term patient recovery is possible. These data reveal the importance of new therapeutic strategies discovery, targeting specifically GSCs.

ERBB4 is a tyrosine kinase type membrane receptor that has been associated with nervous system embryonic development and related to various tumorigenesis processes. This receptor plays different roles depending on the tumor type. In this work we observed that it plays a crucial role in cerebellum development and in the control of progenitor cells migration. Moreover, its activation in progenitor and MB cells made them more resistant to apoptotic stimuli. This suggests that its abnormal activation might protect cells from apoptosis, providing resistance to chemo- or radiotherapy. When analyzing ERBB4 expression in the different MB subgroups, we observed that it was highly expressed in subgroup 4 MBs, and that was related to a lower survival, more significantly in this subgroup. Interestingly, in this subgroup an altered signaling pathway has not yet been described. Therefore, these results show the ERBB4 importance as a subgroup 4 and a prognostic marker. To elucidate ERBB4 function in MB cells, we inhibited *in vitro* its expression and observed a reduction in cell viability and apoptosis activation. In line, we showed *in vivo* a reduction in self-renewal, initiation and progression capacity. Likewise, we observed ERBB4 expression enrichment in the MBSC subpopulation. Moreover, ERBB4 silencing significantly decreased the proliferative and self-renewal capacity of MBSCs. Thus, in this work we reveal ERBB4 as a potential new therapeutic target in MB and we propose its inhibition as a complementary strategy in combination with existing therapies, with the aim of reducing chemo- and radiotherapy doses to alleviate its serious side effects.

On its part, SOX1 transcription factor plays a fundamental role in embryonic development and stem cell maintenance in adulthood. Its role in oncogenesis has been widely described, revealing it as a tumor suppressor in different cancer types. However, in contrast to what has been published so far, in our work, SOX1 oncogenic role has been demonstrated in both GBM and MB.

Specifically, regarding SOX1 role in MB, we demonstrated that its expression is elevated in SHH subgroup tumors compared to others, using public databases. Related to

this, we observed a higher SOX1 expression in MB cell lines belonging to the SHH subgroup. Likewise, we showed that high SOX1 expression levels correlate with a worse patients' prognosis, and more significantly in SHH subgroup patients. Furthermore, when we analyzed the different SHH pathway genes in these patients, we observed that SOX1 could be a better subgroup and prognosis biomarker than any of the SHH pathway genes. With the aim of clarifying SOX1 role in the MB progression and malignant phenotype, we silenced its expression in MB cells, and observed a decrease in cell proliferation and viability *in vitro*, and in tumor formation and progression *in vivo*. In line, we observed that SOX1 expression increases in MBSCs and that its genetic silencing decreases their self-renewal capacity. Notably, this phenotype was more drastic in SHH subgroup cells, further relating SOX1 to this MB subgroup. Altogether, these results point out a SOX1 fundamental role in MB progression, and more specifically in the SHH subgroup, suggesting that SOX1 could constitute a new therapeutic target in MB.

In the GBM context, we showed SOX1 over-expression compared to healthy tissue, both in our cohort and in accessible databases. In addition, we observed that SOX1 high expression levels are directly associated with a worse prognosis in patients, as we observed in MB, suggesting its potential utility as prognostic marker. With regard to intratumor heterogeneity, we found SOX1 high enrichment in GSCs, both in patients-derived cells and in cells grown in stem cells selective medium. Regarding its regulation in GBM, we showed that SOX1 is regulated by SOX2, a key transcription factor of SOX family involved in embryogenesis and neurogenesis processes. Thus, SOX1 silencing in GBM cells led to a significant decrease in their proliferation capacity, self-renewal ability, and differentiation potential. In line, we observed *in vivo* a reduction in their tumor initiation and progression capacity. All these results demonstrate an important role of SOX1 in GBM development and GSCs maintenance, which are responsible of treatment resistance and tumor recurrence.

Altogether, this thesis has demonstrated a hitherto undescribed ERBB4 and SOX1 role in MB and GBM, as essential genes for these tumors' maintenance. Furthermore, we have described in this work for the first time that SOX1 acts as an oncogene in brain tumors such as MB and GBM. Considering the characteristics of these tumors and the urgent need to find new therapeutic targets and alternative strategies, this work

postulates ERBB4 and SOX1 inhibition as promising therapeutic approaches to combat chemo- and radiotherapy resistance and reduce the current doses toxicity. In addition, ERBB4 and SOX1 might be used as prognostic markers, and also as markers for two different subgroups in the case of MB.

Resumen

A pesar de que en las últimas décadas los avances realizados para tratar el cáncer han supuesto grandes mejoras en lo que respecta a la supervivencia de los pacientes, muchos tipos de tumores presentan resistencia a sus tratamientos, recurren y se diseminan, comprometiendo con ello la supervivencia de los pacientes. Además, las altas dosis de radioterapia y quimioterapia necesarias acarrean graves secuelas permanentes, especialmente en pacientes pediátricos. Uno de los factores que contribuyen a los procesos de resistencia a la terapia de los tumores es la heterogeneidad celular, tanto inter- como intratumoral. Por una parte, la heterogeneidad intertumoral dificulta el establecimiento de tratamientos efectivos para todos los pacientes, lo que aumenta la necesidad de una terapia personalizada. A su vez, la heterogeneidad intratumoral, es decir, la presencia de distintos tipos celulares dentro del mismo tumor, se debe a la existencia de una población de células madre tumorales que son las responsables no solo de la iniciación tumoral, sino también de la metástasis, recurrencia y resistencia a las terapias utilizadas. Debido a la presencia de estas células también en tumores del sistema nervioso central, el objetivo principal de esta tesis fue el de encontrar terapias dirigidas para eliminar dichas células madre tumorales.

La desregulación de aquellos genes relacionados con el desarrollo embrionario y el mantenimiento de las células madre embrionarias y adultas parece ser crítica para el desarrollo y la progresión del fenotipo canceroso. En este trabajo, se ha estudiado el papel de diferentes mecanismos moleculares implicados en la regulación de las células madre y del desarrollo embrionario en los procesos de tumorogénesis del meduloblastoma (MB) y del glioblastoma (GBM), dos tumores del sistema nervioso central.

El MB es el tumor sólido más común en la infancia, y se localiza en el cerebelo. Se origina debido a la desregulación del proceso de desarrollo del cerebelo, por lo que el MB se considera un tumor de origen embrionario. Aunque la supervivencia de los pacientes ha aumentado hasta alcanzar el 70-90 % en los últimos años, las altas dosis de quimioterapia y radioterapia necesarias para eliminar el tumor causan graves secuelas

neurológicas permanentes en los pacientes, haciendo patente la necesidad de hallar nuevas estrategias terapéuticas que permitan reducir los efectos secundarios de los tratamientos actuales. El MB presenta una elevada heterogeneidad intertumoral, identificándose distintos subgrupos en función de qué vías de señalización están alteradas, clasificando los tumores en los subgrupos WNT, SHH, Grupo 3 y Grupo 4. Cabe destacar que en los últimos dos subgrupos todavía no se ha encontrado qué vía de señalización es la causante de la formación y la progresión del tumor. En el MB también se ha demostrado la existencia de una subpoblación de células madre de MB (MBSCs), que son las causantes tanto de la recurrencia del tumor como de la resistencia a los tratamientos actuales.

Por otro lado, el GBM es el tumor cerebral más común, agresivo y maligno que se da en los adultos, con una supervivencia media de 15 meses tras el diagnóstico. Estudios recientes han revelado una gran cantidad de mutaciones genéticas y alteraciones moleculares que dirigen el proceso de tumorogénesis de este tumor, describiéndose así diferentes subgrupos de la enfermedad. Además, al igual que en el MB, se ha descrito la existencia de las células madre de glioma (GSCs), también causantes de la resistencia a los tratamientos actuales y de la recurrencia del tumor. Se ha de tener en cuenta que hoy en día no existe un tratamiento eficaz para tratar estos tumores y que ningún paciente consigue recuperarse de esta enfermedad. Estos datos revelan la importancia de la búsqueda de nuevos tratamientos y dianas terapéuticas, dirigidas específicamente a esta población de GSCs.

ERBB4 es un receptor de membrana con actividad tirosina quinasa que se ha relacionado con el desarrollo embrionario del sistema nervioso, en concreto con procesos de migración neuronal. Además, también está implicado en procesos de tumorogénesis, jugando papeles contrapuestos dependiendo del tipo de tumor. En este trabajo, observamos que este receptor tiene una función esencial en el desarrollo del cerebelo, controlando la población de las células progenitoras y su proceso de migración. Además, demostramos que la activación de este receptor en células progenitoras del cerebelo, y también en células de MB, hace que éstas sean más resistentes a los estímulos apoptóticos. Esto sugiere que su sobreactivación podría proteger a dichas células de estímulos apoptóticos, proporcionándoles resistencia frente a la quimioterapia o la

radioterapia. Por esta razón, decidimos profundizar en el estudio de la función de ERBB4 en el desarrollo y progresión del MB. En primer lugar, mediante el análisis de datos disponibles en bases de datos, observamos que ERBB4 se encontraba altamente expresado en los MBs del subgrupo 4, el subgrupo más común. Además, encontramos que la alta expresión de este receptor se asociaba con una menor supervivencia de los pacientes, siendo esta diferencia aún más significativa entre los pacientes del subgrupo 4. Cabe destacar que aún no ha sido descrita la vía de señalización alterada causante de la generación del tumor en este subgrupo, por lo que estos resultados demuestran la utilidad de este receptor, no solo como marcador con valor pronóstico, sino también como posible marcador de dicho subgrupo. Para dilucidar la función de ERBB4 en las células de MB, inhibimos la expresión de este receptor mediante partículas lentivirales y observamos una reducción en la viabilidad celular junto a una activación de la apoptosis. Asimismo, al inyectar estas células en ratones inmunodeprimidos comprobamos que la capacidad de auto-renovación, de iniciación y de progresión tumoral se reducen con el silenciamiento de ERBB4. Igualmente, observamos un enriquecimiento de la expresión de este receptor en las MBSCs y también que su silenciamiento disminuía significativamente la capacidad proliferativa y de auto-renovación de estas células. Así pues, en este trabajo revelamos que ERBB4 podría ser una nueva diana terapéutica en MB y proponemos su inhibición como estrategia a utilizar, en combinación con las terapias existentes, con el objetivo de reducir las dosis de quimio- y radioterapia utilizadas actualmente, para paliar, en parte, los graves efectos secundarios de las terapias actuales.

Por otra parte, el factor de transcripción SOX1 tiene un papel fundamental en el desarrollo embrionario y el mantenimiento de las células madre en la edad adulta. Su papel en procesos de oncogénesis se ha descrito ampliamente, revelándose como un supresor tumoral en diferentes tipos de tumores. Sin embargo, al contrario de lo publicado hasta el momento, en este trabajo se ha demostrado el papel oncogénico de SOX1 tanto en GBM como en MB.

En primer lugar, en lo que respecta al papel de SOX1 en MB, en este trabajo describimos, haciendo uso de datos disponibles en bases de datos públicas, que su expresión se encuentra elevada en los tumores del subgrupo SHH en comparación con

los otros subgrupos. En relación a esto, observamos una mayor expresión de este factor de transcripción en las líneas celulares de MB pertenecientes al subgrupo SHH. Asimismo, comprobamos que un alto nivel de expresión de SOX1 se correlaciona con un peor pronóstico de los pacientes, haciéndose más notable esta diferencia en los pacientes del subgrupo SHH. Es más, al analizar diferentes genes de la vía de SHH en estos pacientes, observamos que SOX1 podría ser mejor biomarcador de dicho subgrupo, además de ser mejor marcador pronóstico que cualquiera de los genes de la vía de SHH. Con el objetivo de esclarecer el papel de SOX1 en la progresión y el fenotipo maligno del MB, silenciamos su expresión mediante partículas lentivirales en células provenientes de este tipo tumoral, observando una disminución de la proliferación y de la viabilidad celular, así como de la formación y de la progresión tumoral al inyectar estas células en ratones inmunodeprimidos. En esta línea, observamos una expresión aumentada de SOX1 en las MBSCs y que su silenciamiento genético disminuye la capacidad de auto-renovación de dichas células. Cabe destacar que este fenotipo es más drástico al realizar los experimentos en células pertenecientes al subgrupo SHH, reforzando la implicación de SOX1 con este subgrupo de MBs. Todo ello evidencia el papel fundamental de este factor de transcripción en la progresión del MB, en concreto de los del tipo SHH, y sugiere que SOX1 podría constituir una nueva diana terapéutica en MB. Por ello, sería interesante buscar nuevas terapias dirigidas a inhibir dicho factor de transcripción.

En el caso del GBM, en este trabajo demostramos que SOX1 se encuentra sobre-expresado en GBM en comparación con el tejido sano, tanto en nuestra cohorte como en bases de datos accesibles. Además, y al igual que en el MB, observamos que los altos niveles de expresión de SOX1 están directamente asociados con un peor pronóstico de los pacientes, lo que sugiere su utilidad como marcador pronóstico. En lo que respecta a la heterogeneidad intratumoral, observamos que este factor de transcripción está altamente enriquecido en las GSCs, tanto en las derivadas de pacientes como en células cultivadas en medio selectivo para célula madre. Respecto a su regulación, demostramos que en GBM, SOX1 está regulado por otro miembro de su familia, SOX2, un factor de transcripción implicado en procesos de embriogénesis y neurogénesis. Así, al realizar ensayos de silenciamiento de SOX1 en células de GBM observamos una disminución significativa de las propiedades malignas de estas células, como son la capacidad de

proliferación, la habilidad de auto-renovación y el potencial de diferenciación. Además, al inyectar las células silenciadas en ratones inmunodeprimidos, observamos una disminución de la capacidad de iniciación y progresión tumoral de las células de GBM. Todos estos resultados indican un papel importante de SOX1 en el desarrollo de este tumor y en el mantenimiento de la población de las GSCs, causantes de la resistencia al tratamiento y la recurrencia tumoral.

En conjunto, en este trabajo hemos demostrado un papel hasta ahora no descrito de ERBB4 y SOX1 en MB y en GBM, en el que se han revelado como genes esenciales para el mantenimiento y la malignización de estos tumores. Además, en este trabajo hemos descrito por primera vez la función de SOX1 como un oncogén. Teniendo en cuenta las características de estos tumores y la necesidad de encontrar nuevas dianas y estrategias terapéuticas, este trabajo propone la inhibición de ERBB4 y SOX1 como una nueva estrategia terapéutica prometedora para combatir la resistencia a las terapias actuales e intentar reducir las dosis empleadas con el fin de reducir los efectos secundarios generados. Además de proponerse como nuevas dianas terapéuticas, en este trabajo hemos demostrado que ERBB4 y SOX1 podrían ser utilizados como marcadores pronósticos, y en el caso del MB, también como marcadores de dos subgrupos diferentes.

Table of contents

Abbreviations

A	ALDH	Aldehyde dehydrogenase
	ANKRD1	Ankyrin repeat domain 1
	APBB2	Amyloid beta precursor protein binding family B member 2
	APC	Adenomatous polyposis coli
	AR	Amphiregulin
	ATCC	American Type Culture Collection
	ATOH1	Atonal homolog 1
B	BCA	Bicinchoninic acid
	bFGF	Basic fibroblast growth factor
	BMP	Bone morphogenetic protein
	BSA	Bovine serum albumin
	BTC	Betacellulin
C	CAF	Cancer associated fibroblasts
	cC3	Cleaved-caspase-3
	CCND1	Cyclin D1
	CDC25a	Cell division cycle 25A
	CDH13	Cadherin 13
	CDK6	Cyclin dependent kinase 6
	CDK15	Cyclin dependent kinase 15
	CDKN2A	Cyclin dependent kinase inhibitor 2A
	cDNA	Complementary DNA
	CEACAM1	CEA cell adhesion molecule 1
	CGNP	Cerebellar granule neuron progenitor cells
	CHI3L1	Chitinase 3 like 1
	CHK1	Checkpoint kinase 1
	CHK2	Checkpoint kinase 2
	CNS	Central nervous system
	CO_2	Carbon dioxide
	CSC	Cancer stem cell
	CSF	Cerebrospinal fluid
	CSI	Cranio-spinal irradiation
	CT	Computer tomography
	CXCL16	C-X-C motif chemokine ligand 16
	CYT	Cytoplasmic domain
D	DAB	3,3'Diaminobenzidine
	DAPI	4'6-diamino-2-phenylindole
	DCLK1	Doublecortin like kinase 1
	DDX31	DEAD-box helicase 31
	DEPC	Diethyl pyrocarbonate
	dH_2O	Distilled water
	DNA	Deoxyribonucleic acid
E	E2F7	E2F transcription factor 7
	EGF	Epidermal growth factor
	EGFR	Epidermal growth factor receptor
	EGL	External granule cell layer
	ELDA	Extreme limiting dilution analysis
	EMT	Epithelial-mesenchymal transition
	ERBB4	ERBB2 receptor tyrosine kinase 4

	ESC	Embryonic stem cell
	EtOH	Ethanol
F	FBS	Foetal bovine serum
	FGF	Fibroblast growth factor
	FGF5	Fibroblast growth factor 5
	FGFR1	Fibroblast growth factor receptor 1
	FKPM	Fragments per kilobase of exon model per million reads mapped
	FUT4	Fucosyltransferase 4
G	GABRA1	Gamma-aminobutyric acid type A receptor subunit alpha 1
	GAD1	Glutamate decarboxylase 1
	GAPDH	Glyceraldehyde-3-Phosphate Dehydrogenase
	GBM	Glioblastoma
	GFAP	Glial fibrillary acidic protein
	GNS	Glioma neural stem
	GO	Gene ontology
	GSC	Glioma stem cell
	GSK3β	Glycogen synthase kinase 3 beta
H	H2AFX	H2A histone family member X
	HBEGF	Heparin-binding EGF-like growth factor
	Het	Heterozygous
	HIF	Hypoxia inducible factor
	HMG	High-mobility group
	HRP	Horseradish peroxidase
I	ICD	Intracellular domain
	IDH	Isocitrate dehydrogenase
	iEGL	Inner external granule cell layer
	IF	Immunofluorescence
	IFITM1	Interferon induced transmembrane protein 1
	IGFBP3	Insulin like growth factor binding protein 3
	IGL	Internal granule cell layer
	IHC	Immunohistochemistry
	IL1α	Interleukin 1 alpha
	IL1R1	Interleukin 1 receptor type 1
	IL6	Interleukin 6
	IL7R	Interleukin 7 receptor
	IL18R1	Interleukin 18 receptor 1
	iPSC	Induced pluripotent stem cell
J	JM	Juxtamembrane domain
K	KCl	Potassium chloride
	KLF4	Krueppel-like factor 4
	KO	Knock out
L	LCA	Large cell anaplastic
	LLG	Low-grade glioma
M	MAPK	Mitogen activated kinase-like protein
	MB	Medulloblastoma
	MBEN	Medulloblastoma with extensive nodularity
	MBSC	Medulloblastoma stem cell
	MERTK	MER proto-oncogene tyrosine kinase
	MET	Mesenchymal-epithelial transition

	MGMT	O-6-methylguanine-DNA methyltransferase enzyme
	MGP	Matrix gla protein
	miRNA	microRNA
	ML	Molecular layer
	MMP7	Matrix metallopeptidase 7
	MOI	Multiplicity of infection
	MRI	Magnetic resonance imaging
	mRNA	Messenger RNA
	mTOR	Mechanistic target of rapamycin kinase
	MTT	3-(4,5-dimethylthiazol-2-yl)-2,5-diphenyltetrazolium bromide
	MYC	v-myc avian myelocytomatosis viral oncogene homolog
	MYCN	Neuroblastoma-derived v-myc avian myelocytomatosis viral related oncogene
N	NEFL	Neurofilament light
	NF-κB	Nuclear factor kappa B
	NF1	Neurofibromin 1
	NGN1	Neurogenin-1
	NRG	Neuregulin
	NSC	Neural stem cell
O	O/N	Overnight
	O_2	Oxygen
	oEGL	Outer external granule cell layer
	OLIG2	Oligodendrocyte transcription factor 2
	OSMR	Oncostatin M receptor
P	PBS	Phosphate buffered saline
	PDGFRA	Platelet derived growth factor receptor alpha
	PFA	Paraformaldehyde
	PFKP	Phosphofructokinase platelet
	PHH3	Histone H3 (phospho S10)
	PI3K-AKT	Phosphoinositide-3-kinase/protein kinase B
	PI3K/PIK3R1	Phosphoinositide-3-kinase/phosphatidylinositol 3-kinase regulatory subunit alpha
	PL	Purkinje cell layer
	PLAC8	Placenta associated 8
	POSTN	Periostin
	POU3F2	POU class 3 homeobox 2
	PRRX1	Paired related homeobox 1
	PTCH1	Patched 1
	PTEN	Phosphatase and tensin homolog
	PTHLH	Parathyroid hormone-related protein
R	Rb	Retinoblastoma
	RL	Rhombic lip
	RNA	Ribonucleic acid
	RT	Room temperature
	RT-qPCR	Real time quantitative polymerase chain reaction
S	SALL2	Spalt like transcription factor 2
	SDS	Sodium dodecyl sulfate
	SDS-PAGE	Sodium dodecyl sulphate-polyacrilamide gel electrophoresis
	SEM	Standard error of the mean
	SEMA5A	Semaphorin 5A
	SHH	Sonic Hedgehog
	shRNA	Short hairpin RNA

	SLC12A5	Solute carrier family 12 member 5
	SMO	Smoothened
	SNCAIP	Synuclein alpha interacting protein
	SOCS2	Suppresor of cytokine signaling 2
	SOD2	Superoxide dismutase 2
	SOX	Sex-determining region Y (SRY)-box
	SOX1	SRY-box 1
	SOX2	SRY-box 2
	SOX3	SRY-box 3
	SOX4	SRY-box 4
	SOX9	SRY-box 9
	STAT3	Signal transducer and activator of transcription 3
	STAT5A	Signal transducer and activator of transcription 5A
	STAT5B	Signal transducer and activator of transcription 5B
	SVZ	Subventricular zone
	SYP	Synaptophysin
	SYT1	Synaptotagmin 1
T	TAC	Transcriptome Analysis Console
	TACE	Tumor necrosis factor-α converting enzyme
	TBS-T	Tris buffered saline 0.01 % Tween 20
	TCGA	The Cancer Genome Atlas
	TERT	Telomerase reverse transcriptase
	TGF-α	Transforming growth factor-α
	THBS1	Thrombospondin 1
	TK	Tysorine-kinase
	TMZ	Temozolomide
	TNF	Tumor necrosis factor
	TP63	Tumor protein P63
U	UNC	University of North Carolina
V	VCAM1	Vascular cell adhesion molecule 1
	VEGFA	Vascular endothelial growth factor A
W	WB	Western blot
	WHO	World Health Organization
	WT	Wild type
	β-actin	Beta actin

Introduction

1. Cancer

Nowadays, cancer is the non-contagious illness that generate more deaths, only surpassed by cardiovascular diseases. Moreover, since lifespan is increasing year after year, the incidence of different type of cancers is incrementing. The following data demonstrate this affirmation: in 2012, 14 million new cases had been diagnosed and more than 8 million deaths caused by cancer had been documented (Ferlay et al., 2015). In contrast, in 2018, there were more than 18 million new diagnosed cancer cases, and 9.5 million deaths caused by this disease (Ferlay et al., 2019). Moreover, both incidence and mortality are expected to continue to increase in the coming years.

Cancer is caused by a malignant transformation of common cells from the body. This transformation process is performed through different phases, with genetic and epigenetic changes caused by different factors, such as environmental oness. The last ones create genetic, epigenetic and transcriptional modifications, and when the accumulation of these modifications reach a threshold, the cells undergo the malignant transformation.

In 2000, Hanahan and Weinberg detailed the 6 specific abilities tumor cells present and that differences them from the non-malignant cells. These described abilities include: proliferative signaling support, growth suppressors evasion,, replicative immortality enabling, , invasion and metastasis activation, angiogenesis induction, , cell death resistance and cellular energetics' deregulation (Hanahan and Weinberg, 2000)[**Figure I1**]. 11 years later, the same authors redefine these hallmarks including 4 new abilities that tumor cells present: immune system escape, tumor promoting inflammation, genome instability and mutation and deregulation of cellular energetics. Altogether, they conclude that different tumors may have common molecular mechanisms, and that finding those mechanisms may lead to the validation of new therapeutic targets (Hanahan and Weinberg, 2011).

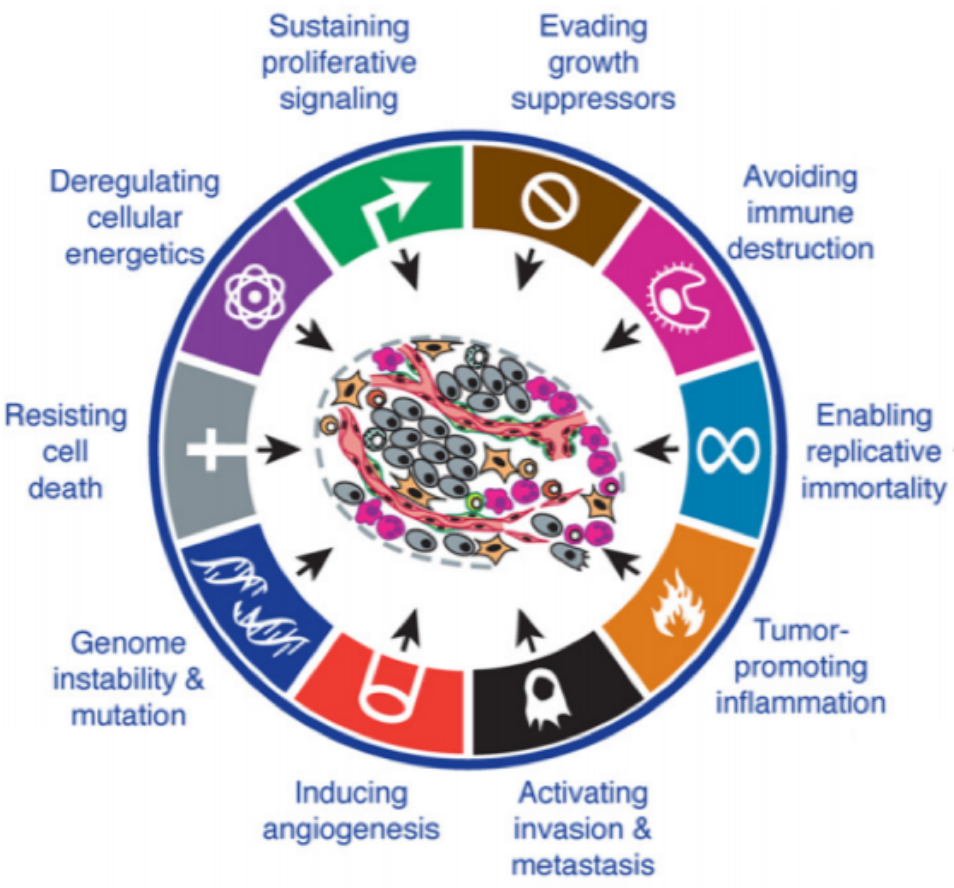

Figure I1. Representative image of the specific characteristics of tumor cells. Modified from Hanahan and Weinberg, 2011.

Although in the last decades there have been great improvements in regards to tumors' treatment, nowadays some tumor types are still incurable and present resistance to the applied therapies. It is the reason why tumors relapse and develop metastasis. This phenomenon doesn't occur in all type of tumors, and even within the same type of cancers, tumors act in different manners according to their subgroups and their development stages. This is due to the heterogeneity of the tumors

1.1. Inter- and intra-tumor heterogeinty

Although, in general terms, a large number of tumors present some common alterations, significant molecular differences are presented between the same type of tumors from different patients. This heterogeneity is known as inter-tumor

heterogeneity. In fact, different tumors present a great variety of different genetic and epigenetic alterations, which are responsible of differences in i) the phenotypes, ii) the response to treatments and iii) the prognostic of patients.

There are different reasons why this heterogeneity occurs. First, it is probably due to the origin of the tumor, as tumors of the same tissue could be developed from different type of cells (Visvader, 2011). The second reason could be tumor development itself, which is a random, dynamic and uncontrolled process, thus the emergence of multiple molecular alterations may appear in a short time. Third, these alterations are conditioned and could be supported by extrinsic factors in the tumor microenvironment (Tlsty and Coussens, 2006). Hence, all this heterogeneity causes significant differences between patients' outcome and, thus, complicates the diagnosis and the selection of the appropriate treatment for each patient, making clear the necessity of finding new biomarkers for patients' stratification and personal treatment (Nowell, 1976).

Moreover, heterogeneity can be also found inside the same tumor (denominated as intra-tumor heterogeneity). This makes difficult the characterization of each tumor and consequently, specific treatment design. Intra tumor heterogeneity also promotes treatment resistance, and thus, progression and recurrence of the disease (McGranahan and Swanton, 2017). In addition, genome sequencing analysis has demonstrated that in the same tumor coexist several tumor cells clones that are genetically different with distinct phenotypes (Burrell et al., 2013). In line with this, genetically different subclones have been described in the primary tumor and metastasis of the same patient, which demonstrates that secondary tumors may arise from a minority of cells within the primary. These reduced tumor subclones could stay in dormancy for years, which complicates the establishment of effective new therapeutic strategies (Ding et al., 2010; Vignot et al., 2013).

Different theories have emerged to explain this intra-tumor heterogeneity. The most known ones are the clonal evolution or stochastic model and the cancer stem cell or hierarchic model.

1.1.1. Stochastic or clonal evolution model

The clonal evolution model postulates that all the cells of the tumor have the same growth and division potential, since each cell has the capacity to self-renew (giving rise to two daughter cells with similar characteristics to the original cell) or differentiate (originating two daughter cells oriented to cellular differentiation) (Nakahata et al., 1982). In this model, the cells do not follow an organization system, since all the cells contribute equally to tumor growth (Dingli et al., 2007), and the cell clones that present the most beneficial characteristics regarding their environment will expand and displace the other cell clones, at the same time experimenting new modifications that will perpetuate the heterogeneity (Greaves and Maley, 2012; Nowell, 1976). In this process of tumor evolution, the cellular plasticity constitutes a non-inheritable source of heterogeneity that also promotes phenotypic differences between tumor cells (Marusyk and Polyak, 2010) and has important implications in the therapy resistance and metastatic dissemination (Marusyk et al., 2012).

1.1.2. Cancer Stem Cells or hierarchical model

The other theory or model is the cancer stem cell or hierarchic model. In almost all tumors a subpopulation of tumor cells with stem cell characteristics has been found, named as cancer stem cells (CSCs). This discovery leads to the appearance of the model or theory of CSCs. This theory suggests a hierarchic organization in which the tumor is generated from a CSC, which by symmetric divisions auto-renews its population, generating cells with the same stemness capacity than the mother cell, and by asymmetric divisions generates more differentiated daughter cells, with properties of limited proliferation that constitute the bulk of the tumor (Reya et al., 2001) [**Figure I2**]. This hierarchy, however, is not unidirectional, since it does not go only from a dedifferentiated state to a more specialized one. Thanks to Takahashi and Yamanaka, evidences that differentiated cells could revert their state and go back to stem cell characteristics under determined conditions or in presence of certain factors had emerged (Takahashi and Yamanaka, 2006). In cancer, this process of dedifferentiation towards CSCs would also be feasible, which would allow and increase the adaptability of

different types of cancer to antitumor therapies (Chaffer et al., 2011; Heddleston et al., 2011).

The hierarchical model or the CSCs model does not invalidate the concept of clonal evolution regarding tumor progression, but complements it by adding the concept of a cellular hierarchy in which CSCs are the origin of the tumor and are the source of the heterogeneity, due to their indefinite self-renewal capacity and elevated plasticity (Peitzsch et al., 2013). For this reason, CSCs can produce cells with different grades of differentiation and can also experiment transdifferentiating processes giving rise (in cancer context) to highly invasive cells with mesenchymal phenotype (Liu et al., 2013; Ricci-Vitiani et al., 2008) or even stromal cells like pericytes or endothelial cells (Cheng et al., 2013).

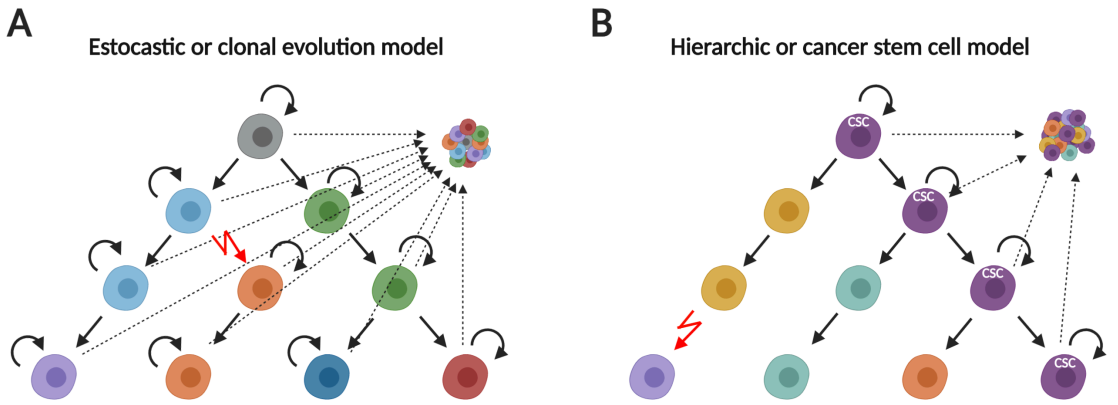

Figure I2. Principal models or theories of tumor heterogeneity. (**A**) In accordance with the clonal evolution theory, the somatic alterations that affect the cell of origin give place to multiple clones, with different sensitivity to the therapies and capacity to proliferate and survive. These cellular clones of the tumor are genetically instable, suffer genetic alterations and the clones with the most aggressive phenotype will be the ones will survive to the therapies. All the cells of the tumor have the capacity to maintain and expand the tumor. (**B**) The model or theory of the stem cells defends that only a minoritarian population known as cancer stem cells (CSC) has the capacity of self-renewal and limitless proliferation that give rise to clones with very different genetic profiles. Created with BioRender.com.

CSCs reside in niches, which are anatomically distinct regions within the tumor microenvironment. These niches are responsible for maintaining the principle properties of CSCs, such as plasticity preservation, protection from immune system and metastasis facilitation (Plaks et al., 2015).

Besides cancer cells, tumors also contain other cell types such as the immune system cells, the endothelial cells of the surrounding blood vessels and the stroma cells (fibroblasts and pericytes). All of them form the denominated tumor microenvironment, a complex system in which tumor cells and non-tumor cells communicate and influence each other (Junttila and de Sauvage, 2013). Nowadays, it is well described that the influence of the tumor microenvironment is very important for the progression of the tumor. A clear example of this premise is the induction of angiogenesis that tumor cells promote and that allows them to achieve nutrients and oxygen, in addition to disseminate through blood vessels (Hanahan and Weinberg, 2011). Other clear demonstration of the relevance of this microenvironment is the fact that some recent antitumor therapies that are been studied are targeting stroma cells, such as cancer associated fibroblasts (CAFs), which, as a result of their oncogenic context, are phenotypically and functionally different from the normal fibroblasts, and promote the proliferation and the invasive capacity of tumor cells (Calgani et al., 2016).

Thus, taking all this information together, we can conclude that different mechanisms contribute to the intra-tumor heterogeneity, including genetic mutations, tumor microenvironment and the existence of tumor cell subpopulations with self-renewal and multipotency ability, the subpopulation denominated as cancer stem cells (CSCs), which have specific characteristics that are following explained.

1.1.2.1. Stem cells characteristics

For understanding the biology of CSCs, first it is necessary to define the specific properties of an adult stem cell. A normal adult stem cell is defined by two main characteristics, shared with CSCs, including pluripotency and self-renewal capacity (Lobo et al., 2007):

- Pluripotency: a capacity of a non-differentiated stem cell to differentiate into distinct cellular linages. Depending on that capacity, there are different levels of "potency" (Bozdag et al., 2018):

  - *Totipotency*: is the ability to generate a hole organism from one cell. Embryonic cells within the first couple of cell divisions after fertilization are the only cells that are totipotent.

- *Pluripotency*: is the ability to generate cells of different linages of the three germinal layers (except for the placenta) from one cell.

- *Multipotency*: is the ability of generating different type of cells, but all of them belonging to the same linage. In this level are located the adult stem cells.

- *Unipotency*: is the ability to generate a single cell type.

- **Self-renewal capacity**: It is the ability of cells to self-perpetuate using both symmetric and asymmetric divisions. Thanks to this process, stem cells retain their undifferentiated state (by symmetric division) and maintain or increase their number as needed (by asymmetric divisions), thus creating new, more specialized cells necessary for the maintenance of the organism (He et al., 2009).

According to this classification, adult stem cells are multipotent cells, capable of generating different cell types, but all of them belonging to the same tissue or cell lineage. They are distributed throughout the adult organism, but located in very specific regions of the organs called stem cell niches, and are responsible for the formation of new cells in order to replace those eliminated by apoptosis, necrosis or senescence processes. They are cells, therefore, essential for the maintenance of homeostasis of the organism and tissue regeneration (Blanpain and Fuchs, 2014). These cells are predominantly in a quiescent state (in G0 phase), non-dividing, but they are able to exit this state in response to a stress stimulus, thus, entering in the cell cycle, expanding and differentiating (Arai et al., 2004).

Among other characteristics of the stem cells, it has been observed that these cells are smaller (Li et al., 2015a) and present lower metabolism activity, aspects that are related with their quiescent state. Moreover, they present high expression levels of aldehyde dehydrogenase enzyme (ALDH) (Dolle et al., 2015), express specific surface markers and develop a high efflux of substances by ATP Binding Cassette Subfamily G Member (ABCG) membrane transporters, reason why they can be distinguished by a low accumulation of fluorescent substances like Hoechst 33342 or Rhodamine 123 (Goodell et al., 1996; Jones et al., 1996; Leemhuis et al., 1996).

The capacity for self-renewal and the potentiality of stem cells are properties that are shared with cancer cells, so it does not seem unreasonable to think that some type of stem cells, or the transformation of somatic cells into stem cells, could be involved in the process of tumorigenesis.

1.1.2.2. CSCs' characteristics

As well as normal stem cells, CSCs also present distinctive characteristics of size, markers, metabolism and substances' efflux (Bleau et al., 2009; Li et al., 2015a). It has been demonstrated that CSCs are specifically resistant to conventional treatments. Several factors or mechanisms participate in this resistance, such as DNA damage reparation mechanisms, alteration of the cell cycle control, drug expulsion processes, certain signaling pathways activation and tumor microenvironment influence (Borovski et al., 2011). Following, the main specific characteristics involved in treatment resistance of the CSCs are described.

Self-renewal capacity: conferred by symmetric and asymmetric divisions (Al-Hajj and Clarke, 2004). This is guided by the activation of several signaling pathways during embryonic development and tissues homeostasis. Among them WNT/β-Catenin, Notch and Sonic Hedgehog (SHH) pathways can be found (Borah et al., 2015; Karamboulas and Ailles, 2013).

Quiescence: where cells stay in G0 phase of the cell cycle, in which they don't divide. However, they can exit it and reintroduce in the cell cycle in response to physiological stimuli. Quiescence makes CSCs resistant to conventional treatments, since most of the therapies target proliferating cells and thus, don't influence the quiescent cells (Najafi et al., 2019). Moreover, quiescence could also explain the tumor recurrence and metastasis, since CSCs could be maintained quiescent for long periods and wake up inducing tumor progression in the same place or disseminating (Recasens and Munoz, 2019).

Highly active DNA damage reparation: this process has been related to CSCs' resistance to radio- and chemotherapy, since these cells have the ability to activate rapidly the machinery to repair DNA damage and, thus, go ahead in the cell cycle (Abdullah and Chow, 2013).

Cellular plasticity: is part of normal biology in development and adult homeostasis to respond to stimuli and overcome cellular stress. In cancer cells, this ability confers chemoresistance (Deheeger et al., 2014). Using this plasticity, CSCs can perform a transition between a more proliferative state, with an epithelial nature, and a more quiescent and invasive one, with a mesenchymal nature. This process of epithelial-mesenchymal transition (EMT), or its reverse mesenchymal-epithelial (MET), have been studied in the context of cancer biology and their relation with CSCs and metastasis (Mani et al., 2008; Morel et al., 2008; Nieto et al., 2016). This plasticity is a challenge for therapies, since EMT increases the invasion and dissemination capacity of cells, while decreases the proliferation, thus, conferring resistance to chemotherapy (Singh and Settleman, 2010). Moreover, reversion to an epithelial phenotype by MET allows cells to resume the proliferation that is required for tumor growth in distant organs, thus inducing metastasis (Korpal et al., 2011; Ocana et al., 2012; Tsai et al., 2012).

Moreover, the following characteristics are also present in CSCs: ABC transporters' increment (Di and Zhao, 2015; Fletcher et al., 2010), low ROS levels (Singer et al., 2015), high ALDH activity (Deng et al., 2010; Huang et al., 2009; Ma and Allan, 2011; Marcato et al., 2011) and apoptosis protection (Capper et al., 2009; Maji et al., 2018; Qi et al., 2015; Steinbichler et al., 2018).

Apart from these characteristics that confer treatment resistance to CSCs, the expression of some markers could be used to identify and isolate them. On the one hand, they express specific surface markers, such as CD34 (Bonnet and Dick, 1997; Lapidot et al., 1994), CD133 (Hemmati et al., 2003; Singh et al., 2004b), CD44 and CD15 (Ajani et al., 2015; Al-Hajj and Clarke, 2004; Read et al., 2009). However, in many cancers there is no consensus regarding the value and specificity of the different surface markers, since their expression can vary during tumor growth and may be heterogeneous between patients and even in the same tumor (Medema, 2013).

On the other hand, CSCs also express higher levels of stem cell markers. OCT4, SOX2 and NANOG transcription factors and components of WNT/B-Catenin, Notch and SHH signaling pathways have been related to the phenotype of these stem cells (Hadjimichael et al., 2015; Liu et al., 2013).

All these CSCs' characteristics are highly relevant, since they make them responsible for tumor progression and therapy resistance. So, taking this into account, CSCs could become the specific targets of new therapies, and once they are eliminated, it would be enough to use conventional therapies to eliminate differentiated cells and thus reach a stable regression of the tumor (Singh et al., 2004a). Thus, new therapies targeting CSCs should be used in combination with classical therapies to reach an optimal result.

1.1.2.3. Origin of CSCs

Even if the specific characteristics of CSCs are well known, the identity of the normal cells that acquire the changes that promote the capacity of tumor initiation and progression is still unknown (Perez-Losada and Balmain, 2003; Visvader, 2011). In this respect, it is known that this process requires accumulation of alterations and is improbable to occur in the half-life of an adult cell. That is why it is thought that CSCs are derived from self-renewable normal stem cells or progenitor cells that acquire self-renewal capacity thanks to mutations [**Figure I4**], which has been demonstrated in various types of cancers (Alcantara Llaguno et al., 2009; Blanpain, 2013).

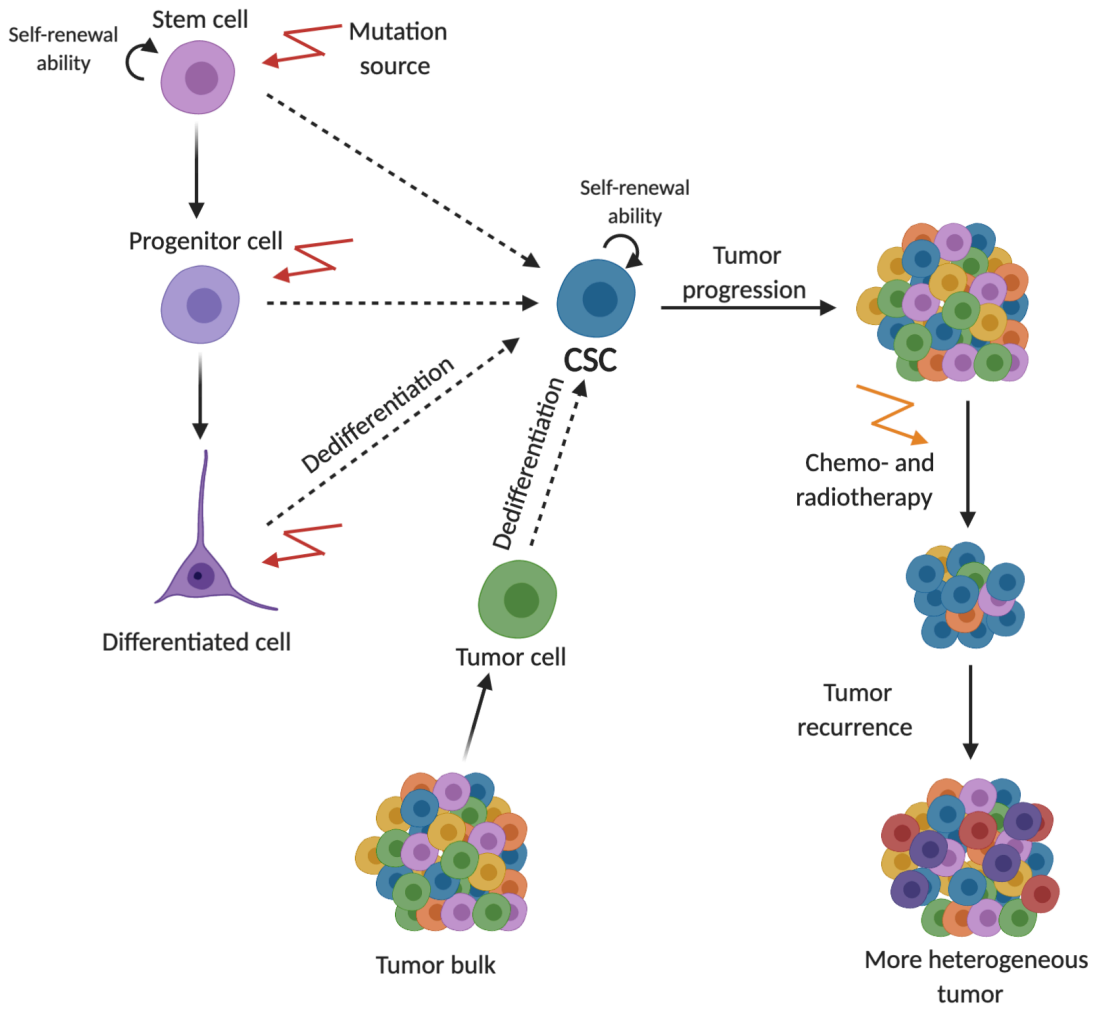

Figure I3. Cancer stem cells could originate from specific mutations in stem cells, progenitor cells, or even differentiated cells, due to dedifferentiation process. Moreover, CSCs can be also originated from dedifferentiation of differentiated tumor bulk cell. CSCs has the ability to promote tumor progression and to resist to chemo- and radiotherapy. This is the reason why they are responsible of tumor recurrence, creating a more heterogeneous tumor after treatment. Created with BioRender.com.

Another hypothesis to explain CSCs origin suggests that cells in the bulk of the tumor are able to dedifferentiate and become CSCs [**Figure I3**]. Differentiation processes are strictly regulated by epigenetic mechanisms and are generally unidirectional and irreversible processes (Cantone and Fisher, 2013). However, the capacity of reprograming completely differentiated somatic adult cells into the denominated induced pluripotent stem cells (iPSC) by ectopic introduction of OCT3/4, SOX2, KLF4 and c-MYC factors (Takahashi and Yamanaka, 2006) indicates that dedifferentiation is a feasible process. In the case of the dedifferentiation of differentiated tumor cells to CSCs, this process has been demonstrated to occur at least in gliomas (de la Rocha et al., 2014;

Friedmann-Morvinski et al., 2012; Lee et al., 2008; Moon et al., 2011). Moreover, embryonic stem cell (ESC) markers have been identified in CSCs, postulating that these cells could originate from ESCs as a consequence of mutations in the first developmental stages (Schoenhals et al., 2009).

Altogether, the identification of these crucial cell populations may allow earlier detection of malignancies and better prediction of tumor behavior, and ultimately may lead to preventive therapies for individuals at high risk of developing cancer (Visvader, 2011)

2. Central Nervous system tumors

Central nervous system (CNS) tumors constitute a heterogeneous group of neoplasms that, even if they are rare, share a considerable morbidity and mortality rate, especially in children and young adults, constituting respectively 30 % and 20 % of cancer deaths (McNeill, 2016).

CNS tumors include brain tumors, which could be very heterogeneous regarding they aggressiveness and mortality rate. More than 120 brain tumor types have been described by the National Brain Tumors Society, and they are classified by the World Health Organization (WHO) regarding their cellular origin and aggressiveness. The most common CNS tumors in children are pilocytic astrocytoma, embryonal tumors and malignant gliomas, whereas the most common ones in adults are meningiomas, pituitary tumors and malignant gliomas (McNeill, 2016).

2.1. Medulloblastoma

Brain tumors are the most common solid tumors in children, and among them medulloblastoma (MB) is the most frequent one, representing around the 20 % of the CNS tumors in childhood (Bartlett et al., 2013). These tumors form a heterogeneous group of embryonal tumors of the cerebellum. In fact, 4 different MB molecular subgroups have been described (WNT, SHH, Group 3 and Group 4), which will be addressed later (Taylor et al. 2012). All subtypes of MBs are classified by the WHO as grade IV lesions, the highest grade of malignancy according to this classification (Louis et al., 2016). MB arises in the cerebellum due to an abnormal development of this brain structure, this is the reason why these tumors are named as embryonal tumors. It is suspected to originate from the dysregulation of various discrete neuronal stem or progenitor cell populations during early development (Northcott et al., 2019).

This tumor affects around 5 children per 1 million individuals (Ostrom et al., 2018) and the most common age of appearance is between 6 and 8 years, although some MBs

can occur during the first years of life or during adulthood (Northcott et al., 2019). The diagnosis of this tumor is based on clinical symptoms, imaging by magnetic resonance imaging MRI (both of the brain and total spine, in order to assess primary tumor and to screen for macroscopic metastases), cerebrospinal fluid (CSF) cytology (in order to detect microscopic metastases) and an integrated histopathological and molecular analysis (Northcott et al., 2019).

Standard therapy is based on surgical resection, in order to remove the tumor, followed by cytotoxic chemotherapy and, in non-infants (defined as patients younger than 3 years of age), radiation. The most widely used chemotherapeutic agents are cisplatin, carboplatin, vincristine, cyclophosphamide and lomustine. Owing the propensity of MBs to metastasize within the CNS, the most successful radiation therapy is the irradiation of the entire cranio-spinal axis, being the most common one the cranio-spinal irradiation (CSI) with a focal boost on the primary tumor (Northcott et al., 2019). However, treatment outcome depends on the age of the patient and the histological and molecular features of the tumor. Moreover, current therapy, principally CSI, causes severe, widespread side effects, such as permanent neurocognitive disability, neuroendocrine dysfunction, psychological deficits and secondary malignancies among others (Musial-Bright et al., 2011; Saury and Emanuelson, 2011). Thus, the goal of both chemo- and radiotherapy is to deliver the minimum required dose to reach the maximal disease control using the least toxic agents, in this way trying to avoid the severe side effects. However, 30 % of surviving patients relapse after the initial treatment (Kadota et al., 2008; Musial-Bright et al., 2011).

Furthermore, almost 30 % of patients with MB present disseminated tumor in the moment of the diagnostic (Park et al., 1983). MBs normally spread from the CSF, and the most common dissemination is leptomeningeal. However, metastases outside the CSF can occur, even if are rare. They normally appear in the bone, in the lymph nodes or in the lung (Rochkind et al., 1991).

The therapeutic approach used nowadays has improved the survival rate of patients up to a 70-90 %, but it can vary depending on the age of the patient and the type of tumor (Coluccia et al., 2016). The overall survival for patients older than 3, with a gross

total resection of their tumor and non-metastatic at the moment of the diagnosis is between 70 and 85 % (Gajjar et al., 2006; Oyharcabal-Bourden et al., 2005; Packer et al., 2006). However, for patients younger than 3, with a subtotal resection and/or metastatic at the moment of the diagnosis (which are considered as high-risk patients), the overall survival is lower that 70 % (Gajjar et al., 2006; Gandola et al., 2009; Jakacki et al., 2012), since they cannot receive CSI because of the risk of promoting a second neoplasia (Kumar et al., 2017).

2.1.1. Cerebellum development

As mentioned before, MB originates due to an aberrant cerebellum development. The cerebellum is located inferior to the cerebrum and posterior to the brainstem (Iulianella et al., 2019). Even if it has been thought to be important to control only motor functions, recent studies have suggested that alterations in this brain structure may be related to non-motor diseases, such as autism spectrum (Ito, 2008; Schmahmann, 2004; Schmahmann and Caplan, 2006; Strick et al., 2009; Timmann et al., 2010).

The cerebellum is organized in four dense layers: an internal granule cell layer (IGL), the Purkinje cell layer (PL), the molecular layer (ML, comprised by interneurons), and the external granule cell layer (EGL) [**Figure I4**]. The complete development of the cerebellum structure occurs postnatally, taking place in the first 2 years of live in humans, that correlates with the first 21 days in mouse (Butts et al., 2014a).

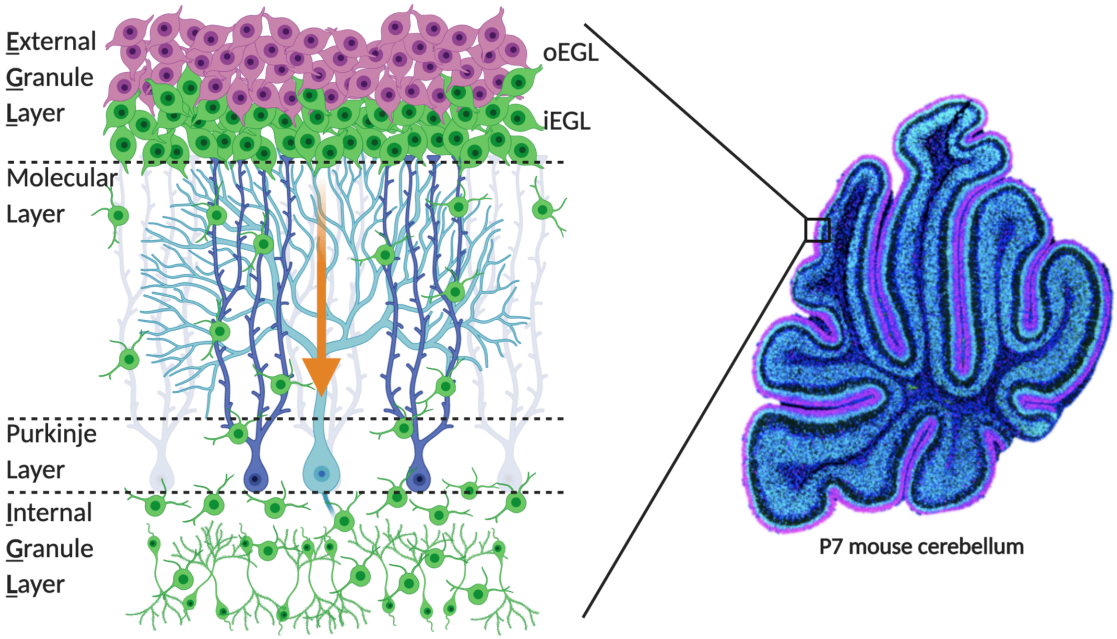

Figure I4. Cerebellar structure and CGNPs migration. Cerebellum outer layer is composed by 4 main layers, i) the external granule layer (EGL), also composed by two layers, the outer (oEGL) and inner (iEGL) layers ii) the molecular layer iii) the Purkinje cell layer and iv) the internal granule layer (IGL). At birth, CGNPs are located in the EGL, the ones in the oEGL are more proliferative, whereas the ones in the iEGL has stopped proliferating to start migrating to the IGL through the Bergman glia fibers (located in the molecular layer) and finally differentiated into neurons in the IGL. Orange arrow represents the direction of CGNPs' migration. Created with BioRender.com.

To make a long story short, cerebellum development needs a well-regulated rate of proliferation and differentiation of the cerebellar granule neuron progenitor cells (CGNPs). In the first stages these cells undergo a rapid expansion in the EGL, and afterwards, they exit the cell cycle and migrate internally through Bergmann radial fibers to the IGL, where they differentiate into interneurons (Mainwaring and Kenney, 2011; Rakic, 1971), resulting in a completely developed cerebellum.

In more detail, CGNPs derive from the rhombic lip (RL) (Wingate and Hatten, 1999), whose development is completely dependent on the function of *Atoh1/Math1*, which is induced by bone morphogenetic protein (BMP) signals (Alder et al., 1999). As development of the cerebellum progresses, the retreat of fibroblast growth factor (FGF) signaling depresses BMP signals, and consequently promotes the formation of the first migratory populations derived from *Atoh1* expressing RL progenitors, which give rise to both cerebellar neurons and extra-cerebellar nuclei in ventral hindbrain (Green et al., 2014). In the embryonic day 13 in mouse, these precursor cells generate migratory CGNPs

(Machold and Fishell, 2005), leave the RL and migrate tangentially forming a proliferative layer in the surface of the cerebellum, the EGL. This is a layer in which the CGNPs are in a proliferative state. Here they begin a variable number of rounds of amplification by symmetric divisions in order to generate a wide number of progenitor cells (Espinosa and Luo, 2008). For this stage onwards, the EGL splits into two layers, an upper or outer one containing dividing CGNPs (oEGL) and a lower or inner EGL layer containing newly generated CGNPs (iEGL) [Figure I4] (Chedotal, 2010). Subsequently, cells located in the iEGL stop proliferating and give rise to inwardly, radially migrating post-mitotic CGNPs that switch their migration pattern from tangential to radial and translocate along the fibers of the Bergmann glia to the forming IGL, where they will differentiate into neurons (Komuro and Rakic, 1998; Kuhar et al., 1993). However, how CGNPs switch from a proliferative state in the oEGL to differentiation in the iEGL is still poorly understood.

Even if it is thought that CGNPs only originate from RL, Wojcinski et al. demonstrate that there is a second source of these cells that is only mobilized under specific conditions. They demonstrated that Nestin-positive glial cells, which embryonically originate in the cerebellar ventricular zone, act as a progenitor reservoir in the adult cerebellum to supply newborn CGNPs upon cerebellar damage, such as the one caused after irradiation (Wojcinski et al., 2017). This finding gives us hope for the regenerative properties of the cerebellum after therapies against cancer, such as chemotherapy or radiation.

The whole process of proliferation, migration and differentiation of CGNPs is well-regulated by several signaling pathways. SHH-Patched (PTCH1) and WNT signaling pathways are key regulators of this process. On the one hand, *Shh* is secreted by the Purkinje cells and acts directly on the proliferation of CGNPs in the oEGL, and indirectly influences the differentiation of Bergmann or radial glia, which consequently stimulates CGNPs differentiation and migration to the IGL (Dahmane and Ruiz i Altaba, 1999). In the absence of this protein, PTCH1 (Shh receptor) inhibits Smoothened (SMO)-GLI signaling pathway, but in the presence of Shh, PTCH1 releases the negative regulation that is exerting to SMO, thus activating the signaling pathway and promoting cell proliferation of the CGNPs [Figure I5] (Wechsler-Reya and Scott, 2001). On the other hand, WNT signaling pathway presents a similar mechanism of action, since in the absence of WNT,

the multiprotein complex formed by Axin, Glycogen synthase kinase 3 beta (GSK3β) and Adenomatous polyposis coli (APC) phosphorylates cytoplasmic β-Catenin, promoting its degradation. However, in the presence of WNT, its binding to Frizzled receptor inhibits the GSK3β, in turn inhibiting the function of the multiprotein complex. That way, β-Catenin will accumulate and translocate to the nucleus, promoting cell cycle progression of the CGNPs [**Figure I5**] (Haegele et al., 2003). Moreover, *NeuroD1* seems to be also important for the exit of the CGNPs from the cell cycle in the EGL, since it downregulates *Atoh1* expression, thereby promoting the migration of these cells to the IGL (Butts et al., 2014b).

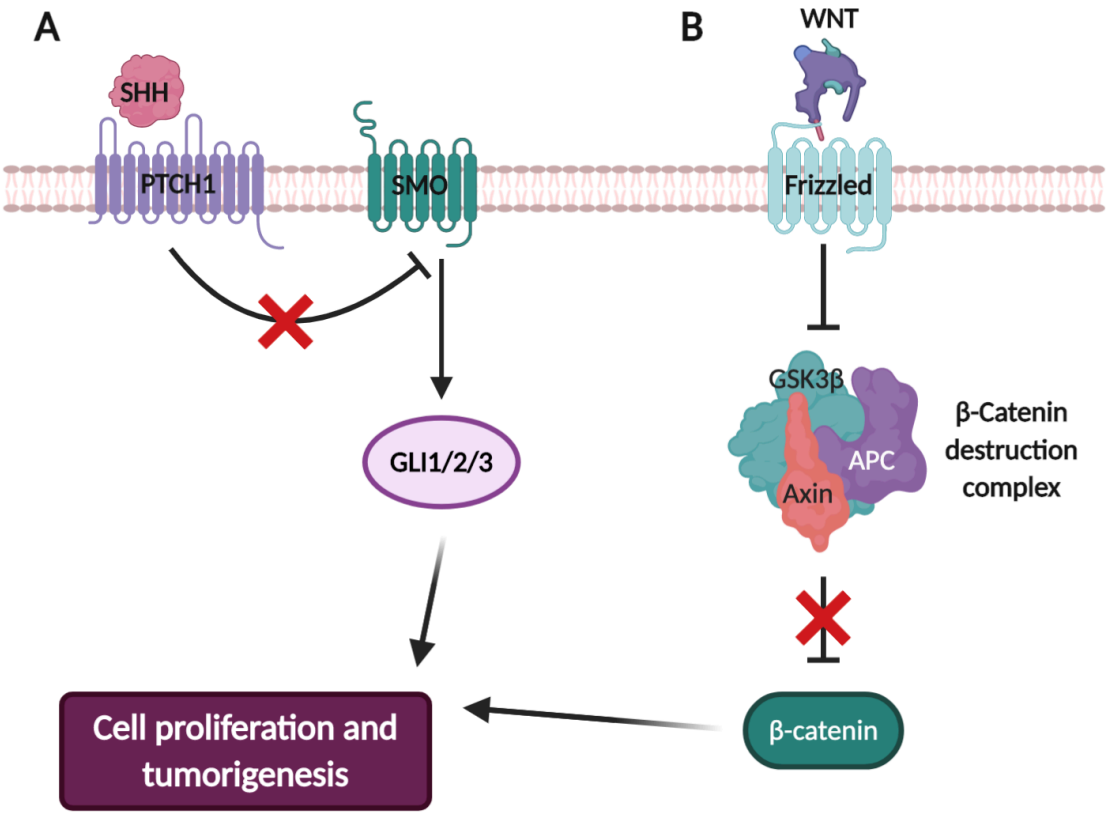

Figure I5. SHH/PTCH1 and WNT signaling pathways. (**A**) The SHH ligand inactivates the PTCH1 receptor allowing SMO to become active. Red cross represents the release of the inhibition exerted by PTCH1 on SMO when SHH is present. SMO activates GLI proteins, a family of transcription factors that turn on the expression of different target genes, giving rise to cell proliferation and tumorigenesis. (**B**) The binding of WNT to Frizzled receptor activates a cascade of downstream events, resulting in the activation of β-Catenin destruction complex. The red cross represents the release of the inhibition exerted by β-Catenin destruction complex on β-Catenin. As a consequence, β-Catenin activates and promotes the transcription of genes that promote cell proliferation and tumorigenesis. Adapted from (Aldaregia et al., 2018). Created with BioRender.com.

2.1.2. Origin of medulloblastoma

When a dysregulation of the cerebellar development process occurs and the transition between proliferation and differentiation of the cells from the EGL is disrupted, medulloblastoma progression may occur due to the incapacity of the cells to exit from a proliferative state and enter in a differentiation process (Grimmer and Weiss, 2006). As a consequence of this excessive proliferation, cells will continue proliferating and will form the tumor (Marino, 2005). The loss of equilibrium between proliferation and differentiation may be caused by an alteration of the signaling pathways mentioned above, for example, due to an excessive activation of both WNT or SHH-PTCH1 signaling pathways, proof of it are the WNT and SHH medulloblastoma mice models (Dey et al., 2012; Gibson et al., 2010; Goodrich et al., 1997).

Kadin et al. first proposed that the origin of medulloblastoma is the CGNPs for the EGL of the cerebellum (Kadin et al., 1970). Even if now it is clear that SHH MBs arise from this group (Schuller et al., 2008; Yang et al., 2008), recent findings have demonstrated that other medulloblastomas originate from different cell localizations. First, some years ago, Gibson et al. demonstrated that subgroups of medulloblastoma have different developmental origins, discovering that some WNT medulloblastomas were arisen from the dorsal brainstem cells (Gibson et al., 2010). Later, Grammel et al. discovered that some SHH medulloblastomas were arising from the granule neuron precursors of the cochlear nuclei of the brainstem (Grammel et al., 2012). Moreover, two independent studies also reported a different cell of origin for Group 3 MBs, as this subgroup MBs are characterized by high levels of MYC, they appear to derive from cerebellar stem cells (Kawauchi et al., 2012; Pei et al., 2012). Finally, in the case of Group 4 MBs, the most prevalent group, their origin is not clear, even if it has been demonstrated that several cell types can give rise to this type of tumor (Kumar et al., 2017). Even though it has been described that different subgroups of medulloblastoma have distinct cells of origin, it is interesting to note that all these cells have in common stem cell properties, and that in medulloblastomas the majority of the cells have stem-like appearance (Kumar et al., 2017).

2.1.3. Medulloblastoma classification

Until some years ago, MBs were classified based on their histopathological features. Specifically, they were classified in three main subgroups: the classic, the desmoplastic-nodular and the large cell anaplastic (LCA) MBs. In 2007, the classification performed by the WHO defined four distinct histological subgroups: desmoplastic-nodular, large cell, anaplastic and MB with extensive nodularity (MBEN), being the first one the one with the best prognosis (Louis et al., 2007). This classification changed completely in 2011, when Northcott and colleagues, using a bioinformatic analysis of transcriptional data from two cohorts of Toronto and Moscow, discovered the existence of four distinct molecular variants of MB, which they denominated as WNT, SHH, Group C and Group D (Northcott et al., 2011). These findings, together with additional studies, gave rise to a conference in Boston in 2010, where the discussant reached a consensus of the existence of four MB subgroups, that they named WNT, SHH, Group 3 and Group 4 (Taylor et al., 2012). Finally, in a more recent study, where 763 MB samples were analyzed using the similarity network fusion approach, Cavalli and colleagues identified new subtypes within the previously described four MB subgroups. The results they obtained suggest 12 subtypes, two within WNT MBs, four within SHH MBs, three within Group 3 MBs and three within Group 4 MBs (Cavalli et al., 2017). Main features of these subtypes and the relationship between the different classifications are summarized in **Figure I6.**

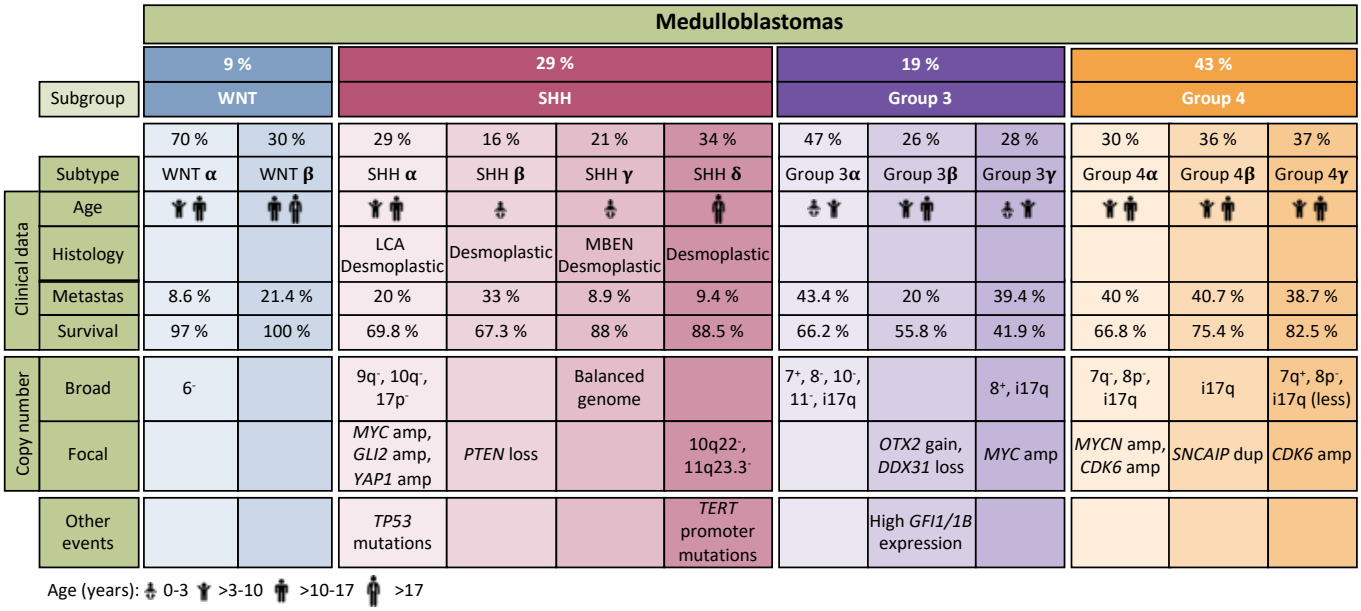

Figure I6. Image summarizing the main clinical and molecular characteristics of the different subtypes according to Cavalli classification. Modified from Taylor et al., 2012 .

2.1.3.1. WNT subgroup

The main characteristic of this subgroup MBs is the aberrant activation of the WNT/β-Catenin signaling pathway (Clifford et al., 2006). The patients belonging to this subgroup present the best prognosis; however, it is the less common one. In the last classification conducted by Cavalli and colleagues, two subtypes within the WNT subgroup were identified: WNT α and WNT β. The main molecular difference between these two subtypes is that WNT α tumors present monosomy of chromosome 6, a chromosome where *β-Catenin* encoding gene is located, whereas WNT β tumors are normally diploid for this chromosome [**Figure I6**]. Moreover, the other main difference of these two subtypes is presented in the age of appearance of the tumor. While WNT α tumors are commonly presented in children and adolescents, WNT β tumors appear in adolescents and adults [**Figure I6**] (Cavalli et al., 2017).

2.1.3.2. SHH subgroup

The tumors belonging to this subgroup are characterized by the aberrant activation of SHH signaling pathway. Different genes that participate in this pathway could be mutated in these tumors: *SHH*, *PTCH1*, *SMO*, *SUFU*, *GLI1* and *GLI2* among others.

Regarding the clinical features, patients diagnosed with SHH MBs present an intermediate prognosis, with the exception of infants, who have a good prognosis.

In the last classification four different subtypes within the SHH subgroup have been defined: SHH α, SHH β, SHH χ and SHH δ [**Figure I6**] (Cavalli et al., 2017). The SHH α subtype mainly affects to children and adolescents and its particular characteristic is that it is the only one presenting *TP53* mutations (Cavalli et al., 2017). Furthermore, this subtype tumors present enrichment of genes involved in DNA repair and cell cycle progression. Regarding to SHH β and SHH χ, these subtypes affect mainly to infants, but the survival rate varies between both of them. As it is shown in **Figure I6**, SHH β tumors are characterized by *phosphatase and tensin homolog* (*PTEN*) loss and they present the lowest survival rate within all SHH MBs, presenting a 67.3 % of survival at 5 years [**Figure I6**]. Moreover, Cavalli and colleagues identified enrichment in the developmental signaling pathways in SHH β and SHH χ subtypes. Finally, SHH δ subtype MBs present as a main characteristic enrichment in mutations of *Telomerase reverse transcriptase* (*TERT*) promoter (Cavalli et al., 2017) [**Figure I6**].

2.1.3.3. Group 3 subgroup

Among all MB subgroups, this is the one that shows the worst overall survival, presenting a median survival rate of 66.7 ± 76.6 % at 2 years (Jiang et al., 2017). To date, a specific altered signaling pathway that is responsible of originating the disease has not been identified. In the last classification three different subtypes has been described within this subgroup: Group 3α, 3β and 3χ. Regarding chromosomic alterations, the first one is characterized by the loss of chromosome 8q, chromosome that is encoding *v-myc avian myelocytomatosis viral oncogene homolog* (*MYC*). However, tumors belonging to the Group 3β subtype are characterized by the activation of the *GFI1* and *GFI1B* oncogenes, amplification of *OTX2*, and loss of *DEAD-box helicase 31* (*DDX31*) on chromosome 9. Finally, tumors of subtype Group 3χ present amplification of *MYC* as a consequence of a gain of the chromosome 8q [**Figure I6**] (Cavalli et al., 2017).

In this last classification the signaling pathways implicated in each subtype has been also characterized. In this regard, it has been described that Group 3α tumors present an enrichment of photoreceptor, muscle contraction and primary cilium-related

genes, while Group 3β and 3χ present enrichment in protein translation pathways. Moreover, Group 3χ also presents enrichment in genes related to telomere maintenance [**Figure I6**] (Cavalli et al., 2017).

2.1.3.4. Group 4 subgroup

The Group 4 MBs are the most common subgroup, representing the 40 % of all MBs. As happens with Group 3 MBs, in these tumors the signaling pathway that is originating the disease has not been identified yet. Cavalli and colleagues have identified three different subtypes within the Group 4 MBs: Group 4α, 4β and 4χ. The main chromosomic characteristics of Group 4α tumors are amplification of *neuroblastoma-derived v-myc avian myelocytomatosis viral related oncogene* (*MYCN*) and *cyclin dependent kinase 6* (*CDK6*), chromosome 8p loss and chromosome 7q gain. Regarding Group 4β tumors, they present duplication of *synuclein alpha interacting protein* (*SNCAIP*) and ubiquitous i17q. Finally, Group 4χ tumors are characterized by the amplification of *CDK6*, loss of chromosome 8p and gain of chromosome 7q, as present also Group 4α MBs, but in this case with the absence of *MYCN* amplification [**Figure I6**] (Cavalli et al., 2017).

In regard to the data obtained by Cavalli and colleagues about the differentially expressed signaling pathways, they identified an activation of migration related pathways in Group 4α, and an activation of *mitogen activated kinase-like protein* (*MAPK*) and *fibroblast growth factor receptor 1* (*FGFR1*) signaling pathways in Group 4β. Finally, in Group 4χ tumors *phosphoinositide-3-kinase/protein kinase B* (*PI3K-AKT*) and *ERBB2 receptor tyrosine kinase 4* (*ERBB4*)-mediated nuclear signaling pathways activation has been identified [**Figure I6**] (Cavalli et al., 2017).

2.1.4. MBSCs theory

In the last decades the increasing interest to understand the molecular mechanism underlying the formation, progression and recurrence of MB has revealed an important role of CSCs as a principal driver of MB initiation and relapse (Azzarelli et al., 2018). As it has been previously mentioned, several tumors present intratumor heterogeneity in which a small fraction of tumor cells called CSCs present stem properties

and the ability to proliferate and maintain the tumor growth (Clarke et al., 2006). Briefly, these cells are characterized by having self-renewal (a key property to regulate the oncogenic potential) and differentiation capacities (Manoranjan et al., 2012). In the last years CSCs has been described in several solid and hematopoietic tumors (Batlle and Clevers, 2017), including MB (Singh et al., 2003). These CSCs seem to reside in a perivascular niche, in a microenvironment composed of supportive cells, extracellular matrix and factors needed to maintain cancer stemness (Calabrese et al., 2007). These MB stem cells (MBSCs) present neural stem and progenitor features as they are characterized by CD133, SOX2, Musashi1, NES, CD15 and BMI1 expression (Ahmad et al., 2015; Hemmati et al., 2003; Read et al., 2009). All these genes are also expressed in neural stem cell (NSC) (Cai et al., 2002; Kaneko et al., 2000; Lessard and Sauvageau, 2003; Park et al., 2003; Uchida et al., 2000; Zappone et al., 2000).

In addition to present high expression of some NSC markers, several signaling pathways and most relevantly CD133, WNT, SHH, Notch, PI3K/AKT and MYC, have been demonstrated to control CSCs cell cycle and growth. (Cordeiro et al., 2014; Guessous et al., 2008).

CD133. Physiologically, CD133 induces WNT/β-Catenin signaling (Mak et al., 2012) and has also been described as an important regulator of PI3K-AKT signaling pathway in CSCs (Wei et al., 2013). The first MBSCs that had been isolated from human tissue were CD133 and Nestin positive and had shown an improved proliferation, self-renewal and differentiation capacity, since they had the ability to grow forming clusters similar to neurospheres *in vitro* and were able to produce tumors *in vivo* (expressing NSC markers such as Nestin) when they were transplanted into immunocompromised mice forebrains (Singh et al., 2003). Moreover, when injecting a small number of $CD133^+$ cells (100 cells) into immunocompromised mice, MB formation was confirmed, whereas when injecting the same amount of $CD133^-$ cells, tumor formation failed (Singh et al., 2004b). These results demonstrate the importance of this gene expression in tumor initiation process. Moreover, CD133 has also been related to apoptosis as well as radiotherapy and chemotherapy resistance (Blazek et al., 2007; Dean et al., 2005).

SHH pathway. This signaling pathway is activated by hedgehog ligands that bind to the PTCH1 receptor and maintain tumor growth and cell stemness (Enguita-German et al., 2010).

Notch pathway. This signaling pathway is required for controlling growth and proliferation of neural stem/progenitor cells, but also embryonal tumors (Pierfelice et al., 2008), including MB (Fan and Eberhart, 2008)(Wang et al., 2017b).

PI3K-AKT pathway. This signaling pathway has been demonstrated to play an important role in embryonic stem cells renewal (Wang et al., 2017a) and in the maintenance of CSCs in solid tumors (Dubrovska et al., 2009; Zhou et al., 2007), including MB (Frasson et al., 2015; Hambardzumyan et al., 2008).

MYC family. MYC proteins have been associated with MBs and more specifically with Group 3 MBs, while MYCN amplification is a characteristic of SHH and Group 4 MBs [**Figure I6**]. It has been also demonstrated that spheres cultured from MYCN-driven mice MBs express neuronal markers (such as *Neurogenin-1 (Ngn1), Synaptophysin (Syp), Oligodendrocyte transcription factor 2 (Olig2)* and *Sox9*) and when transplanted orthotopically into mice, spheres were able to form massive tumors which mimic human MBs (Swartling et al., 2012).

As mentioned when explaining CSC theory, these cells are able to survive chemo- and radiotherapy, thus contributing to failure of treatment with multiple drugs, since they have characteristics such as quiescence, activation of pro-survival/anti-apoptosis pathways and interaction with microenvironmental factors (Cojoc et al., 2015). MBSCs are also considered to be the responsible of common events as therapy resistance and tumor recurrence (Kumar et al., 2017). Moreover, CSCs has been also associated with tumor dissemination through EMT (Mani et al., 2008). Therefore, it is necessary to find new therapeutic strategies targeting this type of cells in order to avoid both therapy resistance and tumor recurrence.

2.2. Glioblastoma

In adults, the most common brain tumors are gliomas. These tumors are derived from glial cells, which are cells of a neuroepithelial origin that are responsible for the protection and maintenance of neurons. Gliomas constitute the 50 % of all brain and CNS tumors. Both from clinical and histological aspects, they are very heterogeneous tumors, and range from low proliferative to very aggressive tumors. Histologically, gliomas are classified into 4 groups: Grade I, II, III and IV, named as pilocytic astrocytoma, diffuse astrocytoma, anaplastic astrocytoma and glioblastoma, respectively (Louis et al., 2007).

Based on this classification, glioblastoma (GBM) is considered the type of glioma with the highest grade according to the WHO, which has classified the tumors according to histopathological and clinical criteria (Louis et al., 2007). Even if it is one of the 4 groups of gliomas, its incidence is very high, representing 12-15 % of the brain tumors and almost 50 % of all gliomas (Ostrom et al., 2014). It is considered the most aggressive and malign brain tumor, with an incidence ranging between 1-5 cases per 100,000 individuals per year (Ostrom et al., 2014). It could appear in any age, but it is preferably presented in adults, demonstrating its peak of apparition between 45 and 65 years of age. GBM is one of the tumors with worst prognosis, presenting an average survival of the patients that does not exceed 15 months of live and an associated 5-year survival of less than 5 % (Stupp et al., 2009).

As mentioned before, almost all of these tumors arise from glia cells. The GBM are mainly localized in both brain hemispheres, although they can originate in any location of the brain or the spinal cord. Their main characteristic is that they are very infiltrating tumors inside the brain, even if it is not common that they spread to other parts of the body, since this tumor cells do not intravasate into blood vessels (Bernstein and Woodard, 1995). GBM are characterized by a widely cellular spread within the brain, a diffuse distribution pattern in the tissue, an uncontrolled proliferation, a high genetic instability, apoptosis resistance, and by the presence of highly vascularized areas and necrotic areas (Furnari et al., 2007). Moreover, these tumors show a remarkable inter and intra-tumor heterogeneity in different levels: cellular, genetic, molecular, clinic and

histopathological among others. Moreover, they present cellular hierarchy in regard to their morphology.

GBM are diagnosed through both neuroimaging techniques, such as MRI or computer tomography (CT) scans, and tissue samples, even if they have some limitations (Shankar et al., 2017). Regarding the symptomatology, patients commonly suffer of headache, convulsions, loss of memory and behavioral changes, which are due to the increased intracranial pressure because of the presence of the tumor. Furthermore, they can also present other indicatives of the disease, such as loss of movement, instability, language disfunction and other cognitive disorders (Yamanaka, 2008).

These tumors are treated by a combination of therapies that could vary depending if the GBM is of new diagnostic or recurrent. For new diagnosed GBM, first, the resection of the tumor is needed, which frequently is not complete, due to its infiltration and localization near vital structures of the brain. Surgery allows reducing the symptoms. Next, the patients are given a combination of focal radiation therapy and chemotherapy for 6 weeks (Stupp et al., 2005). More precisely, the chemotherapeutic agent that is used to treat GBM tumors is the alkylating agent Temozolomide (TMZ), due to its ability to cross the blood brain barrier (Brada et al., 1999; Ostermann et al., 2004). After this first approach, treatment continues with adjuvant TMZ for 5 days a month during 6 months (Stupp et al., 2002; Stupp et al., 2009). However, despite the fact that this treatment has been partially effective (2.5 months survival improvement) (Stupp et al., 2005), tumors usually reappear in the same location and with a more aggressive character.

For recurrent tumors, the most used treatment is chemotherapy. The election of the chemotherapeutic agents depends on different factors, but if any has been used before, normally a different chemotherapeutic agent is administered in order to avoid the resistance mechanisms (Hou et al., 2006). The main treatment for recurrent tumors is the bevacizumab (Agha et al., 2010; Norden et al., 2008), a monoclonal anti-angiogenic antibody against the vascular endothelial growth factor.

2.2.1. GBM classification

From the clinical point of view, GBM are classified in two main groups: primaries and secondaries. The primaries, or also known as *de novo*, appear without clinical evidences of any malignant precursor and are the most common ones, representing the 90 %. The secondaries, however, come from the low-grade gliomas' progression (Ohgaki and Kleihues, 2013).

GBM can be also classified following their specific molecular alterations. Recent high-throughput molecular analyses have allowed conducting this molecular classification and have highlighted the high inter-tumor heterogeneity that GBM present (Brennan et al., 2013; Cancer Genome Atlas Research, 2008). Based on the results published by The Cancer Genome Atlas (TCGA), the different alterations present in GBM have been determined, which affect mainly to three signaling pathways: tyrosine-kinase (TK) type receptors' signaling pathways, p53 signaling pathway and retinoblastoma (Rb) signaling pathway (Brennan et al., 2013; Cancer Genome Atlas Research, 2008). Moreover, according to the TCGA, GBM have been classified into 4 molecular subtypes considering genetic and epigenetic alterations, treatment response and prognosis (Verhaak et al., 2010). According to this classification, the following GBM subtypes have been described: proneural, neural, classic and mesenchymal [**Figure I7**].

2.2.1.1. Proneural subtype

Generally, tumors belonging to this subtype are secondary GBM and are associated with an earlier appearance. They are also characterized for presenting a longer overall survival.

Regarding the alterations presented in these tumors, the most frequent ones that are characteristic of this subtype of GBM are the overexpression *platelet derived growth factor receptor alpha* (*PDGFRA*) and the mutations in *isocitrate dehydrogenase 1* (*IDH1*) and *phosphoinositide-3-kinase/phosphatidylinositol 3-kinase regulatory subunit alpha* (*PI3K/PIK3R1*). However, they can also present several alterations, such as, loss or mutations in *TP53*, *cyclin dependent kinase inhibitor 2A* (*CDKN2A*) and *PTEN*, expression

of proneural and oligodendrocyte markers and activation of hypoxia inducible factor (HIF), PI3K and PDGFR signaling pathways.

2.2.1.2. Neural subtype

Their genetic expression pattern is the most similar to a healthy brain and the tumor cells appear to have a differentiated phenotype, since they express neuron, astrocyte and oligodendrocyte markers, such as *neurofilament light* (*NEFL*), *gamma-aminobutyric acid type A receptor subunit alpha 1* (*GABRA1*), *synaptotagmin 1* (*SYT1*) and *solute carrier family 12 member 5* (*SLC12A5*). They also present amplification or overexpression of *epidermal growth factor receptor* (*EGFR*).

2.2.1.3. Classic subtype

This subtype GBMs are mainly characterized by mutations, amplifications and/or overexpression of *EGFR*. Moreover, they also present loss or mutation of *PTEN*, loss of *CDKN2A*, overexpression of *NES* and activation of the Notch and SHH signaling pathways.

2.2.1.4. Mesenchymal subtype

This subtype tumors are the ones that present the most necrotic areas, together with the expression of genes associated to inflammation, such as *tumor necrosis factor* (*TNF*) and *nuclear factor kappa* (*NF-κB*). Moreover, other alterations like loss or mutation of *neurofibromin 1* (*NF1*), *TP53* and *PTEN* and overexpression of *MET*, *chitinase 3 like 1* (*CHI3L1*), *CD44* and *MER proto-oncogene tyrosine kinase* (*MERTK*) can be found in this subtype tumors.

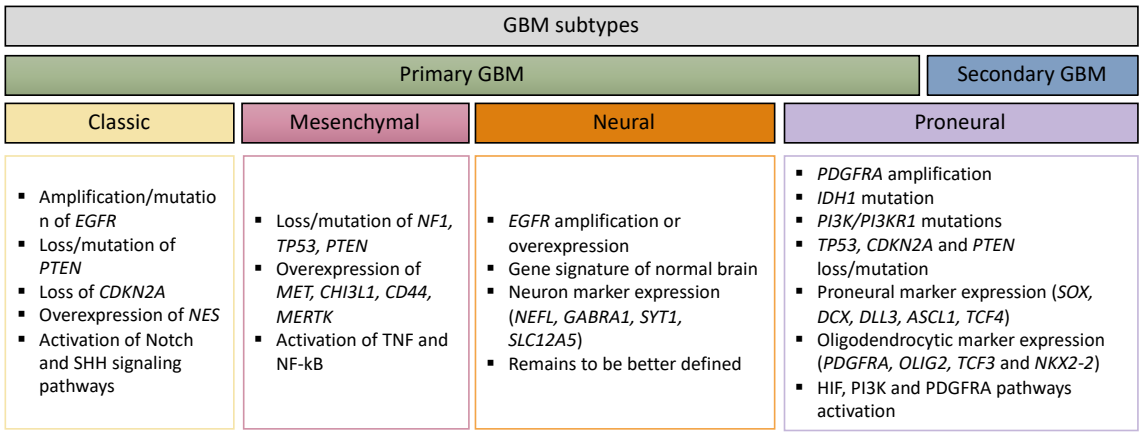

Figure I7. GBM classification according to their main alterations. Modified from (Van Meir et al., 2010).

The importance of this classification resides in the prediction of the patients' survival and their response to the conventional treatments, enabling the application of personalized therapy. For example, in the classic and mesenchymal subtypes the therapy is going to be more effective than in the other subtypes (Phillips et al., 2006). However, recently, and based on the information obtained due to the advanced molecular analyses conducted in the last years, this classification has been updated by the WHO in order to improve and make more precise the diagnosis of these tumors. This new classification [Table I1] considers both molecular and histological characteristics, reason why it integrates the genotypic and phenotypic parameters and classifies the GBM within astrocytic and oligodendrocytic tumors based on the *isocitrate dehydrogenase IDH* mutation. The following ones are the groups described by this classification: *IDH* wild type, *IDH* mutant and a third group as GBM NOS, in which the diagnosis is reserved due to the impossibility of fully evaluating *IDH* (Louis et al., 2016). Nowadays, *IDH* mutational status, rather than subtypes described by Verhaak and colleagues, is the routine diagnostic molecular marker to differentiate among GBM tumors (Louis et al., 2007).

Table I1. GBM subtypes based on WHO current classification that integrates both molecular and histological parameters. Adapted from (Louis et al., 2016).

Characteristics	GBM *IDH*-wild type	GBM *IDH*-mutant
Precursor lesion	Primary GBM, *de novo*	Secondary GBM, generated from diffuse or anaplastic astrocytoma
Frequency	90 %	10 %
Average age at diagnosis	62 years	44 years
Average survival after treatment	15 months	31 months
Major mutations (proportion)	*TERT* promotor (72 %) T*P53* (27 %) *EGFR* amplification (35 %) *PTEN* (24 %)	*TERT* promotor (26 %) *TP53* (81 %) *ATRX* (71 %)

2.2.2. Glioma stem cells theory

As mentioned before, GBM present a high intratumor heterogeneity, and as in other tumors, the presence of CSCs has been demonstrated, denominated as glioma stem cells (GSCs) (Galli et al., 2004; Singh et al., 2004b). Different origins of these cells have been postulated. On the one hand, it is thought that GSCs could originate from NSCs that are present in the adult brain, which present self-renewal and multipotency

capacities to generate the main differentiated cells of the CNS, including neurons, astrocytes and oligodendrocytes [Figure I8] (Temple, 2001). The theory that GSCs originate from NSCs has been demonstrated by overexpressing oncogenes or deleting tumor suppressor genes in embryonic and early postnatal cells, resulting in the formation of astrocytoma in mice (Bachoo et al., 2002; Holland et al., 2000; Huse and Holland, 2009; Kwon et al., 2008; Zhu et al., 2005). When analyzing these tumors, the results obtained demonstrated that they were localized in the subventricular zone (SVZ), one of the NSCs niche in the brain, (Doetsch et al., 1997) suggesting that these tumors were generated from NSCs.

On the other hand, it has been also proposed that GSCs could be originated by the dedifferentiation of normal adult cells of the brain, like astrocytes, neurons or oligodendrocytes (de la Rocha et al., 2014) [Figure I8]. Several works have induced the dedifferentiation of astrocytes to GSCs in *p53* deficient mice by *Ras* (Lee et al., 2008) or *Nanog* (Moon et al., 2011) oncogenes transduction. That this type of dedifferentiation can occur has also been demonstrated *in vivo* in gliomas, by the inactivation of *NF1* and *p53* in astrocytes and neurons (Friedmann-Morvinski et al., 2012). Moreover, by the genetic mapping of the state of the cellular chromatin, Suvà and colleagues identified 4 transcription factors (POU class 3 homeobox 2 (POU3F2), SOX2, Spalt like transcription factor 2 (SALL2) and OLIG2) in proneural GBM that were able to reprogram the differentiated tumor cells into GSCs [Figure I8] (Suva et al., 2014). These transcription factors were essential to maintain the tumorigenic capacity of these cells, suggesting that mediators of stem cell programs could confer the oncogenic capacities to the CSCs.

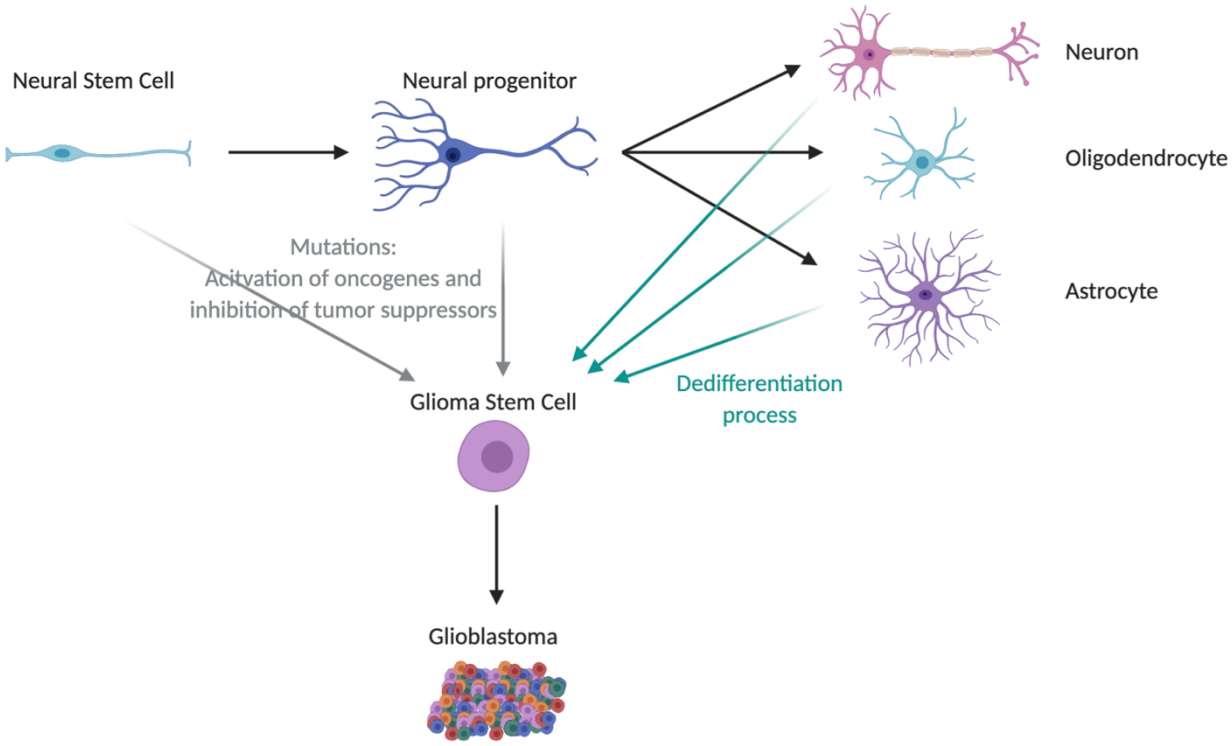

Figure I8. Origin of glioma stem cells (GSCs). GSCs could originate from neural stem or progenitor cells due to mutations that provoke activation of oncogenes and inhibition of tumor suppressors. Neural stem cells originate neural progenitors, and then they differentiate into the three main neural cells: neurons, astrocytes and oligodendrocytes. These three differentiated cells could also originate GSCs, due to a process of dedifferentiation. Finally, GSCs are the responsible of tumor origination. Created with BioRender.com.

GSCs have been characterized by mRNA analysis, differentiating proneural and mesenchymal GSCs, while they demonstrate a correspondence with proneural and mesenchymal high-grade gliomas respectively (Bhat et al., 2013; Mao et al., 2013). Proneural GSCs share some similarities with the fetal NSCs, while mesenchymal GSCs are more similar to adult NSCs (Morokoff et al., 2015; Ricci-Vitiani et al., 2008). These GSCs are more aggressive, invasive, angiogenic and resistant to therapies than the proneural ones. Moreover, the mesenchymal GSCs are mostly derived from primary or *de novo* GBM, whereas the proneurals have been also found in secondary GBM and in grade III gliomas (Mao et al., 2013; Nakano, 2015).

GSCs present specific characteristics, among them they are characterized for expressing several markers, such as CD133, CD15, A2B5 and NES. Moreover, they present

some characteristics that are usual in CSCs: ALDH1 activity, low proteasome activity and high ABC transporters activity (Ludwig and Kornblum, 2017).

As the theory of the CSCs decamines, GSCs have also been related to therapy resistance. Even if treatments for GBM have improved in the last decades, these continue to be ineffective. Although they initially regress, these tumors end up recurring. Since conventional therapies directly target proliferative cells, the undifferentiated and quiescent GSCs population can lead to therapy resistance and frequently to tumor recurrence (Ajani et al., 2015; Carrasco-Garcia et al., 2013). Moreover, GSCs resistance to both chemotherapeutic agents and radiotherapy has been demonstrated (Bao et al., 2006; Liu et al., 2006). Indeed, several studies have related the DNA-damage repair activity to radiotherapy resistance (Bao et al., 2006; Cheng et al., 2011; King et al., 2017; Short et al., 2011). Regarding chemotherapy resistance, it has been described that the expression of the O-6-methylguanine-DNA methyltransferase enzyme (MGMT), responsible for eliminating the methyl groups of the DNA, contributes to GSCs resistance to TMZ (Qiu et al., 2014).

Other studies have demonstrated that GSCs present a higher activation of ATM, checkpoint kinase 1 (CHK1) and checkpoint kinase 2 (CHK2) kinases, and a slowdown of the cell cycle in front of radiation, thus, these cells achieve an efficient DNA repair which results in radio-resistance (Bao et al., 2006; Ropolo et al., 2009). It has been also demonstrated that GSCs express higher levels of anti-apoptotic proteins such as BCL-2 than differentiated tumor cells (Tagscherer et al., 2008). Moreover, the high expression of ABCG2 cellular transporters, which play an important role in the drug efflux, have been related to the chemo-resistance of GSCs (An and Ongkeko, 2009).

Furthermore, it has been shown that GSCs overexpress genes that take part in NOTCH and SHH signaling pathways, and that their pharmacological inhibition using gamma-secretase and cyclopamine, respectively, induce the sensitization of GSCs to treatments such as TMZ (Ulasov et al., 2011).

Related to therapy resistance, cellular plasticity has been described to be a phenomenon that occurs in several tumors, where differentiated cells could turn into CSCs in response to the pressure induced by chemo or radiotherapy. First of all, it has

been observed that GSCs from cell lines and patient derived cells augmented in response to TMZ treatment both *in vitro* and *in vivo*, and that these cells came from the conversion of differentiated tumor cells into GSCs, which expressed stem cell markers such as CD133, SOX2, OCT4 and NES and presented a high tumorigenic phenotype (Auffinger et al., 2014). This conversion from differentiated tumor cells to GSCs in response to treatment has also been demonstrated when the application of TMZ induces an overexpression of HIF and cells become into GSCs, showing elevated expression levels of CD133 (Lee et al., 2016). In concordance with this affirmation, it has been also demonstrated the dedifferentiation of differentiated tumor cells toward GSCs in response to stress such as hypoxia (Safa et al., 2015). Furthermore, it has been determined that other treatments such as irradiation could regulate the dedifferentiation of GBM cells in a process that implicates to survivin dependent signaling pathway (Dahan et al., 2014).

In summary, the evidences presented indicate that GSCs are the responsible not only for tumor formation and maintenance (de la Rocha et al., 2014), but also for treatment resistance (Carrasco-Garcia et al., 2013; Liu et al., 2006).

Overall, GBM's high heterogeneity hinders diagnosis and adequate therapeutic intervention, emphasizing the need to identify biomarkers that allow a correct patient stratification and tailored therapy. Moreover, the dismal prognosis of GBM highlights the need to unravel the critical molecular mechanisms underlaying its progression to develop novel personalized therapeutic strategies.

3. ERBB receptors

ERBB receptors are a family of tyrosine kinase growth factor receptors. This family is composed by 4 members: the epidermal growth factor receptor ERBB1, best known as EGFR, ERBB2 (HER2), ERBB3 (HER3) and ERBB4 (HER4). As they are membrane receptors, they need the binding of a ligand for their activation. These receptors can be stimulated by at least six different epidermal growth factor (EGF) family hormones, including EGF, transforming growth factor-α (TGF-α), amphiregulin (AR), betacellulin (BTC), heparin-binding EGF-like growth factor (HBEGF), epiregulin and epigen, and the family of neuregulins (NRG), composed by 4 members (NRG1-4) [**Figure I9**] (Buonanno and Fischbach, 2001; Segers et al., 2020; Wang, 2017). When the ligand binds to the receptor, the dimerization of the receptor happens, allowing both its homodimerization and heterodimerization with another member of the family. Homodimers are normally formed by ERBB1 and ERBB4, while heterodimers can be formed by ERBB1 and ERBB2, ERBB3 and ERBB2, and ERBB4 and ERBB2 (Vermeulen et al., 2016). The binding of the ligand to the receptors activates different intracellular signaling pathways, such as RAS/MAP-Kinase and PI3K/AKT ones, thus regulating cell migration, proliferation, survival and differentiation (Roskoski, 2014).

3.1. ERBB4

ERBB4 is a 180 kDa protein and, as the other members of the family, is composed by an extracellular ligand binding domain, a single transmembrane domain and an intracellular domain (ICD). In the case of ERBB4, the ICD contains a functional tyrosine kinase enzyme and a C-terminal tale (Veikkolainen et al., 2011). This receptor has several ligands that can activate it: betacellulin (Riese et al., 1996a), epiregulin (Komurasaki et al., 1997), HBEGF (Elenius et al., 1997b) and the four members of NRG (NRG1-4) (Carraway et al., 1997; Harari et al., 1999; Plowman et al., 1993; Zhang et al., 1997). The only ligands specific for ERBB4 are NRG3 and NRG4 [**Figure I9**].

ERBB4 is the unique receptor of the family that undergoes alternative splicing, having at least two different isoforms expressed at the same time. As a result of

alternative splicing, different ERBB4 variants are produced, differing in the extracellular juxtamembrane (JM) (Elenius et al., 1997a) and intracellular cytoplasmic (CYT) (Elenius et al., 1999) domains. Regarding the variants differing in the JM domain, there is one lacking the exon 16 (JM-b) (Elenius et al., 1997a) and other one having this exon (JM-a) (Gilbertson et al., 2001). In this exon is encoded the tumor necrosis factor-α converting enzyme (TACE), one of the enzymes responsible for the regulated intramembrane proteolysis (Rio et al., 2000). Thus, the isoforms having the exon 16 could be cleaved and, consequently, the activated intracellular kinase domain could be moved into the cell and translocate to the nucleus acting as a transcription factor [**Figure I9**] (Ni et al., 2001; Ni et al., 2003; Vidal et al., 2005). Additionally, there are two different isoforms that differ in the CYT domain: CYT-1 and CYT-2, the first one contains the exon 26 while the second one does not [**Figure I9**] (Elenius et al., 1999). This exon encodes the domain that can mediate specific coupling to SH2 and WW domain-containing proteins, such as PI3K (Elenius et al., 1999) and ubiquitin ligases (Sundvall et al., 2008). The isoforms produced by the alternative splicing have different functions and activate different cell processes, such as cell growth, survival and apoptosis (Veikkolainen et al., 2011).

ERBB4 is linked to two main intracellular signaling pathways: RAS-MAPK-ERK and PI3K-AKT pathways [**Figure I9**]. When ERBB4 is activated, and thus phosphorylated, it induces a sustained activation of RAS-MAPK-ERK pathway, and in consequence activates cell-cycle cessation and differentiation (Iwakura and Nawa, 2013; Ortega et al., 2012). In the case of CYT-1 isoform, the phosphorylation of the Y1056 residue results in p85 adaptor recruitment to activate PI3K-AKT signaling, inducing both chemotaxis and survival (Kainulainen et al., 2000), whereas CYT2 isoform has not the ability to activate the PI3K-AKT signaling pathway. Regarding JM-a isoform, it is susceptible to proteolytic cleavage by TACE and χ-secretase, which releases an 80 kDa ERBB4 fragment, named ERBB4-ICD. This fragment will be released to the cytoplasm and will interact with the transcription factor signal transducer and activator of transcription 5A (STAT5A), subsequently translocating to the nucleus to act as a transcription factor (Sundvall et al., 2010; Vidal et al., 2005).

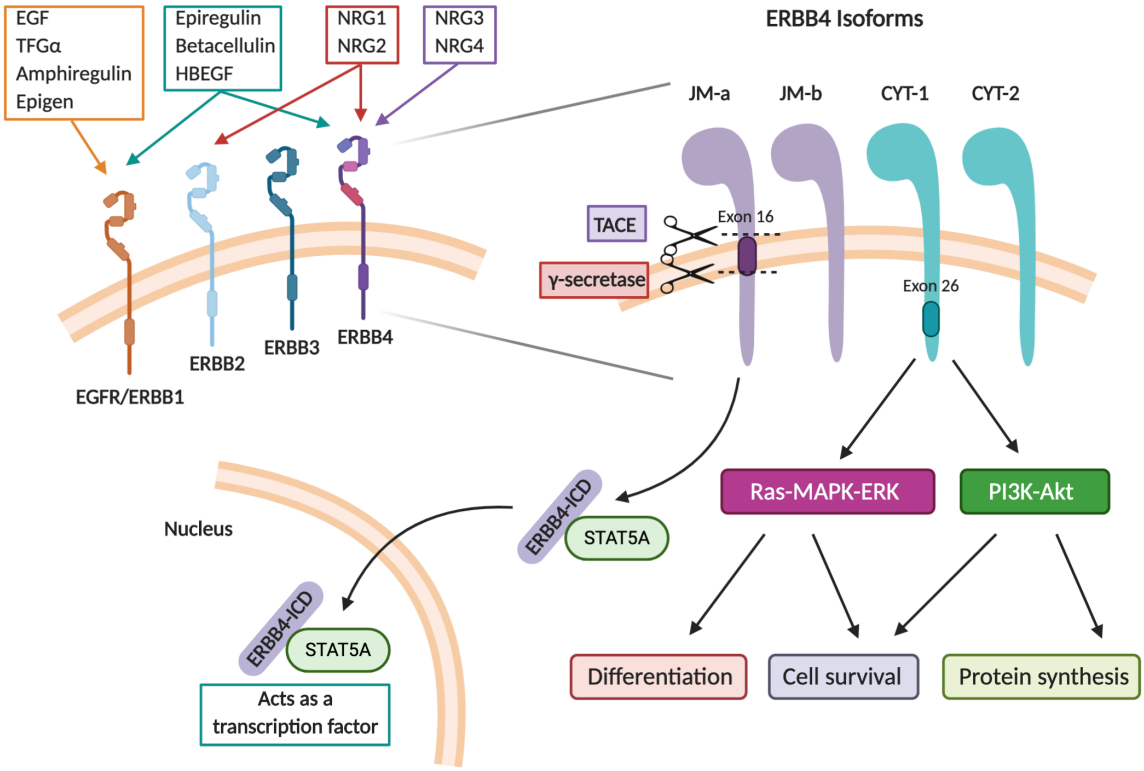

Figure I9. ERBB receptors, their ligands and ERBB4 receptor isoforms and their intracellular signaling. On the top left the 4 ERBB receptors are presented, showing the different ligands that can activate them. On the top right the alternative splicing of ERBB4 is represented, showing the different isoforms generated as a consequence of the splicing in the JM and the CYT domain. JM-a isoform can be cleaved and release to the cytoplasm, whereas JM-b isoform cannot. Moreover, CYT-1 isoform has the ability to activate PI3K, whereas CYT-2 has not. Different combinations of these variations create the 4 isoforms. Down is represented the intracellular signaling of ERBB4. ERBB4 acts mainly through ERK and Akt signaling pathways, regulating cell differentiation, survival and protein synthesis. ERBB4 JM-a isoform can be cleaved by TACE and χ-secretase resulting in an 80 kDa ERBB4-ICD protein, which will dimerize with STAT5A, resulting in a nuclear translocation. Adapted from Segers et al., 2020; Wang, 2017 and Veikkolainen et al., 2011. Created with BioRender.com.

3.1.1. Implication of ERBB4 in CNS and cerebellum development

ERBB4 receptor plays an important role in the development, ranging from embryogenesis to the development of heart, skin and CNS (Segers et al., 2020; Tidcombe et al., 2003), where is specifically involved in the development of the neural crest, myelination and neuronal migration and pathfinding (Birchmeier, 2009). Moreover, activated ERBB4 promotes neurogenesis and neuronal differentiation and survival (Gerecke et al., 2004; Ghashghaei et al., 2006; Min et al., 2011). In fact, knockout mice for the ERBB4 present defects in the hindbrain (Golding et al., 2000).

Regarding cerebellum, ERBB4 is expressed in CGNPs and it is involved in cerebellar development (Pinkas-Kramarski et al., 1997; Vullhorst et al., 2009), since ERBB4 knockout mice present deficits in neuronal migration, cerebellar heterotopias, alterations in number and distribution of specific subpopulations of interneurons, deficiencies in the astrocytic and oligodendrocytic lineages, and additional insults in major brain structures (Perez-Garcia, 2015). In fact, it has been demonstrated that this receptor is expressed in the cerebellum during its development, and that ERBB4-mediated signaling in the glia is essential for the movement of the CGNPs along the radial glial fibers (Elenius et al., 1997a; Rio et al., 1997).

Furthermore, ERBB4 ligands are also implicated in CNS and cerebellum development (Opanashuk et al., 1999). For instance, HBEGF has been identified to be expressed during cerebellum development both in the EGL and the IGL, and also in cerebellar Purkinje cells (Hayase et al., 1998; Kornblum et al., 1999; Nakagawa et al., 1998; Piao et al., 2005). Moreover, NRG have been demonstrated to be expressed in the cerebellum and participate in neuronal migration (Gilbertson et al., 1998; Rio et al., 1997).

3.1.2. ERBB4 in cancer and MB

Overexpression and activation of ERBB receptors is often associated with poor patient outcomes and advanced tumor states and has been proven as therapeutically relevant in breast, colon and other tumors (Muraoka-Cook et al., 2008). Whereas the other members of the ERBB family have been related to aggressive forms of different tumor types (Hyman et al., 2018; Hynes and Lane, 2005; Vermeulen et al., 2016), ERBB4 presents growth inhibiting properties and it is downregulated in aggressive tumors, suchas breast cancer (Muraoka-Cook et al., 2008; Naresh et al., 2006). However, several controversies about the anti- or pro-oncogenic role of ERBB4 appeared in the last years. This could be explained by the multiple ligands that can activate ERBB4, its numerous intracellular phosphorylation sites, the presence of alternative splice variants, the different intracellular signaling pathways affected, and the different downstream responses in different cell types and disease stages (Segers et al., 2020).

In more detail, the vast majority of published studies indicate that ERBB4 inhibits or has no effect on tumor growth, including breast and hepatocellular cancer (Liu et al., 2017; Muraoka-Cook et al., 2006). However, a limited number of studies indicate that ERBB4 may have a growth stimulating effect on certain tumor cells such as in colorectal cancer, gastric cancer, and melanoma (Prickett et al., 2009; Williams et al., 2015; Xu et al., 2018). These data demonstrate the dual role of this receptor, which is dependent of the tumor type.

Few evidences have been published regarding the role of ERBB4 in MB. On the one hand, it has been shown that human tumor samples express higher levels of this receptor than the healthy cerebellum (Zeng et al., 2009). Moreover, its high expression has been correlated with a poor prognosis (Bal et al., 2006; Gilbertson et al., 1997). It has been also demonstrated that ERBB4 isoforms are differentially expressed in MB (Ferretti et al., 2006; Gilbertson et al., 2001). Finally, a recent study has reported an oncogenic role for aberrant ERBB4-mediated signaling in MB, specifically in Group 4 patients, through a proteomic and phosphoproteomic approach (Forget et al., 2018).

4. SOX transcription factors

SOX (sex-determining region Y (SRY)-box) genes are a family of transcription factors distinguished by a conserved high-mobility group (HMG) DNA-binding domain. This family is composed by 20 members, and these are classified into 8 groups based on their HMG sequence identity (Schepers et al., 2002). Members within the same group may have overlapping expression patterns, share biochemical properties, and perform synergistic or distinct functions. These transcription factors play an essential role in embryonic and postnatal development, and in stem cells regulation and maintenance, especially in the CNS (Pevny and Placzek, 2005; Sarkar and Hochedlinger, 2013).

The activity and expression of SOX proteins are regulated at multiple levels. They interact with other factors to carry out their function. However, the expression of SOX factors is regulated by themselves or by other members of the family. Their expression is also regulated both post-transcriptionally, by miRNAs, and post-translationally, by modifications such as phosphorylation, sumoylation, acetylation, methylation and glycosylation, which affect their activity, stability and intracellular localization (Kamachi and Kondoh, 2013). Their activity is also modulated by the protein-protein interactions. Specifically, SOX proteins recognize and bind to components of SHH and WNT signaling pathways, in which SOX-GLI and SOX-β-Catenin interactions, respectively, are involved in their activity (Bernard and Harley, 2010; Malki et al., 2010; Oosterveen et al., 2012).

As mentioned before, SOX factors play an important role in the embryonic development during early gastrulation, sex determination, hematopoiesis and neurogenesis. During these processes, their function is necessary for the maintenance of stem cell pool and also to determine the commitment of certain cell populations in the development of differentiated tissues, highlighting the prominent role they play in the CNS. Historically these genes have been defined as crucial genes in embryonic development. However, recent studies demonstrate that their activity is not exclusive of development period, but also they are expressed in adult stem cells (Sarkar and Hochedlinger, 2013).

There is a growing body of evidence indicating that mutations and dysfunction of SOX factors are involved in several human diseases, including a variety of cancers. In fact, it has been thought that the genes implicated in tumor progression could coincide with genes involved in embryonic development, due to their activity in stem cells and the nexus between these cells and cancer. In general, some of the members of these transcription factors family act as oncogenes while the others are tumor suppressors (Castillo and Sanchez-Cespedes, 2012). Example of this affirmation are SOX2, SOX4, SOX9 and SOX10, which display an oncogenic role in different type of tumors, such as lung and esophageal squamous cell carcinomas, small cell lung cancer, colorectal cancer, melanoma and GBM (Bass et al., 2009; Carrasco-Garcia et al., 2016; Castillo et al., 2012; Garros-Regulez et al., 2016a; Matheu et al., 2012; Sun et al., 2014). Besides, SOX17 and SOX11 present a tumor suppressor function in some other tumor types, such as gastrointestinal tumors, mantle cell lymphomas, colorectal cancers, cholangiocarcinomas and GBM (de la Rocha et al., 2014; Du et al., 2009; Kuo et al., 2015; Li et al., 2015b; Merino-Azpitarte et al., 2017).

4.1. SOX1

SOX1 (SRY-box 1) is a member of SOXB1 subgroup, a group also comprising SOX2 (SRY-box 2) and SOX3 (SRY-box 3). It has been less studied than the other members of the group, but its important role in promoting neurogenesis has been already described (Kan et al., 2004).

4.1.1. Implication of SOX1 in CNS and cerebellum development

During development, SOX1B subgroup members show different expression patterns. While SOX1 is the earliest known neuroectoderm linage specific marker, which is activated during gastrulation, SOX2 and SOX3 show broader expression patterns that turn on at the pre-implantation and epiblast stages, respectively (Wood and Episkopou, 1999)(Venere et al., 2012). SOX1 is expressed in telencephalic neurons of the ventral striatum throughout development (Ekonomou et al., 2005). In the absence of SOX1, the early differentiation of these neurons appears normal but migration to the proper location is affected (Ekonomou et al., 2005). Thus, SOX1 has been described as a key

regulator of neural progenitor identity and neural cell fate determination, since it maintains the ability of proliferation and differentiation of these progenitors from early development to adult stages (Aubert et al., 2003; Kan et al., 2004; Pevny et al., 1998; Venere et al., 2012). Moreover, SOXB1 group members are co-expressed in the neural stem cell population and show certain degree of functional redundancy (Bylund et al., 2003; Pevny and Placzek, 2005).

Interestingly, SOX1 plays an important role in cerebellar development, since it has been described to be expressed in the Bergmann glia progenitors (Alcock and Sottile, 2009; Sottile et al., 2006). These cells are essential for the development and correct arborization of Purkinje cells, and consequently the correct migration of CGNPs to the IGL, thus forming a correct cerebellum.

4.1.2. SOX1 in cancer

To date, SOX1 has been described to play a tumor suppressor role in several tumor types, such as ovarian, hepatocellular, cervical and nasopharyngeal cancers, where its expression appears silenced by hypermethylation of its promoter (Guan et al., 2014; Lin et al., 2013; Su et al., 2009; Tsao et al., 2012), since hypermethylation of tumor suppressors contributes to carcinogenesis (Dawson and Kouzarides, 2012). Mechanistically, SOX1 acts as a tumor suppressor via the interaction with β -Catenin, consequently inhibiting WNT signaling pathway (Guan et al., 2014; Tsao et al., 2012).

Regarding the activity of SOXB1 members in GBM, the oncogenic function and clinical relevance of SOX2 are well established, most of its roles being linked to GSC regulation (Alonso et al., 2011; Gangemi et al., 2009; Garros-Regulez et al., 2016a; Garros-Regulez et al., 2016b; Ikushima et al., 2009). In contrast, little is known about the expression or function of SOX1 and SOX3. Interestingly, microarray analysis in SOX2 knock-down glioma cells identified SOX1 and SOX18 among the almost 500 genes whose expression was altered (Fang et al., 2011).

Moreover, even if SOX2 and SOX3 have been described as oncogenes in medulloblastoma (Ahlfeld et al., 2013; Gong et al., 2018; Treisman et al., 2019; Vanner et al., 2014), no studies have been published to date relating SOX1 to this tumor.

Hypothesis

ERBB4 and SOX1 play an important role in brain development and stem cell maintenance, as well as in the pathogenesis of different tumors. However, little is known about a potential role of SOX1 in brain tumors such as GBM and, specially, MB, despite its key role in neural embryonic development and its previous implication as a tumor suppressor in different tumor types has been described. In addition, ERBB4 role in MB is not clear, mainly due to the complex molecular network associated with its signaling function. Taking this background into account, we intended to go deeper into the function of both proteins in adult and pediatric brain tumors.

We hypothesize that ERBB4 and SOX1 play a role in MB pathogenesis, and that SOX1 is also involved in the carcinogenesis of GBM, through regulating CSCs proliferation and self-renewal capacity, which might be contributing to the therapy resistance showed by these tumors.

Objectives

1. To characterize the role of ERBB4 in MB.
    a. To characterize the function of ERBB4 in cerebellum development and in CGNPs.
    b. To analyze the expression of ERBB4 among MB subgroups and to determine its impact in patients' survival.
    c. To study the effect of ERBB4 silencing in medulloblastoma cell lines and MBSCs, both *in vitro* and *in vivo*.
2. To characterize the role of SOX1 in MB.
    a. To analyze the expression of SOX1 among MB subgroups and to evaluate its impact in patients' survival.
    b. To investigate the effect of SOX1 silencing in medulloblastoma cell lines and MBSCs, both *in vitro* and *in vivo*.
    c. To study the main downstream signaling pathways following SOX1 silencing.
3. To characterize the role of SOX1 in GBM.
    a. To analyze the expression of SOX1 in healthy and GBM samples and to assess its impact in patients' survival.
    b. To investigate the effect of SOX1 silencing in GBM cell lines and GSCs, both *in vitro* and *in vivo*.
    c. To study the effect of SOX1 overexpression in glioblastoma cell lines and GSCs.

Materials and methods

1. Human samples

Human glioblastoma samples were provided by the Basque Biobank for Research-OEHUN (http://www.biobancovasco.org). Data for GBM and LGG was downloaded using TCGAAssembler. The methods and experimental protocols in human samples were carried out in accordance with relevant guidelines, and all study participants signed the informed consent form. The study was approved by the ethic committee of Biodonostia Health Research Institute and Hospital University Donostia.

2. Experimental animals

With the aim of addressing the hypothesis of this work we took advantage of several mice strains. The mice strains used, as well as their main description and reference, are summarized in Table M1.

Mice were housed in specific pathogen-free barrier areas of the Biodonostia Health Research Institute and the Neuroscience Research Center at University of North Carolina (UNC), and handled in compliance with the animal research regulations specified in the European Union Directive [2010/63/EU] and in the University of North Carolina Institutional Animal Care and Use Committee approved protocol 16-099. All studies were approved by Biodonostia Health Research Institute and the University of North Carolina Animal Care and Use Committees. Mice were maintained in ventilated racks under controlled humidity, light cycle, temperature, food and water, always fulfilling the criteria established for this species. Whenever possible, all experiments were performed in age-matched or littermates' mice and blind to the experimental condition of the animals. For brain and cerebellum extraction and for tumor extraction, animals were anesthetized with isoflurane (880393HO, Abbvie), and sacrificed using CO_2 or decapitation, depending on the age of the animal.

Table M1. Different mice used in the studies.

Name	Complete strain name	Description	Reference
Foxn1nu/ Foxn1nu	Hsd: Athymic Nude-Foxn1 nu (Athymic Nude)	Athymic and hairless mice, with lack of T cells	The Jackson Laboratories, https://www.jax.org/strain/007850
NOD-SCID	NOD.CB17-Prkdcscid/ NcrCrl	Absence of functional T cells and B cells	The Jackson Laboratories, https://www.jax.org/strain/001303
C57BL/6J	C57BL/6J	No genetic alterations	The Jackson Laboratories, https://www.jax.org/strain/000664
SmoM2	Gt(ROSA)26Sortm1(Smo/EYFP)Amc	Cre-mediated excision results in the constitutive expression of the Smo/EYFP fusion gene and unrestrained Hedgehog signaling, forming MBs spontaneously	The Jackson Laboratories, https://www.jax.org/strain/005130 (Mao et al., 2006)
Conditional ErbB4 KO	ErbB4loxP/loxP	ErbB4 gene flanked by two loxP sites to make a conditional ErbB4 KO when crossing them with Cre mice	(Golub et al., 2004)
hGFAP-Cre	hGFAP-Cre	Mice expressing Cre in hGFAP positive cells	(Zhuo et al., 2001)

To examine the expression of ErbB4 in cerebellum development, as no genetic alterations were required, *C57BL/6J* mice strain was used. To determine the role of ErbB4 in cerebellar development and apoptotic resistance of CGNPs, conditional ErbB4 KO mice were crossed with hGFAP-Cre mice to generate ErbB4 KO or Het mice, lacking one copy or both of ErbB4 gene respectively, and specifically in CGNPs. In order to clarify the implication of ErbB4 in MBs' apoptotic resistance, conditional ErbB4 KO mice, SmoM2 mice and hGFAP-Cre mice were crossed, generating hGFAP-Cre; SmoM2;ErbB4KO or hGFAP-Cre;SmoM2; ErbB4Het mice, thus generating mice with constitutive expression of Smo signaling pathway and lacking both copies or one copy of ErbB4 gene respectively. Because of Smo signaling constitutive activation, these mice formed MB spontaneously within 15-17 days after birth. To assess tumor formation and progression and to avoid the rejection of the injection of human cells, immunocompromised *nude* mice, Foxn1^{nu}/ Foxn1^{nu} mice, were used.

3. Cell culture

The summary of the media used in the culture of cells isolated from mice and of human cell lines is represented in Table M4.

3.1. CGNPs isolation and culture

Plates were first treated with Poly-L-Lysine (P4832, Sigma-Aldrich) for one hour at room temperature (RT). Depending on the plate size, different volumes of Poly-L-Lysine was used in order to cover the entire plate surface. Once the incubation was completed, the plate was washed 3 times with Hank's Balanced Salt Solution (HBSS, 14175-095, Gibco) supplemented with 6 g/L glucose (G8769, Sigma-Aldrich). Once the plate was washed, half of the appropriate final volume of Dulbecco's Modified Eagle Medium Nutrient Mixture F-12 (DMEM/F12, 11330-032, Gibco) supplemented with 100 U/mL penicillin and 100 µg/mL streptomycin (15140122, Gibco), 1 % N2 (17502048, Gibco), 1 % KCl 2.5 M and 10 % foetal bovine serum (FBS, 10270106, Gibco) was added. Then, the plate was incubated at 37 ºC until the cells were seeded. Needed treatments, were added to this media if required. The concentrations used for each treatment are specified in Table M2.

For CGNP isolation, pups were sacrificed at postnatal day 5-7 (p5-7) by decapitation; their cerebella were removed and collected in tubes containing HBSS + Glucose. Then, HBSS + Glucose was removed and cerebella were dissociated with 0.25 % Trypsin (T4424, Sigma) by incubating them at 37 ºC for 5 minutes. In order to inactivate the trypsin, 1 mL CGNP-DMEM/F12 + 10 % FBS media was added to the tubes containing the tissue. Next, to remove the media and trypsin, the tubes were placed in ice until the precipitation of the dissociated tissue. Afterwards, mechanic dissociation was performed using 1 mL of HBSS + Glucose. Then, the tubes were placed in ice for 2 minutes and the supernatant was collected in a new tube. The precipitated tissue was mechanically dissociated again repeating the same steps and mixing the first supernatant with the one collected in the second dissociation. Finally, the collected supernatants were centrifugated at 100 g for 1.5 minutes 3 times, supernatant was discarded and the cell pellets were resuspended in the appropriate volume of CGNP-DMEM/F12 + 10 % FBS to seed them in the previously treated plate. Cells were incubated for 4 hours at 37 ºC, at

95 % of humidity, 21 % of O_2 and 5 % of CO_2. Then, the media was removed and CGNP-DMEM/F12 media without FBS was added. Then the cells were incubated in the same conditions for 24 h. Lastly, these cells were collected for further experiments.

Table M2. Concentrations, timing and references of the treatments used with CGNPs.

Drug	Concentration	Time of treatment	Reference	Manufacturer
Shh	0.5 µg/mL	24 hours	464-SH	R&D technologies
hNRG1	100 nM	24 hours	4730-10	BioVision
HBEGF	100 nM	24 hours	4267-10	BioVision
Dexamethasone	200 µM	24 hours	D4902	Sigma

3.2. Human cell lines

All characteristics and detailed information of the cell lines used in this work are summarized in **Table M3**.

D283Med, D341Med, CHLA-01-Med and CHLA-01R-Med MB cell lines and U87MG (U87), U373MG (U373), U251MG (U251), A172 and T98G glioma cell lines were obtained from the American Type Culture Collection (ATCC). DAOY and UW228 MB cell lines were kindly provided by Dr. Castresana (Universidad de Navarra, Unav, de la Rosa et al., 2016). All glioma cell lines and DAOY, UW228 and D283Med MB cell lines were grown as adherent cell lines in Dulbecco's Modified Eagle Medium (DMEM, 41966029, Gibco) supplemented with 10 % FBS (10270106, Gibco), 2 mM L-Glutamine (25030024, Gibco), 100 U/mL penicillin and 100 µg/mL streptomycin (15140122, Gibco). In order to detach the adherent cells, 0.05 % trypsin/EDTA (25300054, Gibco) was used, incubating the cells in contact with it for 5 minutes at 37 ºC.

D341Med cell line was grown as spheres in suspension in DMEM supplemented with 20 % FBS; 2 mM L-Glutamine, 100 U/mL penicillin and 100 µg/mL streptomycin.

CHLA-01-Med and CHLA-01R-Med cell lines were grown in suspension in DMEM/F12 (11514436, Thermo Fisher) supplemented with 2 mM L-Glutamine, 100 U/mL penicillin, 100 µg/mL streptomycin, 2 % B27 (11514436, Thermo Fisher), 20 ng/mL epidermal growth factor (EGF, A15E9644, Sigma-Aldrich) and 20 ng/mL basic fibroblast growth factor (bFGF, PHG0023, Gibco).

Glioma Neural Stem 166 (GNS166) and 179 (GNS179) cell lines were kindly provided by Dr. Steve Pollar (MRC Centre for Regenerative Medicine and Edinburgh Cancer Research Centre, University of Edinburgh) and GB1 and GB2 cell lines were established in Dr. Ander Matheu's laboratory. These cell lines were grown in DMEM/F12 media, supplemented with 1.34 % D-(+)-Glucose solution 45 % (G8769, Sigma-Aldrich), 2 mM L-Glutamine, 100 U/mL penicillin and 100 µg/mL streptomycin, 1 % of N2 and 2 % B27, 20 ng/mL EGF and 20 ng/mL bFGF. To get an adherent culture, 1:500 of laminin at 1 mg/ml (L2020, Sigma-Aldrich) was added to the media. In order to detach these cells, accutase (A1110501, Gibco) was used, incubating the cells in contact with this enzyme for 5 minutes at 37 ºC.

Table M3. Cell lines characteristics used in this work.

Cell line	Type of cell	Origin	Culture media	Come from
A172	Glioma	GBM	DMEM + 10 % FBS	ATCC (CRL-1620)
T98G	Glioma	GBM	DMEM + 10 % FBS	ATCC (CRL-1690)
U87MG	Glioma	Astrocytoma	DMEM + 10 % FBS	ATCC (HTB-14)
U251MG	Glioma	GBM	DMEM + 10 % FBS	ATCC
U373MG	Glioma	GBM	DMEM + % 10 FBS	ATCC (HTB-17)
GNS166	Glioma Stem Cell	GBM	DMEM/F12	Dr. Steve Pollard (MRC)
GNS179	Glioma Stem Cell	GBM	DMEM/F12	Dr. Steve Pollard (MRC)
GB1	Glioma Stem Cell	GBM	DMEM/F12	Donostia University Hospital's patient
GB2	Glioma Stem Cell	GBM	DMEM/F12	Donostia University Hospital's patient
DAOY	MB	MB	DMEM + 10 % FBS	Dr. Castresana (Unav)
UW228	MB	MB	DMEM + 10 % FBS	Dr. Castresana (Unav)
D283 Med	MB	MB	DMEM + 10 % FBS	ATCC (HTB-185)
D341 Med	MB	MB	DMEM + 20 % FBS	ATCC (HTB-187)
CHLA-01-Med	MB	MB	CHLA-DMEM/F12	ATCC (CRL-3021)
CHLA-01R-Med	MB metastasis	Pleural fluid	CHLA-DMEM/F12	ATCC (CRL-3034)
HEK 293T	Embryonic kidney	Kidney	DMEM + 10 % FBS	ATCC (CRL-1573)

All cell lines were maintained in standard conditions at 37 ºC of temperature, 95 % of humidity, 21 % of O_2 and under 5 % of CO_2 pressure. All the cell culture procedures have been performed under laminar flow hoods of class II security (Class II Biohazard Safety Cabinets, ESCO). Cell lines were regularly tested for mycoplasma.

Table M4. Cell specific culture medias and components used in this work.

Name of the media	Media's components	Cells
DMEM + 10 % FBS	DMEM + 10 % FBS + 2 mM L-Glutamine + 100 U/mL penicillin + 100 µg/mL streptomycin	DAOY, UW228, D283Med, U87MG, U373M, U251MG, A172, T98G and HEK 293T
DMEM + 20 % FBS	DMEM + 20 % FBS + 2 mM L-Glutamine + 100 U/mL penicillin + 100 µg/mL streptomycin	D341Med
DMEM/F12	DMEM/F12 + 1.34 % D-(+)-Glucose solution 45 % + 2 mM L-Glutamine + 100 U/mL penicillin + 100 µg/mL streptomycin + 1 % N2 + 2 % B27 + 20 ng/mL EGF + 20 ng/mL bFGF	GNS166, GNS179, GB1, GB2 and CSC oncospheres
CHLA-DMEM/F12	DMEM/F12 + 2 mM L-Glutamine + 100 U/mL penicillin + 100 µg/mL streptomycin + 2 % B27 + 20 ng/mL EGF + 20 ng/mL bFGF	CHLA-01-Med and CHLA-01R-Med
CGNP-DMEM/F12	DMEM/F12 + 100 U/mL penicillin + 100 µg/mL streptomycin + 1 % N2 + 1 % KCl 2.5 M (+ 10 % FBS)	CGNPs

3.3. Genetic expression modulation by lentiviral infections

For lentiviral infections, the following constructs have been used: lentiviruses harboring plKO.1 puro (8453, Addgene) and pWXL-GFP (122257, Addgene) plasmids as control (empty vector), plKO.1 shSOX1.1 and plKO.1 shSOX1.5 plasmids (NM_005986, Sigma) for SOX1 expression silencing, SOX1 plasmid (kindly provided by Dr. Stevanovic) for SOX1 overexpression, and plKO.1 shERBB4.2 and plKO.1 shERBB4.3 (NM_005235, Sigma) for ERBB4 silencing. Prior to lentivirus generation, all the plasmids were verified by enzymatic digestions, selecting the appropriate enzyme for each plasmid. Restriction enzymes were selected by uploading the full plasmid sequence to the Restriction Mapper version 3 (Blaiklock, 2018). The buffers and amount of enzyme were used according manufacturer instructions. In all cases, the mix without enzyme was used as control. Products migration was performed in an agarose (8067, Condalab) gel for band size determination and analysis.

Lentiviruses were generated at the Viral Vector Unit of Centro Nacional de Investigaciones Cardiovasculares. 200 x 10^3 cells were lentivirally transduced with different plasmids. Lentiviral infections were performed with a multicity of infection (MOI) of 10 for 6 h in each cell line appropriate media and in the presence of 2 µg/mL polybrene (H9268, Sigma-Aldrich). The efficiency of these transductions was certified after 48 h by observing cells fluorescence under the microscope Nikon Eclipse TS-100 or by adding 2 µg/mL puromycin (P8833, Sigma-Aldrich) to the media.

4. Functional assays

4.1. Proliferation assay

For each experiment cells were seeded in duplicate in 6-well-plates (P6, 3506, Corning™). 2.5 x 10^4 cells were cultured in each well in a final 2 mL volume media. At days 1, 3 and 5 post-culture, cells were detached with trypsin and then counted. The obtained results were represented graphically, showing the total number of cells per experimental condition in each time point.

4.2. Measurement of CSCs proliferation and self-renewal capacity

For CSC proliferation assays, cells were plated at a density of 10 x 10^3 cell per well in triplicate (for each experimental condition) in tissuenon-treated P6. CSCs were incubated in DMEM/F12 media containing EGF and bFGF. 300 µL of fresh media were added twice a week. To analyze the proliferation capacity, the number of formed primary (1^{ry}) oncospheres was counted after 10 days culture. After, oncospheres were mechanically and enzymatically disaggregated with accutase for 5 min to obtain a single-cell suspension and re-plated at the same cell concentration to form secondary (2^{ry}) oncospheres. To analyze the self-renewal capacity of this oncospheres, 2^{ry} oncospheres were counted after 10 days culture.

4.3. Colony formation assay

For each experimental condition, 0.5 x 10^3 cells were seeded in 3 wells of a P6, in a final volume of 2 mL. Cells were maintained in culture for 10 days and the media was

renewed 5 days later. At day 10 after seeding, cells were fixed adding 0.5 mL of 37 % paraformaldehyde (PFA) to the culture media and incubated for 30 min at RT in agitation. Next, media and PFA were removed and fixed cells were stained with 5 % Giemsa (1.09204.0500, Merck) diluted in phosphate buffer saline (PBS, 14190094, Gibco). Cells were again incubated for 30 minutes at RT in agitation. Finally, Giemsa was removed and the wells were washed with distilled H_2O (dH_2O) and dried. Lastly, formed colonies were counted.

4.4. Cell viability assay (MTT)

In order to measure cell viability, a colorimetric assay based on the 3-(4,5-dimethylthiazol-2-yl)-2,5-diphenyltetrazolium bromide (MTT) metabolism was performed. This assay assesses the purple crystals of the formazan formed due to the reduction of the MTT reactive by the succinate-dehydrogenase enzyme present in the viable cells.

4.4.1. DAOY and UW288 cell lines

To perform this assay, 0.5 x 10^3 cells per well were cultured in sextuplicate (per experimental condition) in 96-well plates (P96, 3585, Corning™). After 96 hours of incubation at 37 ºC and 5 % CO_2, 0.44 mg/mL MTT (M2128, Sigma-Aldrich) was added. After additional 3.5 h incubation at 37 ºC and 5 % CO_2, the well contents were removed and formed purple crystals in each well were resuspended in 150 µL DMSO (D2650, Sigma-Aldrich). In order to dissolve the crystals, the plate was incubated shaking at RT for 15 min. Afterwards, the absorbance of each well was measured at 570 nm by the Multiskan Ascent plate reader (Thermo Scientific).

4.4.2. D283Med cell line

In this case, 5 x 10^3 cells per well were seeded in P96 plates , in sextuplicate (per experimental condition). After 96 hours of incubation at 37 ºC and 5 % CO_2, 0.44 mg/mL MTT (M2128, Sigma-Aldrich) was added. After additional 3.5 h incubation at 37 ºC and 5 % CO_2, 100 µL of isopropanol (I9516, Sigma-Aldrich) + 0.01 M HCl were added per well to the culture media, and the purple crystals were resuspended by pipetting. Finally, the

absorbance of each well was measured at 570 nm by the Multiskan Ascent microplate reader (Thermo Scientific).

4.5. Migration assay

To assess the cells migration capacity, 24 h before seeding the cells for the experiment, the FBS was removed, changing the media to FBS free media. To perform these experiments, 6.5 mm Transwell® chambers with 8.0 µm pore polycarbonate membrane inserts (3422, Corning) were used. Before culturing the cells in these inserts, they were humidified with FBS free media by incubating them for 1 h at 37 ºC and 5 % CO_2. Then, 2.5 x 10^4 cells were seeded in each insert, using FBS free media, in a total volume of 100 µL. As a chemoattractant to make the cells migrate through the polycarbonate membrane media with FBS was used. So, inserts were placed in 24-well plates (P24, 3527, Corning™) and 500 µL of media with FBS was added in the wells below the inserts, allowing the contact of the FBS-media with the polycarbonate membrane. Cells were then incubated for 48 h at 37 ºC and 5 % CO_2.

Next, cells that had migrated were stained adding 300 µL of Cell Stain (90144, Millipore) solution in a P24 well, placing the inserts in the wells and incubating them stirring for 20 min at RT. Afterwards, the inserts were washed with dH_2O and dried. Pictures of the migrated cells were taken with an Eclipse TS100 (Nikon) microscope. For the migrated cells quantification, polycarbonate membranes were unstained with 200 µL of Straction Buffer (90145, Millipore), adding this volume to P24 plate well, placing the insert above and incubating them stirring for 15 min at RT. Finally, 100 µL of the Straction Buffer were placed into a P96 plate well. The absorbance was measured at 570 nm in a MultiSkan Ascent microplate reader (Thermo Scientific) using the Ascent software.

4.6. Cytometry assays

4.6.1. Cell cycle assay

Cell cycle assay was used in order to quantify the percentage of the cultured cells in each phase of the cell cycle. To perform this assay 1 x 10^6 cells were collected and washed once with 1X PBS. Next, they were resuspended in 300 µL of 1X PBS and fixed by adding 700 µL 100 % cold ethanol (EtOH, ET00111000, Scharlab) drop wise and by

vortexing. The cells were fixed in a final 70 % ethanol and incubated overnight (O/N) at -20 ºC. After, these cells were washed once, centrifuging them at 1,000 g for 5 min at RT. The supernatant was discarded and 1 mL of 1X PBS was added, centrifugation and discarding the supernatant again. Once the cells were washed, they were stained in 500 µL of 1X PBS, 0.1 mg/mL RNAse A (R4875, Sigma-Aldrich) and 0.05 µM TO-PRO-3 (T3605, LifeTech) and incubated for 30 min at 37 ºC in the dark. Cells were then passed through a SH800S (Sony) cytometer and TO-PRO-3 emission was measured using the 638 nm laser and 665/30 nm filter. Cell droplets were discarded and results were analyzed using the SH800S Cell Sorter Software.

4.6.2. Cell apoptosis assay

Cell apoptosis rate in the cultures was measured by Annexin-V staining. For this, Annexin-V Alexa Fluor 488 conjugate apoptosis detection kit (A13201, Thermo Fisher) was used according to the manufacturer instructions. First, around 1 x 10^6 cells were harvested and washed once in PBS. Next, the cells' pellet was resuspended in 1 mL of annexin-binding buffer (10 mM HEPES, 140 mM NaCl and 2.5 mM CaCl2, at pH 7.4). Afterwards, 5 µL of annexin V conjugate was added per 100 µL of cell suspension, as well the SYTOX Blue, in order to stain dead cells. Then, the samples were incubated at RT for 15 min. After this incubation period, 400 µL of annexin-binding buffer were added, mixed gently and the samples were kept on ice until they were analyzed using a flow cytometer (Beckman Coulter Gallios). The number of positive cells was calculated as the percentage of the total cells relative to the control experimental condition.

4.7. In vivo carcinogenesis assay

4.7.1. Subcutaneous tumors' formation

Subcutaneous tumor formation assays were performed using 6-8-week-old immunocompromised Foxn1^{nu}/ Foxn1^{nu} mice. These mice present a mutation in the FOXn1 gene, an essential gene in thymus and hair development, so they lack mature T cells (www.jax.org/strain/007850). Subcutaneous injection was performed in these mice, in the inferior two flanks. To complete these injections, cells were collected and washed with 1X PBS and finally were resuspended in the appropriate concentration in 1X PBS.

100 µL of this suspension were injected in each mice flank, then mice were examined twice a week, by measuring the size of the formed tumors with a caliber until the end point of the experiment (until tumors reached the maximum length of 15 mm). Tumors' volumes were calculated using $V = (L \times W^2 \times 0.5)$ equation, where L represents the biggest length of the tumor and W represents the shortest one.

Tumor initiation assay was also performed. On this aim, different cell dilutions were injected. The minimum number of cells necessary to initiate tumor formation can be calculated thanks to the Extreme Limiting Dilution Analysis (ELDA, Hu and Smyth, 2009) platform.

4.7.2. Stereotaxic brain tumors´ formation

Brain tumors' formation experiments were performed in 6-8-week-old NOD-SCID mice, which lack B and T lymphocytes. Considering that this strain allows both xenogeneic and halogenic transplantation, it is considered the perfect mouse model to perform human cell transferences and xenografts (www.jax.org/strain/001303). Injected cells, being stem like GNS166 cells, were detached from the plate using accutase enzyme, then washed with 1X PBS and resuspended at the desired volume and concentration in 1X PBS.

For each mouse, 1×10^5 cells were injected in a total volume of 1 µL using a 75 RN, 26s ga 2'' Hamilton syringe (HA-87930, Teknokroma Analítica) in the right hemisphere of the striatum. The injections were performed using a stereotaxic instrument (Kopf Instruments) [**Figure M1**] in the following coordinates: Bregma: + 1.00 mm posterior, -2 mm left side and -2.5 mm depth, following the protocol established by Dr. Pollard (Pollard et al., 2009), with a constant flow of 0.05 µL/min.

After the injection, mice were examined twice a week in order to detect tumor appearance signals as weight and functional abilities' loss or other deterioration signals. When there was any evidence of tumor appearance, mouse brains were extracted and fixed in 4 % PFA (158127-5006, Sigma-Aldrich) in order to investigate them later.

During the experiments, to detect weight loss, mice were weighed once a week using a weighing scale (TE15025, Sartorious).

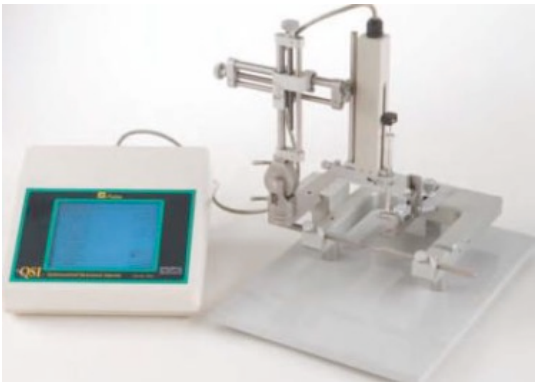

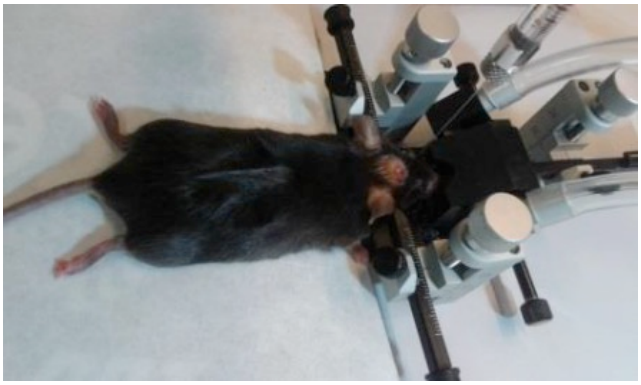

Figure M1. Representative images of stereotaxic instrument (Kopf Instruments) and injection.

5. Protein analyses

5.1. Protein extraction and quantification

Cells were collected, centrifuged for 5 min at 8000 g (microcentrifuge 22R, Beckman Coulter) to discard the supernatant and washed once with 1X PBS. The obtained cell pellets were lysate in 80-120 µL (depending the number of cells in each pellet) of Lysis Buffer (1 % NP-40, 150 mM NaCl, 5 mM EDTA, 50 mM NaF, 30 mM $Na_4P_2O_7$, 1 mM Na_3VO_4, 50 mM Tris-HCl pH 7.4), supplemented with a different protease inhibitors mix (P8340, Sigma-Aldrich), phosphatase inhibitors cocktail (P5726, Sigma-Aldrich) and the inhibitor of serine proteases phenylmethanesulfonyl fluoride (PMSF, P7626, Sigma-Aldrich) at a 100 µM concentration. Pellets were maintained for 30 min on ice and then centrifuged at 13000 g for 10 min at 4 °C for cellular debris precipitation. Supernatants containing whole cell protein extracts were collected and protein concentration was quantified by the colorimetric bicinchoninic acid assay (BCA) using a calibration line performed with 5 different concentrations of bovine serum albumin (BSA)

(Pierce BCA assay kit 23227, Thermo Scientific). Absorbance was measured at 570 nm in a MultiSkan Ascent spectrophotometer (Thermo Scientific).

5.2. Western Blot

For Western Blot (WB) technic, one fifth of loading buffer 5X (312.5 mM Tris pH 6.8, 10 % sodium dodecyl sulfate (SDS), 50 % glycerol, 0.5 % bromophenol blue and 5 % β-mercaptoethanol) was added to the desired amount of protein (ideally between 20-30 µg). Samples were then incubated at 95 ºC for 5 min in order to denaturalize them and were separated by molecular weight by sodium dodecyl sulphate-polyacrilamide gel electrophoresis (SDS-PAGE).

1.5 mm thick polyacrylamide gels were used, composed by stacking gel (4.5 % polyacrylamide) and separating gel (10 % for proteins of 100-300 kDa and 15 % for proteins between 15-99 kDa). When necessary, fror proteins size separation, commercial polyacrylamide gels (4561085, BioRad) were used, with a gradient of 4 % to 15 % polyacrylamide. Electrophoresis was performed using an electrophoresis buffer (Tris 20 mM, glycine 0.2 M, SDS 0.1 % and pH 8.3) and the power supply BioRad HC Power Pac for 60-90 min (depending on the protein size) at 120 V. Proteins were transferred to a nitrocellulose membrane (Amersham Protran 0.2 µm NC; 10600001, GE Healthcare Life Science). Transfer was performed with a transfer buffer (Tris 25 mM, 192 mM glycine, 20 % methanol, pH 8.6) for 90 min at 220 mA. To avoid the unspecific reactivity of primary antibodies the membrane was blocked with Tris Buffered Saline 0.01 % Tween 20 (TBS-T, 8221840500, Merck Millipore) and 5 % skim milk powder (70166, Sigma-Aldrich) for 1 h at RT. The nitrocellulose membranes were incubated for 15-18 h at 4 °C with different primary antibodies, see **Table M5**, following the manufacturer recommendations.

After the incubation with primary antibodies, membranes were washed 3 times for 5 min with TBS-T and incubated with the corresponding horseradish peroxidase (HRP)-conjugated secondary antibody [**Table M5**] for 1 h at RT. Finally, membranes were washed 3 times with TBS-T. Protein detection was performed by chemiluminescence using NOVEL ECL Chemi Substrate (WP20005, Thermo Fisher) for highly expressed proteins and Luminata Crescendo Western HRP Substrate (WBLUR0100, Millipore) and

SuperSignal West Femto Maximun Sensitive Substrate (#34096, ThermoFisher) for low expression proteins. Light signal was recorded by iBrightFL1000 (Invitrogen).

Table M5. Primary and secondary antibodies used in the WB technique.

Primary antibodies					
Recognized antigen	**Used dilution**	**Diluted in**	**Produced in**	**Supplier**	**Reference**
SOX1	1:250	TBS-T 5 % milk	Rabbit	Cell Signaling	4194
SOX2	1:500	TBS-T 5 % milk	Rabbit	Millipore	AB5603
ERBB4	1:250	TBS-T 5 % milk	Rabbit	Cell Signaling	4795S
P-ERBB4	1:300	TBS-T 0.5 % milk	Rabbit	Cell Signaling	4757S
Cleaved-caspase-3 (cC3)	1:300	TBS-T 0.5 % milk	Rabbit	Cell Signaling	9664S
CD133	1:300	TBS-T 5 % milk	Rabbit	Abcam	ab16518
SOX9	1:500	TBS-T 5 % milk	Rabbit	Millipore	AB5535
$P27^{KIP}$	1:500	TBS-T 5 % BSA	Rabbit	BD Bioscience	BD610241
β-ACTIN	1:10,000	TBS-T 5 % milk	Mouse	Cell Signaling	3700S
Secondary antibodies					
Antibody	**Used dilution**		**Produced in**	**Supplier**	**Reference**
Goat anti-rabbit HRP	1:1,000		Goat	Santa Cruz	sc-2004
Goat anti-mouse HRP	1:1,000		Goat	Santa Cruz	sc-2005

5.3. Cell immunofluorescence

Cells were seeded in 8-well immunofluorescence plates (154534, LabTek Thermo) and when they got the ideal confluence, cells were fixed with 4 % PFA for 10 min at RT. Next, cells were washed 3 times with 1X PBS and were blocked and permeabilized with 1X PBS 5 % FBS and 0.3 % Triton X-100 (T8787, SigmaAldrich) for 1 h at RT. Fixed cells were incubated for 15-18 h at 4 ºC with the appropriate primary antibody for each experiment [Table M6]. After this incubation, cells were washed 3 times with 1X PBS and were incubated with the correspondent secondary antibody [Table M6] for 1 h at RT in darkness. Then, after washing the secondary antibody 3 times, cell chromatin was stained for 2 min with HOESCTH (33342, Sigma-Aldrich) at 1 μg/mL and slides were mounted using Fluoro-Gel mounting media (17985-10, Aname) or cell chromatin was stained and slides mounted using Vectashield Hard set Mounting Medium with 4'6-diamino-2-

phenylindole (DAPI) counterstain (H1500, Vector Laboratories). Cell immunofluorescence (IF) was evaluated with Eclipse 80i microscope and processed with NIS Element Advances Research (Nikon) software.

Table M6. Primary and secondary antibodies used for cell IF.

Primary antibodies				
Antigen	**Used dilution**	**Produced in**	**Supplier**	**Reference**
Histone H3 (phospho S10) (PHH3)	1:2,000	Mouse	Abcam	ab14955
ß-Catenin	1:250	Mouse	BD Bioscience	610153
Cleaved-caspase-3 (cC3)	1:500	Rabbit	R&D systems	AF835
Secondary antibodies				
Antibody	**Used dilution**	**Produced in**	**Supplier**	**Reference**
Alexa Fluor® 488 Goat Anti-Rabbit IgG (H+L) Antibody	1:500	Goat	Invitrogen	A11034
Alexa Fluor® 555 Goat Anti-Mouse IgG (H+L) Antibody	1:500	Goat	Invitrogen	A21422
Alexa Fluor® 555 Goat Anti-Rabbit IgG (H+L) Antibody	1:500	Goat	Invitrogen	A21244

5.4. Tissue immunofluorescence

After dissecting the tissue, brains were fixed in 4 % PFA for at least 48 h. Tissue was processed and embedded in paraffin at the UNC Center for Gastrointestinal Biology and Disease Histology core. Sections were deparaffinized, and antigen retrieval was performed using a low-pH citric acid-based buffer. Staining was performed with assistance from the UNC Translational Pathology Laboratory. Slides were scanned using the Leica Biosystems Aperio ImageScope software (12.3.3). The primary and secondary antibodies used to perform the immunofluorescences are summarized in **Table M7**. The primary antibodies used are the following: anti-phospho-ERBB4 (P-ERBB4, PA5-38501, ThermoFisher, Waltham, MA, USA), anti-HBEGF (1:500, sc-365182, SantaCruz, Dallas, TX, USA), NeuN (MAB377, Millipore, Burlington, MA, USA), GAD1, and GFAP (Z0334, Dako,

Santa Clara, CA, USA). Where indicated, nuclei were counterstained with DAPI (catalog number D1306; Life Sciences, St. Petersburg, FL, USA).

Table M7. Primary and secondary antibodies used for tissue IF.

Primary antibodies			
Antigen	**Produced in**	**Supplier**	**Reference**
p-ERBB4	Rabbit	Thermo Fisher	PA5-38501
Hbegf	Mouse	Santa Cruz	sc-365182
NeuN	Mouse	Millipore	MAB377
GAD1	Rabbit	Invitrogen	PA5-21397
GFAP	Rabbit	Dako	Z0334
Secondary antibodies			
Antibody	**Produced in**	**Supplier**	**Reference**
Alexa Fluor® 488 Goat Anti-Rabbit IgG (H+L) Antibody	Goat	Invitrogen	A11034
Alexa Fluor® 488 Donkey Anti-Mouse IgG (H+L) Antibody	Donkey	Invitrogen	A21202
Alexa Fluor® 555 Goat Anti-Mouse IgG (H+L) Antibody	Goat	Invitrogen	A21422
Alexa Fluor® 555 Donkey Anti-Rabbit IgG (H+L) Antibody	Donkey	Invitrogen	A31572

5.5. Tissue immunohistochemistry

Immunohistochemistry (IHC) was performed to identify the expression of the proteins of interest in the brains and subcutaneous tumors generated in animal models.

Tumors and brains were extracted and fixed in 4 % PFA for at least 48 h at RT. Afterwards, tissues were embedded in paraffin and cut in 4 µm thick sections using a microtome. Then, the slides were deparaffined, rehydrated by successive baths in decreasing alcohols percentages and incubated in boiling citrate buffer for 10 min for antigenic recovery. Endogenous peroxidase was blocked in 5 % hydrogen peroxidase in methanol for 15 min. Next, samples were incubated in blocking solution (PBS, 0.3 % Triton X-100 and 5 % FBS) supplemented with the corresponding primary antibody [**Table M8**]

at 37 ºC for 2 h. After incubation with the primary antibody, the slides were washed and incubated with the appropriate secondary antibodies [Table M8]. Following, samples were incubated for 10 min at RT with 3,3'Diaminobenzidine (DAB, SPR-DAB-060, Spring Bioscience), getting as a product of the reaction oxidized DAB, a brown precipitate in the tissue. The nuclei were stained by incubating the samples for 19 min at RT with hematoxylin (6765004, Shandon). Finally, the stained slides were observed with an Eclipse 80i microscope and processed by the NIS Elements Advances Research (Nikon) software or were digitally acquired using an Aperio ScanScope XT (Aperio).

Table M8. Primary and secondary antibodies used for tissue IHC.

Primary antibodies			
Antigen	**Produced in**	**Supplier**	**Reference**
SOX1	Rabbit	Cell Signaling	4194
SOX2	Rabbit	Millipore	AB5603
PML	Rabbit	Bethyl Laboratories	A301-167A
Nrg1	Mouse	Thermo Fisher	MA5-12896
KI67	Rabbit	Abcam	ab15580
Cleaved-caspase-3 (cC3)	Rabbit	R&D systems	AF835
Secondary antibodies			
Antibody	**Produced in**	**Supplier**	**Reference**
MACH 3 Rabbit HRP-Polymer	Rabbit	BioCare Medical	M3R531
MACH 3 Mouse HRP-Polymer	Mouse	BioCare Medical	M3M530

For hematoxylin/eosin staining, fixed and paraffinized brain slides were subjected to hematoxylin and eosin staining using a Varistain Gemini ES (A78000014, Thermo Fisher) following the manufacturers instructions. Briefly, the slides were deparaffinized and rehydrated by successive baths in decreasing alcohols percentages. Next, they were submerged in hematoxylin for 2 min. After washing the slides with hot water, they were finally stained with eosin (6766008, Shandon) for 1 s.

6. Gene expression analysis

6.1. Ribonucleic acid extraction

Total ribonucleic acid (RNA) was extracted from cell lysates and from fresh tissue. Regarding the tissues, samples were homogenized in a tissue-lyser (Quiagen Retsch MM300) before adding TRI Reagent Solution (AM9738, Life Technologies). Cells were directly lysed with TRI Reagent Solution. The same procedure was used for cell pellet and tissue RNA extraction. After the complete disaggregation, 200 µL chloroform were added (C2432, Sigma-Aldrich) and gently mixed. After an incubation of 10 min at RT, samples were centrifuged at 13,000 g at 4 ºC for 10 min. The aqueous phase formed in the centrifugation was transferred into a diethyl pyrocarbonate (DEPC, 159220, Sigma-Aldrich) treated 1.5 mL microcentrifuge tube. Next, 500 µL of 2-propanol (I9516, Sigma Aldrich) and 1 µL of glycogen (at 5 µg/µL) (AM9510, Ambion) were added to each sample. After 10 min incubation at RT, samples were centrifuged at 13,000 g at 4 ºC for 22 min. Supernatant was discarded and the pellet was washed twice with 75 % EtOH by centrifugation. The remaining RNA pellet was dried and eluted in RNAse free water (10977-035, Invitrogen). Finally, RNA concentration was measured by spectrophotometry at 260 and 280 nm with a Nanodrop-1000 (Thermo Scientific).

6.2. Reverse transcription

For retro-transcription experiments, Maxima First Strand complementary DNA (cDNA) Synthesis Kit for real time quantitative polymerase chain reaction (RT-qPCR) with dsDNase Kit (K1671, Thermo Scientific) was used. cDNA synthesis was performed starting from a total RNA amount of 2 µg. Samples were incubated at different temperatures following the manufacturer instruction in a BioRad C1000 Thermal Cycler. Specifically, this retro-transcription protocol is based on an incubation phase of 10 min at 25 ºC, followed by 30 min at 50 ºC and 5 min at 85 ºC. The obtained cDNA was diluted in RNase free water up to a concentration of 4 ng/µL.

6.3. Real Time Quantitative Polymerase Chain Reaction (RT-qPCR)

Gene expression determination via messenger RNA (mRNA) was performed by RT-qPCR, starting with 20 ng of cDNA. The reaction was performed using the reaction mix Absolute SYBR Green mix (4368706, Applied Biosystem) or KiCqStart SYBR Green ReadyMix (KCQS01, Sigma-Aldrich) and 0.01 µM of primers (forward and reverse) specific for the target gene. The sequences of the primers in this work are summarized in Table M9.

RT-qPCR reactions were performed in two different ways depending on the reaction mix used. When using Absolute SYBR Green mix, the reactions were performed in the Light Cycler 96 (Roche) thermocycler following the temperature cycles defined by the manufacturer. Briefly, the program consists in 1 cycle of 120 s at 50 °C, 1 cycle of 600 s at 95 °C, 41 cycles of 15 s at 95 °C, 60 s at 60 °C and a last cycle of 10 s at 95 °C followed by 60 s at 60 °C and 1 s at 97 °C. When using the KiCqStart SYBR Green ReadyMix, the reactions were performed in the CFX984 real-time thermal cycler (BioRad) following the temperature cycles defined by the manufacturer. Briefly, the program consists in a cycle of 120 s at 50 ºC, a cycle of 600 s at 95 ºC, 40 cycles of 15 s at 95 ºC and 60 s at 60 ºC, dissociation of 5 s at 65 ºC, and then heat until 95 ºC gradually at 0.5 ºC/s. To correct the possible differences of the loaded sample amount, *β-actin* and *Glyceraldehyde-3-Phosphate Dehydrogenase (GAPDH)* were used for the mice and human samples normalization, respectively. Relative quantification was calculated using $2^{-\Delta\Delta Ct}$ method, in which the normalized gene expression of the sample is calculated taking as reference a control sample. Results are represented as fold change.

Table M9. Primers sequences used in RT-qPCR reactions.

Gene	Sense/Forward sequence (5' → 3')	Antisense/Reverse sequence (5' → 3')
Human		
ANKRD1	TGAGTATAAACGGACAGCTC	TATCACGGAATTCGATCTGG
BOC	CAAGGTCACAAATTCCTCTG	CATCTCCACTTCATACAAGC
CCND1	AGGAAGAGCCCCAGCCATG	GTTCCTCGCAGACCTCCAG
CD133 (Chapter 1 and 2)	AAGCATTGGCATCTTCTATG	TTTGCTCTGGAGTTTCATTC
CD133 (Chapter 3)	GCTCAGACTGGTAAATCCCC	GACTCGTTGCTGGTGAATTG
CEACAM1	CCACCTAACAAGATGAATGAAG	GAATCTCCTAGTGATGAGGG
CNPase	AAGAGCTGGGGAACCACAAG	GAGCCTTCCCGTAGTCACAA
CTNNB1	AGGGCTTACTGGCCATCTTT	AAACGCACTGCCATTTTAGC
ERBB4	AGGGTGATGATCGTATGAAG	TCTTGCTCTGGAAGTATAGATG
FUT4	ACAAAATCATCTGTTGGGAC	AGCAGATAAGCACTTTCAAC
GFAP	GGAAGATTGAGTCGCTGGAG	ATACTGCGTGCGGATCTCTT
GAPDH (Chapter 1 and 2)	ACAGTTGCCATGTAGACC	TTGAGCACAGGGTACTTTA
GAPDH (Chapter 3)	ATGGGGAAGGTGAAGGTCGG	GACGGTGCCATGGAATTTGC
HBEGF	GCTTATATACCTATGACCACAC	GTACCTAAACATGAGAAGCC
IGFBP3	AATCATCATCAAGAAAGGGC	GAACTTCAGGTGATTCAGTG
IL6	GCAGAAAAAGGCAAAGAATC	CTACATTTGCCGAAGAGC
MYC	GGCTCCTGGCAAAAGGTCA	CTGCGTAGTTGTGCTGATGT
NESTIN (Chapter 1 and 2)	ATGGAGACGTCGCTG	ACAGCCAGCTGGAAC
NESTIN (Chapter 3)	AGACTTCCCTCAGTTTAGG	CAGGTGTCTCAAGGGTAGCAG
NRG1	GTGGAATCAAACGCTACATC	AAAGGTCTTTCACCATGAAG
OCT4	TTCAGCCAAACGACCATC	CAGGTTGCCTCTCACTCG
p27^{KIP}	GCAACCGACGATTCTTCTAC	CTTCTGAGGCCAGGCTTCTT
PML (Chapter 1 and 2)	AGAGGATGAAGTGCTACG	TACAGCTGCATCTTTCCC
PML (Chapter 3)	CATCACCCAGGGGAAAGA	CATCACCCAGGGGAAAGA
POSTN	ATACTCTCCAGTGTTCTGAG	TTGGCAGAATCAGGAATTAG
PTHLH	GCTATTATTTCAGAGGAAGCG	CTCGGGACTTATTTAGCAAC
SEMA5A	CTATAAAGAAATTGGCCCCTG	ACAACAAGTTCTTTCTGTCC
SOD2	ATCATACCCTAATGATCCCAG	AGGACCTTATAGGGTTTTCAG
SOX1 (Chapter 1 and 2)	TGCTTGTTCTGTTAACTCAC	AAAGAACCTCAGAGAGAGTC
SOX1 (Chapter 3)	AGACCTAGATGCCAACAATTGG	GCACCACTACGACTTAGTCCG
SOX2 (Chapter 1 and 2)	ATAATAACAATCATCGGCGG	AAAAAGAGAGAGGCAAACTG
SOX2 (Chapter 3)	TACAGCATGTCCTACTCGCAG	GAGGAAGAGGTAACCACAGGG
SOX9	AGCGAACGCACATCAAGAC	CTGTAGGCGATCTGTTGGGG
THBS1	GTGACTGAAGAGAACAAAGAG	CAGCTATCAACAGTCCATTC
TP63	CAGCCTATATGTTCAGTTCAG	CAGTCCATGCTAATCTCAATC
VCAM1	ACTTGATGTTCAAGGAAGAG	TCCAGTTGAACATATCAAGC
Mouse		
ErbB4	GGCAATCTCATCTTTCTTGT	GACTGTATGTTCAGGAAACC
Hbegf	GAGCTATAGGAACCTTCAGAG	ATCGGAAATGAATGAAGACG
Nrg1	TAGTCACAGCTGGAGTAATG	CTGAGGAAGCTGTTACATTC

6.4. Microarray performing and analysis

The microarray analysis of gene expression was performed starting from 0.5 µg of the MB cells mRNA, both controls (plKO) and ERBB4 or SOX1 silencing (shERBB4 or shSOX1) cells, using Clariom S Human (902926, Thermo Fisher) microarray chips. The

microarray procedure was performed by Biodonostia Genomics Facility. The analysis of differential expression was performed using Transcriptome Analysis Console (TAC 4.0, Thermo Fisher), where the genes differentially expressed compared to the distinct experimental conditions were selected according to their *p-value* significance (lower than 0.05 and a fold-change higher than 2). Finally, the altered pathways identification with ERBB4 or SOX1 silencing and genes contributing in these pathways were obtained using the GSEA software (Broad Institute), program that integrates the selected genes in pathways depending on their most significant biological relationship according to the bibliography.

6.5. RNAscope In Situ Hybridization analysis

RNAscope was performed by the UNC Translational Pathology Laboratory with the RNAscope 2.5 Duplex Assay (ACD Bio-Systems) according to the ACD protocol for fresh-frozen tissue, in order to detect RNA expression directly in the tissue. ERBB4 (Cat No. 311,801) probe was used in this work.

7. Statistical analysis

Results of the present work are represented with the standard error of the mean (SEM), also indicating the number of experiments (*n*). Each experiment was repeated at least 3 times in an independent manner. If not otherwise indicated, all statistical analyses were calculated using the statistical Student's t-test for normal distributions. Two-tail statistical significance is represented as: *p≤0.05; ** p≤0.01; *** p≤0.001, one-tail as ≠ and ns as non-significant. Correlations and survival curves data was analyzed with GraphPad Prism 5 software (GraphPad Software, Inc. CA, USA). For genes correlation assessment, Spearman analysis was used. For the evaluation of the survival curves statistical significance, Log-Rank Test was performed.

Results

CHAPTER 1

ERBB4 is required for cerebellar development and malignant phenotype of medulloblastoma

ERBB4 is expressed in the inner part of the external germinal layer during cerebellum development

First, we investigated the expression of ErbB4 in the cerebellum in *wt* mice. For this aim, we measured its mRNA levels in the whole developing cerebellum at different time points (postnatal day 7 (p7), p14, and p18). We observed that *ErbB4* levels were similar at the different stages of the cerebellum development [**Figure R1-1.A**]. Next, in order to assess the topography of this receptor expression, we performed an RNAscope analysis and immunofluorescence assays in p7 mice cerebellum. These experiments revealed that *ErbB4* is expressed in the inner part of the EGL [**Figure R1-1.B**], whereas the expression of the active form of ErbB4 (P-ErbB4) is observed in the whole EGL [**Figure R1-1.C**]. This layer, where ErbB4 appears to be expressed, constitutes the proliferative layer of the developing cerebellum. Specifically, the external part of the EGL is very proliferative, whilst the inner part is the more differentiated side.

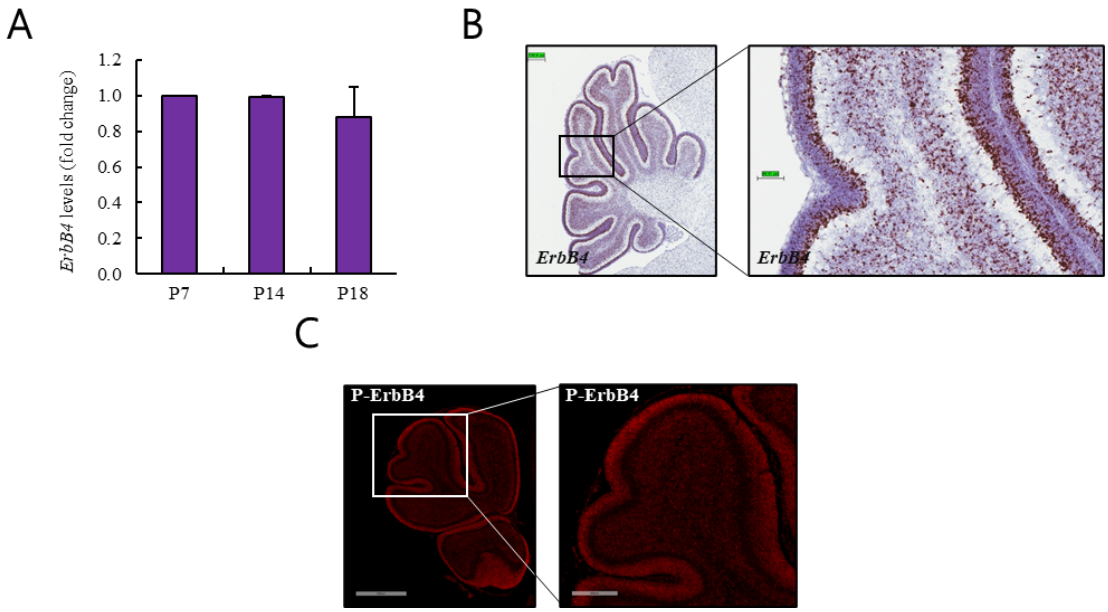

Figure R1-1. ErbB4 is expressed in the EGL during cerebellar development. (**A**) *ErbB4* mRNA expression in mice cerebellum at postnatal day 7 (p7), p14, and p18. (**B**) Representative RNAscope images of *ErbB4* mRNA expression in p7 mouse cerebellum ($n \geq 3$). Scale bars: left image = 199.8 µm and right image = 49.91 µm. (**C**) Representative immunofluorescence images of P-ErbB4 protein expression in p7 mouse cerebellum ($n \geq 3$). Scale bars: left image = 600 µm and right image = 200 µm.

Regarding ErbB4 receptor activation, different ligands exist. Among them, Hbegf and Nrg1 are the most relevant ones. Hbegf is expressed in developing cerebellum by Purkinje cells and it seems to be the dominant ligand in this brain structure (Kornblum et al., 1999). Besides, Nrg1 expression has been observed in the cerebellum EGL (Gilbertson et al., 1998). In this work, the expression of both ligands was measured at p7, p14, and p18 stages of cerebellum development by RT-qPCR. The results showed that the expression of *Hbegf* increases from p7 to p18 in a regular manner, whilst *Nrg1* expression remains constant during this period of time [**Figure R1-2.A**]. Moreover, with the aim of investigating their localization *in vivo,* Hbegf and Nrg1 expression was assessed by immunofluorescence and immunohistochemistry assays. The results showed that Hbegf is expressed in the outer part of the IGL [**Figure R1-2.B**], where cells differentiated to neurons. However, Nrg1 expression was very low or undetectable [**Figure R1-2.C**]. Altogether, these results revealed the different pattern of expression of ErbB4 ligands during cerebellar development *in vivo*.

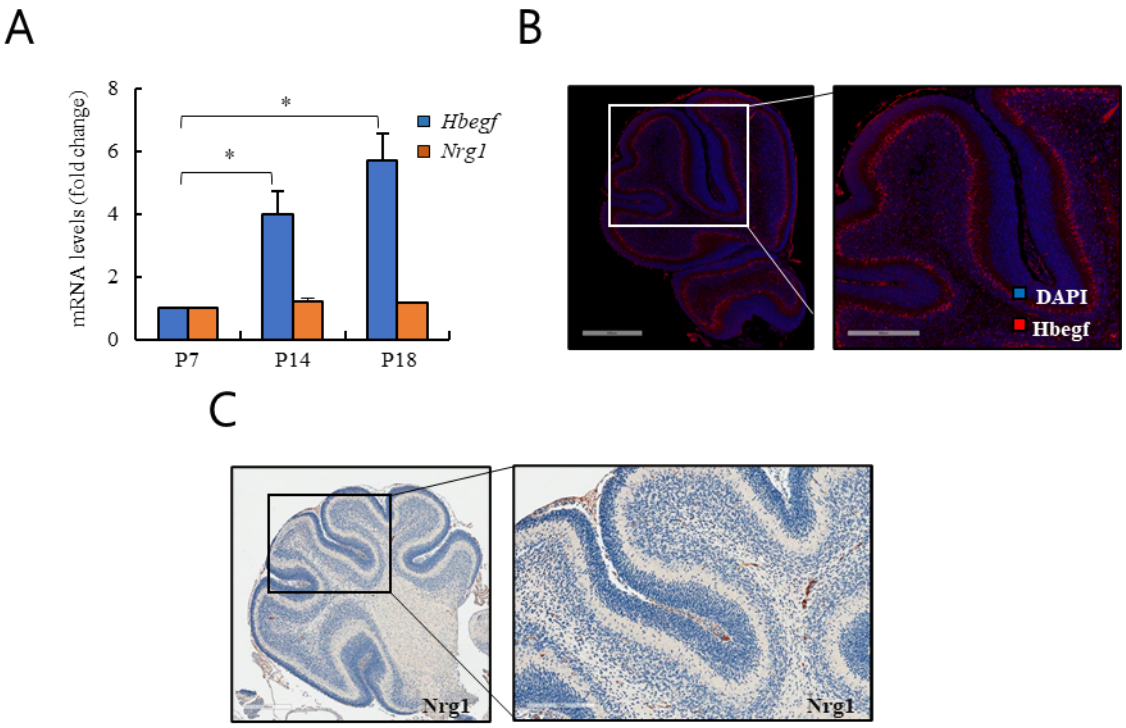

Figure R1-2. ErbB4 ligands present different expression pattern during cerebellar development. (**A**) *Hbegf* and *Nrg1* mRNA expression in mice cerebellum at p7, p14 and, p18. (**B**) Representative immunofluorescence images of Hbegf protein expression in p7 mouse cerebellum ($n \geq 3$). Scale bars: left image = 500 µm and right image = 300 µm. (**C**) Representative immunohistochemistry images of Nrg1 protein expression in p7 mouse cerebellum. Scale bars: left image = 400 µm and right image = 200 µm.

ERBB4 is essential for normal CGNP migration during cerebellar development

To assess the role of ERBB4 in CGNPs *in vivo*, we took advantage of *ErbB4* mutant or *knock out* (*KO*) mice (Gassmann et al., 1995). First, we analyzed and compared the cerebella of p20 control and *ErbB4 KO* mice by Hematoxylin and Eosin and immunofluorescence staining. At this time point, all the CGNPs should have migrated to the IGL and should have differentiated into neurons in this layer. However, the Hematoxylin and Eosin staining images of the *ErbB4 KO* mice showed that CGNPs were still located in the EGL at p20 [**Figure R1-3**]. These results confirm that ErbB4 is essential in CGNPs migration during cerebellar development.

Furthermore, we investigated different cell type markers in order to determine the localization of each cell type in both control and *ErbB4 KO* mice cerebella. In the images obtained, we could detect NeuN positive stained cells that remain in the EGL in the mutant mice cerebella. These results suggest that the neuronal differentiation

process of the CGNPs was not disrupted by the lack of *ErbB4* [Figure R1-3]. On the contrary, immunofluorescence performed for the Purkinje cell Glutamate decarboxylase 1 (Gad1) marker (Kirsch et al., 2012) showed disorganization in the Purkinje cells in *ErbB4 KO* mice [Figure R1-3], since they did not form the straight layer that can be observed in the images of *wt* mice cerebella. Moreover, when analyzing glial fibrillary acidic protein (Gfap) astrocyte marker, immunofluorescence images of *ErbB4* mutant mice cerebella also demonstrated disorganization of these cells [Figure R1-3], which form the radial glia from where CGNPs migrate through to get to the IGL.

All the results obtained demonstrate that ErbB4 has an essential role in the organization and normal development of the cerebellum and that its deficit causes aberrant migration and differentiation of the CGNPs.

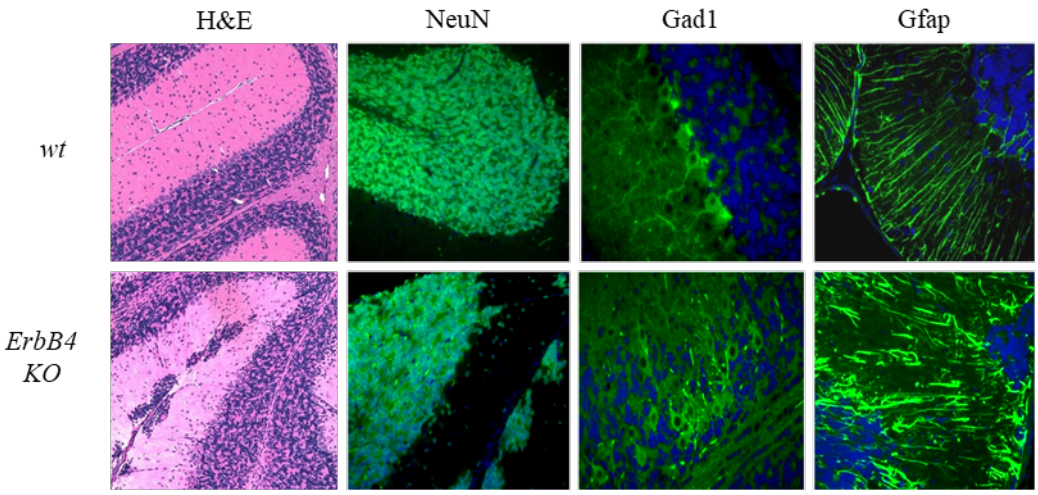

Figure R1-3. *ErbB4* deletion impairs migration during cerebellar development. Representative immunofluorescence images of the indicated proteins in p20 *wt* and *ErbB4 KO* mouse cerebella.

ERBB4 is expressed in cultured CGNPs, and its activation protects cells from an apoptotic stimulus in vitro and in vivo

To further investigate the role of ErbB4 when it is activated in CGNP cells population, p5 mice cerebella were isolated and these cells were cultured *in vitro*. Afterwards, CGNPs were treated with exogenous Shh, with the aim of maintaining them in a proliferative status, and with exogenous Hbegf and human NRG1 (hNRG1), in order to activate the ErbB4 receptor. In the performed experiments, the treatment with

exogenous Hbegf obtained a low activation of ErbB4 [**Figure R1-4.A**], since differences in P-ErbB4 levels when performing Western Blot analysis were very low when comparing treated and untreated CGNPs. However, when treating the cells with exogenous hNRG1, a strong activation of ErbB4 could be observed, as there was a significant increase in P-ErbB4 levels [**Figure R1-4.A**]. These results show that there is a different response of ErbB4 to both ligands *in vivo* and *in vitro*.

Next, CGNPs from *wt* and *ErbB4* mutant mice cerebella were cultured and treated again with exogenous Shh, hNRG1, and dexamethasone (a cell apoptosis activator). The results in *wt* mouse cultures showed that when ErbB4 is activated with hNRG1, cells are less sensitive to dexamethasone apoptosis activation. In fact, Western Blot analysis of cleaved-Caspase-3 (cC3) expression showed lower expression levels of this apoptosis marker in *wt* mouse cultures [**Figure R1-4.B**]. However, when the same experiments were repeated with *ErbB4 KO* mice cultured cells, the results show an augmented cC3 levels even when cells were treated with exogenous hNRG1 [**Figure R1-4.B**]. These results demonstrate that specifically ErbB4 receptor, and no other members of the family, is the responsible of apoptotic protection in CGNP cells.

To characterize the role of ErbB4 not only in normal development, but also in tumorigenesis process, $ErbB4^{loxP/loxP}$ mice were crossed with *hGFAPcre; SmoM2* mice. The last ones' special characteristic is that they develop MB spontaneously within 15–17 days after birth (Mao et al., 2006). First, we analyzed the tumors obtained in the pups acquired after this breeding. When we compared *ErbB4 Het* mice, with one copy of the *ErbB4* gene in Gfap expressing cells, with *KO* mice, which totally lack *ErbB4* expression in Gfap expressing cells, the results obtained by Western Blot analysis showed an increment in cC3 levels in p15 *KO* mice tumors compared with tumors obtained from p15 *Het* mice [**Figure R1-4.C**]. These phenotypes were replicated in p17 *KO* and *Het* mice tumors [**Figure R1-4.D**]. All these results demonstrate that ErbB4 confers resistance to apoptosis not only in healthy CGNPs *in vitro*, but also in tumor cells *in vivo*, thus suggesting the inhibition of ErbB4 as a possible therapeutic approach to activate apoptosis in MB cells.

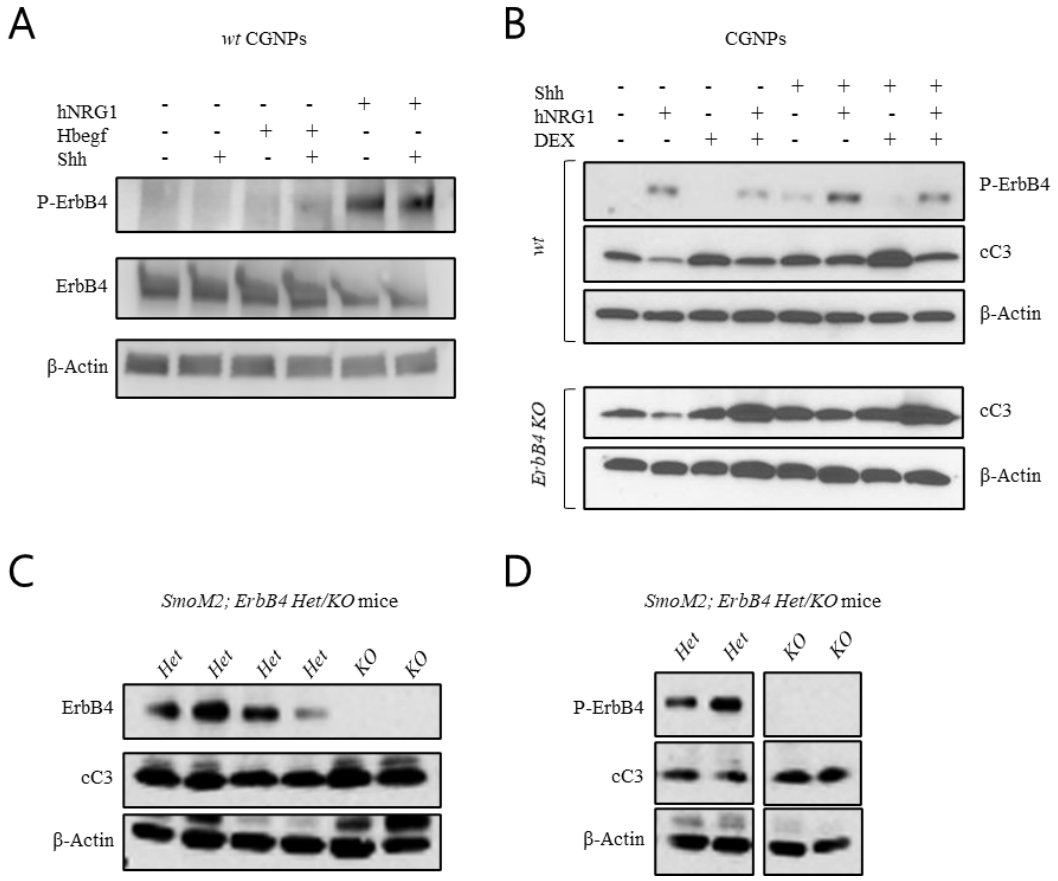

Figure R1-4. ErbB4 activation protects CGNPs and MB tumor cells from apoptosis. (**A**) Western Blot analysis of P-ErbB4, ErbB4 and β-Actin of CGNPs from p5 *wt* mice treated with the indicated compounds ($n \geq 3$). (**B**) Western Blot analysis of P-ErbB4, cC3 and β-Actin of CGNPs from *wt* and *ErbB4 KO* p5 mice treated with the appropriate compounds ($n \geq 3$). Western Blot analysis of P-ErbB4, cC3 and β-Actin obtained from (**C**) p15 and (**D**) p17 cerebellum from *SmoM2; ErbB4 Het* or *KO* mice ($n \geq 3$).

The higher expression that ERBB4 presents in Group 4 medulloblastomas is associated with poor clinical outcome

To investigate the ERBB4 impact on human MB progression, we analyzed the expression of *ERBB4* in different databases of human clinical biopsies from MB tumors. First, we investigated the expression of *ERBB4* in the four different established MB groups. The results obtained show that Group 4 MBs were the ones presenting the highest expression of *ERBB4* in all the analyzed databases [**Figure R1-5.A–D** and **Table R1-1.A-D**]. Moreover, we studied the expression of *ERBB4* in various human MB cell lines, detecting higher expression levels of this receptor in cells belonging to Group 4 (D283Med, D341Med, CHLA-01-Med, and CHLA-01R-Med) compared to DAOY and UW228 cell lines belonging to SHH subgroup [**Figure R1-6**].

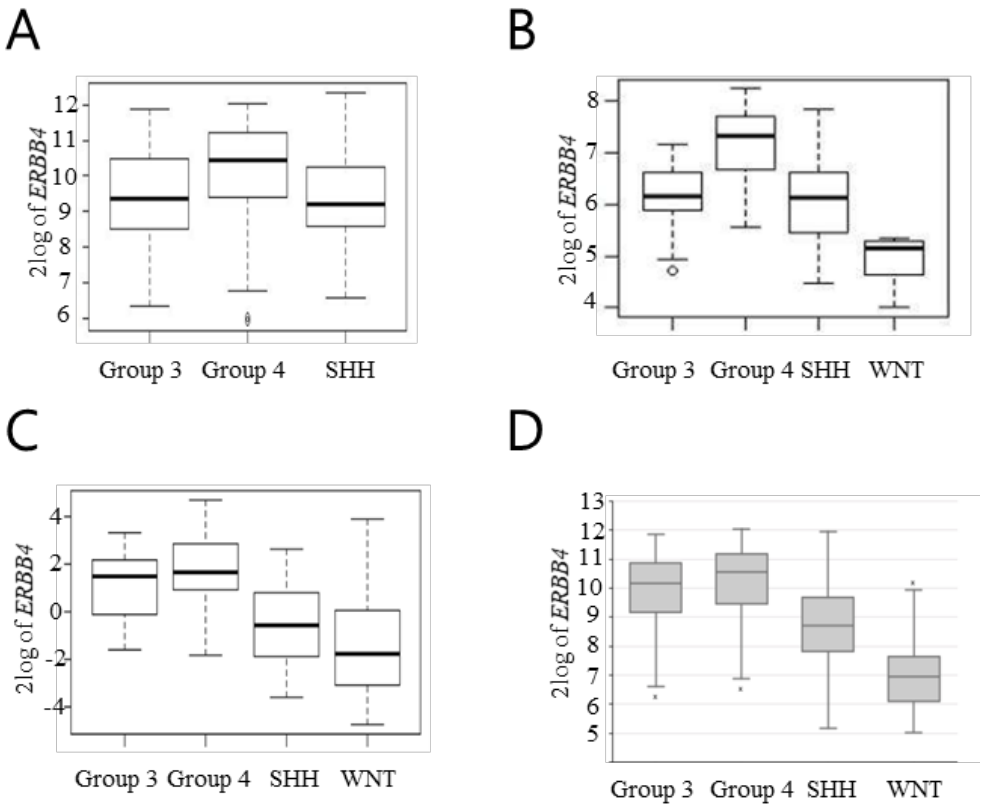

Figure R1-5. Group 4 MBs present high levels of *ERBB4*. Boxplot of the log2 of *ERBB4* expression in the indicated MB subgroups in (**A**) Northcott et al. (2012) cohort (*n* = 1087), (**B**) Robinson et al. (2012) cohort (*n* = 76), (**C**) Remke et al. (2011) cohort (*n* = 64), and (**D**) Cavalli et al. (2017) cohort (*n* = 612).

Table R1-1. p-values of the differences of *ERBB4* expression between the different MB subgroups in Northcott PA et al. 2012 cohort (n = 1087), Robinson G et al. 2012 cohort (n = 76), Remke M et al. 2011 cohort (n = 64) and Cavalli FMG et al. 2017 cohort (n = 612).

Northcott PA et al. 2012 (n = 1087)			
T test	**WNT**	**Group 3**	**Group 4**
SHH	-	N/S	1.67×10^{-6}
Group 3	N/S	-	8.76×10^{-5}
Group 4	1.67×10^{-6}	8.76×10^{-5}	-
Robinson G et al. 2012 (n = 76)			
T test	**WNT**	**SHH**	**Group 4**
WNT	-	0.0135	3.73×10^{-8}
SHH	0.0135	-	0.0017
Group 4	3.73×10^{-8}	0.0017	-
Remke M et al. 2011 (n = 64)			
T test	**WNT**	**SHH**	**Group 4**
WNT	-	N/S	9.84×10^{-5}
SHH	N/S	-	0.00017
Group 4	9.84×10^{-5}	0.00017	-

Cavalli FMG et al. 2017 (n = 612)				
T test	**WNT**	**SHH**	**Group 3**	**Group 4**
WNT	-	9.5×10^{-17}	1.7×10^{-34}	3.4×10^{-57}
SHH	9.5×10^{-17}	-	8.0×10^{-15}	4.2×10^{-35}
Group 3	1.7×10^{-34}	8.0×10^{-15}	-	9.8×10^{-3}
Group 4	3.4×10^{-57}	4.2×10^{-35}	9.8×10^{-3}	-

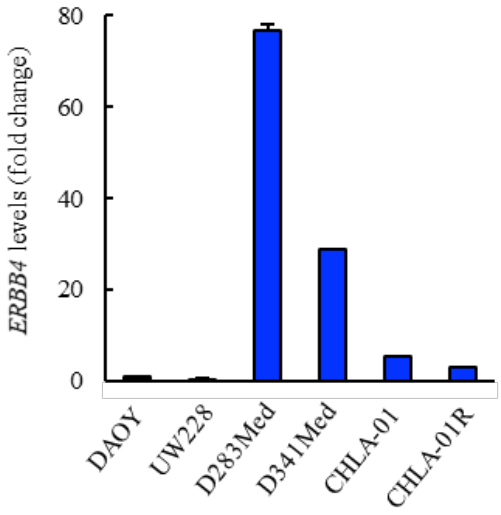

Figure R1-6. MB cell lines belonging to Group 4 express higher *ERBB4* levels. *ERBB4* mRNA expression levels in the indicated MB cell lines ($n \geq 3$).

Furthermore, we investigated the correlation between *ERBB4* expression levels and clinical characteristics of the patients in publicly available datasets of the Cavalli cohort. Strikingly, high *ERBB4* expression levels were associated with shorter overall survival in Group 4 MBs (*p-value* = 1.8×10^{-3}) [**Figure R1-7.A**]. Furthermore, high *ERBB4* expression levels were also associated with shorter overall survival when analyzing all the patients (*p-value* = 0.012) [**Figure R1-7.B**]. Taken all together, these results show that *ERBB4* expression correlates with poor prognosis in all MBs. Moreover, its expression is especially elevated in Group 4 samples, where its high levels could be a promising prognostic biomarker.

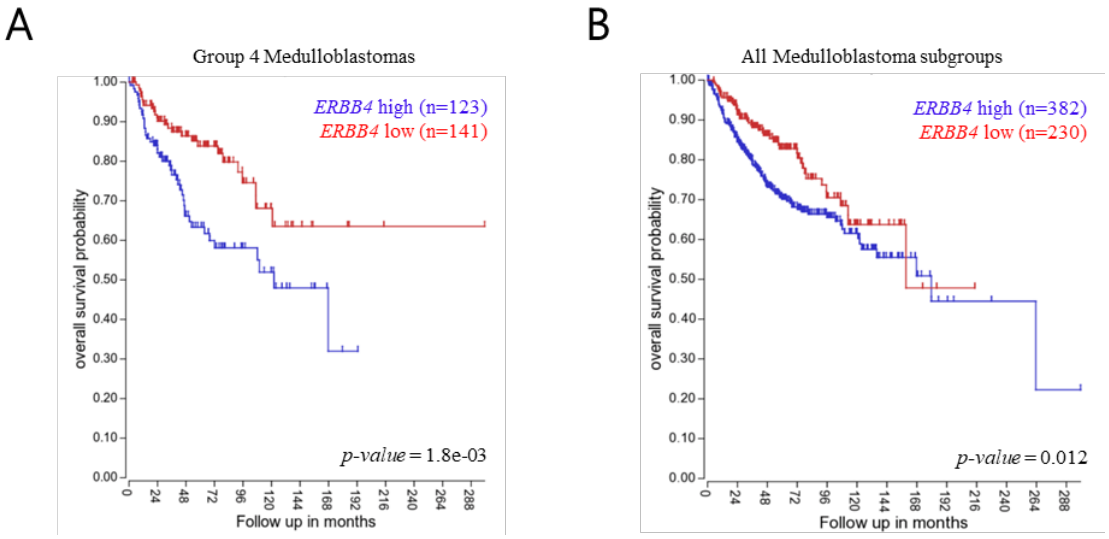

Figure R1-7. High *ERBB4* levels are associated with poor clinical outcome. Kaplan-Meier curves for the Cavalli et al (2017) cohort's (**A**) Group 4 patients' and (**B**) all patients' overall survival rates based on *ERBB4* expression obtained from hgserver1.

ERBB4 knock-down decreases cell viability and activates apoptosis in human medulloblastoma cells in vitro and in vivo

Next, we investigated whether ERBB4 plays a role in MB progression. To reach this goal, we knocked-down *ERBB4* expression in two human MB cell lines (DAOY and D283Med) with two independent short hairpin RNAs (shRNAs). First, we verified the effective inhibition of *ERBB4* by Western Blot and RT-qPCR analysis when using both *shERBB4* constructs (*sh2* and *sh3*) [**Figure R1-8.A-B**]. Functionally, this silencing promoted a significant decrease of more than 2-fold in cell growth rates in both MB cell lines measured by cell counting at different time points [**Figure R1-8.C-E**].

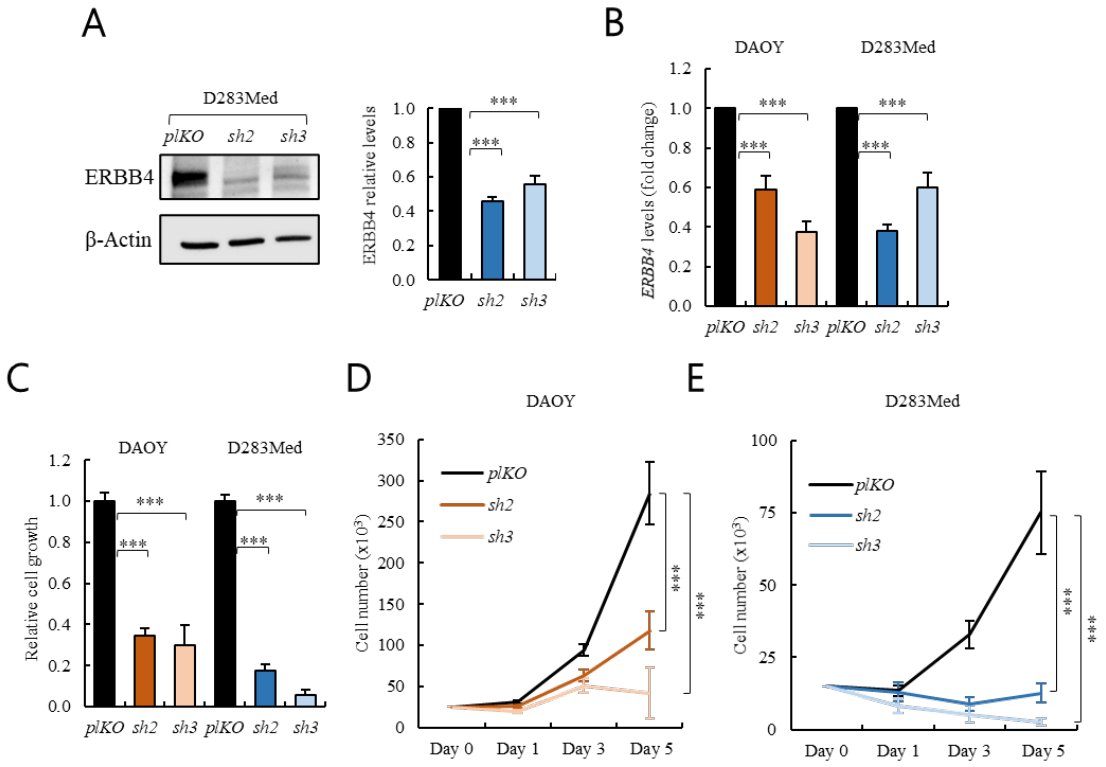

Figure R1-8. ***ERBB4*** **knock-down impairs MB cell growth** ***in vitro.*** (**A**) Representative image and quantification of Western Blot analysis of ERBB4 in control (*plKO)* and *shERBB4* (*sh2* and *sh3*) D283Med cells (n = 4). (**B**) *ERBB4* mRNA expression in control (*plKO)* and *shERBB4* (*sh2* and *sh3*) cells ($n \geq 9$). (**C**) Relative cell growth at day 5 comparing *plKO* with *sh2* and *sh3* cells ($n \geq 3$). *plKO*, *sh2* and *sh3* (**D**) DAOY and (**E**) D283Med cells number at day 1, 3 and 5 after seeding ($n \geq 3$).

To assess if the reduction observed in the cell number was related to an inhibition of proliferation or to a reduction of cell viability, we carried out MTT studies to assess cell viability and immunofluorescence assays to detect proliferative cells. In line with our previous results, MTT studies showed a diminished cell viability rate in *ERBB4* silenced DAOY and D283Med cells [**Figure R1-9.A**]. Nevertheless, these phenotypes did not seem to correlate with a reduction in proliferation, considering that the number of cells positive for the proliferative marker phospho-histone H3 (PHH3) was similar between the three conditions in DAOY cells [**Figure R1-9.B**]. Thus, we can conclude that *ERBB4* silencing impairs cell viability, but it does not stop cell cycle, and consequently cell proliferation.

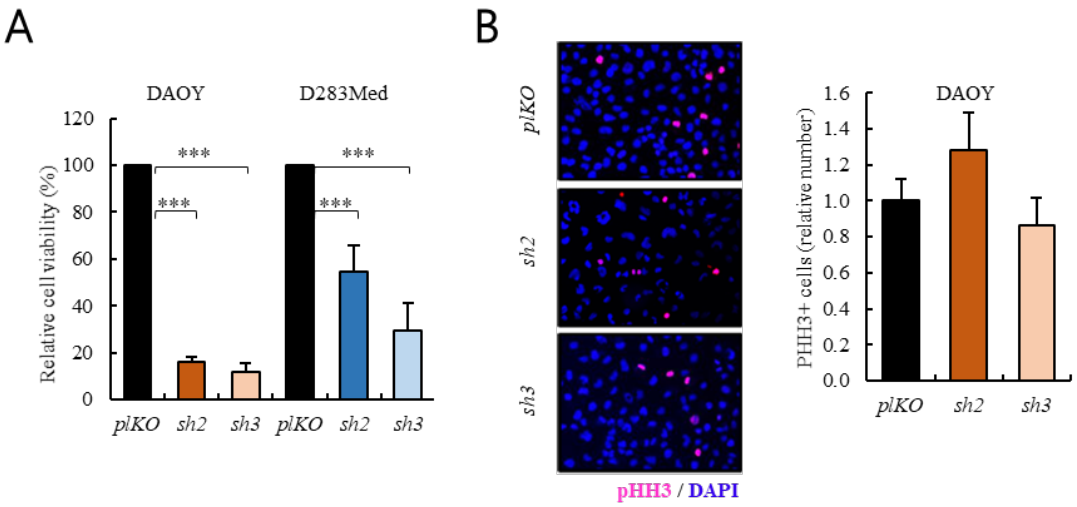

Figure R1-9. *ERBB4* knock-down impairs MB cell viability *in vitro*. (**A**) Cell viability assessment by MTT in *sh2* and *sh3* relative to *plKO* cells ($n \geq 6$). (**B**) Representative images and quantification of PHH3 positive cells in *sh2* and *sh3* relative to *plKO* DAOY cells ($n \geq 3$).

To clarify the origin of the decreased cell viability but not of cell proliferation, we performed a cell cycle assay. This assay is based on quantifying the cells' number in each cell cycle phase, thus providing the information about the cell cycle status in each experimental condition. The results showed an increase in subG0/G1 in *ERBB4* knock-down cells comparing to control cells [**Figure R1-10.A-B**], suggesting an increased cell death of these MB cells when knocking-down *ERBB4*. We confirmed this increase in the apoptosis by quantifying the number of cells positive for both cC3 and Annexin-V apoptotic markers. We found an elevated number of positive cells for the both markers in DAOY and D283Med *sh2* and *sh3* cells comparing to *plKO* experimental condition [**Figure R1-10.C-E**].

Finally, we also investigated the role of *ERBB4* in the MB cell migration ability. We observed that *ERBB4* knock-down resulted in a significant decrease in the migration potential of DAOY MB cells [**Figure R1-10.D**].

Altogether, these results further highlight the relevance of ERBB4 in maintaining critical cellular phenotypes, mainly apoptosis and migration, during homeostasis and pathological conditions.

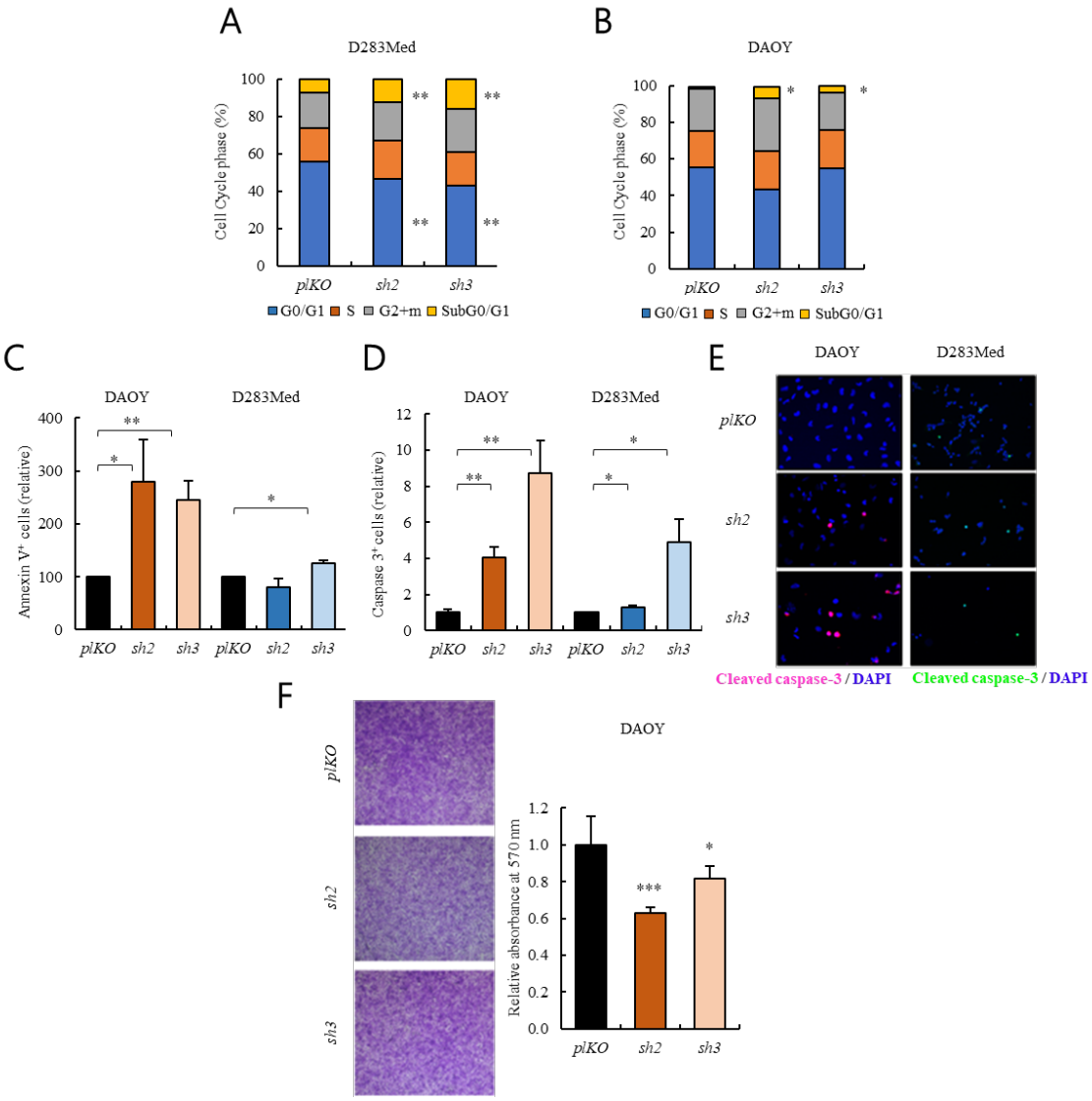

Figure R1-10. *ERBB4* knock-down increases apoptosis of MB cells *in vitro*. Cell cycle assay measuring the number of cells in each cell cycle phase in *plKO, sh2* and *sh3* (**A**) D283Med and (**B**) DAOY cells ($n \geq 3$). (**C**) Percentage of Annexin-V positive cells in *plKO, sh2* and *sh3* DAOY and D283Med cells ($n \geq 3$). (**D**) Immunofluorescence quantification of cC3 positive cells in *sh2* and *sh3* relative to *plKO* DAOY and D283Med cells ($n \geq 4$). (**E**) Representative immunofluorescence images of cC3 positive cells in *plKO*, *sh2* and *sh3* DAOY and D283Med cells ($n \geq 4$). (**F**) Representative images and quantification of the migration assay in DAOY cells ($n \geq 3$).

Next, we wanted to extend the results obtained *in vitro* to determine whether ERBB4 could regulate tumor growth *in vivo.* For this aim, we injected *sh2* and *sh3* DAOY and D283Med cells subcutaneously in immunocompromised mice. Interestingly, we observed a significant decrease of *shERBB4* DAOY and D283Med cells tumor growth of over 70 %, especially with *sh3* experimental condition, which did not form tumors in D283Med cells [**Figure R1-11.A-B**]. To validate these results, the weight of generated

tumors was measured, showing a lower weight for tumors generated from knocked-down cells than for tumors generated from control cells [**Figure R1-11.A-C**]. Moreover, tumors molecular analysis by immunohistochemistry revealed increased apoptosis, characterized by higher cC3 positive cells, and decreased proliferation, since they presented lower KI67 positive cells, in *sh2* DAOY and D283Med cells [**Figure R1-11.D-E**]. Taken together, all these results showed that ERBB4 is required for MB cell survival and, thus, tumor progression.

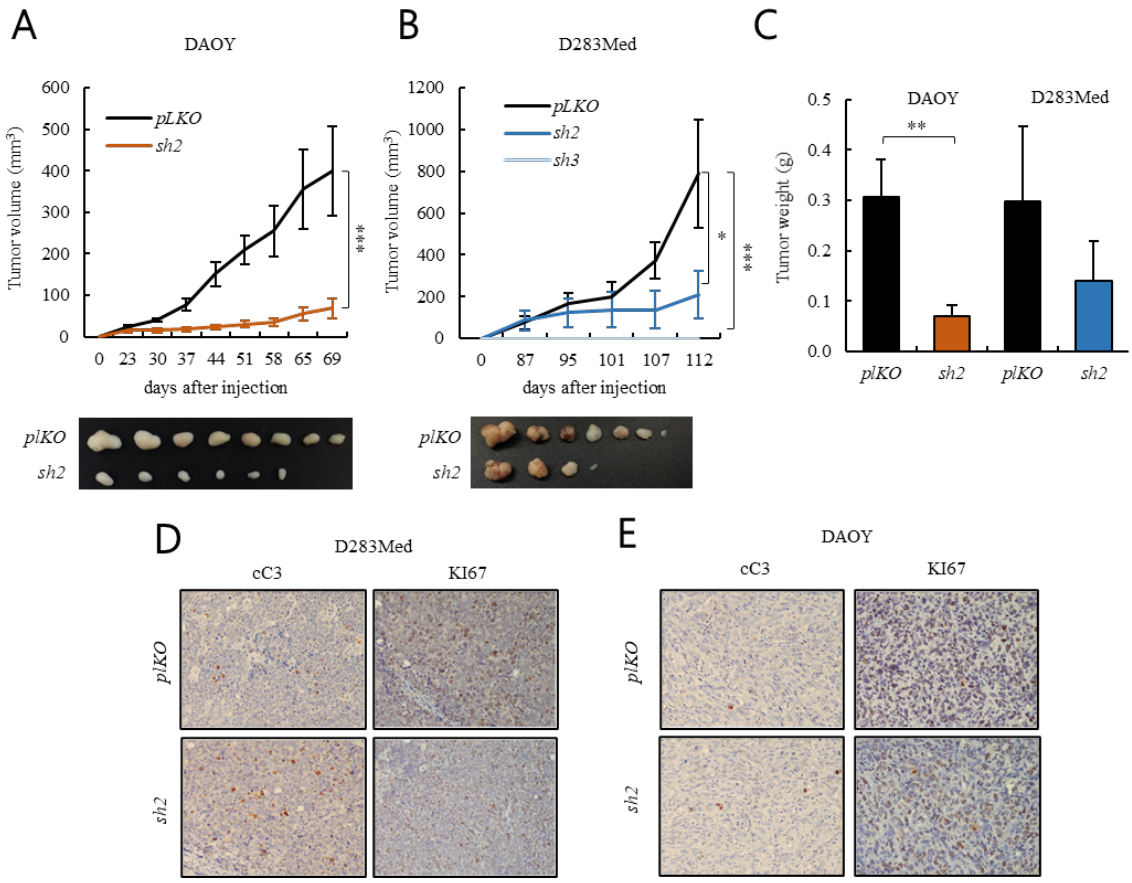

Figure R1-11. *ERBB4* knock-down reduces tumor progression *in vivo*. Volume of tumors generated after subcutaneous injection of (**A**) DAOY and (**B**) D283Med *plKO*, *sh2* and *sh3* cells ($n \geq 8$) at the indicated time points. (**C**) Quantification of tumors' weight generated after subcutaneous injection of DAOY and D283Med *pLKO* and *sh2* cells (n = 8). Representative images of the immunohistochemical staining of cC3 and KI67 in tumors generated after subcutaneous injection of (**D**) DAOY and (**E**) D283Med *pLKO* and *sh2* cells ($n \geq 3$).

ERBB4 is highly expressed in MBSCs and its knock-down inhibits stem cells activity

With the aim of investigating the role of ERBB4 in MBSCs, we cultured DAOY and UW228 MB cell lines (with low endogenous levels of *ERBB4*) and D283Med and D341Med cell lines (with high expression of *ERBB4*) in the presence of serum and in stem cell specific media to induce oncospheres formation. First, we verified whether the stem cell specific culture condition increased the expression of some of the well-established MBSC markers: *CD133*, *Fucosyltransferase 4 (FUT4)*, *SOX2* and *NESTIN* (Read et al., 2009; Singh et al., 2003; Vanner et al., 2014). RT-qPCR and Western Blot analysis demonstrated that in all cell lines, the cells cultured as oncospheres presented higher levels of these MBSC markers compared to the expression of MB cell lines cultured in the presence of serum [Figure R1-12.A-C]. Interestingly, we observed that oncospheres formed from DAOY and UW228 cell lines showed higher expression levels of *ERBB4* than cells cultured in the presence of serum [Figure R1-12.C-D].

To further analyze the relation between *ERBB4* and MBSC markers expression, we performed a correlation analysis of *ERBB4* gene expression with *CD133* and *FUT4* genes expression in all human MB cell lines. The results showed a positive correlation between *ERBB4* and both MBSC markers' expression [Figure R1-12.E-F], thereby linking *ERBB4* high levels expression to MBSCs activity.

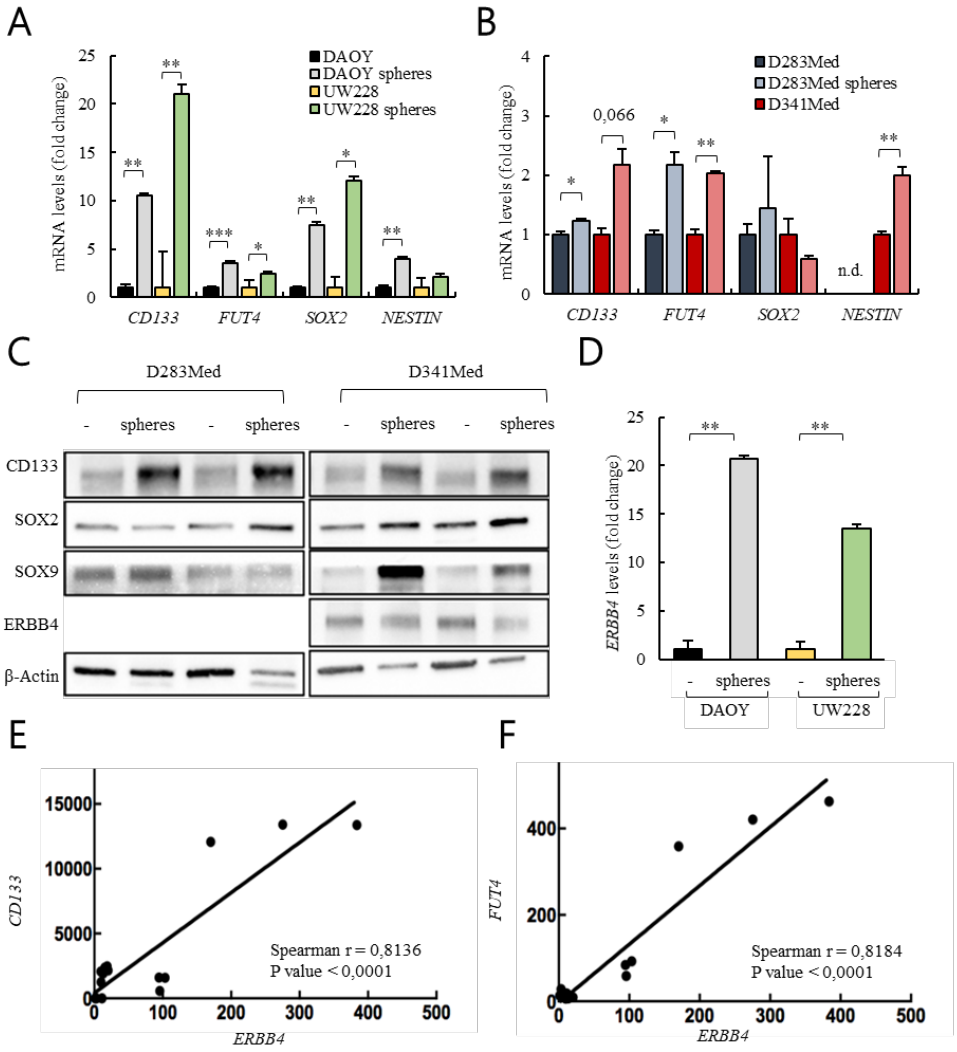

Figure R1-12. *ERBB4* is overexpressed in MBSCs. (**A**) mRNA levels of the indicated stem cell markers of DAOY and UW228 cells grown in serum or in stem cell media as oncospheres ($n \geq 3$). (**B**) mRNA levels of the indicated stem cell markers of D283Med or D341Med cells grown in serum or in stem cell media as spheres ($n \geq 3$). (**C**) Western Blot analysis of the indicated proteins in protein extracts of cells grown in serum (D283Med or D341Med) or in stem cell media as oncospheres ($n \geq 3$). (**D**) *ERBB4* mRNA expression levels of DAOY and UW228 cells grown in serum and stem cell media ($n \geq 3$). Correlation between (**E**) *CD133* and (**F**) *FUT4* expression levels with *ERBB4* expression levels in different MB cell lines (DAOY, UW228, D283Med, D341Med, CHLA-01-Med, and CHLA-01R-Med) ($n \geq 3$).

To directly explore the role of ERBB4 in the MBSCs activity, we cultured DAOY and D283Med cells with *ERBB4* knock-down in stem cell specific media allowing them to form oncospheres, and then we quantified the number of oncospheres formed. The results showed a marked decrease in the ability of the cells with *ERBB4* knocked-down to form oncospheres, both in DAOY and D283Med cells [**Figure R1-13.A**]. Moreover, we measured the ability to form secondary oncospheres, by disaggregating the primary oncospheres and seeding them again. We found that the ability to form secondary oncospheres was

also significantly impaired in *sh2* and *sh3* DAOY MB cells [**Figure R1-13.B**]. In line with these results, *ERBB4* silencing significantly decreased the ability of colony formation [**Figure R1-13.C**]. Altogether, these results suggest that ERBB4 has an important role in the maintenance of MBSCs.

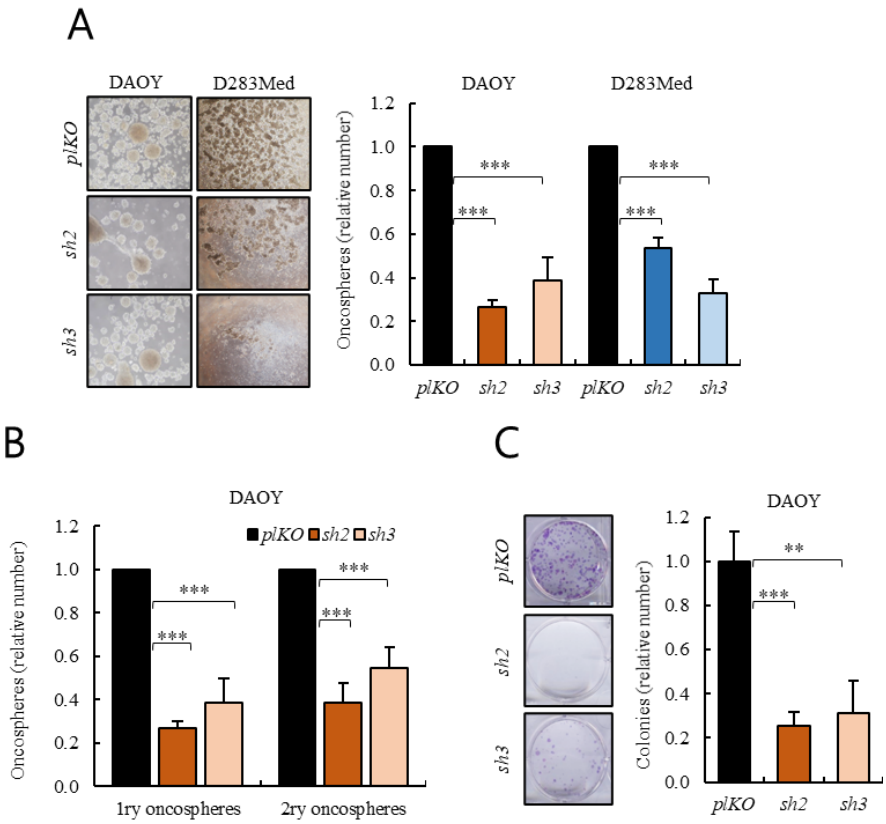

Figure R1-13. ***ERBB4* expression regulates MB stem cell (MBSC) activity *in vitro*.** (**A**) Representative images and quantification of the oncospheres' number formed from the indicated conditions in DAOY and D283Med cells ($n \geq 4$). (**B**) Quantification of the number of 1ry and 2ry oncospheres formed from *plKO*, *sh2* and *sh3* DAOY cells ($n \geq 3$). (**C**) Representative images and quantification of the colonies' number formed from the indicated conditions in DAOY cells ($n \geq 3$).

With the objective to further characterize the impact of ERBB4 in MBSCs activity, we moved to *in vivo* experiments. We injected limited dilution concentrations of knocked-down *ERBB4* DAOY and D283Med cells subcutaneously in immunocompromised mice. Strikingly, the frequency of tumor initiation in DAOY cells was 1 in 475,710 and 1 in 946,994 in *sh2* and *sh3* cells, respectively, compared to 1 in 99,524 in the control cells [**Figure R1-14.A,C**]. Moreover, the tumor initiation in D283Med cells was 1 in 1,649,864 and infinite in *sh2* and *sh3* cells, respectively, compared to 1 in 441,838 in the empty vector harboring cells [**Figure R1-14.B,D**]. These differences in stem cell frequenciy

between the tested experimental conditions were all statistically significant. These results confirm that *ERBB4* inhibition limits tumor initiation and reveal its essential role in MBSCs activity.

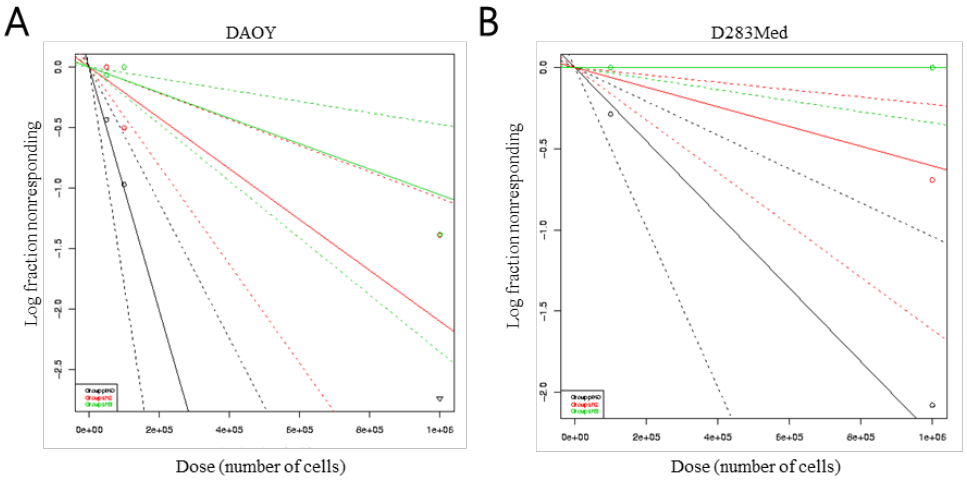

C

DAOY

Confidence intervals for 1/(stem cell frequency)			
Group	Lower	Estimate	Upper
plKO	178331	99524	55543
sh2	923105	475710	245151
sh3	2112051	946994	424610

D

D283Med

Confidence intervals for 1/(stem cell frequency)			
Group	Lower	Estimate	Upper
plKO	960525	441838	203244
sh2	4397369	1649864	619018
sh3	Inf	Inf	2937513

Figure R1-14. *ERBB4* expression regulates MBSC activity *in vivo*. (**A**) Frequency of tumor initiation after subcutaneous injection of 1 x 10^6, 1 x 10^5 and 5 x 10^4 DAOY cells transduced with *plKO, sh2* and *sh3* in nude mice. (**B**) Frequency of tumor initiation after subcutaneous injection of 1 x 10^6 and 1 x 10^5 D283Med cells transduced with *plKO, sh2* and *sh3* in nude mice. The incidence of tumor initiation was measured using ELDA platform (black line represents *plKO* condition, red line represents *sh2,* and green line represents *sh3*). Number of stem cells needed to initiate a tumor in the indicated conditions with (**C**) DAOY and (**D**) D283Med cells.

ERBB4 knock-down alters multiple processes and pathways in medulloblastoma cells

Finally, we wanted to investigate the pathways from which ERBB4 is acting in MB cells to promote a tumorigenic activity. In order to identify the pathways altered when knocking-down *ERBB4* expression, we carried out a transcriptomic analysis of *plKO*, *sh2*, and *sh3* DAOY cells. We found that in *sh2* DAOY cells, 293 genes were upregulated whereas 395 genes were downregulated. Regarding *sh3* DAOY cells, 724 genes appeared upregulated whereas 997 genes were downregulated. All the identified genes presented

a *p-value* lower than 0.05 and a fold-change higher than 2. After identifying the altered genes in each *shERBB4*, we sorted out the common genes for both shRNAs, and found 179 genes upregulated and 297 downregulated. These common genes were further selected and used to perform a gene enrichment analysis with the Gene Ontology (GO) gene sets, considering biological processes. The results obtained in this gene enrichment analysis were consistent with our functional studies previously performed, since processes such as cell motility, morphogenesis, development, cell growth and proliferation, and cell signaling were downregulated when knocking-down *ERBB4* [**Figure R1-15.A**]. On the contrary, cell death and response to stimulus processes were increased [**Figure R1-15.B**].

Among the identified common genes, lower expression levels of stem cell markers such as *CD133*, *Doublecortin like kinase 1 (DCLK1)*, *LIN7*, *SRY-box 4 (SOX4)*, *SERPINE3*, or *Tumor protein P63 (TP63)*; genes involved in motility-related pathways such as *Paired related homeobox 1 (PRRX1)*, *Matrix metallopeptidase 7 (MMP7)*, or *Claudin*; genes related to cell signaling as *FOS* or *JUN*; or cancer-related genes such as *K-RAS* were detected in *shERBB4* cells compared to *plKO* cells. On the other hand, genes related to cell differentiation (*Fibroblast growth factor 5; FGF5*), cell apoptosis (*Amyloid beta precursor protein binding family B member 2 (APBB2)*, *Ankyrin repeat domain 1 (ANKRD1)*, *Placenta associated 8 (PLAC8)*), response to stress (*H2A histone family member X (H2AFX)*, *SERPINE1*, *Cadherin 13 (CDH13)*, *Vascular endothelial growth factor A (VEGFA)*) and cell cycle and division (*CDK6*, *Cyclin dependent kinase 15 (CDK15)*, *Cyclin D1 (CCND1)*, *E2F transcription factor 7 (E2F7)*, *Cell division cycle 25A (CDC25a)*) displayed a higher expression in knocked-down cells.

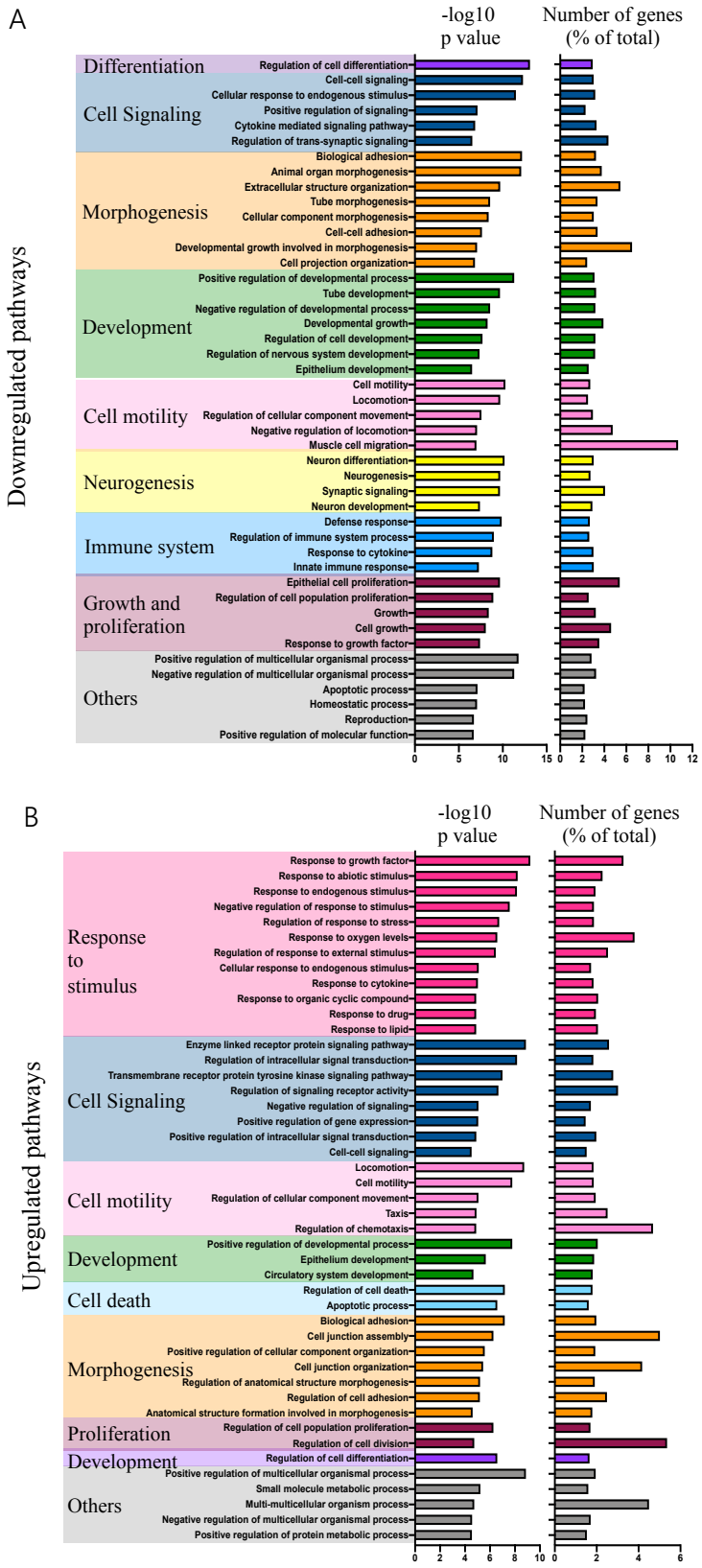

Figure R1-15. *ERBB4* knock-down alters multiple pathways of MB cells. (**A**) Downregulated and (**B**) upregulated pathways in *sh2* and *sh3* DAOY cells compared with *plKO* cells when performing a GO gene set biological processes analysis from Clariom S microarray results. The *p-value* and the percentage of genes deregulated in each pathway are represented in the figure.

Moreover, we also performed a gene enrichment analysis but, in this case, based on hallmark gene sets. The results showed alterations in genes' expression related to cell cycle or stress response, thus finding a good correlation between both datasets that reinforce the GO gene sets analyses' results. Furthermore, the data also revealed dysregulation in inflammation- or metabolism-related pathways [**Figure R1-16.A-B**]. Indeed, we observed a decreased expression of genes or inflammation markers such as *Signal transducer and activator of transcription 3 (STAT3)*, *Oncostatin M receptor (OSMR)*, *Interleukin 1 receptor type 1 (IL1R1)*, *Interleukin 18 receptor 1 (IL18R1)*, *C-X-C motif chemokine ligand 16 (CXCL16)*, *Interferon induced transmembrane protein 1 (IFITM1)*, *Suppresor of cytokine signaling 2 (SOCS2)*, and *Matrix gla protein (MGP)*, whilst we found an elevated expression of *Interleukin 1 alpha (IL1α)*, *Interleukin 7 receptor (IL7R)* and *Signal transducer and activator of transcription 5B (STAT5B)* among others, or *Phosphofructokinase Platelet (PFKP)* related to metabolism, in cells with *ERBB4* knock-down.

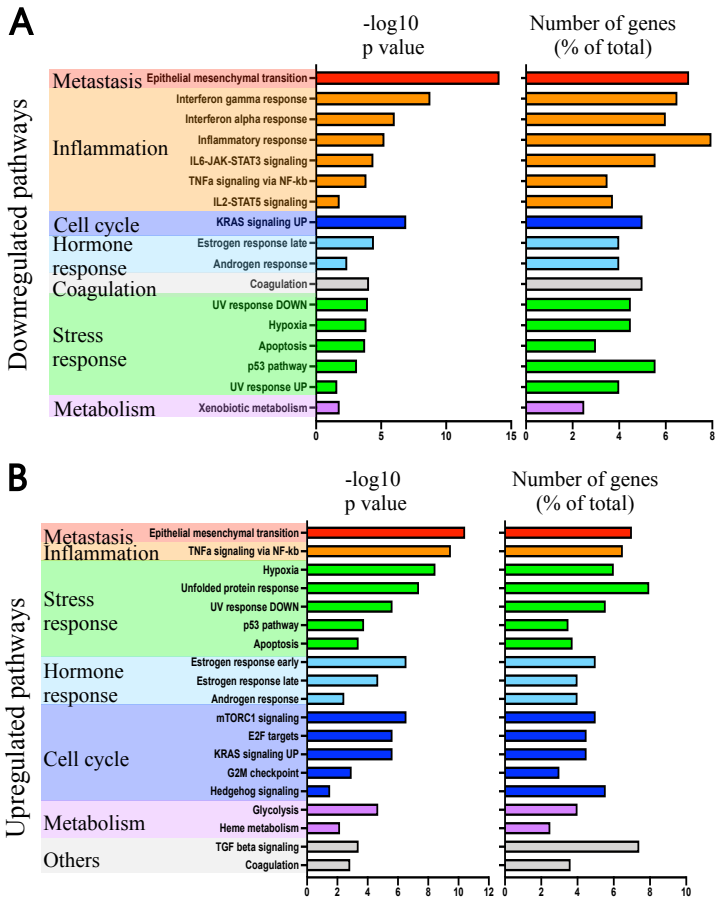

Figure R1-16. *ERBB4* knock-down alters multiple pathways of MB cells. (**A**) Downregulated and (**B**) upregulated pathways in *sh2* and *sh3* DAOY cells compared with *plKO* cells when performing a hallmark gene set analysis from Clariom S microarray results. The *p-value* and the percentage of genes deregulated in each pathway are represented in the figures.

Next, based on the literature, we moved our attention to genes that had been already related to MB. We validated in DAOY and D283Med cells some of the downregulated genes, such as *Periostin (POSTN)* (Zhu et al., 2019), *BOC* (Mille et al., 2014), *Vascular cell adhesion molecule 1 (VCAM1)* (Liang et al., 2015), and *TP63* (Forster et al., 2014) as well as some of the upregulated ones, such as *ANKRD1* (Jimenez et al., 2017), *Thrombospondin 1 (THBS1)* (Zhou et al., 2010), *NRG1* (Gilbertson et al., 1998), *PTHLH* (Katoh and Katoh, 2009), and *HBEGF* [**Figure R1-17.A-C**]. Altogether, these analyses revealed the underlying molecular mechanisms of ERBB4 activity in MB cells.

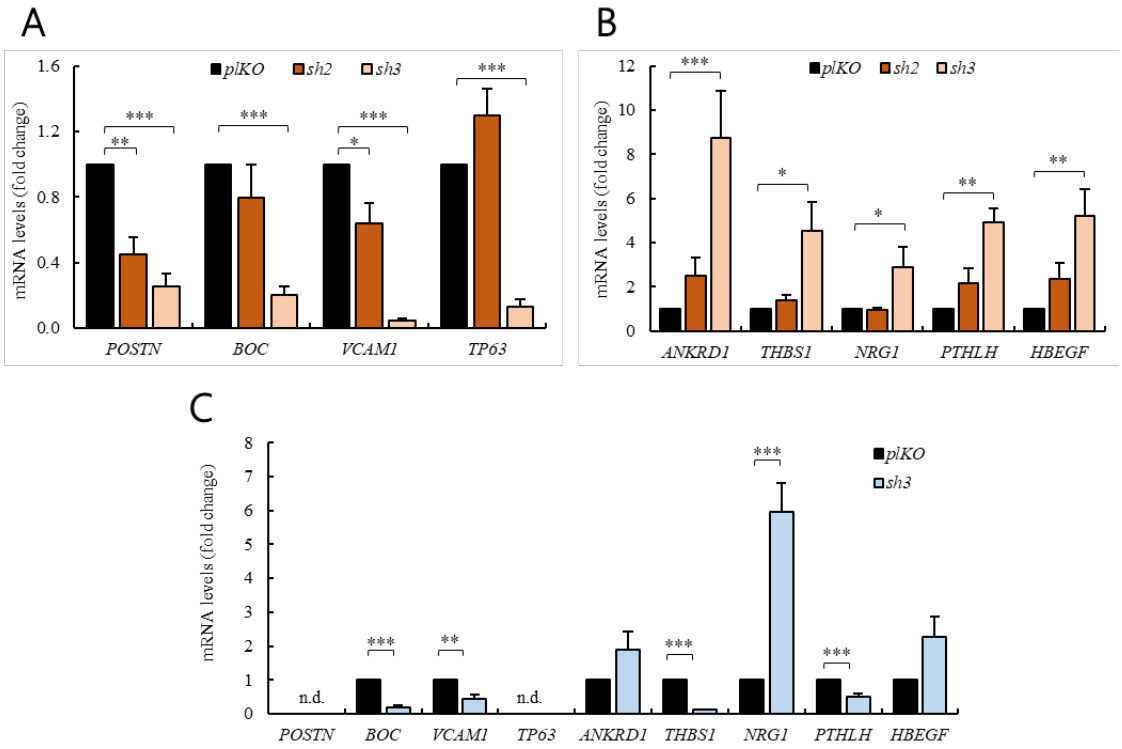

Figure R1-17. *ERBB4* knock-down alters multiple pathways of MB cells. mRNA levels of (**A**) downregulated and (**B**) upregulated genes in control (*plKO*) and *shERBB4* (*sh2* and *sh3*) DAOY cells ($n \geq 3$). (**C**) mRNA levels of downregulated and upregulated genes in *plKO* and *sh3* D283Med cells ($n \geq 3$).

To characterize the impact of the identified pathways and genes in MB and their relation with ERBB4, we moved to clinical samples. First, we completed a correlation study between the expression of *ERBB4* and the validated genes, taking advantage of the publicly available Cavalli FMG et al. (2017) cohort. We considered only Group 4 patients' data. The results showed a statistically significant positive correlation between *ERBB4* and two genes (*BOC* and *TP63*) found to be downregulated when knocking-down *ERBB4* [**Figure R1-18.A**]. We found also a statistically significant negative correlation between *ERBB4* and all of the genes that shown to be upregulated when *ERBB4* was knocked-down. Three of them (*THBS1*, *NRG1*, and *PTHLH*) showed statistically significance [**Figure R1-18.B**].

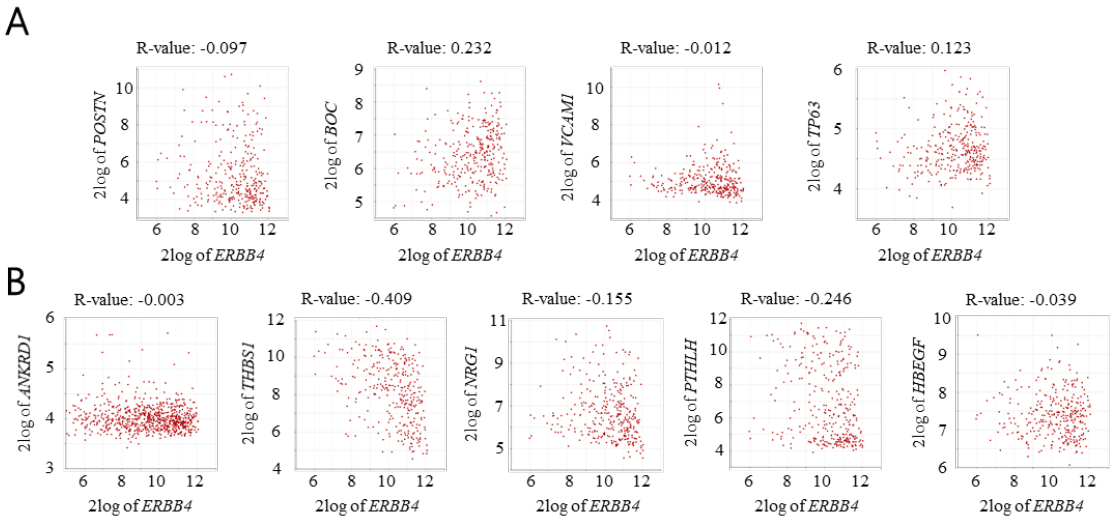

Figure R1-18. Correlation between *ERBB4* and ERBB4 downstream genes' expression in human samples of Group 4 MBs. Correlation analysis of (**A**) downregulated (*POSTN p-value* = 0.079, *BOC p-value* = 2.38 x 10^{-5}, *VCAM1 p-value* = 0.835, and *TP63 p-value* = 0.027) and (**B**) upregulated (*ANKRD1 p-value* = 0.955, *THBS1 p-value* = 1.48 x 10^{-14}, *NRG1 p-value* = 5.17 x 10^{-3}, *PTHLH p-value* = 6.91 x 10^{-6}, and *HBEGF p-value* = 0.482) genes with *ERBB4* expression for Cavalli cohort Group 4 patients' (*n* = 326) data. All results were obtained from hgserver1.

Afterwards, we performed the same analysis, but in this case, considering all patients' data from the same cohort. The results were not as consistent as the ones acquired when analyzing only the data of the patients belonging to the Group 4 [**Figure R1-19.A-B**]. Thus, these results reinforce the relation between these genes and *ERBB4* expression, especially in the Group 4 MBs.

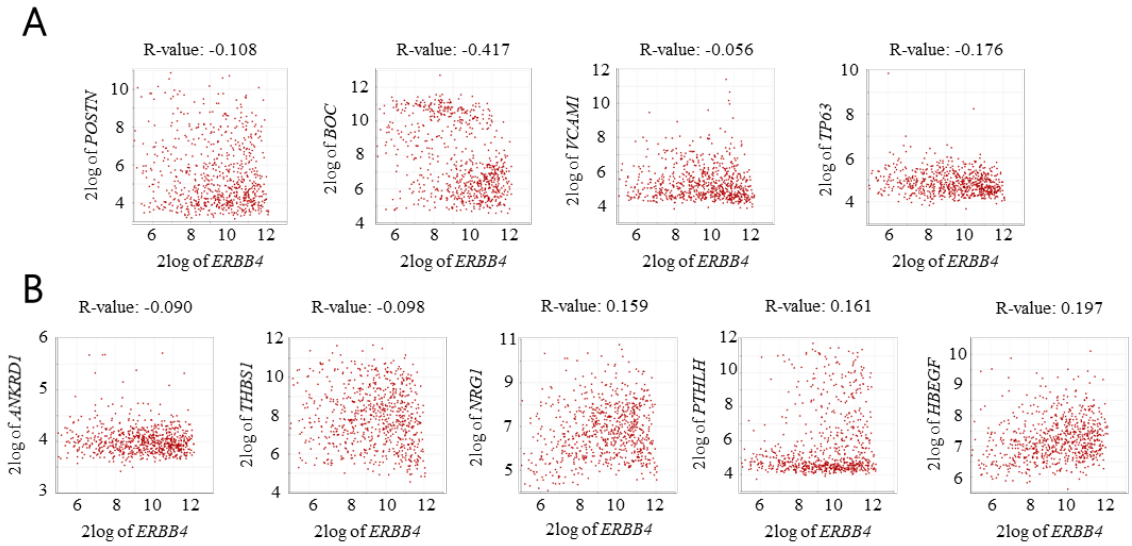

Figure R1-19. Correlation between *ERBB4* and ERBB4 downstream genes' expression in human samples of MB. Correlation analysis of (**A**) downregulated (*POSTN p-value* = 2.91 x 10^{-3}, *BOC p-value* = 2.08 x 10^{-33}, *VCAM1 p-value* = 0.121, and *TP63 p-value* = 9.54 x 10^{-7}) and (**B**) upregulated (*ANKRD1 p-value* = 0.013, *THBS1 p-value* = 6.78 x 10^{-3}, *NRG1 p-value* = 1.07 x 10^{-5}, *PTHLH p-value* = 7.95 x 10^{-6}, and *HBEGF p-value* = 3.95 x 10^{-8}) genes with *ERBB4* expression for Cavalli FMG et al. 2017 cohort's all patients' (*n* = 612) data. All results were obtained from hgserver1.

After these two studies, we analyzed the expression of the selected genes in the different subgroups using the information of all patients from the same cohort. We found that three of the downregulated genes (*BOC*, *VCAM1*, and *TP63*) followed the same pattern as *ERBB4* and showed a higher expression in Group 4 MBs [**Figure R1-20.A-B**].

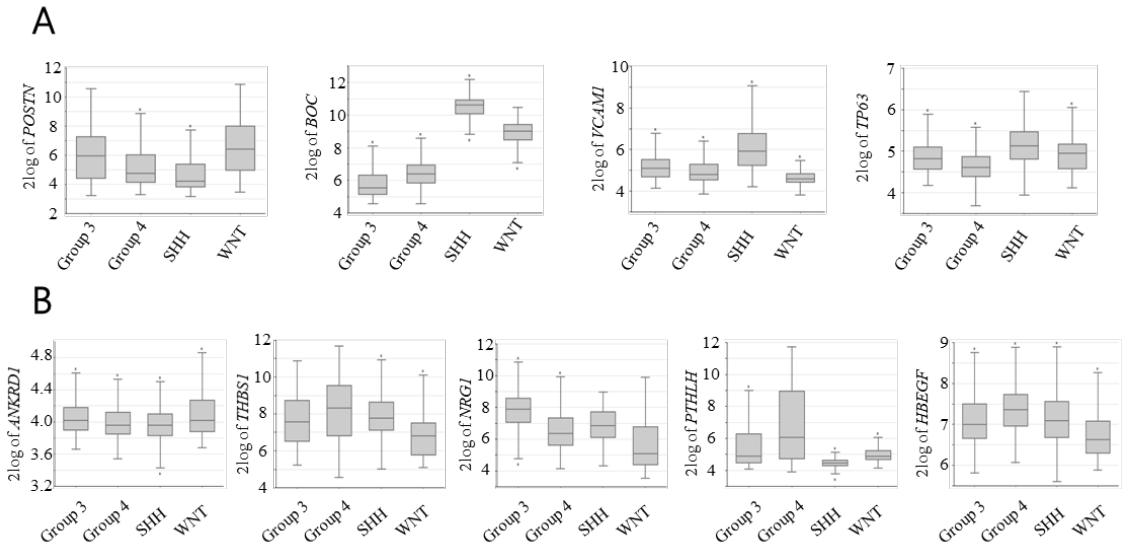

Figure R1-20. Expression of ERBB4 downstream genes in human samples of MB. Boxplot of the log2 of (**A**) downregulated and (**B**) upregulated genes in the indicated MB subgroups in Cavalli cohort (*n* = 612). All results were obtained from hgserver1.

Finally, we performed a correlation analysis between the expression of the genes selected from the microarray and patient outcome. We found that altered *VCAM1*, *TP63*, *ANKRD1*, *THBS1*, and *PTHLH* expression levels significantly correlated with lower patient survival in Group 4 MB samples [**Figure R1-21.A-B**]. Moreover, we carried out the same analysis in all MB subgroups. The results showed an elevated *ANKRD1* and *NRG1* expression that correlated with lower patient survival [**Figure R1-22.A-B**].

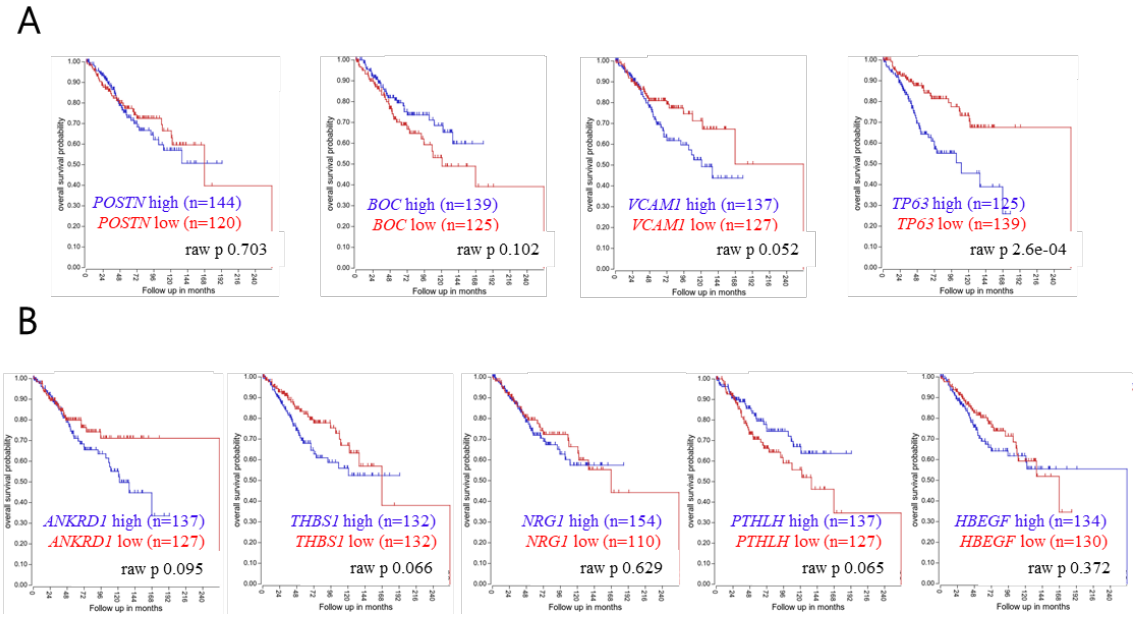

Figure R1-21. Clinical impact of ERBB4 downstream genes in MB human samples. Kaplan-Meier curves for the Cavalli cohort Group 4 patients' overall survival rates based on (**A**) downregulated and (**B**) upregulated expression (*p-values* are indicated in each graph). All results were obtained from hgserver1.

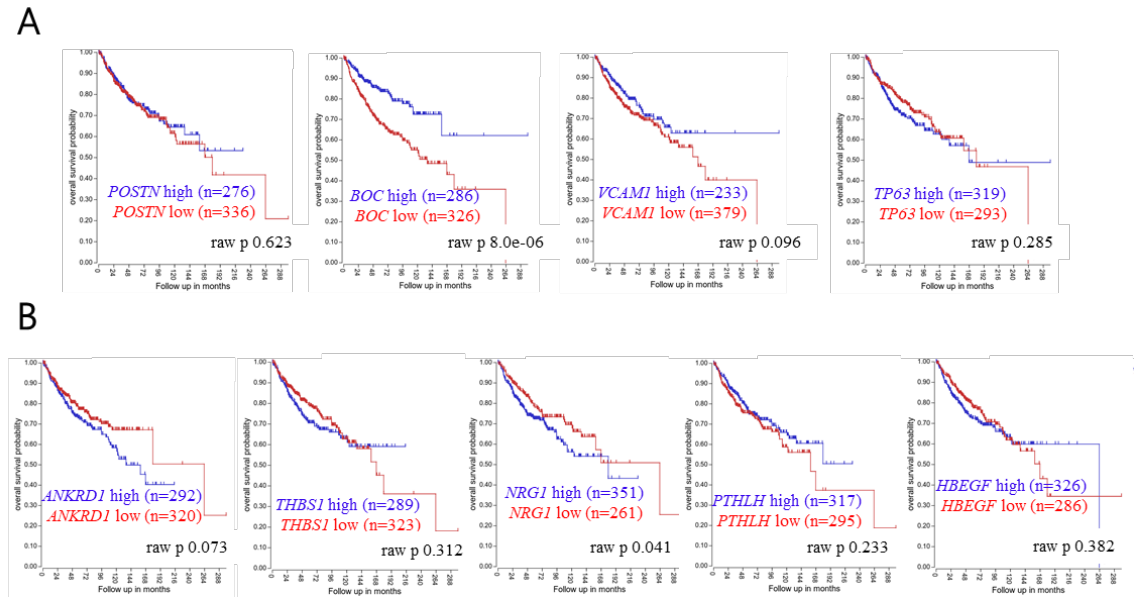

Figure R1-22. Clinical impact of ERBB4 downstream genes in Group 4 MB human samples. Kaplan–Meier curves for the Cavalli cohort's all patients' overall survival rates based on (**A**) downregulated and (**B**) upregulated genes (*p-values* are indicated in each graph). All results were obtained from hgserver1.

All these results further extend the findings obtained *in vitro* to clinical samples *in vivo*, and reveal various promising genes and pathways that seem to be related to ERBB4 activity and involved in MB progression.

CHAPTER 2

High SOX1 expression is a hallmark of SHH medulloblastomas and its inhibition depletes tumor malignancy

High SOX1 expression levels are associated with poor clinical outcome in medulloblastoma

First in this section, we wanted to analyze the function and impact of SOX1 transcription factor in MB. For this aim, we analyzed *SOX1* expression in publicly available databases of human MB clinical biopsies (Cavalli et al., 2017; Northcott et al., 2017). First, we compared the *SOX1* expression levels in the different groups of MB. We found that SHH MBs present the highest *SOX1* expression levels in the two analyzed cohorts [**Figure R2-1.A-D**]. We also investigated SOX1 protein levels in the different MB cell lines available in the laboratory, finding that cells belonging to SHH subgroup MBs presented higher levels of SOX1 than cells belonging to Group 3 or 4 [**Figure R2-1.E**].

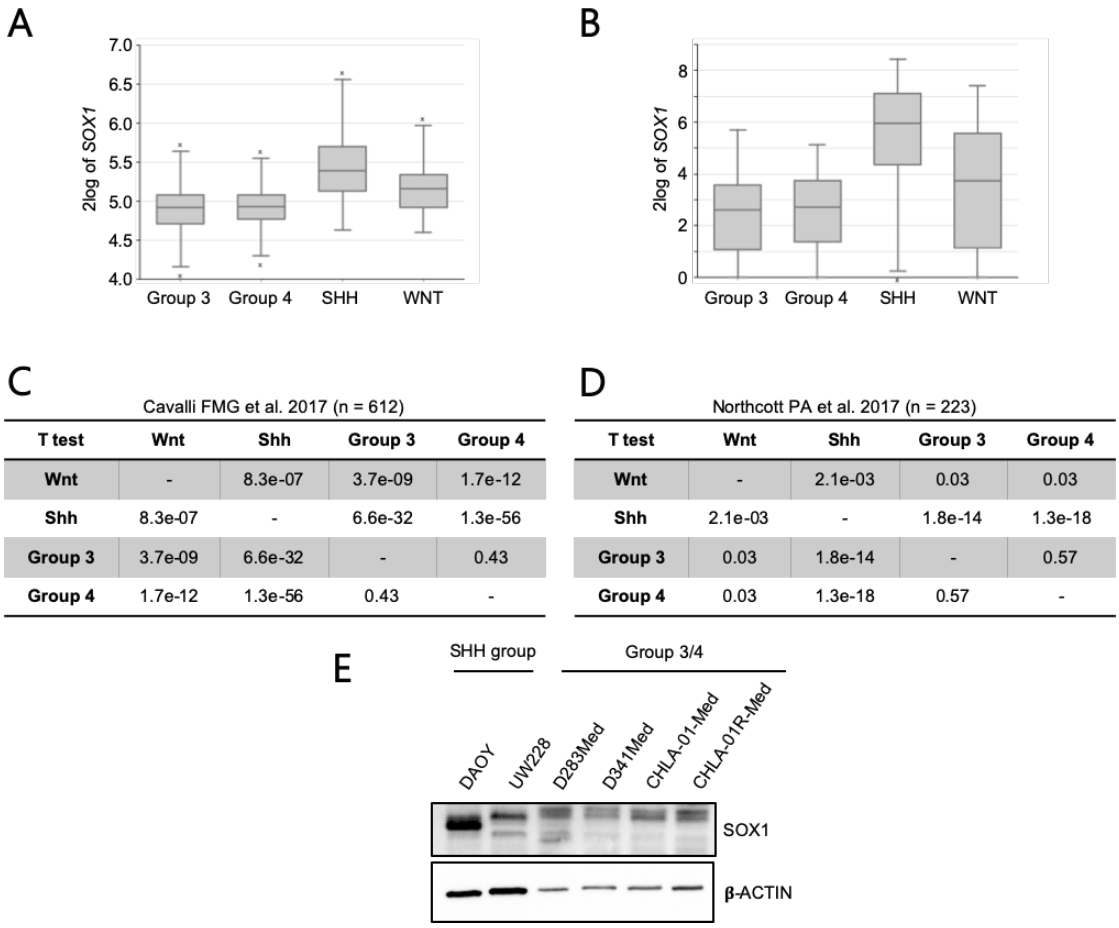

Figure R2-1. High levels of *SOX1* are found in SHH MBs. Boxplot of the log2 of *SOX1* in the indicated MB subgroups (**A**) Cavalli FMG et al. 2017 cohort (*n* = 612) and (**B**) Northcott PA et al. 2017 cohort (*n* = 223). *P-values* of the differences in *SOX1* expression in the indicated MB subgroups of (**C**) Cavalli FMG et al. 2017 cohort (*n* = 612) and (**D**) Northcott PA et al. 2017 cohort (*n* = 223). (**E**) Western Blot analysis of SOX1 protein in SHH subgroup cell lines (DAOY and UW228) and in Group 3 or 4 cell lines (D283Med, D341Med, CHLA-01-Med and CHLA-01R-Med).

Second, we investigated the correlation of patients' survival with *SOX1* expression levels in the Cavalli cohort, by considering all MB patients' and SHH group MBs data. Interestingly, we found that high *SOX1* expression levels were associated with a worse clinical outcome in SHH MBs (*p-value* = 0.018) [**Figure R2-2.A**], but this correlation was not maintained when analyzing all MB groups together (*p-value* = 0.352) [**Figure R2-2.B**]. Thus, these results show that *SOX1* expression is specifically elevated in SHH MBs, where its high levels could be a promising prognostic biomarker.

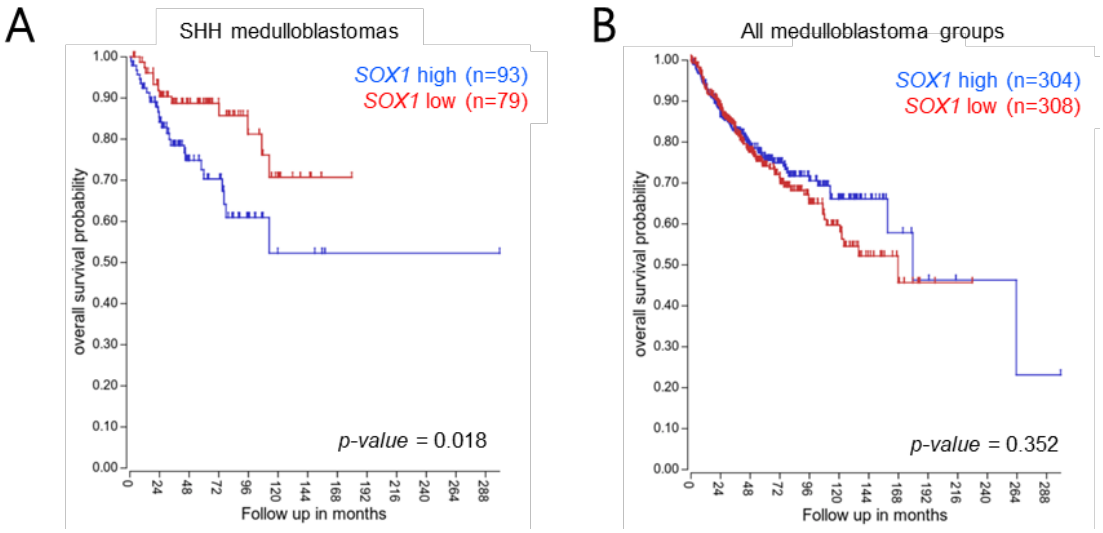

Figure R2-2. High levels of *SOX1* are associated with shorter overall survival. Kaplan-Meier curves for the Cavalli FMG et al. 2017 cohort´s (**A**) SHH group patients' and (**B**) all patients' overall survival rates based on *SOX1* expression obtained from hgserver1.

SOX1 expression seems to be a better biomarker of prognosis in SHH subgroup medulloblastomas than SHH signaling pathway-related genes

To further analyze the potential of *SOX1* expression as both subgroup and prognostic biomarker, we first analyzed the correlation between its expression and those of the genes implicated in SHH signaling pathway (*SHH*, *SMO*, *PTCH1*, *GLI1*, *GLI2* and *GLI3* genes), in all MB subgroups [**Figure R2-3.A**] and only in SHH subgroup MBs [**Figure R2-3.B**]. For this aim, we took advantage of the publicly available Cavalli FMG et al. 2017 cohort's patients' data. We found that all the analyzed genes' expression correlated positively and significantly with *SOX1* expression when analyzing all MBs [**Figure R2-3.A**]. However, when only SHH subgroup MBs were analyzed, only *SMO*, *GLI2* and *GLI3* expression presented a positive, significant correlation with *SOX1* expression [**Figure R2-3.B**].

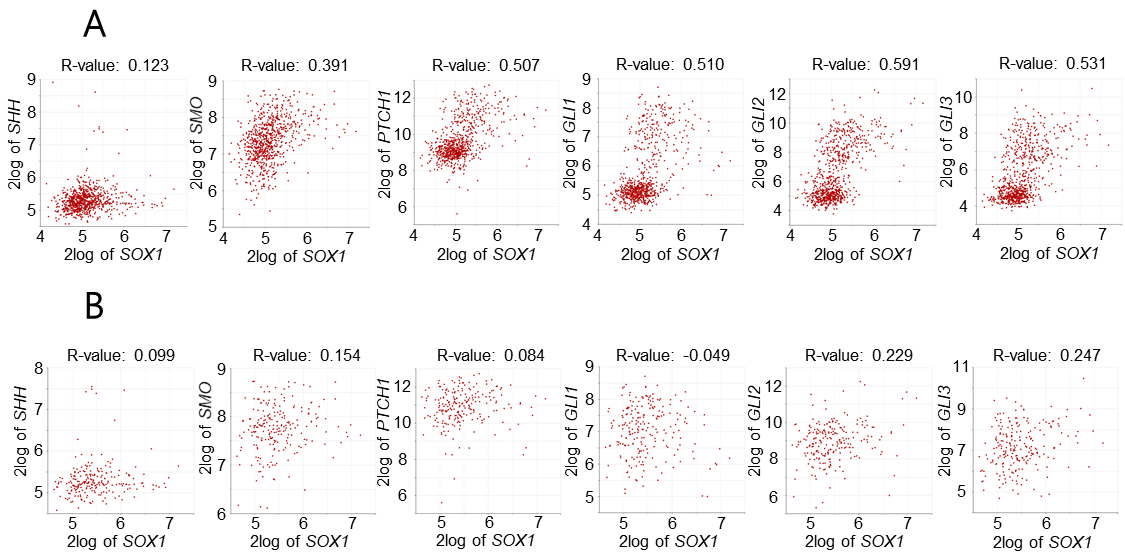

Figure R2-3. *SOX1* correlates positively with SHH signaling pathway genes. (**A**) Correlation analysis between *SOX1* and *SHH* (*p-value* = 6.95 x 10^{-4}), *SMO* (*p-value* = 2.74 x 10^{-29}), *PTCH1* (*p-value* = 3.55 x 10^{-51}), *GLI1* (*p-value* = 1.19 x 10^{-51}), *GLI2* (*p-value* = 6.26 x 10^{-73}) and *GLI3* (1.19 x 10^{-56}), by considering all MB subgroups in Cavalli FMG et al. 2017 cohort (*n* = 612). (**B**) Correlation analysis between *SOX1* and *SHH* (*p-value* = 0.142), *SMO* (*p-value* = 0.021), *PTCH1* (*p-value* = 0.214), *GLI1* (*p-value* = 0.466), *GLI2* (*p-value* = 5.71 x 10^{-4}) and *GLI3* (*p-value* = 1.91 x 10^{-4}), by considering only SHH subgroup MBs in Cavalli FMG et al. 2017 cohort (*n* = 223). All the results were obtained from hgserver1.

Next, we analyzed the SHH signaling pathway genes' expression in the different subgroups of MB in the same cohort. We observed that *SHH*, *SMO* and *GLI3* were not good biomarkers of SHH MB subgroup, in contrast to *PTCH1*, *GLI1* and *GLI2*, since they presented their highest expression levels in this subgroup of the tumor [**Figure R2-4** and **Table R2-1**].

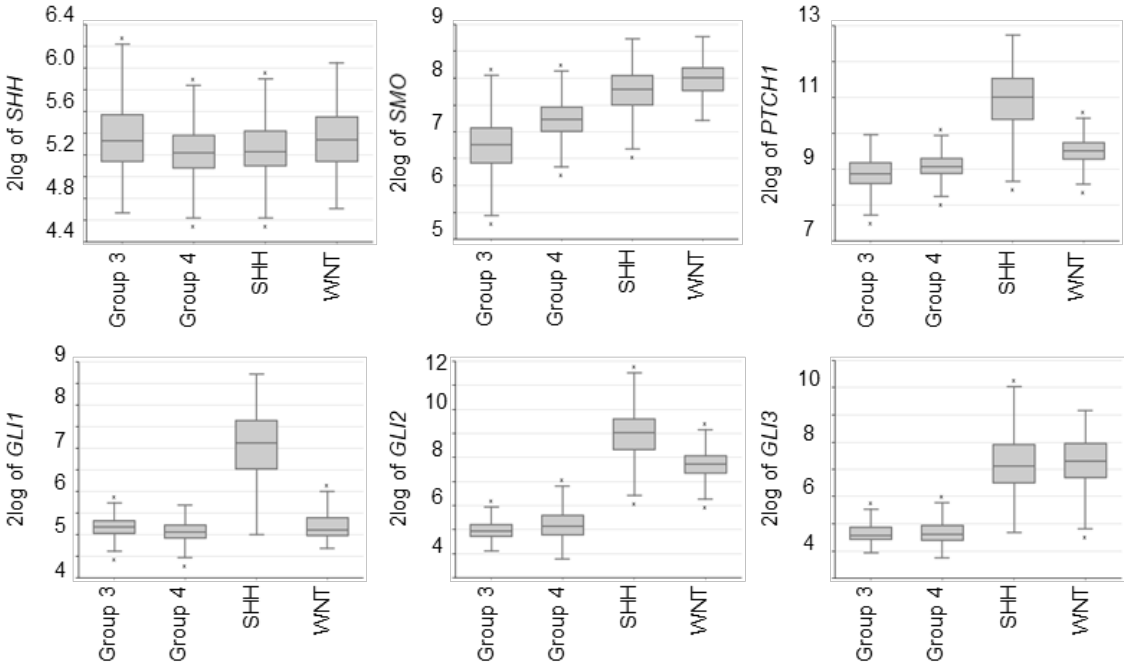

Figure R2-4. SHH signaling pathway genes present varied expression patterns between different MB subgroups. Boxplot of the log2 of *SHH*, *SMO*, *PTCH1*, *GLI1*, *GLI2* and *GLI3* in the indicated MB subgroups in Cavalli FMG et al. 2017 cohort (*n* = 612). All the results were obtained from hgserver1.

Table R2-1. P-values of the differences between the indicated MB subgroups of *SHH, SMO, PTCH1, GLI1, GLI2* and *GLI3* genes' expression in Cavalli FMG et al. 2017 cohort (*n* = 612).

SHH expression				
T test	WNT	SHH	Group 3	Group 4
WNT	-	0.56	0.20	3.0×10^{-3}
SHH	0.56	-	0.02	0.02
Group 3	0.20	0.02	-	3.8×10^{-7}
Group 4	3.0×10^{-3}	0.02	3.8×10^{-7}	-
SMO expression				
T test	WNT	SHH	Group 3	Group 4
WNT	-	8.1×10^{-5}	3.2×10^{-48}	6.7×10^{-48}
SHH	8.1×10^{-5}	-	4.4×10^{-58}	2.1×10^{41}
Group 3	3.2×10^{-48}	4.4×10^{-58}	-	1.5×10^{-29}
Group 4	6.7×10^{-48}	2.1×10^{41}	1.5×10^{-29}	-
PTCH1 expression				
T test	WNT	SHH	Group 3	Group 4
WNT	-	7.8×10^{-25}	2.0×10^{18}	3.6×10^{-17}
SHH	7.8×10^{-25}	-	1.0×10^{-74}	7.3×10^{-121}
Group 3	2.0×10^{18}	1.0×10^{-74}	-	2.3×10^{-8}
Group 4	3.6×10^{-17}	7.3×10^{-121}	2.3×10^{-8}	-
GLI1 expression				
T test	WNT	SHH	Group 3	Group 4
WNT	-	9.3×10^{-50}	0.23	3.9×10^{-6}
SHH	9.3×10^{-50}	-	1.4×10^{91}	6.0×10^{-179}
Group 3	0.23	1.4×10^{91}	-	1.2×10^{-6}
Group 4	3.9×10^{-6}	6.0×10^{-179}	1.2×10^{-6}	-
GLI2 expression				
T test	WNT	SHH	Group 3	Group 4
WNT	-	1.2×10^{-18}	1.2×10^{-86}	1.8×10^{-88}
SHH	1.2×10^{-18}	-	1.4×10^{-140}	2.3×10^{-201}
Group 3	1.2×10^{-86}	1.4×10^{-140}	-	1.6×10^{-4}
Group 4	1.8×10^{-88}	2.3×10^{-201}	1.6×10^{-4}	-
GLI3 expression				
T test	WNT	SHH	Group 3	Group 4
WNT	-	0.53	1.1×10^{-50}	2.3×10^{-111}
SHH	0.53	-	2.2×10^{-74}	2.2×10^{-149}
Group 3	1.1×10^{-50}	2.2×10^{-74}	-	0.26
Group 4	2.3×10^{-111}	2.2×10^{-149}	0.26	-

By analyzing only SHH subgroup patients' data in Cavalli FMG et al. 2017 cohort, we observed no statistical differences in the prognosis of MB patients between high and low levels of *SHH*, *SMO* and *PTCH1* genes expression, with a tendency of low levels linked to worse prognosis [**Figure R2-5**]. Moreover, *GLI3* gene expression did not present statistical significance either, but it showed the opposite tendency, since this gene's high expression seem to be linked to worse prognosis [**Figure R2-5**]. Among the studied genes, only *GLI1* and *GLI2* showed statistical significance, but they presented opposite relations

with prognosis. On the one hand, *GLI1* low expression levels correlated with worse prognosis, whilst *GLI2* low expression levels correlated with better clinical outcome of the patients as previously observed for *SOX1* [Figure R2-5].

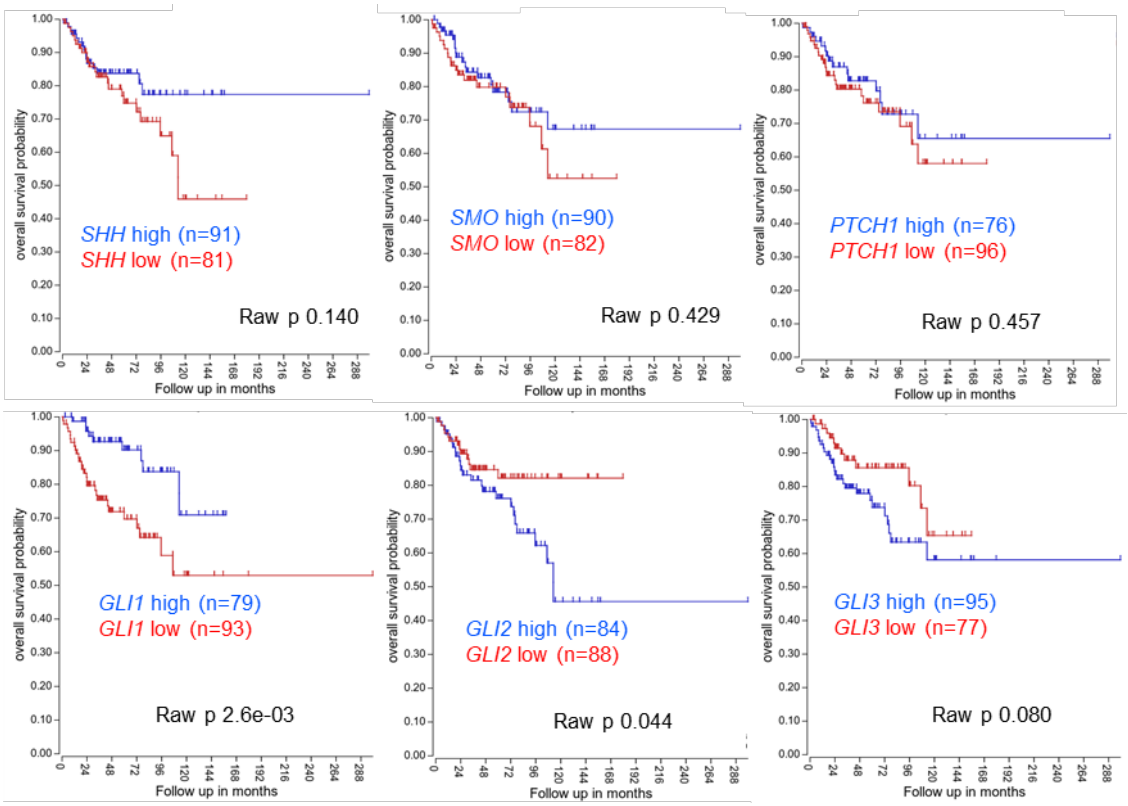

Figure R2-5. SHH signaling pathway genes correlate differentially with patients' prognosis. Kaplan-Meier curves for the Cavalli FMG et al. 2017 cohort´s SHH group patients' overall survival rates based on *SHH*, *SMO*, *PTCH1*, *GLI1*, *GLI2* and *GLI3* expressions. All results were obtained from hgserver1.

Taking all these results into account, the only gene implicated in SHH signaling pathway that seems to be a good subgroup and prognostic biomarker is *GLI2*. As *SOX1* present the same expression pattern and impact on patients' survival, it could be proposed as a novel prognostic and subgroup biomarker for SHH MBs.

SOX1 seems not to be related to other SOX family members in MB

As SOX1 has been described to be controlled by other SOX family members in GBM (Garcia et al., 2017), we wondered if SOX1 could be related to other SOX factors in MB. For this aim, we analyzed the correlation between *SOX1* and *SOX2, SOX4* and *SOX9* members, finding a statistically significant positive correlation between all of them when

considering all MBs [Figure R2-6.A]. However, when considering only the SHH subgroup (expressing higher levels of *SOX1*), we found that only *SOX2* correlates significantly [Figure R2-6.B]. Furthermore, we analyzed the expression of these SOX family members in the different subgroups of MB, finding that *SOX2* and *SOX9,* but not *SOX4*, followed the same pattern as *SOX1* [Figure R2-6.C].

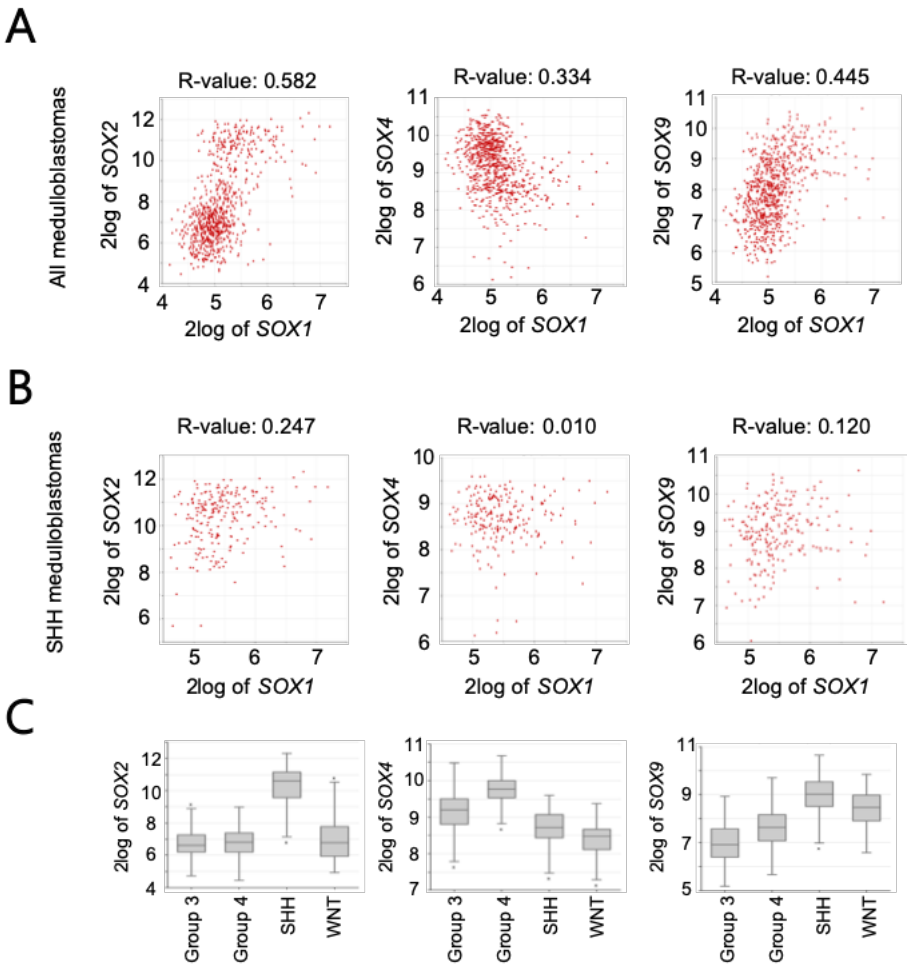

Figure R2-6. *SOX1* correlates positively with other SOX family members only considering all MBs. (**A**) Correlation analysis of *SOX2* (*p-value* = 2.08 x 10^{-70}), *SOX4* (*p-value* = 2.71 x 10^{-21}) and *SOX9* (*p-value* = 2.64 x 10^{-38}) with *SOX1* considering all MB subgroups in Cavalli FMG et al. 2017 cohort (*n* = 612). (**B**) Correlation analysis of *SOX2* (*p-value* = 1.99 x 10^{-04}), *SOX4* (*p-value* = 0.882) and *SOX9* (*p-value* = 0.075) with *SOX1* considering only SHH subgroup MBs in Cavalli FMG et al. 2017 cohort (*n* = 223). (**C**) Boxplot of the log2 of *SOX2*, *SOX4* and *SOX9* in the indicated MB subgroups in Cavalli FMG et al. 2017 cohort (*n* = 612). All results were obtained from hgserver1.

Finally, we also investigated the role as prognostic biomarkers of the three SOX family members considered. First, we performed Kaplan-Meier curves considering all MB patients and we found that only *SOX9* low levels were significantly correlated with poor

prognosis [**Figure R2-7.A**]. Moreover, when performing the same analysis only considering SHH MBs, none of the investigated genes presented a significant correlation with patients' overall survival [**Figure R2-7.B**]. Thus, we concluded that SOX2, SOX4 and SOX9 factors seem not to be correlated with SOX1 in MB.

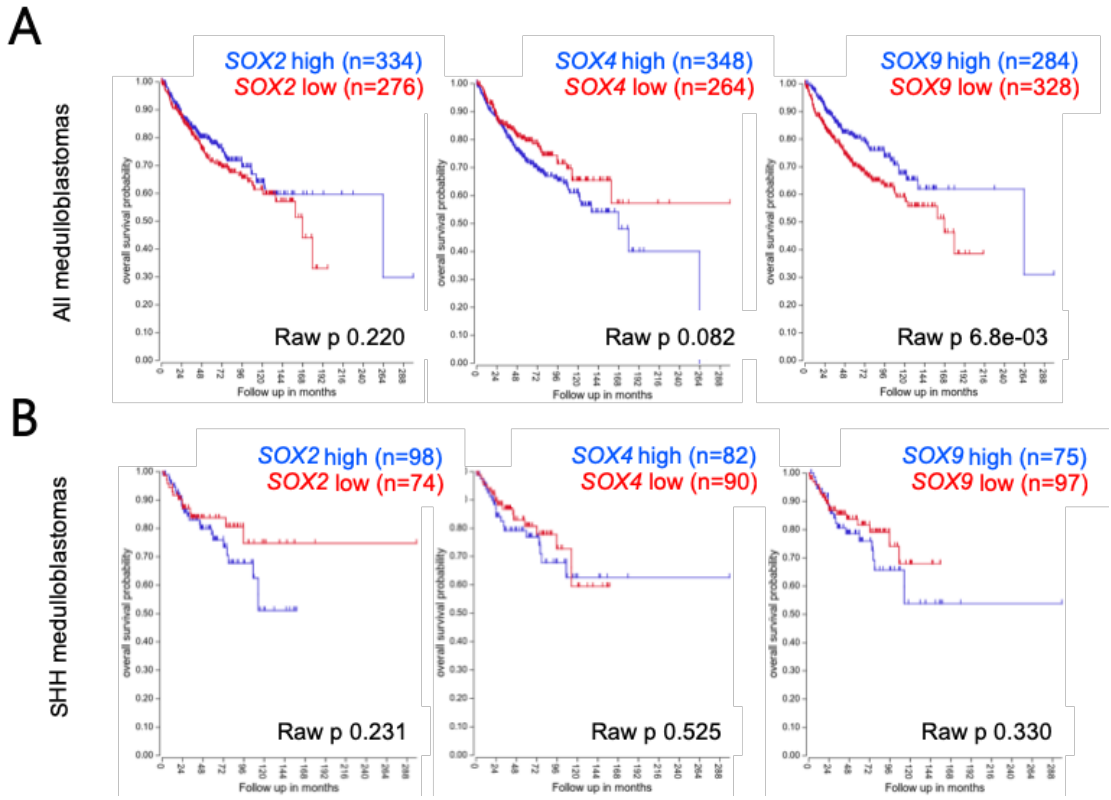

Figure R2-7. SOX family genes correlate differentially with patients' prognosis. (**A**) Kaplan-Meier curves for the Cavalli FMG et al. 2017 cohort patients' overall survival rates based on *SOX2*, *SOX4* and *SOX9* expressions. (**B**) Kaplan-Meier curves for the Cavalli FMG et al. 2017 cohort's SHH subgroup patients' overall survival rates based on *SOX2*, *SOX4* and *SOX9* expressions. All results were obtained from hgserver1.

SOX1 knock-down inhibits cell proliferation and viability in vitro and tumor growth in vivo

In order to determine the role of SOX1 in MB progression, we knocked-down *SOX1* expression in conventional DAOY, UW228 and D283Med human MB cell lines with two independent shRNAs. Effective inhibition of *SOX1* expression was demonstrated by Western Blot analysis using both *shSOX1* constructs (*sh1* and *sh5*) in the three cell lines analyzed [**Figure R2-8.A**]. Functionally, to asses the proliferative capacity of MB cells, we performed a cell counting assay and analyzed the percentage of positivity for the PHH3

mitosis marker. Our results demonstrated that *SOX1* silencing promotes a significant decrease in cell growth rates in all MB cell lines, especially for DAOY and UW228 cells [Figure R2-8.B]. In line with these results, PHH3 positive cell number was also diminished in knocked-down cells comparing with control (*plKO*) cells in DAOY and UW228 cell lines [Figure R2-8.C].

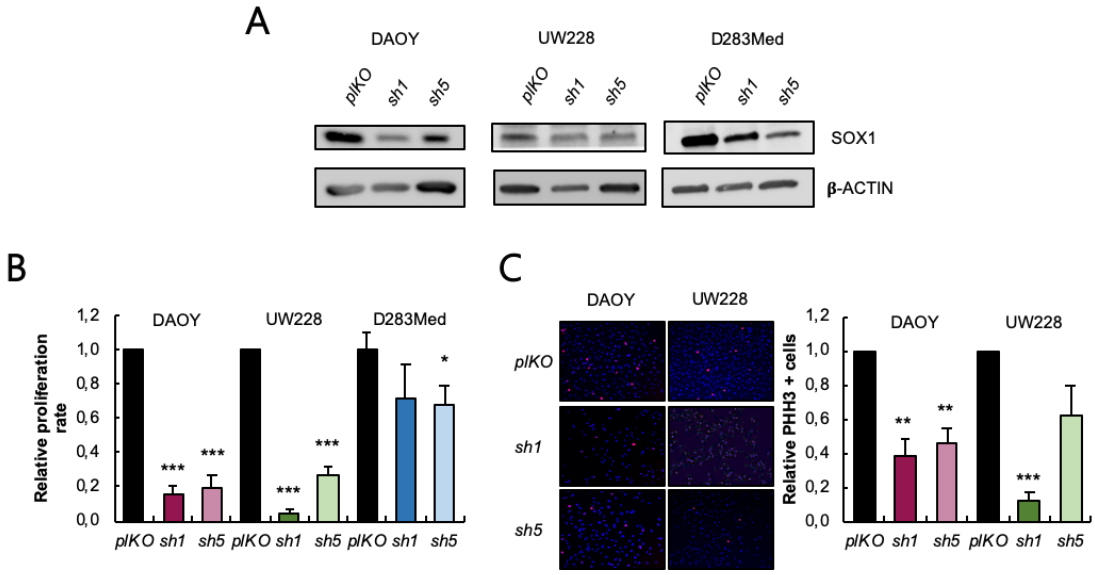

Figure R2-8. *SOX1* knock-down impairs MB cells proliferation *in vitro*. (**A**) Western Blot analysis of SOX1 protein from control (*plKO*) and *shSOX1* (*sh1* and *sh5*) conditions in DAOY, UW228 and D283Med cells ($n \geq 3$). (**B**) Relative cell growth at day 5 comparing *plKO* with *sh1* and *sh5* conditions ($n \geq 3$). (**C**) Representative immunofluorescence images and quantification of phospho-Histone-3 (PPH3) positive cells in *sh1* and *sh5* relative to *plKO* DAOY and UW228 cells ($n \geq 3$).

Moreover, to assess cell viability, we performed an MTT assay showing a decrease in cell viability in DAOY, UW228 and D283Med cells with *SOX1* silencing [Figure R2-9.A]. Furthermore, this silencing also significantly decreased the ability of colony formation in DAOY and UW228 cells, since we observed less formed colonies in silenced cells than in control (*plKO*) ones [Figure R2-9.B].

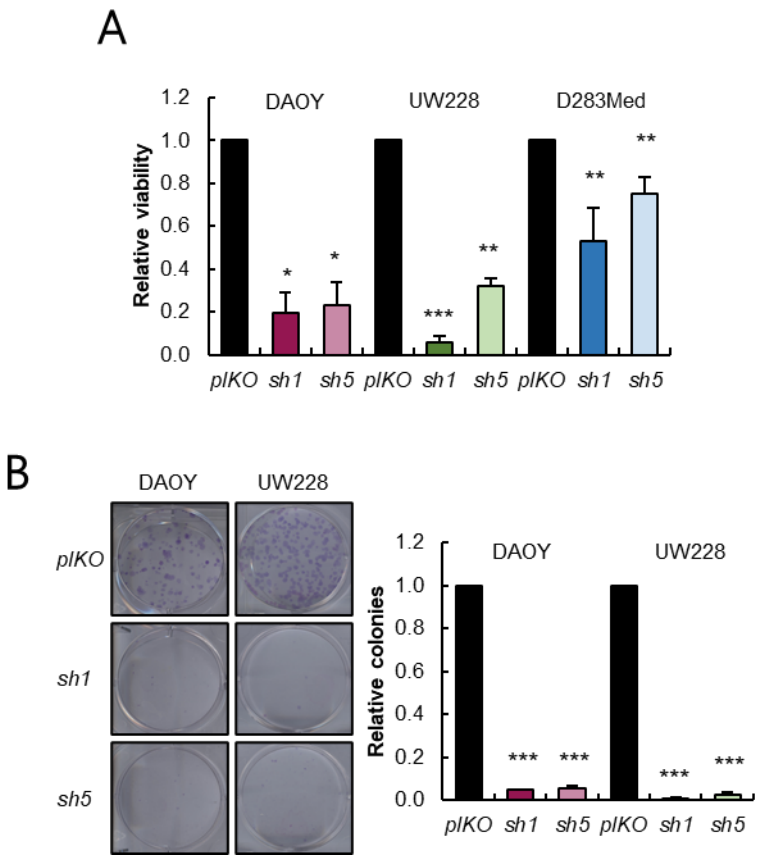

Figure R2-9. *SOX1* knock-down impairs MB cells' viability and colony formation ability *in vitro*. (**A**) MTT studies measuring cell viability in *sh1* and *sh5* relative to *pIKO* DAOY, UW228 and D283Med cells ($n \geq 3$). (**B**) Representative images and quantification of formed colonies for the indicated conditions in DAOY and UW228 cells ($n \geq 3$).

Finally, we determined whether SOX1 regulates tumor growth *in vivo*. For this aim, we injected subcutaneously control and silenced cells in immunocompromised mice. Strikingly, a significant decrease in tumor growth in *shSOX1* DAOY [**Figure R2-10.A**] and D283Med cells was observed [**Figure R2-10.B**]. In line with these results, the weight of tumors generated from *SOX1* knocked-down DAOY cells was smaller than controls [**Figure R2-10.C**]. It is worth to note that *SOX1* silenced D283Med cells formed very few tumors, demonstrating the essential role of SOX1 for tumor initiation [**Figure R2-10.B**]. Altogether, these results point out that SOX1 is required for MB progression.

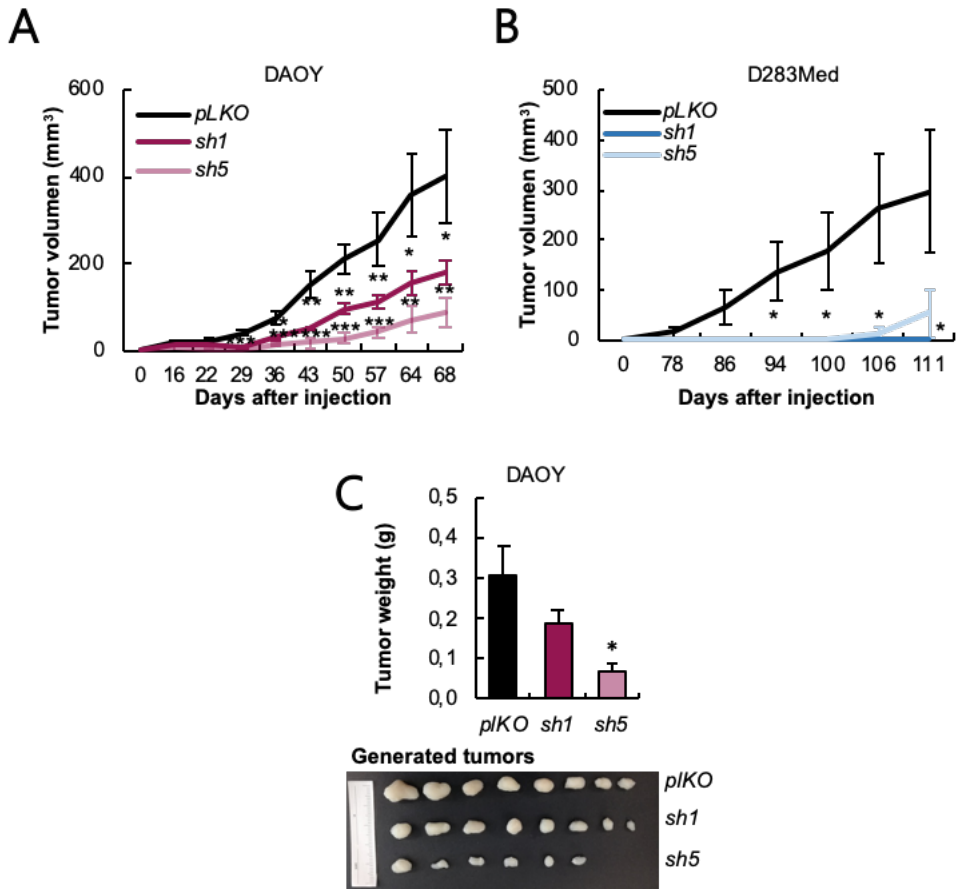

Figure R2-10. *SOX1* knock-down impairs tumor initiation and progression *in vivo*. Tumor volumes generated after subcutaneous injection in nude mice of (**A**) DAOY and (**B**) D283Med *plKO*, *sh1* and *sh5* cells (n = 8) at the indicated time-points are represented. (**C**) Image and quantification of the weight of the generated tumors by DAOY cells.

SOX1 overexpression enhances cell proliferation

To further investigate the role of SOX1 in MB, we enhanced its expression by lentiviral infections in DAOY (high basal SOX1 levels) and D283Med (low basal SOX1 levels). First, we verified the correct overexpression of this transcription factor by Western Blot analysis, observing higher levels in the overexpression condition (*SOX1*) than in the control one (*GFP*) [**Figure R2-11.A**]. Functionally, we performed a cell counting assay to analyze the proliferative capacity of these cells, observing a slight increase in cell proliferation in D283Med cells that was not so clear in DAOY cells [**Figure R2-11.B**].

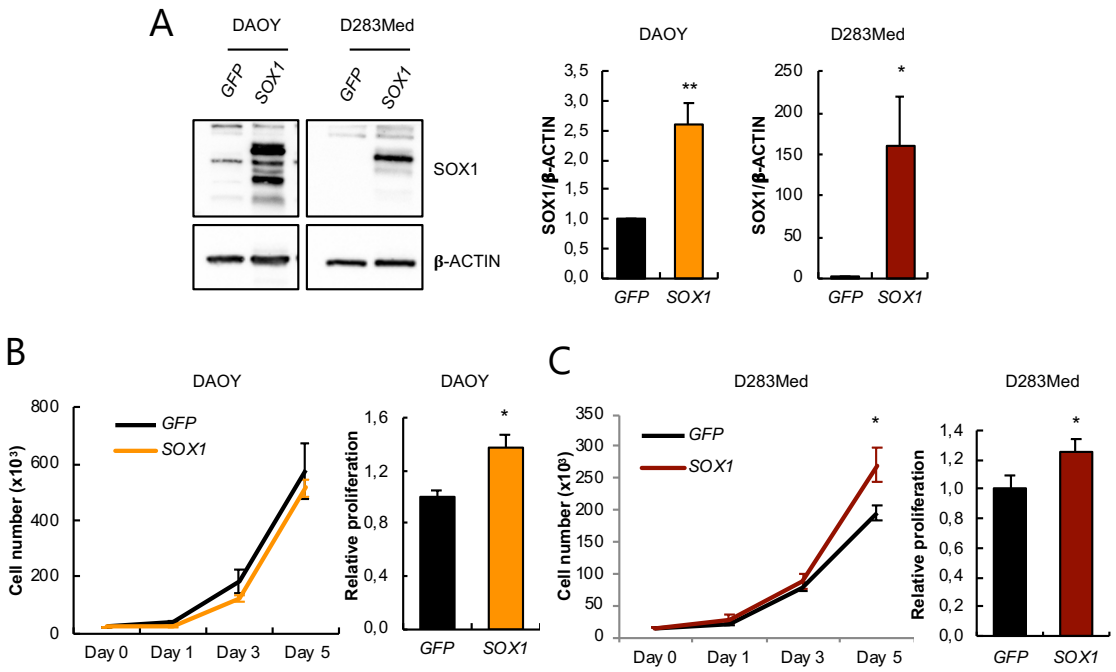

Figure R2-11. *SOX1* upregulation promotes a slight increase in MB cell proliferation. (**A**) Western Blot analysis and protein quantification of SOX1 protein form control (*GFP*) and *SOX1* overexpression conditions in DAOY and D283Med cells ($n \geq 3$). Cell number and relative cell growth at day 5 comparing *GFP* with *SOX1* condition in (**B**) DAOY and (**C**) D283Med cells ($n \geq 3$).

Moreover, we analyzed the positivity for PHH3 (mitosis marker) and KI67 (proliferation marker) in our cell models. In line with the previous cell count results, these experiments demonstrated that *SOX1* overexpression promotes a slight increase in PHH3 and KI67 positive cell number in D283Med cells, but not in DAOY cells [**Figure R2-12.A-B**]. Thus, it seems that SOX1 overexpression is only presenting a phenotype in SOX1 low expressing cells (D283Med), where it may be expected the overexpression to have a stronger impact compared to cells presenting high basal levels of SOX1, such as in DAOY cells. Moreover, the results suggest that SOX1 is essential for MB cells' proliferation.

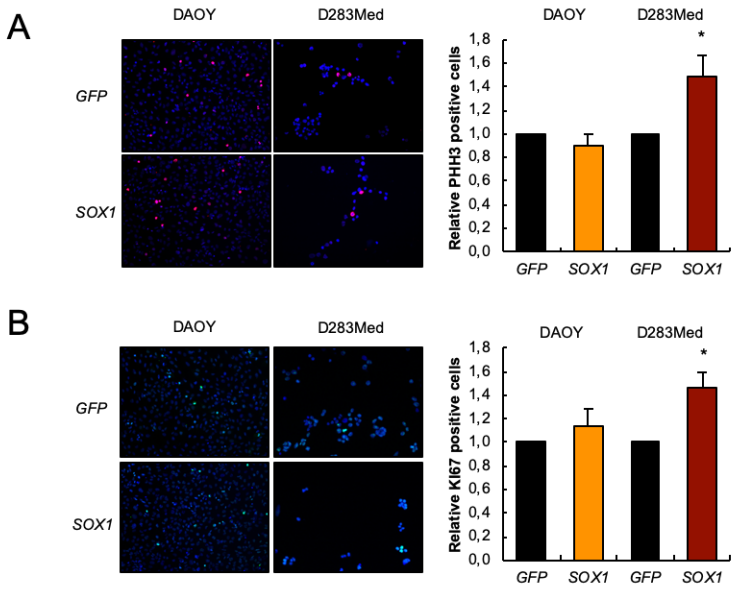

Figure R2-12. *SOX1* overexpression promotes cell proliferation only in D283Med cells. (**A**) Representative immunofluorescence images and quantification of PPH3 positive cells in *SOX1* relative to *GFP* DAOY and D283Med cells ($n \geq 3$). (**B**) Representative immunofluorescence images and quantification of KI67 positive cells in *SOX1* relative to *GFP* DAOY and D283Med cells ($n \geq 3$).

MBSCs express high levels of SOX1 and its knock-down inhibits MBSCs activity

To directly explore the role of SOX1 in MBSCs activity, we first investigated the expression of *NESTIN*, *PML*, *ERBB4* and *CD133* stem cell markers, and $p27^{KIP}$ differentiation marker, in *shSOX1* DAOY cells. RT-qPCR results showed a decrease in stem cell markers' expression in *SOX1* knocked-down cells [**Figure R2-13.A**], while Western Blot analysis showed an increase in the levels of $p27^{KIP}$ differentiation marker[**Figure R2-13.B**].

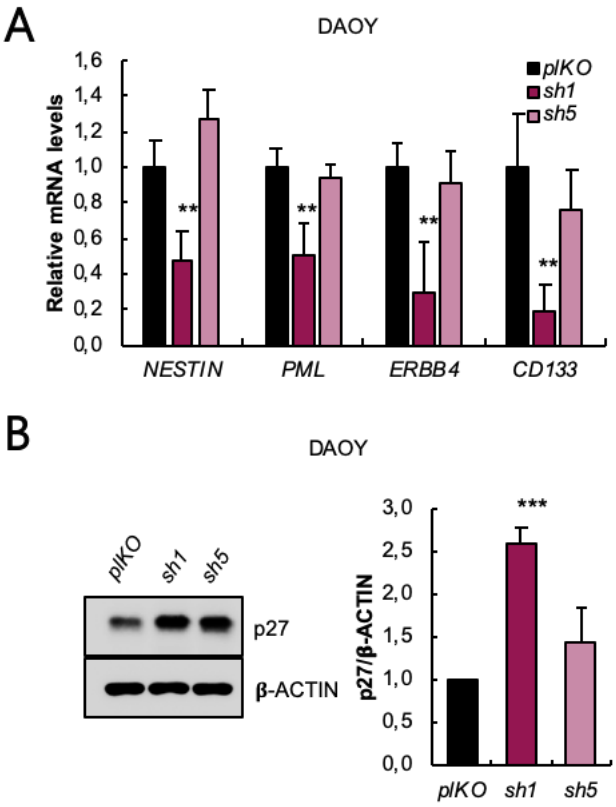

Figure R2-13. *SOX1* knock-down decreases stem cell markers' expression but augments differentiation marker levels. (**A**) mRNA levels of the indicated stem cell markers in *plKO*, *sh1* and *sh5* DAOY cells ($n \geq 3$). (**B**) Western Blot analysis and quantification of $p27^{KIP}$ protein from *plKO*, *sh1* and *sh5* DAOY cell extracts ($n \geq 3$).

To further investigate the role of SOX1 in MBSCs, we cultured the two conventional DAOY and UW228 MB cell lines in different conditions:as adherent monolayer in the presence of serum or in stem cell specific media, to obtain oncospheres. Interestingly, the oncospheres derived from both MB cell lines expressed higher levels of *SOX1* compared to those cultured in the presence of serum [Figure R2-14.A]. In addition, to investigate the role of SOX1 in MBSCs function, we counted the oncospheres formed after culturing *SOX1* knocked-down DAOY, UW228 and D283Med cells in the presence of stem cell medium. This experiment showed a marked decrease in the ability of forming oncospheres in these three cell lines when knocking-down *SOX1* [Figure R2-14.B]. Altogether, these results suggest that *SOX1* have a role in the maintenance of MBSCs.

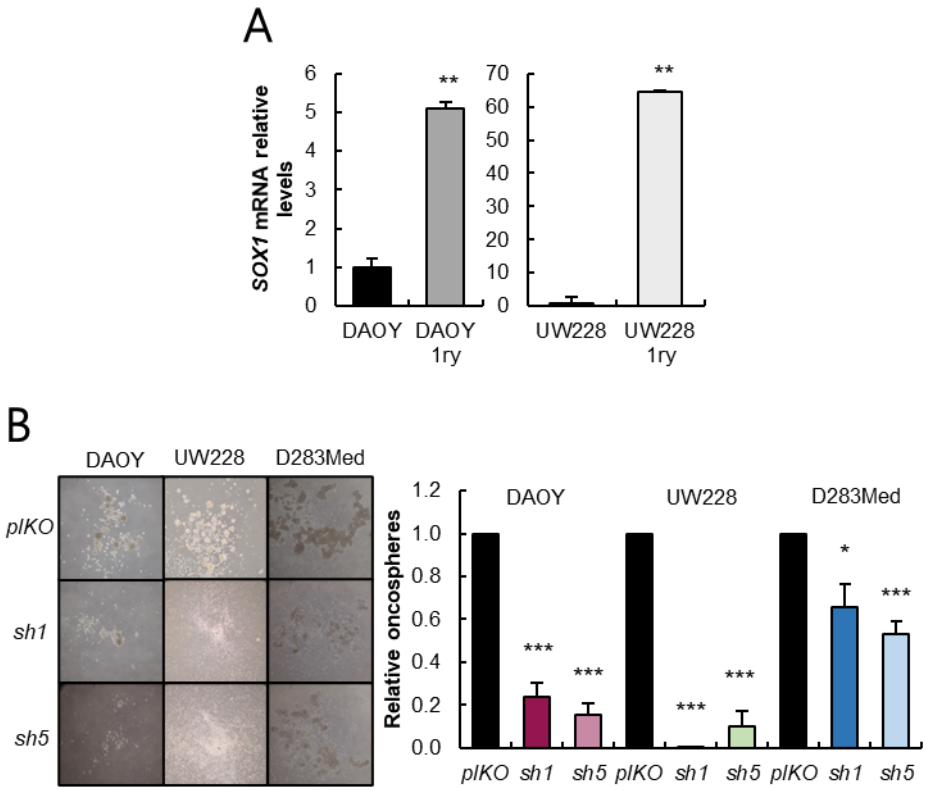

Figure R2-14. *SOX1* expression is upregulated in MBSCs. (**A**) *SOX1* mRNA expression levels of DAOY and UW228 cells grown in serum (DAOY or UW228) or in stem cell media as oncospheres (1ry) ($n \geq 3$). (**B**) Representative images and quantification of the oncospheres formed from *plKO*, *sh1* and *sh5* conditions in the indicated cell lines.

Next, we moved to *in vivo* experiments in order to assess the tumor cells' initiation capacity. For this aim, we injected limited dilution concentrations of knocked-down *SOX1* cells subcutaneously in immunocompromised mice and then we counted the number of tumors formed with DAOY [**Figure R2-15.A**] and D283Med [**Figure R2-15.B**] cells. Strikingly, the frequency of tumor initiating cells necessary to form the tumor was higher in *shSOX1* cells than in controls, both in DAOY [**Figure R2-15.C**] and D283Med [**Figure R2-15.D**] cell lines. Strikingly, the frequency of tumor initiation in DAOY cells was 1 in 475,710 and 1 in 946,994 in *sh2* and *sh3* cells, respectively, compared to 1 in 99,524 in the control cells [**Figure R1-14.A,C**]. Moreover, the tumor initiation in D283Med cells was 1 in 1,649,864 and infinite in *sh2* and *sh3* cells, respectively, compared to 1 in 441,838 in the empty vector harboring cells [**Figure R1-14.B,D**]. The statistical differences in stem cells frequencies between *plKO* and *sh1* was *p-value* = 1 for DAOY and *p-value* = 0.000123 for D283Med cells, and between *plKO* and *sh5* was *p-value* = 0.00074 for DAOY and *p-value*

= 0.0140 for D283Med cells. All these results confirm that *SOX1* inhibition limits tumor initiation, revealing an essential role of this transcription factor in MBSCs activity.

A

64 days after injection		
Group	1000K cells	100K cells
plKO	8/8	5/8
sh1	8/8	5/8
sh5	6/8	0/8

B

112 days after injection		
Group	500K cells	50K cells
plKO	7/8	0/8
sh1	0/8	0/8
sh5	2/8	0/8

C

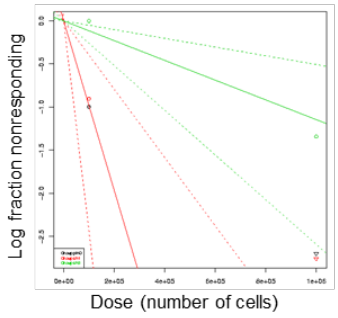

Confidence intervals for 1/(stem cell frequency)			
Group	Lower	Estimate	Upper
plKO	252493	101861	41093
sh1	252493	101861	41093
sh5	1976074	873262	385910

Pairwise tests for differences in stem cell frequencies		
Group 1	Group 2	Pr(>Chisq)
plKO	*sh1*	1
plKO	*sh5*	0.00074
sh1	*sh5*	0.00074

D

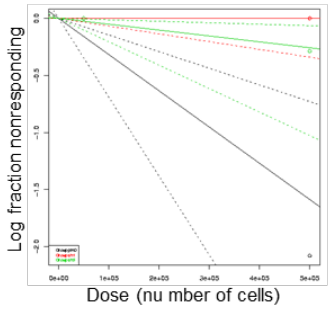

Confidence intervals for 1/(stem cell frequency)			
Group	Lower	Estimate	Upper
plKO	685697	315069	144770
sh1	Inf	Inf	1468757
sh5	7722769	1939287	486980

Pairwise tests for differences in stem cell frequencies		
Group 1	**Group 2**	**Pr(>Chisq)**
plKO	*sh1*	0.000123
plKO	*sh5*	0.0140
sh1	*sh5*	0.0818

Figure R2-15. *SOX1* regulates MBSCs activity. Number of tumors formed in the indicated conditions after subcutaneous injection in nude mice of (**A**) 1 x 10^6 and 1 x 10^5 DAOY and (**B**) 5 x 10^5 and 5 x 10^4 D283Med cells. Frequency of tumor initiation of the indicated conditions in (**C**) DAOY and (**D**) D283Med cells, measured using ELDA platform, is also shown.

SOX1 knock-down alters cell response, motility and cellular morphogenesis-related pathways

Finally, to investigate which pathways could be underlying the phenotype observed when knocking-down *SOX1*, transcriptomic analysis of *plKO*, *sh1* and *sh5* DAOY cells was performed. In *sh1* condition, 560 upregulated and 586 downregulated genes were found when compared to *plKO* control condition. Regarding *sh5* cells, 89 upregulated and 221 downregulated genes were found after comparing with control

cells. All these genes presented a *p-value* lower than 0.05 and a fold-change higher than 2. The gene enrichment analysis was performed with each shRNA gene list separately, using the GO sets and considering the biological processes. The results show a downregulation of genes involved in cell response and motility in both *sh1* [Figure R2-16.A] and *sh5* [Figure R2-16.B] conditions. On the contrary, an increase in genes implicated in cellular morphogenesis was observed in *sh1* [Figure R2-17.A] and *sh5* [Figure R2-17.B] cells.

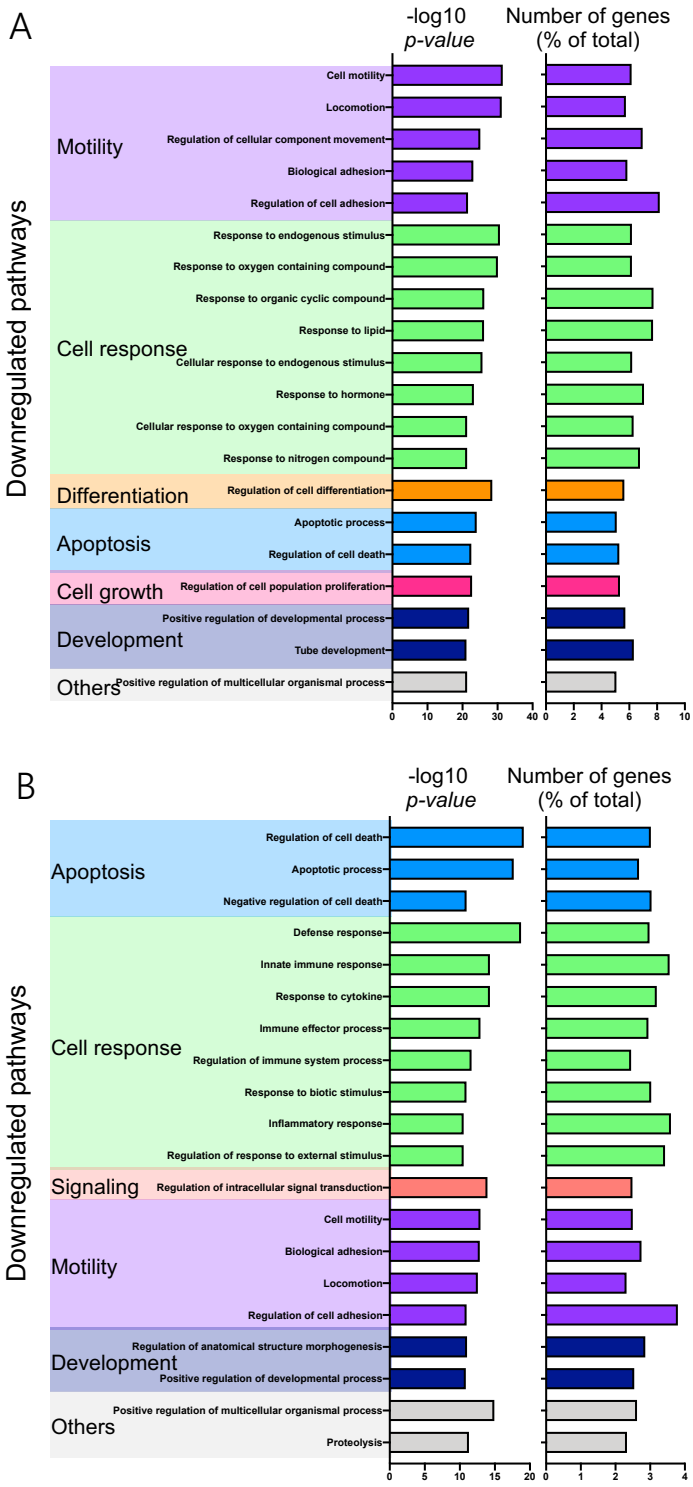

Figure R2-16. *SOX1* knock-down downregulates cell response and motility pathways of DAOY cells. Downregulated pathways in (**A**) *sh1* and (**B**) *sh5* DAOY cells compared with *plKO* cells when performing a GO gene sets biological processes analysis from Clariom S microarray results. The *p-value* and the percentage of genes dysregulated in each pathway is represented in all figures.

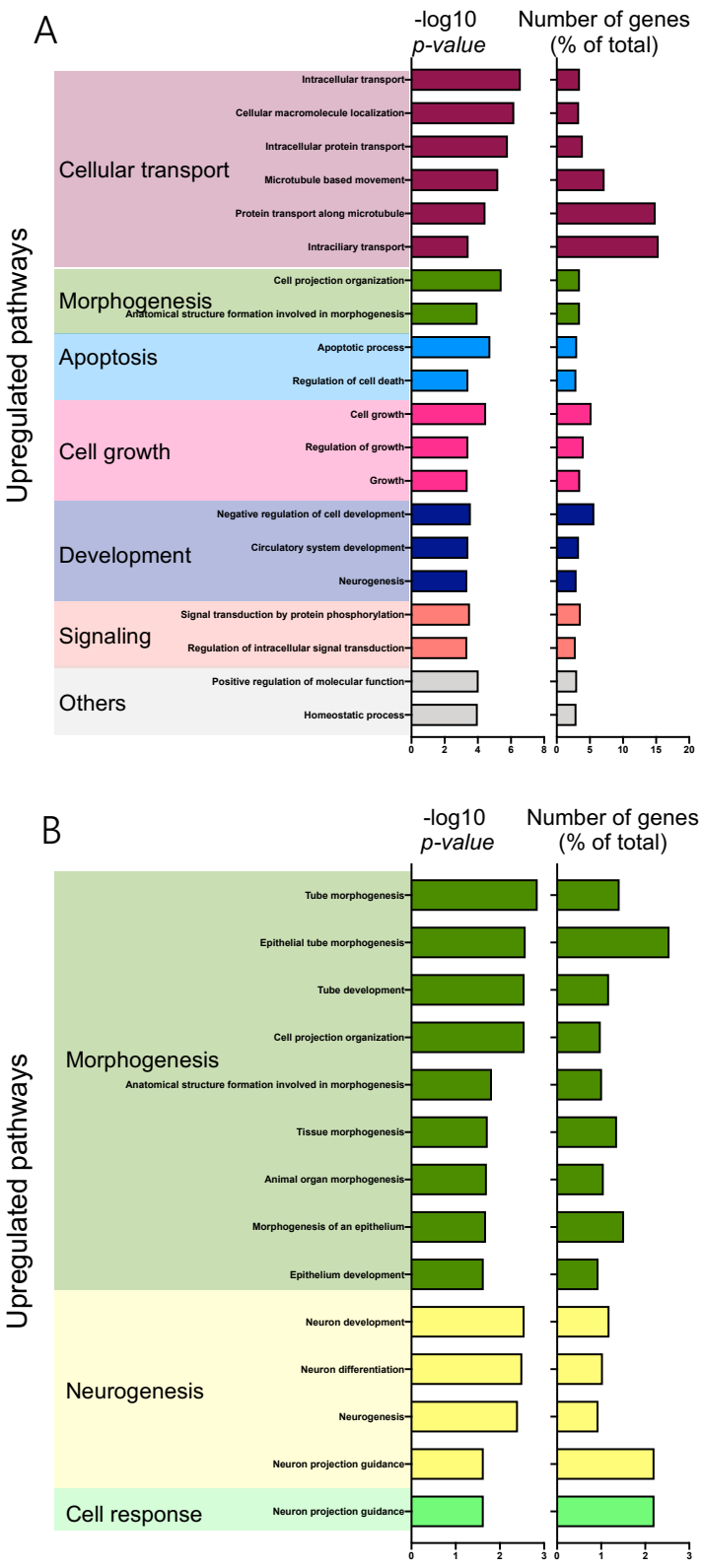

Figure R2-17. *SOX1* knock-down upregulates morphogenesis pathway of DAOY cells. Upregulated pathways in (**A**) *sh1* and (**B**) *sh5* DAOY cells compared with *plKO* cells when performing a GO gene sets biological processes analysis from Clariom S microarray results. The *p-value* and the percentage of genes dysregulated in each pathway is represented in all figures.

We validated some of the genes already linked to MB or cancer based on the literature, such as *Interleukin 6 (IL6)* (Chen et al., 2018), *VCAM1* (Liang et al., 2015), *CEA cell adhesion molecule 1 (CEACAM1)* (Kelleher et al., 2019), *Insulin like growth factor binding protein 3 (IGFBP3)* (Svalina et al., 2016), *Superoxide dismutase 2 (SOD2)* (John et al., 2009) and *Semaphorin 5A (SEMA5A)* (Saxena et al., 2018b). We found by RT-qPCR analysis that all these genes diminished their expression when *SOX1* was knocked-down [Figure R2-18].

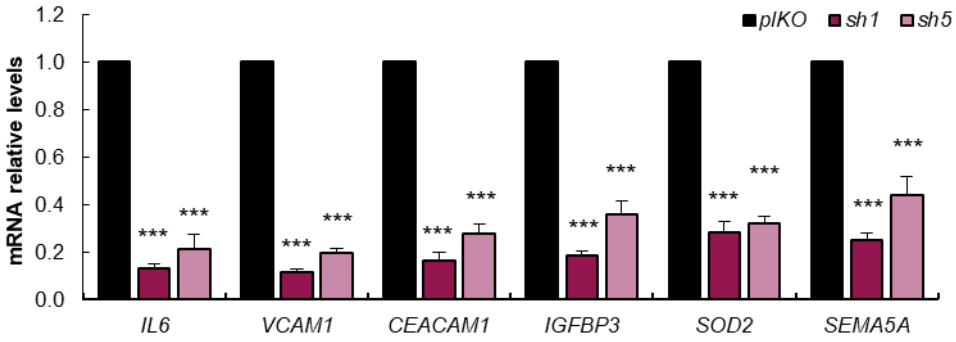

Figure R2-18. *SOX1* downregulates several genes expression. mRNA levels of downregulated genes in *plKO* and *shSOX1* DAOY cells ($n \geq 3$).

To further characterize the impact of the validated genes, we moved to clinical samples and completed a correlation study between *SOX1* and the candidate genes' expression in the Cavalli FMG et al. 2017 cohort, considering both all patients data [Figure R2-19.A] and SHH MB patients' data [Figure R2-19.B]. When analyzing all MB patients, we found a statistically significant and positive correlation between *VCAM1*, *CEACAM1* and *SEMA5A,* and *SOX1* expression [Figure R2-19.A], reinforcing the link between *SOX1* and these genes. However, a negative correlation between *SOD2* and *SOX1* expression was found [Figure R2-19.A]. In addition, when analyzing only the SHH group MB patients' data, only *VCAM1* presented a statistically significant but negative correlation with *SOX1* [Figure R2-19.B], a not expected result. Therefore, the gene expression correlation analyses here performed in MB patients follow a varied pattern depending on the MB subgroup and the particular gene considered, with no clear trends.

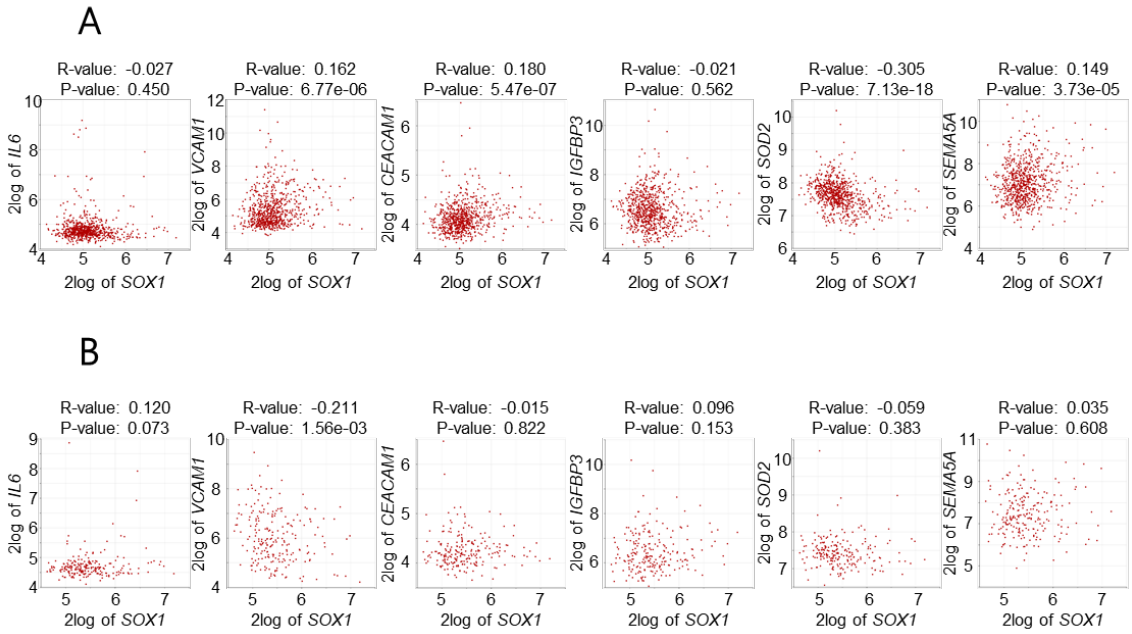

Figure R2-19. Impact of validated genes identified aster transcriptomic analysis in MB clinical samples. Correlation analysis of the validated genes expression with *SOX1* expression taking into account (**A**) all MBs data (IL6 *p-value* = 0.450, *VCAM1 p-value* = 6.77 x 10^{-6}, *CEACAM1 p-value* = 5.47 x 10^{-7}, *IGFBP3 p-value* = 0.562, *SOD2 p-value* = 7.13 x 10^{-18} and *SEMA5A p-value* = 3.73 x 10^{-5}) and (**B**) SHH MBs data (*IL6 p-value* = 0.073, *VCAM1 p-value* = 1.56 x 10^{-3}, *CEACAM1 p-value* = 0.882, *IGFBP3 p-value* = 0.153, *SOD2 p-value* = 0.383 and *SEMA5A p-value* = 0.608) from Cavalli FMG et al. 2017 cohorts' data. All results were obtained from hgserver1.

Moreover, we analyzed the expression level of the validated genesin the different MB subgroups, taking advantage of the same cohort information. Our results showed that *VCAM1*, *CEACAM1* and *SEMA5A* genes are the ones with higher expression in the SHH subgroup MBs compared to the other subgroups [**Figure R2-20**], following similar patterns as *SOX1*, *PTCH1*, *GLI1* and *GLI2* genes. Thus, *VCAM1*, *CEACAM1* and *SEMA5A* genes might be also good SHH MBs biomarkers.

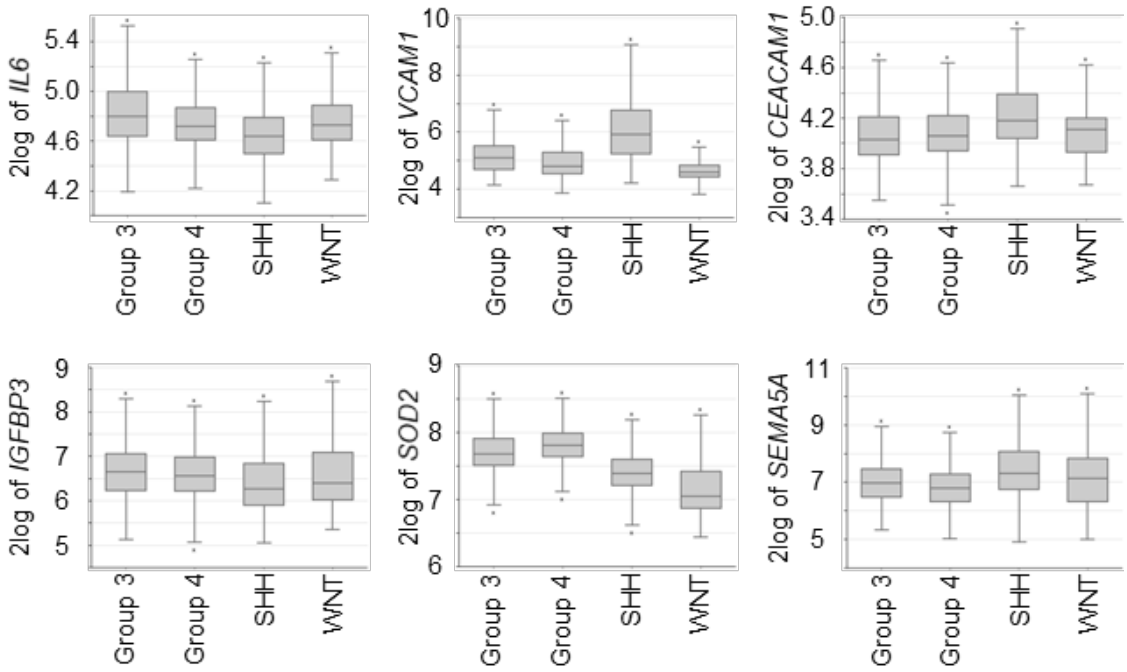

Figure R2-20. Impact of validated genes' expression in the MB clinical samples. Boxplot of the log2 of the indicated genes in the different MB subgroups in Cavalli FMG et al. 2017 cohort (*n* = 612). All results were obtained from hgserver1.

Finally, we studied the validated genes' expressions' correlation with patients' outcome, finding that *IL6* and *SOD2* high expression levels were significantly correlated with poor prognosis when analyzing all MBs [**Figure R2-21.A**]. When repeating the same analysis with SHH subgroup data, *IL6* high expression levels appeared to be statistically correlated with poor prognosis, whereas *VCAM1* high expression levels did so with a better prognosis status [**Figure R2-21.B**]. Therefore, *IL6* is the only gene that follows the same pattern as *SOX1* both in all MBs and in the SHH subgroup, which postulates *IL6* gene expression as a prognosis biomarker candidate in MB.

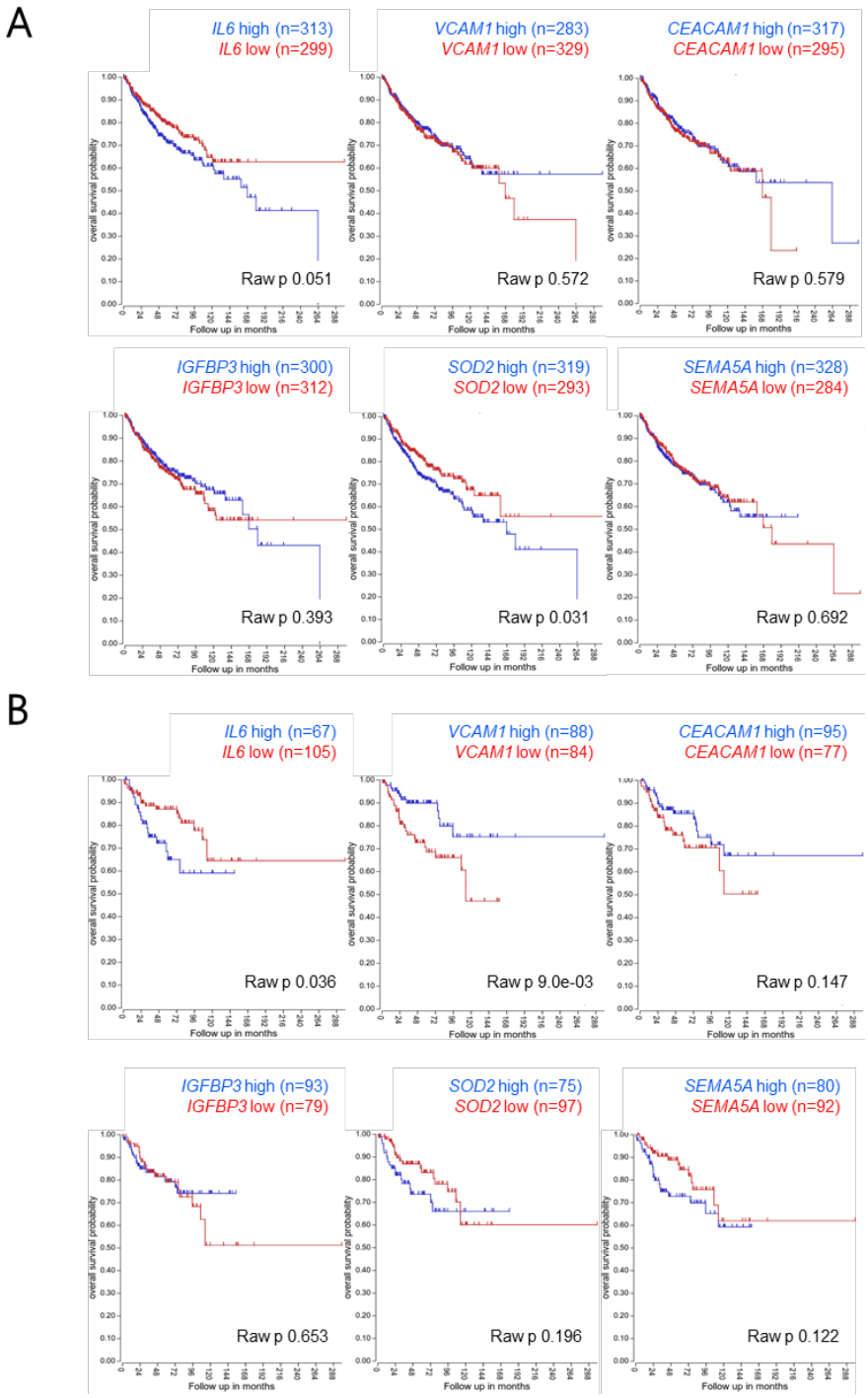

Figure R2-21. Impact of validated genes in MB patients' survival. Kaplan–Meier curves for the Cavalli FMG et al. 2017 cohort's (**A**) all patients' and (**B**) SHH subgroup patients' overall survival rates based on the levels of validated genes obtained in the microarray analysis (*p-values* are indicated in each graph). All results were obtained from hgserver1.

CHAPTER 3

SOX1 presents an oncogenic activity in glioblastoma

High SOX1 expression levels are associated with poor clinical outcome in glioblastoma

To assess the impact of *SOX1* in GBM, we analyzed its expression in human brain tumor biopsies. First, we compared the expression of *SOX1* between human low-grade gliomas (LGG) and healthy brain samples. The results obtained from The Cancer Genome Atlas (TCGA) (Brennan et al., 2013) publicly available datasets showed no differences between the two groups [**Figure R3-1.A**]. Next, we investigated *SOX1* levels in a small GBM cohort derived from Donostia University Hospital. *SOX1* expression in the analyzed tumor biopsies varied between 0.12 and 133 fold change when compared to healthy or normal brain tissue. Interestingly, 18 out of 26 tumors (69.2 %) showed higher levels of *SOX1* with a fold-change greater than 1.5 [**Figure R3-1.B**]. Afterwards, we studied *SOX1* expression in the GBM data from the TCGA cohort and found , even if *SOX1* levels were also highly heterogeneous within the different samples, that GBM presented lower *SOX1* levels than normal brain [**Figure R3-1.C**]. However, when we explored the relation between *SOX1* expression levels and clinical characteristics of the patients in the TCGA cohort, we found that high *SOX1* expression levels were associated with patients' shorter overall survival (*p-value*=0.02) [**Figure R3-1.D**]. Altogether, these results show that *SOX1* expression levels are elevated in a subset of GBM samples and that its expression could be a prognostic biomarker.

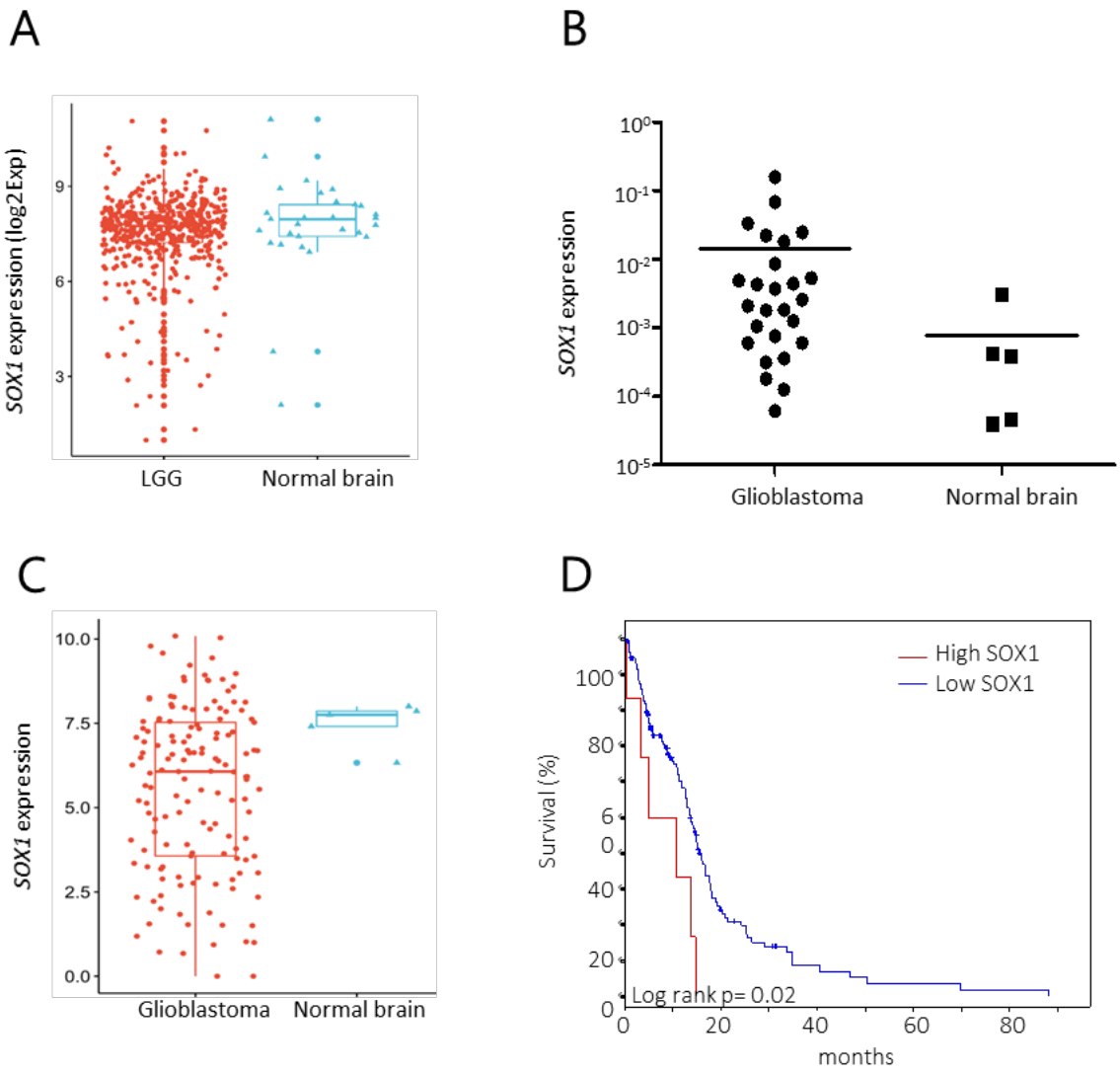

Figure R3-1. High levels of *SOX1* are associated to poor clinical outcome in GBM. (**A**) Boxplot of the *SOX1* fragments per kilobase of exon model per million reads mapped (FPKM) log2 of LGG vs normal healthy brain samples in the TCGA cohort. Wilcoxon test, *p-value* = 0.17. (**B**) *SOX1* mRNA expression levels in GBM samples and normal or healthy brain samples from Donostia University Hospital cohort. (**C**) Boxplot of the log2 of the *SOX1* FPKM of GBM vs normal or healthy brain samples in TCGA cohort. The number of available RNAseq samples for GBM is smaller than for LGG. Wilcoxon test, *p-value* = 0.068. (**D**) Kaplan-Meier curves for the TCGA cohort's patients' overall survival rates based on *SOX1* expression obtained from cbioportal. LogRank test, *p-value* = 0.02.

SOX2 regulates SOX1 expression in glioblastoma

Since *SOX1* is down-regulated in *SOX2*-silenced LN229 glioma cells according to a transcriptomic study (Fang et al., 2011), and as SOX2 activity modulates proliferation and self-renewal in glioma stem cells (Garros-Regulez et al., 2016a), we investigated whether the expression of *SOX1* was regulated by SOX2 in GBM. Interestingly, we found that *SOX2* silencing by an shRNA (*shSOX2*) in U251 glioma cells (which present high endogenous

levels of SOX2, Garros-Regulez et al., 2016a) displayed lower *SOX1* expression than control cells (with normal levels of *SOX2*) [**Figure R3-2.A-B**]. In line with this, *SOX2* ectopic overexpression in U87 glioma cells (with low endogenous SOX2 levels) led to a significant increase in *SOX1* expression [**Figure R3-2.A-B**]. To further study this putative correlation between SOX2 and SOX1, we moved to clinical biopsies and analyzed the expression of both transcription factors in the GBM samples from the Donostia University Hospital cohort. Interestingly, the correlation analysis showed a significant association between *SOX2* and *SOX1* expression in the GBM samples [**Figure R3-2.C**]. Indeed, we found that 60 % of the cohort's biopsies presenting *SOX2* overexpression also showed high levels of *SOX1*, whilst all of the biopsies presenting moderate or low *SOX2* levels also had low *SOX1* levels. Altogether, these results indicate a positive relationship between SOX2 and SOX1, and their belonging to the same signaling pathway.

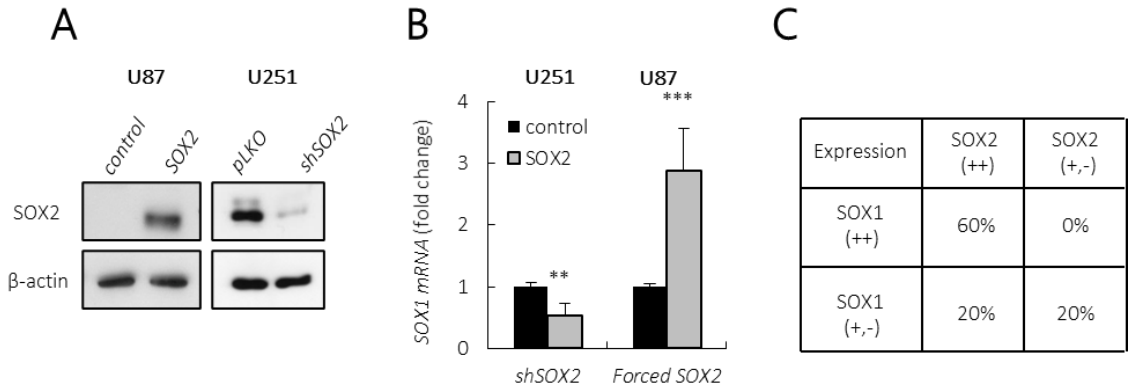

Figure R3-2. *SOX1* correlates with *SOX2* in GBM. (**A**) Western Blot analysis of SOX2 protein expression in U87 cells transduced with ectopic *SOX2* and U251 cells infected with *shSOX2*. (**B**) *SOX1* mRNA expression levels in the indicated GBM cell lines relative to control cells ($n \geq 3$). (**C**) Correlation analysis of *SOX2* and *SOX1* expression in human GBM samples.

SOX1 is enriched in GSCs population

With the aim of investigating the role of SOX1 in GSCs population, we cultured several conventional glioma cell lines as adherent monolayers in the presence of serum (adherent), and as oncospheres in stem cell specific media. First, we analyzed *SOX1* expression levels in the different adherent cell lines. We found high levels of *SOX1* in U251 and U373 cells, and low levels in U87, A172 and T98 cells [**Figure R3-3.A**]. Afterwards, we confirmed that the oncospheres cultured in stem cell specific media expressed higher levels of stem cell markers (*SOX2, CD133* and *OCT4*) [**Figure R3-3.B-D**], which demonstrates an enrichment of stemness activity in parental cells cultured as oncospheres. Interestingly, oncospheres derived from all five glioma cell lines presented also higher levels of *SOX1* comparing with the adherent cells [**Figure R3-3.E**]. It should be noted that in line with their enhanced tumor-propagating activity, these oncospheres are known to be associated with larger and faster-growing tumors formation (Garros-Regulez et al., 2016a).

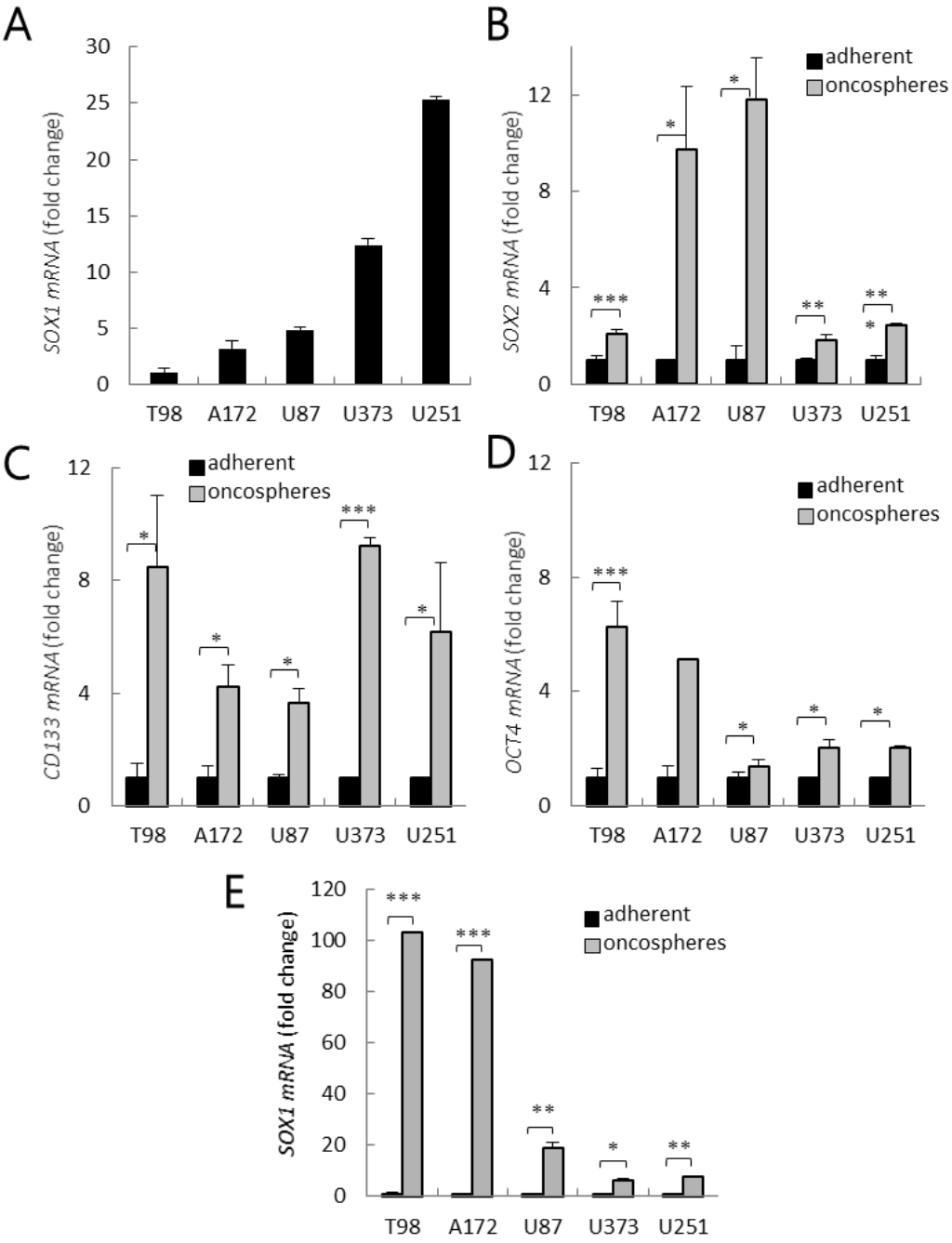

Figure R3-3. *SOX1* is enriched in GSCs population. (**A**) *SOX1* mRNA levels in the indicated glioma cell lines showing different expression levels among them ($n \geq 3$). (**B**) *SOX2*, (**C**) *CD133* and (**D**) *OCT4* stem cell markers together with (**E**) *SOX1* mRNA levels in the indicated glioma cells cultured in stem cell specific media (oncospheres) relative to cells cultured in the presence of serum (adherent) ($n \geq 2$).

To further characterize *SOX1* expression in GSCs, we investigated this gene in primary GSCs derived from human patients. These cells constitute a more similar, and hence relevant, model to the clinical setting. First, we studied *SOX1* expression levels in four independent patient-derived GSC cultures. Our results demonstrated markedly higher *SOX1* levels in GSCs compared to the conventional glioma cell lines [Figure R3-4.A]. Next, we investigated the difference in *SOX1* expression in the GSCs population when we differentiated our four GSCs primary cultures by removing the EGF and b-FGF2 growth factors, and by adding serum. Our results showed that *SOX1* levels were dramatically decreased, by 70 %, in all four differentiated cell lines compared with GSCs cultured in basal conditions [Figure R3-4.B]. Similar results were observed in *SOX2*, *CD133* and *OCT4* stem cell markers [Figure R3-4.C-D], where their expression was significantly decreased when these cells were differentiated. These results demonstrate that *SOX1* levels are highly enriched in the GSCs population and also that high *SOX1* expression correlates with the glioma cell undifferentiated condition.

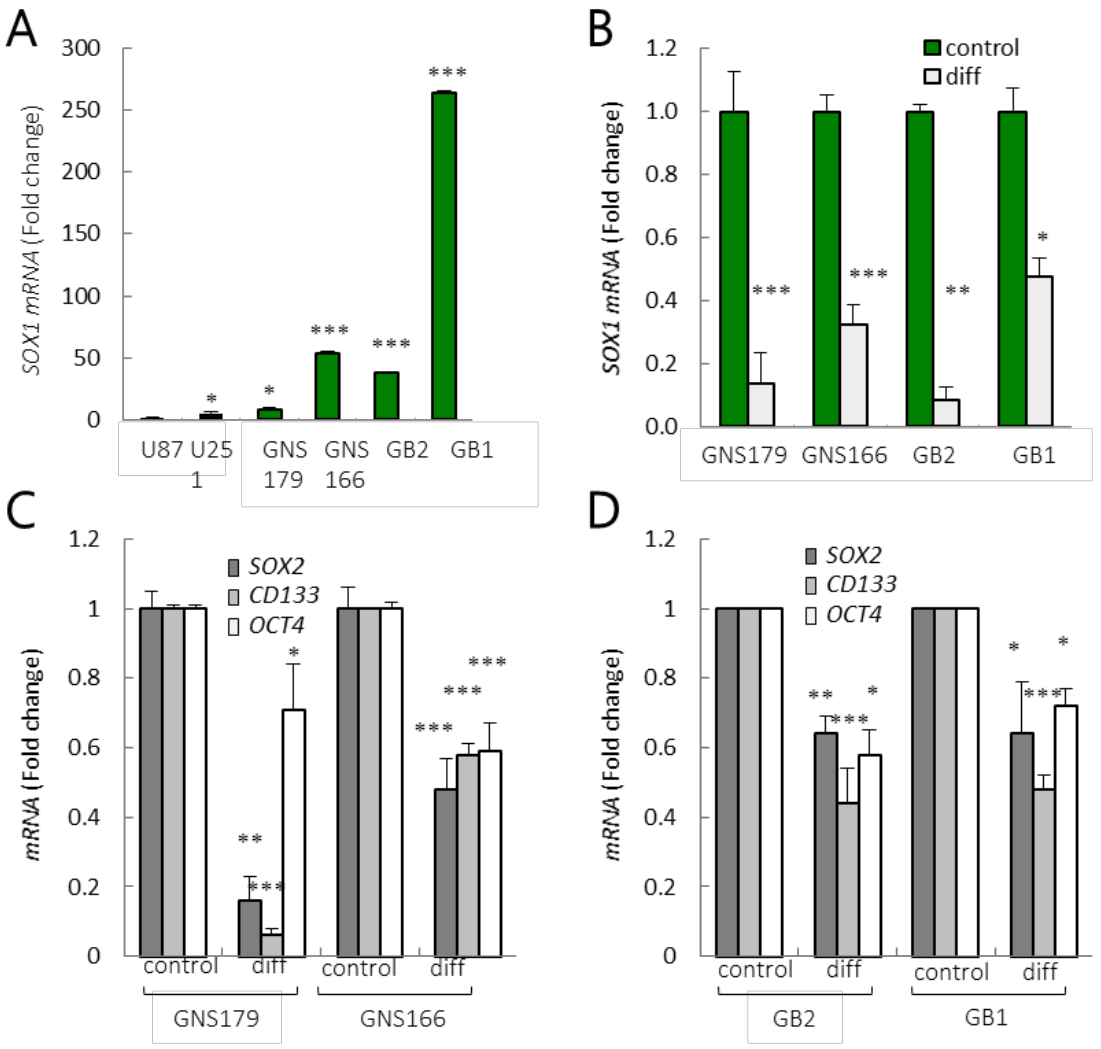

Figure R3-4. *SOX1* is enriched in GSCs population. (**A**) *SOX1* mRNA levels in U87 and U251 glioma conventional cell lines, and four patient derived GSC lines. *SOX1* expression is represented relative to the U87 cell line ($n \geq 3$). (**B**) *SOX1* mRNA levels in four GSC lines cultured in stem cell media (control) compared to differentiated cell lines (diff) ($n \geq 2$). mRNA levels of the indicated stem cell markers grown in stem cell media (control) and differentiation conditions (diff) in (**C**) GNS and (**D**) GB cells ($n \geq 2$).

SOX1 knock-down inhibits GSC activity

To directly and specifically explore the SOX1 role in GSCs activity, we knocked-down *SOX1* expression in a patient-derived cell line (GNS166) using two independent shRNAs. First, we demonstrated an effective inhibition of *SOX1* when using both shRNAs constructs (*sh1* and *sh5*) by RT-qPCR [**Figure R3-5.A**]. Functionally, the silencing of this transcription factor promoted a significant decrease of more than 2-fold in cell growth rates [**Figure R3-5.B**]. Afterwards, we performed MTT studies in order to analyze cell viability. In line with the previous results, MTT studies showed a diminished cell viability

rate in *SOX1* silenced GNS166 cells [**Figure R3-5.C**]. The observed phenotypes correlated also with a diminishment in the number of PHH3 positive cells [**Figure R3-5.D**]. Specifically, the percentage of proliferating cells decreased in more than 70 % in the *sh1* and *sh5* conditions comparing with control condition [**Figure R3-5.D**].

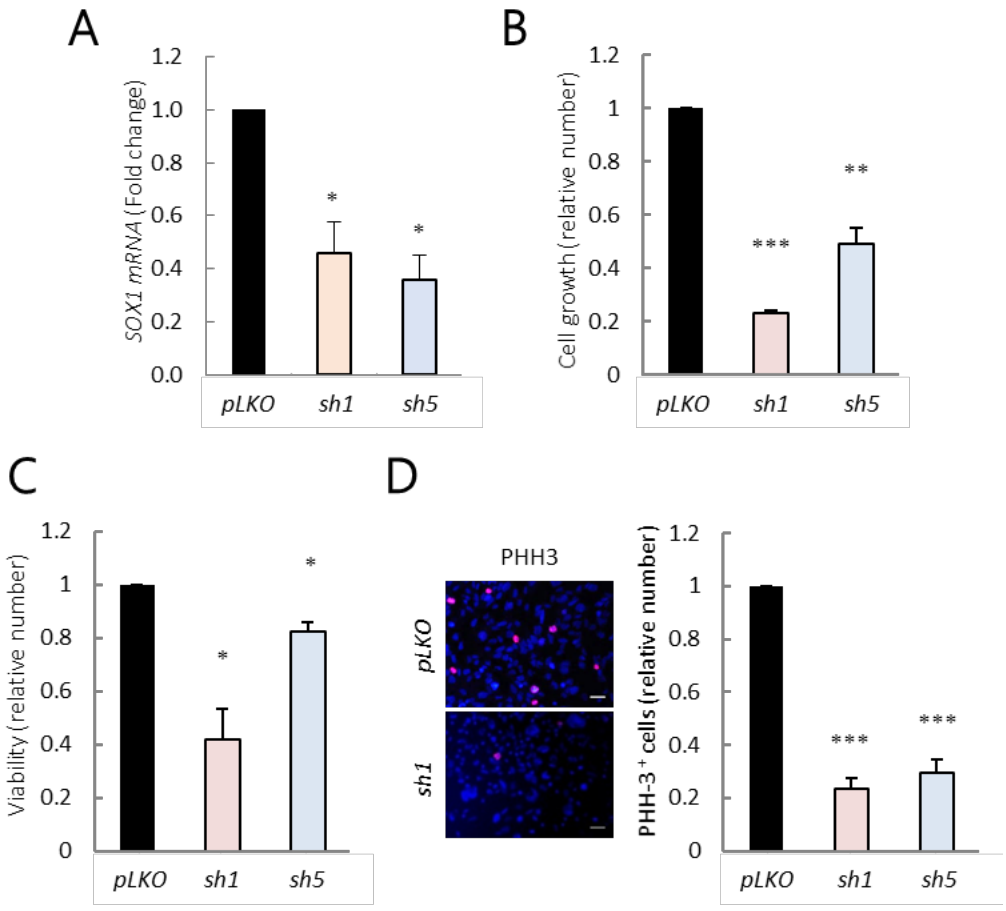

Figure R3-5. *SOX1* knock-down impairs GSCs proliferation and viability. (**A**) *SOX1* mRNA levels in control (*plKO*) and *shSOX1* (*sh1* and *sh5*) GNS166 cells ($n \geq 2$). (**B**) Relative cell growth at day 5 comparing *plKO* and *shSOX1* conditions in GNS166 cells ($n = 3$). (**C**) Cell viability assessment by MTT in *shSOX1* relative to *plKO* GNS166 cells ($n = 3$). (**D**) Representative images and quantification of the PHH3 positive cells in *plKO* and *shSOX1* conditions in GNS166 cells ($n = 3$).

To further determine *SOX1* impact on GSCs' self-renewal regulation ability, we first measured the mRNA expression of several stem cell and differentiation markers in our *SOX1* silenced GSC model. Notably, we observed a reduction in the *NESTIN*, *SOX2*, *SOX9* and *PML* stem cell markers [**Figure R3-6.A**]. Concomitantly, we observed an increase in *GFAP* and $p27^{KIP}$ expression levels, a differentiation marker and a cell cycle inhibitor,

respectively [Figure R3-6.B]. Altogether, these results point out that *SOX1* plays a relevant role in GSC plasticity, by regulating the stemness-differentiation dichotomy.

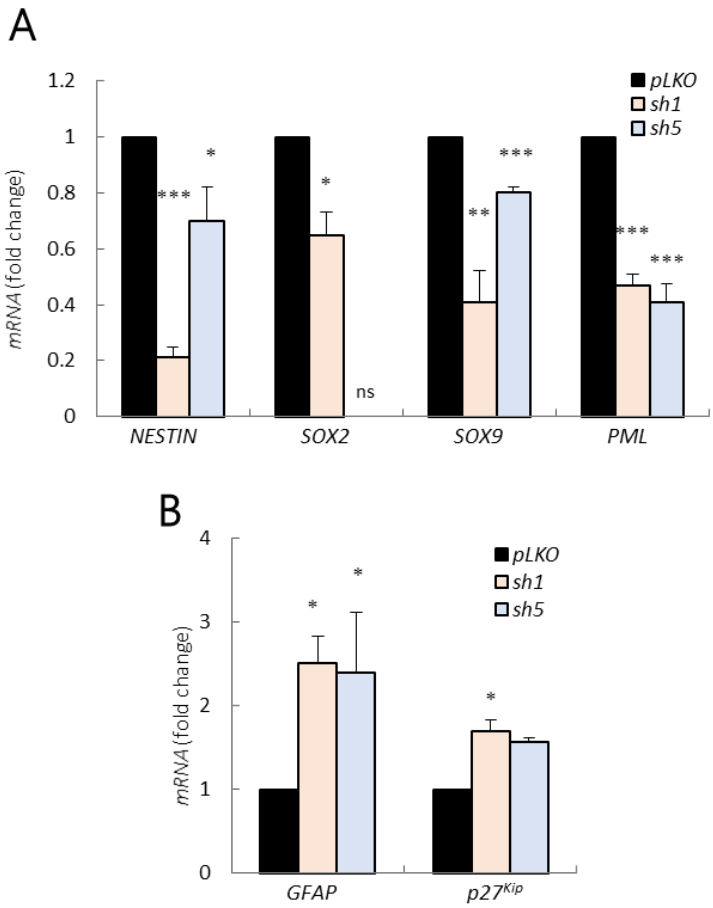

Figure R3-6. *SOX1* knock-down reduces stemness and induces differentiation. (**A**) mRNA levels of the indicated stem cell markers in *sh1* and *sh5* GNS166 cells relative to control (*plKO*) GNS166 cells' expression ($n \geq 2$). (**B**) *GFAP* and $p27^{KIP}$ mRNA levels in the indicated experimental conditions ($n \geq 2$).

The gold standard method to determine the presence of GSCs is to analyze the capacity of the original patient's tumor to replicate that tumor *in vivo* when it is orthotopically transplanted in immunocopromised mice(Lathia et al., 2015). Therefore, *plKO* and *sh1* GNS166 cells were injected intracranially in NOD-SCID mice. Interestingly, *SOX1* silencing significantly delayed GNS166 cells' tumor formation capacity [Figure R3-7]. Thus, our results demonstrated that the median survival for mice injected with *plKO* cells was lower than for the mice injected with *sh1* cells [Figure R3-7]. Specifically, mice injected with *plKO* cells presented a median survival of 27 weeks, whereas mice injected with *sh1* cells survived a median of 42 weeks (an increment of about 50 %). Taken

together, these results show that SOX1 regulates GSCs self-renewal and their tumorigenic activity.

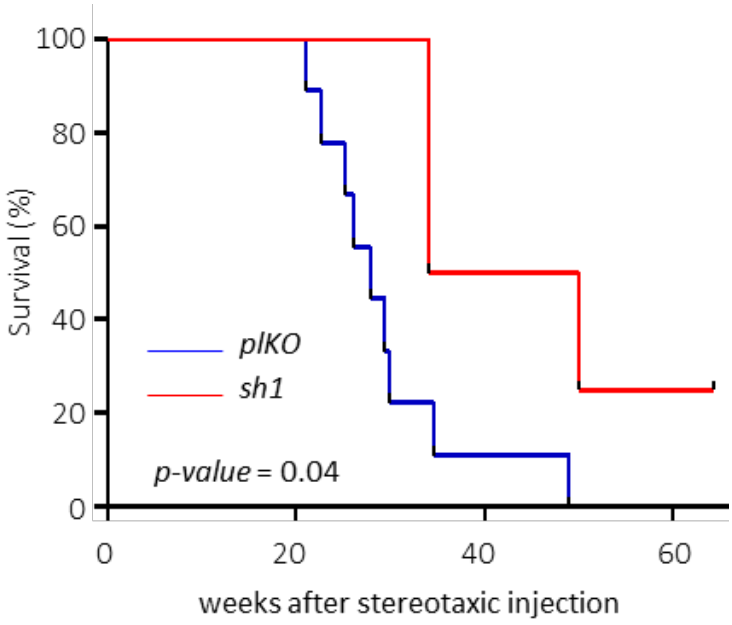

Figure R3-7. *SOX1* knock-down reduces tumor growth *in vivo*. Kaplan-Meier curve representing survival of NOD-SCID mice that were xenotransplantated with *plKO* (n = 9) and *sh1* (n = 4) GNS166 cells.

SOX1 knock-down inhibits U251 glioma cells-related tumor initiation and progression in vitro and in vivo

In order to determine whether the mechanism by which *SOX1* regulates GBM cell proliferation and tumor growth is GSC-specific or broader, we knocked-down *SOX1* expression in the parental U251 cell line. Western blot analysis demonstrated an effective inhibition of SOX1 at protein level [**Figure R3-8.A**]. Tumor-initiation ability, measured by limiting dilution injections, and oncosphere formation assays functionally defines self-renewal capacity of CSCs *in vivo* and *in vitro* respectively (Clevers CSCs premises). Therefore, we tested if *SOX1* silencing could regulate tumor initiation ability *in vivo* by performing subcutaneous inoculations of serial dilutions of U251 cells transduced with empty vector or both *shSOX1* constructs (*sh1* and *sh5*) in immunocompromised mice. In addition, we performed oncosphere formation assays in order to assess self-renewal ability *in vitro*. The limited dilution assay demonstrated that the frequency of tumor initiation was 1/1,050,263 in *sh1* and 1/6,359,439 *sh5* cells compared to 1/108,183 in the

control cells [**Figure R3-8.B**]. In line with these results, *SOX1* silencing markedly decreased the U251 cells ability to generate oncospheres [**Figure R3-8.C**]. Furthermore, at molecular level, *SOX1* silencing in U251 cells decreased *PML* and *SOX2* expression [**Figure R3-8.D**] and up-regulated $p27^{KIP}$ levels [**Figure R3-8.D**]. These results imitate the phenotype obtained in the GSCs performed experiments and further reinforce the robust effect that *SOX1* silencing displays on blocking self-renewal and tumor initiation capacity of glioma cells.

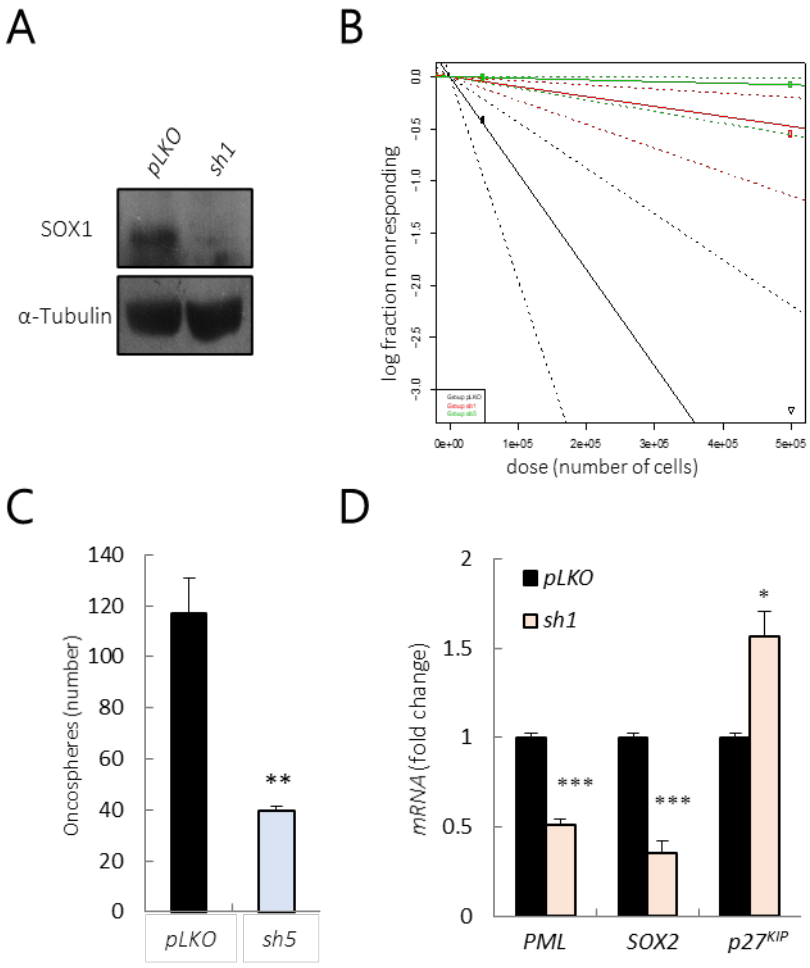

Figure R3-8. *SOX1* knock-down reduces tumor initiation and self-renewal ability in U251 cells *in vivo* and *in vitro*. (**A**) Representative Western Blot image of SOX1 protein expression in U251 cells infected with *plKO* or *sh1* (n = 3). (**B**) Tumor initiation frequency after subcutaneous injection in nude mice of 5 x 10^4 and 5 x 10^4 U251 cells infected with *plKO*, *sh1* and *sh5.* The incidence of tumor initiation was measured using ELDA platform. (**C**) Quantification of the oncospheres formed in the indicated conditions (n = 3). (**D**) mRNA levels of the indicated genes in *sh1* U251 cells relative to *plKO* cells (n = 3).

We went feeper and further evaluated the effect of *SOX1* silencing U251 glioma cells. First, we performed cell counting experiments that revealed a significant reduction

of more than 70 % in cell growth rates in *SOX1*-silenced U251 cells [Figure R3-9A]. Moreover, when analyzing the number of PHH3 positive cells, we detected a reduction of the positivity by a mean of 90 % and 50 % in the case of *sh1* and *sh5,* respectively. This indicates that cell proliferation is dramatically impaired when *SOX1* expression was down-regulated [Figure R3-9B].

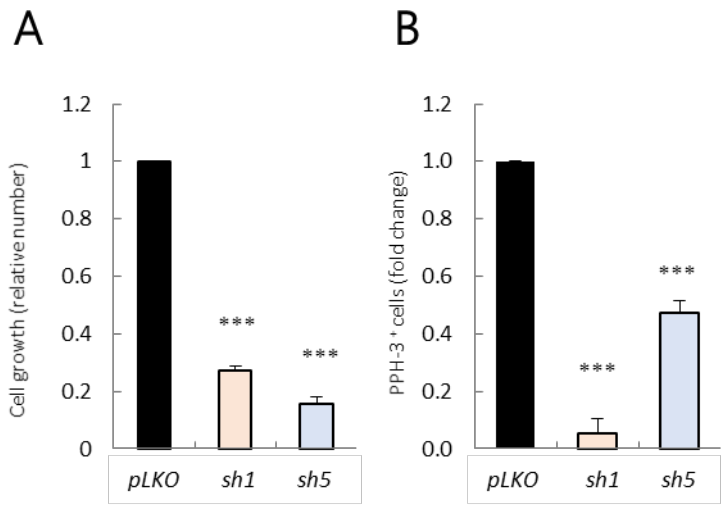

Figure R3-9. *SOX1* knock-down reduces proliferation of U251 cells *in vitro*. (**A**) Relative cell growth at day 5 comparing *plKO* with *sh1* and *sh5* U251 cells (*n* = 3). (**B**) Quantification of PPH3 positive *sh1* and *sh5* U251 cells relative to *plKO* U251 cells (*n* = 3).

Moreover, we investigated the effect of *SOX1* silencing *in vivo*. When injecting subcutaneously *plKO* and both *shSOX1* (*sh1* and *sh5*) U251 cells in immunocompromised mice, we observed a significant decrease in *shSOX1* cells tumor growth [Figure R3-10.A]. Indeed, both *shSOX1* U251 cells formed subcutaneous tumors reaching less than 75 mm^3 in 40 days after injection, while control tumors grew to an average of 550 mm^3 in the same period of time [Figure R3-10.A]. Moreover, the tumors formed from *sh1* and *sh5* U251 cells present a significantly lower weight [Figure R3-10.B].

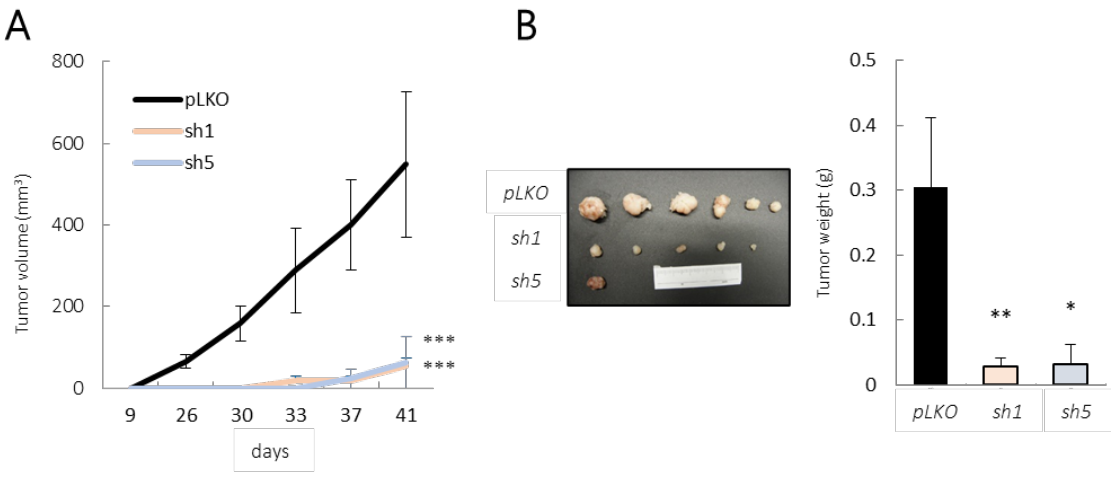

Figure R3-10. *SOX1* knock-down reduces tumor progression of U251 cells *in vivo*. (**A**) Tumorvolume after subcutaneous injection of *plKO*, *sh1* and *sh5* U251 cells at the indicated time points (*n* = 12). (**B**) Picture and average weight of the tumors generated in **A**.

To further characterize the impact of *SOX1* silencing at molecular level *in vivo,* we performed immunohistochemistry analysis in the tumors generated after subcutaneous injection in order to corroborate the impaired tumorigenic ability. Indeed, *sh1* and *sh5* U251 cells derived xenografts displayed lower number of SOX1, KI67, SOX2 and PML positive cells than those derived from control cells [**Figure R3-11**].

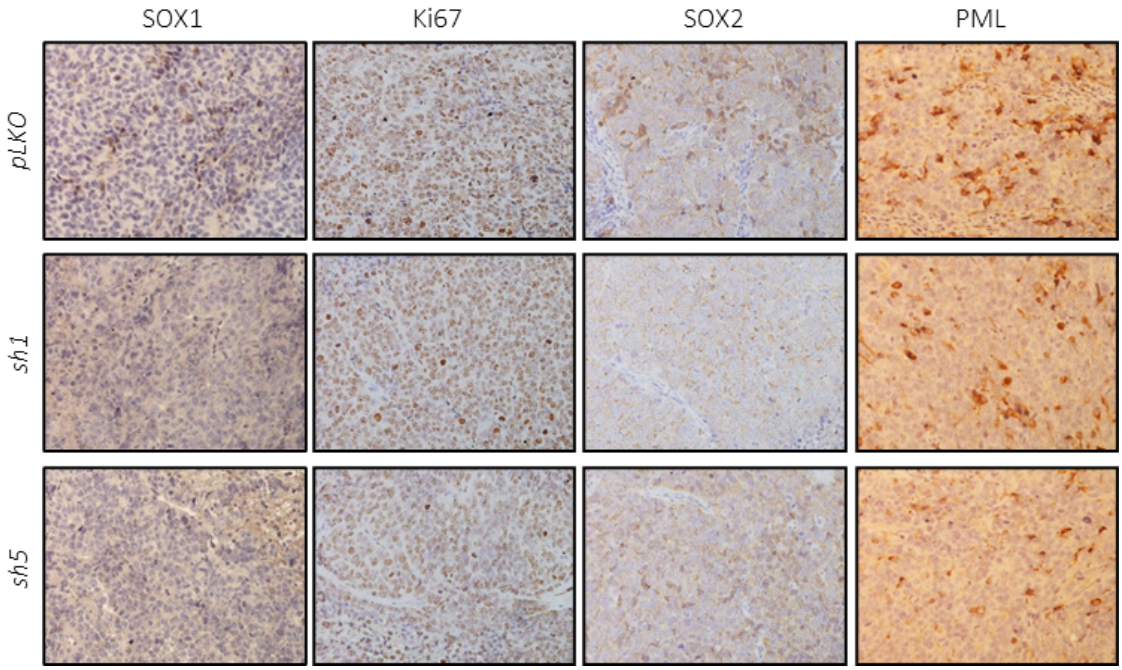

Figure R3-11. *SOX1* knock-down reduces tumorigenic ability of U251 cells *in vivo*. Representative images of the immunohistochemical staining of KI67, SOX1, SOX2 and PML in tumors generated in **figure R3-10.A**.

In summary, *SOX1* genetic silencing induces a strong tumor suppressor phenotype in glioma cells by impairing self-renewal, proliferation, tumor initiation and progression capacity of both glioma cells and GSCs.

SOX1 activity is not mediated by WNT/β-catenin signaling pathway in glioblastoma

Since SOX1 has been described as tumor suppressor in different cancer types through the Wnt/β-catenin signaling pathway (Guan et al., 2014; Tsao et al., 2012), we examined the activity of different proteins belonging to this pathway after *SOX1* silencing in glioma cells and GSCs. CTNNB1, also known as β-catenin, immunofluorescence and immunohistochemistry analysis did not show any clear differences between *plKO* and *shSOX1* U251 cells nor in its expression neither in its nuclear translocation, neither *in vitro* nor *in vivo* [**Figure R3-12.A-B**]. Moreover, we analyzed the expression levels of *β-catenin* and *MYC,* a well-established β-catenin downstream target (Santos et al., 2016), by RT-qPCR in *SOX1*-silenced GNS166 cells, but we did not observe any significant modification in their expression [**Figure R3-12.C**]. To pursue the association between SOX1 and β-catenin, we turned to human GBM biopsies. The results at cellular level were confirmed in the datasets of TCGA cohort, where the correlation analysis did not find any association between *SOX1* and *β-catenin* or *MYC* expression levels [**Figure R3-12.D**]. These results suggest that SOX1 oncogenic activity is not mediated by β-catenin signaling pathway in both GBM cells and clinical samples.

We also studied the expression of *CYCLIN D1*, also known as *CCND1*, an additional β-catenin downstream target (Santos et al., 2016). In this case, *shSOX1* GNS166 cells presented diminished levels of *CYCLIN D1* [**Figure R3-12.C**], and interestingly, its expression was significantly correlated to *SOX1* in the TCGA datasets (*p-value* <0.005) [**Figure R3-12.D**]. These results postulate CYCLIN D1 as a putative mediator of SOX1 activity in GBM.

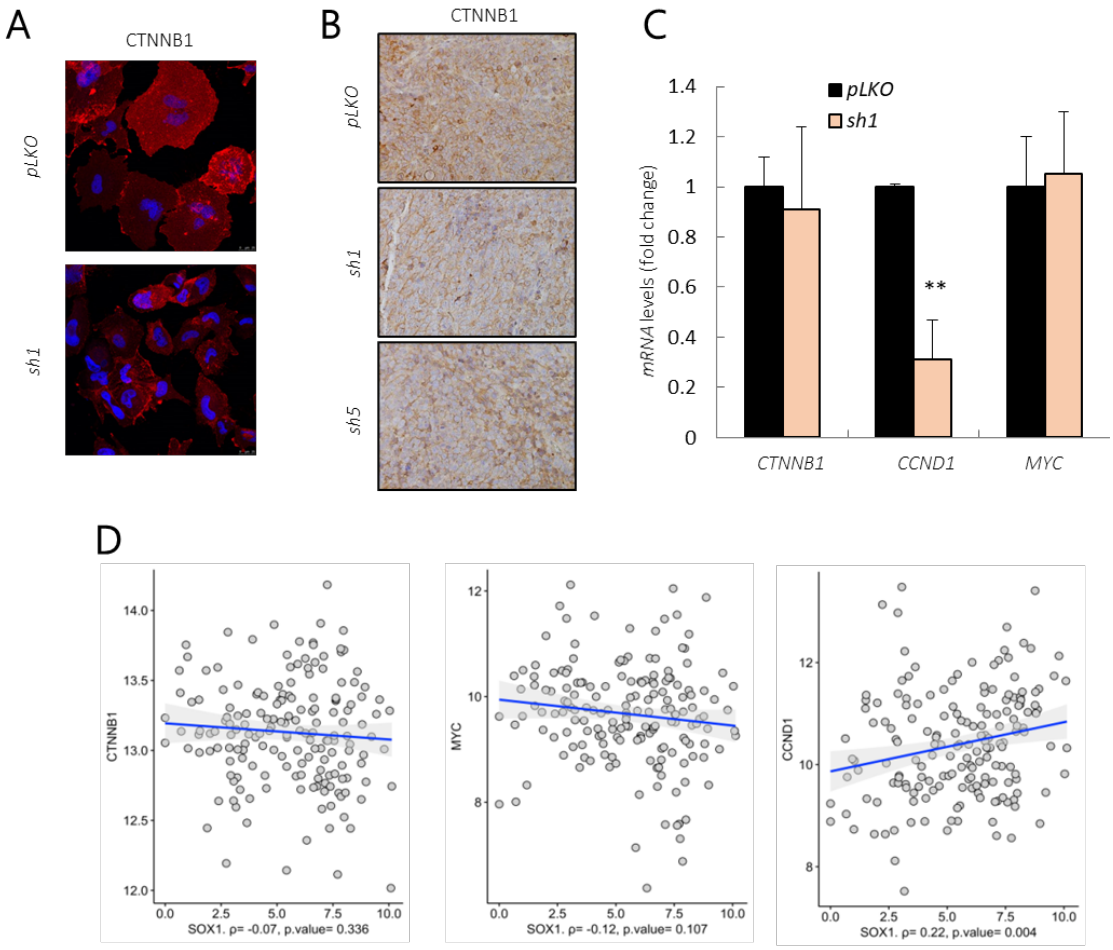

Figure R3-12. SOX1 activity is not mediated by the WNT signaling pathway in GBM. (**A**) Representative images of CTNNB1 immunofluorescence staining in U251 *plKO* and *sh1* cells (n = 4). (**B**) Representative images of CTNNB1 immunohistochemical staining in U251 *plKO, sh1* and *sh5* derived subcutaneous tumors (n = 4). (**C**) mRNA levels of *CTNNB1*, *CCND1* (*CYCLIN D1*) and *MYC* in GNS166 *plKO* and *sh1* cells ($n \geq 2$). (**D**) Scatter plot of log2 of the fragments per kilobase of exon model per million reads mapped (FPKM) of *CTNNB1, MYC* and *CCND1* vs *SOX1* expression. In the x-axis, the correlation and its statistical significance are included.

Ectopic SOX1 overexpression could promote GSCs proliferation and self-renewal

Finally, we introduced a construct encoding *SOX1* gene sequence in GNS166 cells in order to overexpress this gene. We confirmed this overexpression by Western blot analysis and RT-qPCR [**Figure R3-13.A-B**]. First, we analyzed whether *SOX1* overexpression modifies the expression of different stem cell and differentiation markers. In this context, we found that *SOX1* overexpression slightly increased *SOX2* and *PML* stem cell markers

expression [**Figure R3-13.A-B**], whilst decreased *GFAP*, *CNPase* and *p27*^{KIP} differentiation markers' levels [**Figure R3-13.C**].

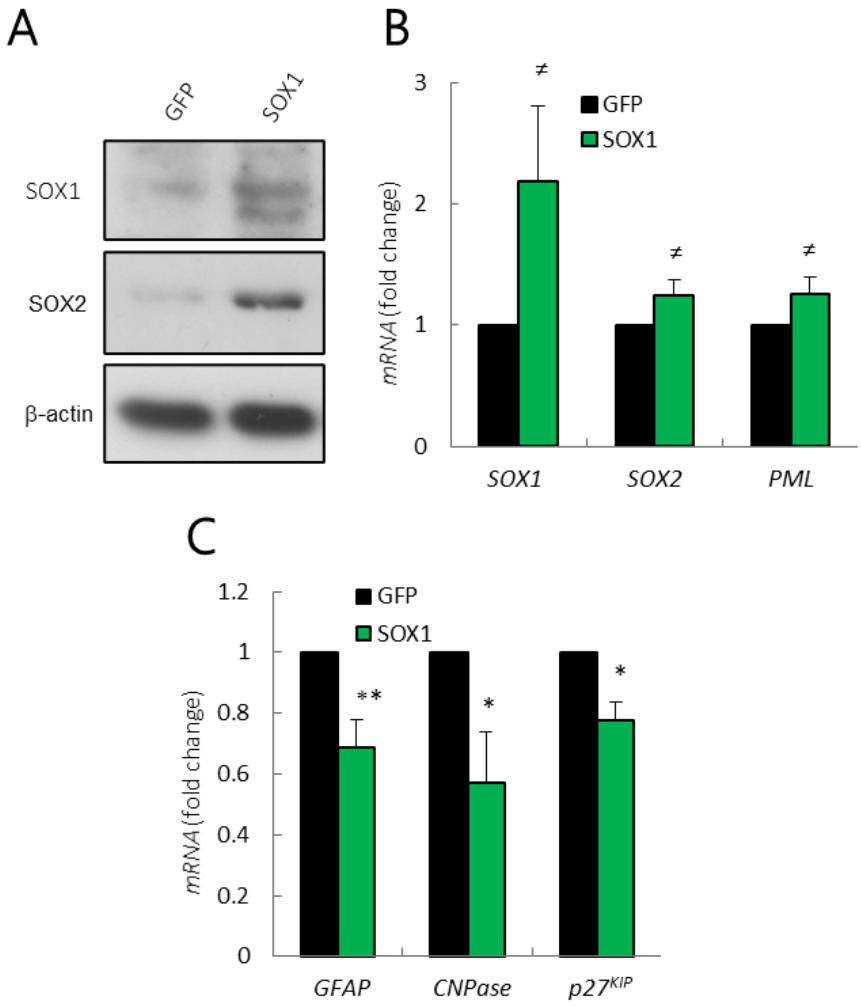

Figure R3-13. *SOX1* overexpression augments stem cell markers' expression and diminished differentiation markers expression. (**A**) Western Blot analysis of SOX1 and SOX2 proteins in GNS166 cells transduced with ectopic *SOX1* (n = 3). (**B**) mRNA levels of the indicated stem cell markers in GNS166 cells transduced with *SOX1* relative to control (GFP) expression ($n \geq 3$). (**C**) mRNA levels of the indicated differentiation markers in the same cells ($n \geq 3$).

Phenotypically, cells with *SOX1* overexpression exhibited moderately higher cell growth curves [**Figure R3-14.A**] and proliferation rates compared to control cells, since they present a higher percentage of PHH3 positive cells [**Figure R3-14.B**]. Altogether, these data reveal that *SOX1* activity is not only necessary for the maintenance but might also promote proliferative and self-renewal activity in GSCs.

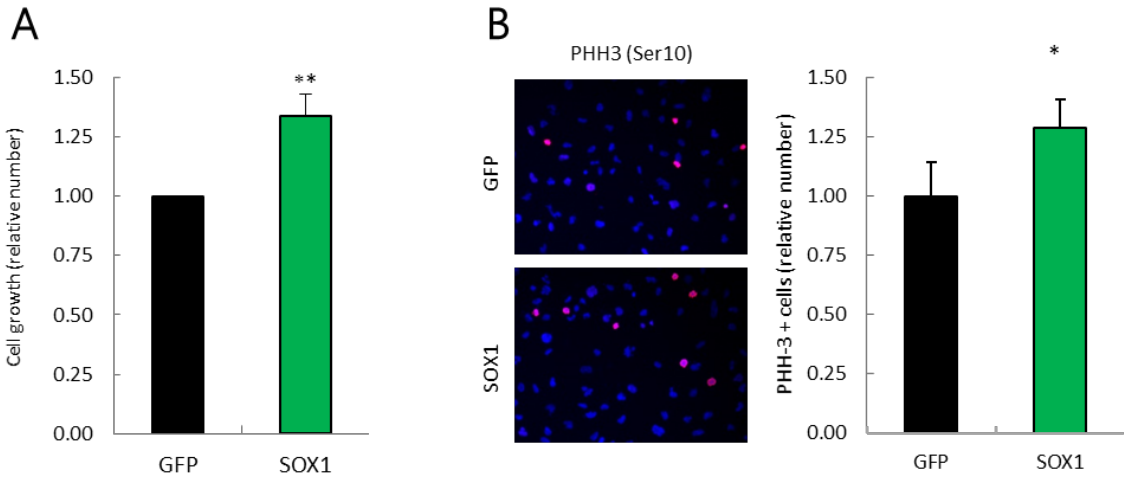

Figure R3-14. *SOX1* overexpression augments GSCs proliferation capacity. (**A**) Relative cell growth at day 5 comparing control (GFP) to *SOX1* overexpressing GNS166 cells (n = 6). (**B**) Representative images and quantification of PHH3 positive cells in *SOX1* overexpressing GNS166 cells compared to control (GFP) condition (n = 6).

Discussion

The complete development of the cerebellum occurs postnatally and it is a well-regulated process by different signaling pathways (Leto et al., 2016), where cerebellar granule cell progenitors (CGNPs) undergo a rapid proliferation stage followed by a differentiation and migration one (Komuro and Rakic, 1998; Kuhar et al., 1993). When a dysregulation of this process occurs and CGNPs continue proliferating, MB tumor can be generated (Grimmer and Weiss, 2006; Marino, 2005; Northcott et al., 2019). This is the most common solid tumor in childhood (Bartlett et al., 2013). Even if 70 % of the patients survive, treatments used nowadays generate incurable side effects (Musial-Bright et al., 2011; Saury and Emanuelson, 2011). Regarding adulthood brain tumors, GBM is the most common and aggressive brain tumor (Ostrom et al., 2014). It presents a very low survival rate (Stupp et al., 2009). For both tumors, the current therapy is ineffective. One of the reasons to explain the failure of current treatments could be the existence of the CSCs, whose presence has been demonstrated in MB and GBM (Galli et al., 2004; Singh et al., 2003; Singh et al., 2004b). These cells are the responsible of treatment resistance and tumor recurrence, since they can stay in a quiescent stage for long periods, thus evading therapies targeting proliferative cells (Recasens and Munoz, 2019). Considering all this information, it seems clear the necessity of finding new therapies for these tumors' treatment, and that targeting CSCs is the most successful strategy.

For this aim we considered ERBB4 and SOX1 genes. On the one hand, ERBB4 is a tyrosine kinase receptor implicated in embryonic development (Segers et al., 2020; Tidcombe et al., 2003) and described to play a role in cerebellum development (Pinkas-Kramarski et al., 1997; Vullhorst et al., 2009). On the other hand, SOX1 is a transcription factor also implicated in early development (Aubert et al., 2003; Kan et al., 2004; Pevny et al., 1998; Venere et al., 2012). Moreover, both of them have been related to different types of cancer (Guan et al., 2014; Hyman et al., 2018; Hynes and Lane, 2005; Lin et al., 2013; Muraoka-Cook et al., 2008; Naresh et al., 2006; Su et al., 2009; Tsao et al., 2012; Vermeulen et al., 2016), acting as tumor suppressors or oncogenes. Moreover, they have been correlated to stemness and proliferative capacity (Birchmeier, 2009; Williams et al., 2015; Wright et al., 2008). Thus, we hypothesize that ERBB4 and SOX1 could, on the one hand, play an essential role in cerebellum development and, on the other hand, in the

development and maintenance of MB and GBM tumors and cancer stem cells activity. We specifically hypothesize that ERBB4 and SOX1 could play an oncogenic role in MB, and that SOX1 also could be is implicated in the carcinogenesis of GBM. Moreover, this implies that they are implicated in CSCs proliferation and self-renewal capacity, thus contributing to therapy resistance.

My thesis results demonstrate that ErbB4 has an important role in cerebellum development, by governing and maintaining CGNPs' proliferation and migration. Moreover, we demonstrated that both SOX1 and ERBB4 are enriched in the CSC pool and that their silencing decreases the proliferative and self-renewal capacity of both differentiated and stem-like cells. In addition, we found that ERBB4 is overexpressed specifically in Group 4 MBs and that SOX1 presents higher expression levels in SHH MBs. Finally, we have showed also that both genes high expression is related to poor patients' survival. Specially, GBM overexpressing SOX1 are related to poor clinical outcome. Considering all these results, we suggest ERBB4 and SOX1 as new prognostic biomarkers and as novel therapeutic targets in MB and GBM brain cancers.

1. ERBB4 is required for cerebellar development and medulloblastoma malignant phenotype

As mentioned before, cerebellum development is a postnatal process, well regulated by different signaling pathways that direct embryonic developmental processes (Leto et al., 2016). If deregulated, these pathways can let to MB formation and progression (Dey et al., 2012; Grimmer and Weiss, 2006; Zurawel et al., 1998).

ERBB4 is a tyrosine kinase membrane receptor essential for the normal neural development and maintenance and involved in cell migration control (Fornasari et al., 2016; Mei and Xiong, 2008; Ortega et al., 2012). Indeed, its genetic deletion leads to neurodevelopmental deficits affecting neuronal migration in multiple brain structures, from the cortex to the cerebellum (Perez-Garcia, 2015).

Considering all these evidences, we hypothesize that ErbB4 could be considered as a key player in neural progenitors' and cerebellum development regulation and MB formation.

1.1. ErbB4 directs CGNPs migration during cerebellar development

In this thesis we firstly wanted to assess the role of ErbB4 in cerebellar development. It has been described that both CGNPs and radial fiber express ErbB4 *in vitro* and *in vivo* (Rio et al., 1997). To investigate the role of this receptor in the cerebellum, we first investigated ErbB4 expression in *wt* mice cerebella. Our analyses indicate that ErbB4 and its active form, P-ErbB4, are expressed in the EGL of the developing cerebellum, the proliferative layer of the cerebellum (Fujita, 1967). This may lead us to think that this membrane receptor is involved in the CGNPs proliferative capacity. Moreover, we took advantage of *ErbB4 KO* mice to investigate the cerebellar structure and different cell types' localization, finding an aberrant cerebellum development. As previous works have also demonstrated (Perez-Garcia, 2015), we found that migration of CGNPs was defective. First, we observed ectopic cell clusters in the EGL,

differentiated into neurons, since they expressed NeuN neuronal marker (Mullen et al., 1992). In a normal cerebellum development, these cells must be located in the IGL. Thus, we concluded that ErbB4 is not guiding CGNPs differentiation process. Same results were obtained by Perez-García (Perez-Garcia, 2015). Second, we observed GFAP-positive radial fibers misalignment, a starting point from where CGNPs migrate to achieve the IGL (Chedotal, 2010). These results point out the essential role of ErbB4 in the CGNPs migratory capacity and in the cerebellar structures formation. In fact, the importance of ErbB4 in different progenitors and neurons migration has been previously described. Indeed, lack of ErbB4 has been associated to a loss of GABAergic interneurons migration to the cortex, where Nrg1 acts as their chemoattractant (Flames et al., 2004). Moreover, lack of ErbB4 causes defects in cranial neural crest cells and cerebellar granule neurons migration (Golding et al., 2000; Tidcombe et al., 2003). It has been also described *in vitro* that Nrg ligands induce radial glia fibers formation (Rio et al., 1997) and that Nrg1/ErbB4 signaling promotes CGNPs migration by Akt/mechanistic target of rapamycin kinase (mTOR) signaling pathway (Yao et al., 2013). Finally, after neuronal migration, it has been demonstrated that Nrg1/ErbB4 signaling plays a crucial role in the neurite outgrowth induction in different cell types, such as hippocampal neurons (Gerecke et al., 2004), cerebellar CGNPs (Rieff et al., 1999) and PC12 cells, which have a neural crest origin (Vaskovsky et al., 2000). These findings reinforce our conclusion regarding ErbB4 essential role in the Bergmann glia formation, and thus, for the CGNPs migration during cerebellar development.

When this receptor ligands were analyzed, we were not able to detect the expression of the most investigated ErbB4 ligand, Nrg1, at protein level. However, we detected its expression in mRNA levels *in vivo*, so we then concluded that our negative result regarding Nrg1 expression in cerebellar tissue was probably due to technical difficulties, such as no appropriate antibody concentration or not selecting the correct antibody. Moreover, we detected Hbegf expression, another, although still controversial, ErbB4 ligand (Sweeney et al., 2000), at protein and mRNA levels. Interestingly, we found *in vivo* that Hbegf expression increases during cerebellar development, reaching the highest levels at p18, when cerebellum is totally developed. These results contradict those of Nakawaga et al. Indeed, they showed an Hbegf peak of expression at p5 and a

gradual expression decrease after p13, even with persistent detectable transcripts (Nakagawa et al., 1998). Nevertheless, their measurements were done in rat cerebella, so this difference can explain the contradictory results. Moreover, in contrast with Hbegf expression, our results show that Nrg1 expression remains at the same levels in the whole cerebellar development, same as *ErbB4* expression. So, we hypothesize that Nrg1 could be the ligand of ErbB4 in this process and that this one is the reason why both present same expression pattern. Regarding Hbegf ligand and ErbB4 receptor locations, surprisingly, we did not observe a colocalization, since we detected Hbegf expression in the IGL of the cerebellum, as other study has also described (Hayase et al., 1998), whereas ErbB4 seems to be located in the EGL. In addition, and confirming our results, Hbegf has been described to be expressed in the whole cerebellum (Piao et al., 2005), specifically in Purkinje cells, which present strong signals (Nakagawa et al., 1998). In line with these results, those obtained by treating CGNPs with Hbegf ligand were consistent, as we were not able to activate the ErbB4 receptor with this ligand *in vitro.* These results demonstrated that Hbegf is expressed in the developing cerebellum, so it must have an important role in this process. However, it does not seem to be related to ErbB4 signaling pathway. Although ErbB4 activation was not reach with Hbegf, we were able to achieve a high activation of the receptor when we treated these cells with Nrg1, demonstrating that this ligand may have a role in ErbB4 activation and function in cerebellar development, in accordance with what Yao et al. has described about the promotion of CGNPs migration by Nrg1/ErbB4 signaling pathway (Yao et al., 2013).

Although the role of Nrg in cerebellar development has been described in several studies [(Gilbertson et al., 1998; Rio et al., 1997), the Hbegf implication in this process has not been well characterized. In fact, even if Hbegf has been describe as an ErbB4 ligand (Elenius et al., 1997b), other studies have described that Hbegf does not activate ErbB4 in the absence of EGFR expression, and thus, it is presumably not its ligand. Instead, Nrg1 is able to activate ErbB4 in the absence of EGFR (Riese et al., 1996b). This might explain why we can activate ErbB4 *in vitro* with Nrg1 but not with Hbegf treatment.

Altogether, we concluded that ErbB4 directs CGNPs migration during cerebellar development, but the role of Hbegf and Nrg1 ligands in regulating this process remains

still unclear. Thus, further investigation will be needed to understand Hbegf-ErbB4 dynamic and interaction *in vivo* in this developmental process.

1.2. ErbB4 protects CGNPs and medulloblastoma cells from apoptosis

ErbB4 is known to protect ventricular myocytes (Fukazawa et al., 2003), neurons (Yan et al., 2017) and PC12 cells (Erlich et al., 2001) from apoptosis. Our data confirms this protection tendency as ErbB4 is also protecting CGNPs and MB tumor cells from apoptosis *in vitro* and *in vivo*. In fact, after treatment with dexamethasone apoptotic drug for CGNPs (Noguchi et al., 2015) and hNRG1, as an ErbB4 activator, both CGNPs and MB tumor cells are more resistant to apoptosis. Since NRG1 could activate other ERBB receptor family members, we confirmed the implication of ErbB4 specifically, and no other members implication, in this apoptosis protection by using *ErbB4 KO* mice CGNPs. In fact, results show that CGNPs coming from ErbB4 KO mouse were not resistant to dexamethasone treatment when treated with hNRG1. Thus, we demonstrated in this mouse model that ErbB4 was the ErbB receptor family member responsible of this apoptotic protection.

On the one hand, since ErbB4 protects CGNPs from apoptosis, we hypothesized that it might drive their proliferation and thus, facilitate MB formation. On the other hand, once the tumor is formed, ErbB4 might help in its progression by protecting tumor cells against apoptotic stimuli, such as anticancer therapies. Thus, according to all these findings, we suggest that ErbB4 would be implicated in MB formation and progression.

1.3. ERBB4 expression is higher in Group 4 MBs and correlates with poor prognosis

Once we observed that ErbB4 presents an important role in cerebellum development and protects both CGNPs and MB cells from apoptosis, and to prove our hypothesis of ERBB4 role in MB formation and progression, we moved to investigate the expression of this receptor in clinical samples.

In silico studies showed that *ERBB4* expression was elevated in MB samples and that its high levels were associated with poor patient survival. These data confirm the

prognostic significance of *ERBB4* expression, and provide the first evidences of *ERBB4* expression as a negative prognostic biomarker in MB. Moreover, its levels are higher in Group 4 MBs comparing with other MB subgroups in the four studied cohorts. While we were carrying out this project, results regarding aberrant ERBB4-SRC signaling in Group 4 MB were published (Forget et al., 2018). Interestingly, when considering only Group 4 patients' data in the survival analysis, *ERBB4* expression levels appeared to be even more significant.

Thus, we suggest that ERBB4 expression could be used as Group 4 MBs biomarker, and that its expression could be also a very useful tool as prognostic biomarker, specifically in this patients' subset.

1.4. ERBB4 promotes tumor progression and its silencing activates apoptosis

To specifically asses the role of ERBB4 in MB, we silenced this receptor expression and then performed different functional assays. My thesis results demonstrated that *ErbB4* experimental silencing significantly impairs cell growth and cell viability as a consequence of apoptosis induction. Although few studies have related ERBB4 with cancer malignant and aggressive phenotype, similar results have been observed in some tumor types. For instance, it has been observed that after ERBB4 suppression in human gastric cancer cells, their proliferation was markedly inhibited both *in vitro* and *in vivo* through PI3K/Akt signaling pathway inhibition (Xu et al., 2018), while another study has confirmed these results in melanoma cells (Prickett et al., 2009). All this information reinforces this thesis results. Furthermore, regarding cell apoptosis activation when inhibiting ERBB4, this phenotype corresponds to the results found *in vivo* in CGNPs and MB cells, where we saw an ErbB4 protective function in response to apoptotic stimuli. Moreover, as mentioned before, several works have related ERBB4 with apoptosis resistance (Erlich et al., 2001; Fukazawa et al., 2003; Yan et al., 2017).

These finding are interesting from the point of view of new therapeutic strategies, since we can hypothesize that ERBB4 inhibition could suppress tumor cells viability and activate their apoptosis, achieving tumor reduction.

1.5. *ERBB4 plays an important role in MBSCs maintenance*

CSCs have been described in many tumor types (Clarke et al., 2006) including MB (Aldaregia et al., 2018; Singh et al., 2003), and they have been described as therapy resistance and tumor recurrence responsible (Azzarelli et al., 2018; Kumar et al., 2017). Regarding MB cells stemness capacity, our results revealed an enrichment of *ERBB4* expression in the MBSCs population, since oncospheres grown in stem cell specific media present higher expression levels of this receptor. It is worth to note that *ERBB4* expression increment when culturing the cells in stem cell specific media, and that it was specially increased in DAOY and UW228 cell lines, but not in the other cell lines. This could be explained by the fact that the other cell lines express intrinsically higher levels of the receptor, thus it is more difficult to see a statistically significant increment when culturing the cells in stem cells specific media. Moreover, since *ERBB4* knocked-down cells present a decreased oncospheres formation capacity *in vitro* and tumor initiation *in vivo,* we confirmed the relevance of ERBB4 in MBSCs activity.

Altogether, we demonstrate that high *ERBB4* levels are involved in maintaining MBSCs population. These results are the first ones demonstrating the high expression of ERBB4 in MBSCs. Moreover, even if these results are the first ones relating *ERBB4* expression to MBSCs, this receptor has been previously related to stem cell function during embryonic developmental processes (Birchmeier, 2009) and to CSCs in human colon cancer (Williams et al., 2015). These results make sense of our results, since ERBB4 has been related to stemness ability in other tissues.

In summary, we concluded that ERBB4 expression is necessary for MBSC maintenance, and that it likely regulates the interplay between self-renewal and differentiation and behaves as an oncogene in MB. Thus, the inhibition of this receptor would be a promising new therapeutic approach, since it would not only reduce the viability and activate the apoptosis of the bulk tumor cells, but also the MBSCs, which remains in a dormant state and are not sensitive to conventional chemo- and radiotherapy (Najafi et al., 2019).

1.6. *ERBB4 silencing upregulates response to stimulus and cell death signaling pathways*

Finally, the work performed in the first chapter of this thesis shows evidence of the altered pathways when silencing *ERBB4*. After performing a transcriptomic analysis of DAOY cells with *ERBB4* silencing, we have observed a downregulation in cell signaling, morphogenesis and development related pathways and an upregulation in response to stimulus, such as growth factors, cytokines, drugs or stress, and cell death. These last findings are considered as advantageous to contemplate a therapy against ERBB4 receptor, since an upregulation of response to stimulus, such radiotherapy or chemotherapy, may reduce tumor resistance, and cell death increase will help for tumor size reduction.

The selected genes to be validated seem to be promising therapeutic targets too, specifically, the parathyroid hormone-related protein *(PTHLH)* and *TP63* genes. On the one hand, *PTHLH* appears upregulated with *ERBB4* silencing and when translating to clinical samples, it negatively correlates with *ERBB4* expression and its low expression levels are related, just as expected, to poor prognosis. PTHLH has been described as a SHH target gene (Sterling et al., 2006), which led us to hypothesize that it is more related to SHH driven MBs. Moreover, this protein high levels have been related to better prognosis in breast cancer (Tran et al., 2018), which goes in the same direction as our results, since ERBB4 silenced cells, which are less tumorigenic, express higher levels of *PTHLH*. However, there are several works that have related PTHLH with cancer progression and osteolytic bone metastasis (Katoh and Katoh, 2009; Yao et al., 2019), which contradicts our results. Thus, we hypothesize that PTHLH role in cancer could be tumor type dependent.

On the other hand, *ERBB4* silencing triggers *TP63* downregulation. In the clinic *TP63* positively correlates with *ERBB4* and its expression is related to worse prognosis. Moreover, both of these genes have been related in different manners to cancer. TP63 has been associated also with cancer and with ERBB4 signaling pathway (Forster et al., 2014; Orzol et al., 2015). TP63 gene encodes p63 protein, one of the p53 protein family members implicated in the regulation of normal stem cells and cancer stem cells

(Galoczova et al., 2018). Specifically, *TP63* is well known for its role in epidermal development. Moreover, it has been described to regulate luminal progenitor function and lactation via NRG1 (Forster et al., 2014). Regarding tumorigenesis, several works have related this transcription factor to cancer, as playing tumor-suppressor and oncogenic dual roles (Orzol et al., 2015). Even if *TP63* gene almost never presents mutations in human cancer, its activity is often increased in several cancers (Orzol et al., 2015) and also implicated in CSCs (Nekulova et al., 2011). All these results propose p63 as a transcription factor that might be mediated by ERBB4, and thus, used as biomarker and new therapeutic target in MB.

Thus, with these analyses we found two different genes that are regulated in some way by ERBB4, and that seem to be good prognostic biomarker and therapy target. However, more studies need to be done in order to investigate their role in MB. However, even if we found some signaling pathways altered with ERBB4 silencing, more experiments would be necessary to find the signaling pathway from where ERBB4 silencing is specifically causing the discovered phenotype.

As a summary of the first chapter of this thesis, our work has identified an important role of ErbB4 in cerebellum development, *ERBB4* expression as highly enriched in the MBSCs pool and its inactivation as significantly impairing their proliferative malignant properties and tumor initiation and progression. Taken together, our data depict a previously unknown role for ERBB4 as a central player of MB biology, prognosis and therapy.

More specifically, we postulate that ERBB4 has an important role in cerebellum development, governing and maintaining CGNPs' proliferation and migration. But it is not clear which one is the specific role of ErbB4 in this brain structure development, and which are the ligands that are activating the receptor in this process. So, further investigation is needed in order to clarify these aspects.

Moreover, we revealed that *ERBB4* is overexpressed in Group 4 MBs, the most common group, and that its high expression levels are associated with shorter overall

patient survival. Furthermore, we demonstrated that ERBB4 inhibition has the ability to reduce MB cells viability and MBSCs stemness ability. Altogether, these results enable the stratification of the patients in terms of ERBB4 expression levels. The prospective of this work is to achieve an effective ERBB4 inhibitor that could be used in combination with traditional chemo and radiotherapy in Group 4 patients or in patients with high ERBB4 expression. The objective of this treatment combination is, first, to target both tumor bulk cells and MBSCs, thus avoiding or hindering tumor recurrence and treatment resistence, and secondly, to reduce the doses of the current therapies in order to reduce their side effects [Figure D1].

2. High SOX1 expression is a hallmark of SHH medulloblastomas and its inhibition depletes tumor malignancy

As mentioned above, MB is generated due to a dysregulation in cerebellum development process (Grimmer and Weiss, 2006). Different genes and signaling pathways that direct this embryonic process has been also implicated in tumor formation, such as WNT and SHH pathways, that are related to MB formation (Dey et al., 2012; Zurawel et al., 1998). There are several evidences that a lot of transcription factors that participate in developmental processes act also as oncogenes, by reactivating necessary processes for tumorigenesis (Suva et al., 2013). Among these transcription factors, SOX1, is a transcription factor essential for maintaining the neural progenitors' proliferation. However, its continued expression leads to neuronal differentiation (Kan et al., 2007). SOX1 absence causes epilepsy (Malas et al., 2003), but its lack could be partially compensated by the other members of the SOXB1 subgroup of transcription factors, SOX2 and SOX3, since it has been demonstrated an overlapping expression pattern of these factors in neural progenitor cells (Bylund et al., 2003; Venere et al., 2012). Interestingly, SOX1 is also implicated in cerebellar development, as it has been described to be expressed in the Bergmann glia progenitors (Alcock and Sottile, 2009; Sottile et al., 2006). Considering all these evidences, we hypothesize that SOX1 could be considered as a key player in neural progenitors' and cerebellum development regulation and MB formation.

2.1. SOX1 could be a better prognostic biomarker for SHH MBs

In the second chapter of this thesis we wanted to assess SOX1 relevance in MB formation and progression. For this aim, we took advantage of publicly available cohorts. We first investigated *SOX1* expression in human MB samples. It is worth to note that it has been previously described that *SOX1* is a negative regulator of WNT/β-catenin signaling pathway in several tumor types (Guan et al., 2014; Mojsin et al., 2015; Song et

al., 2016; Tsao et al., 2012; Yang et al., 2015). Interestingly, the results show that SHH MBs present higher SOX1 expression levels, which are associated with shorter patients' survival. We wondered whether *SOX1* could be used as a patient stratification biomarker in this MBs subtype and if it could be a better biomarker than the SHH signaling pathway genes expression. To achieve this goal, we investigated the expression levels pf SHH signaling pathway different member genes, such as *SHH*, *SMO*, *PTCH1*, *GLI1*, *GLI2* and *GLI3*. We found a positive correlation between these genes and *SOX1* expression. These results reinforced the probable relation between *SOX1* and this signaling pathway and also our hypothesis that SOX1 could be a good SHH group biomarker. Surprisingly, only one of the SHH signaling pathway genes (*GLI2*) seemed to be a good subgroup and prognostic biomarker, since it was the only one presenting the higher expression in SHH subgroup and this high expression was correlated with poor prognosis. The lack of SHH signaling pathway genes overexpression in SHH subgroup can be explained since mutations that lead to constitutive activation of the SHH pathway in medulloblastomas have been identified, usually targeting the *PTCH1*, or less frequently *SUFU* or *SMO*, leading to expression of the oncogenic transcription factor *GLI1* (Pietsch et al., 1997; Raffel et al., 1997; Reifenberger et al., 1998; Taylor et al., 2002; Wolter et al., 1997). However, the correlations between SHH pathway genes and overall survival present worse statistical results than the ones obtained with *SOX1* analysis, highlighting the potential of *SOX1* as a significant biomarker of SHH subgroup. Regarding the evidences relating SOX1 with SHH signaling pathway, a single study has described that SHH supplementation to human embryonic stem cells increases SOX1 expression *in vitro* (Wu et al., 2010), so the relation between them needs to be further investigated.

Moreover, as we have demonstrated in the third chapter of this thesis that SOX1 is regulated by SOX2 in GBM, we wondered if in MB SOX1 could be regulated by different SOX family members. We investigated the relation of SOX2, SOX4 and SOX9 with SOX1 and with MB overall survival, not finding any significative relation between SOX1 and the other SOX members. Thus, we concluded that in MB SOX1 is not regulated by other SOX family members.

All this thesis chapter data confirms the *SOX1* expression significance for patients' stratification and prognostic, showing it as even better than the SHH signaling pathway

genes, and thus, reinforcing our hypothesis. Moreover, the evidence of *SOX1* expression involvement as a negative prognostic biomarker in MB is determined for the first time in this work. Indeed, *SOX1* has been related to several cancer types, but not always with an oncogenic role. In fact, low *SOX1* expression has been correlated with shorter overall survival and poor prognosis in ovarian cancer (Su et al., 2009), human hepatocellular carcinoma (Lou et al., 2015; Tsao et al., 2012), and esophageal squamous cell carcinoma (Kuo et al., 2014; Rad et al., 2016). Until this thesis, high *SOX1* expression has not been correlated with shorter overall survival.

This thesis data and obtained findings demonstrate tumor type dependent SOX1 role in cancer. This SOX1 divergent role could be explained by two different theories. On the one hand, it has been demonstrated that *SOX1* expression is modulated by epigenetic status, since low expression levels of *SOX1* and a better prognosis has been related to these gene's promoter methylation in different tumor types (Guan et al., 2014; Kuo et al., 2014; Tsao et al., 2012). On the other hand, the cellular plasticity and heterogeneity could explain this *SOX1* divergent role, since it has been described that *SOX1* is one of the 19 neurodevelopmental transcription factors that are active and have higher expression in GSCs than in differentiated cells (Suva et al., 2014).

2.2. SOX1 controls tumor proliferation in vitro and in vivo

After analyzing *SOX1* effect in human cohorts, we explored its role in MB cells *in vitro*. For this aim, we knocked-down and enhanced its expression. The experimental silencing in MB cell lines markedly reduced their proliferative capacity and cell viability *in vitro* and delayed tumor formation *in vivo*. However, the overexpression slightly increased the proliferative capacity of MB cells.

As it has been mentioned, SOX1 presents higher expression in SHH subgroup patients. In line with this, the results obtained in this chapter demonstrated that *SOX1* silencing generates a more severe phenotype in DAOY and UW228 cells (SHH subgroup cell lines) than in D283Med cells (Group 3 or 4 cell line) in the performed experiments. This fact further demonstrates the importance of SOX1 in SHH subgroup MBs.

As mentioned before, both this thesis second and third chapters are the first evidence that postulate *SOX1* as an oncogenic and not as a tumor suppressor gene, thus,

relating *SOX1* with tumor cells proliferation. Moreover, even if SOX1 has not been described as tumor proliferation inductor in any other tumor to date, its expression has been related to proliferation in early neuronal progenitors (Kan et al., 2007) and cortical neural progenitors (Elkouris et al., 2011). Considering that MB tumors are originated from neural progenitor cells, the implication of SOX1 in MB proliferation seems coherent.

2.3. SOX1 is overexpressed in MBSCs and mediates their activity

This work results reinforce the SOX1 importance in cancer stem cells, since we found in this study that *SOX1* expression is higher in MBSCs, cultured in stem cell specific media, compared to the parental cells, cultured in the presence of serum. These results demonstrate that *SOX1* high levels are linked to MBSCs population maintenance. Furthermore, *SOX1* knock-down significantly decreased oncosphere formation and self-renewal capacity *in vitro* and tumor initiation *in vivo*. This relation between SOX1 and CSCs has not been described previously. In fact, *SOX1* lower expression have been related with CSCs (Rad et al., 2016).

Furthermore, we detected that silencing of *SOX1* expression downregulated *NESTIN*, *PML*, *ERBB4* and *CD133* stem cell markers expression (Dahlstrand et al., 1995; Ito et al., 2008; Singh et al., 2003; Zhou et al., 2015), and increased the well-known differentiation marker $p27^{KIP}$ expression (Ayrault et al., 2009). An interesting study has demonstrated that $p27^{KIP}$ levels are regulated by *SOX1* in hepatocellular carcinoma (Tsao et al., 2012), reinforcing this protein relevance and its regulation by *SOX1* activity. Moreover, *SOX1* has been found within the genes' set with elevated expression in CD44+/CD24- and CD133+ breast cancer stem cells (Wright et al., 2008), relating also *SOX1* to this stem cell marker.

Altogether, these results show that *SOX1* regulates the interaction between proliferation, self-renewal and differentiation processes that are necessary for MBSCs maintenance. Besides, our results firmly establish that *SOX1* behaves as an oncogene in MB, in contrast to other tumor types such as hepatocellular or nasopharyngeal carcinoma (Guan et al., 2014; Tsao et al., 2012), cervical (Lin et al., 2013), lung (Li and Li, 2015), or breast cancer (Song et al., 2016), where SOX1 displays a tumor suppressor role. Thus,

these results, together with the results obtained in this thesis third chapter, are the first one relating SOX1 to malignant phenotype in cancer. Thus, further research must be done in order to clarify SOX1 role in CSCs and in other brain cancers to consider if maybe it can be related to this phenotype in neural origin tumors.

2.4. SOX1 knock-down alters cell response, motility and cellular morphogenesis related signaling pathways

This thesis transcriptomic analysis shows multiple pathways and genes alteration in *SOX1* knocked-down cells. Specifically, we revealed an upregulation in genes related to cellular morphogenesis and a downregulation in genes involved in cell response and motility. Among these signaling pathways, a reduction in motility could be beneficial for tumor treatment. In fact, as mentioned before, 30 % of MB tumors present metastasis in the moment of the diagnosis (Park et al., 1983), so reduced cellular motility could induce a metastasis diminution. Moreover, even if *SOX1* has not been identified as involved in tumor cells metastasis, it controls neurons migration (Ekonomou et al., 2005), and considering the neuronal origin of MBs, this information can explain our results of reduced expression of cell motility related genes in *SOX1* knocked-down cells.

Moreover, we identified and validated in the microarray analysis a set of 6 genes (*IL6*, *VCAM1*, *CEACAM1*, *IGFBP3*, *SOD2* and *SEMA5A*) as downstream targets of *SOX1* activity in MB cells. IL6 is implicated in a wide range of inflammatory processes and it has been reported as an inductor of MB cells proliferation and viability (Chen et al., 2018). VCAM1 and IGFBP3 have been also related to MB, the first one showing higher expression in SHH subgroup (Liang et al., 2015) and IGFBP3 showing higher expression levels in high risk MBs (Svalina et al., 2016). CEACAM proteins are implicated in cellular adhesion, proliferation, differentiation and tumor suppression, but some of the members of the family, such as CEACAM1 are associated to the malignant phenotype of some tumors (Kelleher et al., 2019). SOD2 has been related to treatment-related ototoxicity in cisplatin treated MBs (Brown et al., 2015). SEMA5A has a dual role in cancer, since it has been demonstrated to be a good prognostic biomarker and suppress proliferation and migration in colon cancer and lung adenocarcinoma respectively (Demirkol et al., 2017; Ko et al., 2020), but it drives melanoma and pancreatic cancer progression (D'Aguanno et

al., 2018; Saxena et al., 2018a). All these genes appear to be downregulated with *SOX1* knock-down. Among them, *CEACAM1, IGFBP3 and SEMA5A* genes seem to have a special interest, since they presented a positive correlation with *SOX1* and exhibit the highest expression levels in SHH MB subgroup patients, following the same pattern as *SOX1*. Even so, none of them presented statistical differences when analyzing the correlation between these genes' expression levels and overall patients' survival. Thus, further investigation might be done in order to investigate the specific relation between these genes and SOX1.

Moreover, as SOX1 is a transcription factor, it can regulate a wide range of genes expression. In this work the specific SOX1 direct targets that are activated or/and inhibited to give rise to the phenotype we found in the cells when inhibiting SOX1 are not demonstrated yet. So next steps will be directed to finding this target genes, with the objective to discover more targetable molecules in order to achieve a good MB treatment.

Altogether, in this thesis second chapter, our work has identified that *SOX1* expression is highly enriched in the MBSCs pool and that its knock-down significantly impairs human MB cells proliferation, self-renewal and tumor initiation and progression. Thus, we hypothesize that SOX1 is a master developmental transcription factor that governs cellular plasticity, heterogeneity and motility. Furthermore, we disclose that SOX1 is overexpressed in SHH MBs compared to the other subgroups and that this high expression is associated with shorter overall patients' survival. Moreover, when comparing the prognostic and subgroup biomarker potential of SHH signaling pathway genes with SOX1, we observed a more promising role for SOX1 than all the genes analyzed regarding prognostic and subgroup biomarker. Collectively, our data detail a previously undescribed *SOX1* role as a central player in MB biology, prognosis and therapy. Moreover, it is the first time that *SOX1* particular role in MB progression and MBSCs pool maintenance has been identified. Hence, we have identified in this work that SOX1 promotes MB malignant progression, and that its expression could be useful for SHH MBs identification.

Regarding the prospective of this work, the identified role of SOX1 in MBSCs, together with the results obtained when inhibiting *SOX1* expression, are interesting for the translational point of view. As mentioned in this thesis, MBSCs are responsible for tumor recurrence and treatment resistance, and targeting them is the ambitious challenge of cancer research. Thus, the establishment of a gene related to tumor proliferation and MBSCs activity allows new studies in order to found an effective SOX1 inhibitor that will target both MBSCs and tumor bulk cells, thus reducing tumor recurrence and therapy resistance. Moreover, as current therapies cause very severe side effects, the best approach would be a combined therapy with SOX1 inhibitors, but using lower doses of the current chemo- and radiotherapy to diminish those side effects [**Figure D1**].

3. SOX1 presents an oncogenic activity in glioblastoma

As mentioned before, several transcription factors that direct developmental decisions might also act as oncogenes by promoting reactivation of programs required for tumorigenesis (Suva et al., 2013). Among them SOX1, the transcription factor that we investigated in this thesis, is an essential transcription factor for proliferation maintenance in the neural stem/progenitor pool. Based on this evidence, SOX1 might be considered as a key player in neural development through the neural/progenitor pool homeostasis maintenance. In the second chapter of this thesis, we have identified the oncogenic role of *SOX1* in MB. Then, we wondered if it would have a similar effect in a non-developmental brain tumor. Thus, we investigated the role of this transcription factor in GBM. It is worth to note that prior to this study, little was known about the impact of SOX1 in GBM and in the GSC population maintenance.

3.1. SOX1 high expression levels are associated with a reduced survival in GBM

In the last chapter of this thesis, we wanted to stufy the role of SOX1 in GBM, the most common and aggressive brain tumor in adulthood. For this aim, we first investigated *SOX1* expression in human brain samples. *SOX1* mRNA expression analysis in a GBM patients' cohort from Donostia University Hospital indicated that *SOX1* expression was slightly up-regulated in approximately 60 % of tumor tissues compared to healthy human brain tissues. Moreover, taking advantage of the publicly available TCGA cohort data, we found that *SOX1* high levels were associated with shorter patient survival. All these data confirm the SOX1 clinic-pathological and prognostic significance in GBM. In fact, as mentioned before, SOX1 protein and/or mRNA low expression has been correlated with shorter overall survival and poor prognosis in ovarian cancer (Su et al., 2009), human hepatocellular carcinoma (Lou et al., 2015; Tsao et al., 2012), and esophageal squamous cell carcinoma (Kuo et al., 2014; Rad et al., 2016). Indeed, together with the second chapter results, it is the first evidence correlating SOX1 high expression with poor patients' outcome in cancer.

As mentioned in previous chapter discussion, the SOX1 dichotomic role in different tumor types is conceivable. In fact, *SOX1* expression could be elevated or decreased depending on the epigenetic status or the cellular heterogeneity and plasticity (Guan et al., 2014; Kuo et al., 2014; Tsao et al., 2012).

3.2. SOX1 is enriched in GSCs and its knock-down inhibits their activity

Regarding cellular heterogeneity and plasticity, our data revealed that *SOX1* expression is enriched in the GSCs population, cultured in stem cell specific media, compared to parental cells, cultured in the presence of serum. Moreover, we found that patient-derived GSCs have higher levels of *SOX1* expression than conventional cell lines. Moreover, these levels decrease when the GSCs are induced to differentiate in the presence of serum. These results demonstrate that high *SOX1* levels maintain GSCs in an undifferentiated state and that the differentiation process decreases the expression levels of this transcription factor. In agreement with this idea and as mentioned before, *SOX1* has been identified within the set of 19 neurodevelopmental transcription factors that are active and have higher expression in GSCs than in differentiated cells (Suva et al., 2014). Furthermore, mapping of chromatin accessibility, before and after differentiation with BMP treatment, identified several enriched motifs for SOXB1 family members, mostly SOX2 but also SOX1, as regulatory regions that failed to be completely silenced in GSC settings (Caren et al., 2015). Moreover, SOX1 has been observed among the genes set with elevated expression in CD44+/CD24− and CD133+ breast cancer stem cells (Wright et al., 2008) and in invasive prostate cancer cells, where *SOX1* promoter was hypomethylated (Mathews et al., 2010). Furthermore, one study has used *SOX1* high expression as GSCs characteristic marker (Bielecka-Wajdman et al., 2017). Together, these results postulate that *SOX1* enrichment in the CSCs population is likely to be mediated by temporal and context dependent epigenetic changes. These findings are supported by the evidence that, during tumor initiation and progression, cancer cells epigenome undergoes multiple alterations thus presenting broad domains of promoter hypermethylation, that contributes to carcinogenesis. This process is induced through tumor suppressor genes and epigenetic regulators inactivation; and also, by the induction of the DNA methylation loss genome-wide (hypomethylation). This is likely affecting

transcription factors important for self-renewal, and therefore, are under selective pressure to maintain or increase their expression in the corresponding cancer cell (Caren et al., 2015; Dawson and Kouzarides, 2012; You and Jones, 2012). However, we did not study the epigenetic status of *SOX1* and its promoter in this thesis chapter, so further research must be done in order to identify this gene epigenetic status in GBM and in GSCs.

Regarding SOX1 role in GSCs activity, we knocked down its expression directly in GSCs. We then observed a marked reduction in their proliferative and self-renewal activity, accompanied by a delayed tumors' formation when cells were xenotransplanted into immunodeficient mouse brains. The same approach with U251 cells generated similar results to the ones obtained with *SOX1* silencing in GSCs. Indeed, *SOX1* knock-down significantly impaired self-renewal and proliferative capability *in vitro* and tumor initiation and progression *in vivo*. These results indicate that *SOX1* expression is necessary for GSC maintenance, that is likely regulating proliferation, self-renewal and differentiation interplay. On the contrary, *SOX1* overexpression in GSCs moderately increased cell growth, proliferation and stem cell markers expression. A complementary study showed that elevated *SOX1* in differentiated glioma cells barely enhanced sphere formation and weakly induced CD133 stem cell marker expression, but failed to initiate tumors in mice that received an orthotopic xenograft (Suva et al., 2014). These results support the notion that *SOX1* elevated expression is essential for maintaining, but not sufficient for promoting GSCs self-renewal. Several additional factors might cooperate to activate stem cell-like properties. Indeed, POU3F2, SOX2, SALL2, and OLIG2 have been shown to be the essential core set of transcription factors for GBM propagation, which are within the 19 transcription factors set (including *SOX1*) required for successful reprogramming of differentiated glioma cells into GSCs (Suva et al., 2014). In summary, our results firmly establish that SOX1 behaves as an oncogene in GBM and that it is regulating glioma cell plasticity. This activity contrasts the evidence available for other cancer types, such as hepatocellular or nasopharyngeal carcinoma (Guan et al., 2014; Tsao et al., 2012), cervical (Lin et al., 2013), lung (Li and Li, 2015), or breast cancers (Song et al., 2016), in which it displays tumor suppressor activity. These data underline the fact that SOX1 activity is cancer context dependent.

3.3. SOX1 promotes tumor cells proliferation independently from WNT/B-catenin signaling pathway

This thesis results have also shown that when knocking down *SOX1* expression in conventional U251 cell lines, the cells lose their proliferative capacity and viability. They also form less and smaller tumors when injected into immunocompromised mice subcutaneously. In regard to these results, and as it has been mentioned before, to our knowledge, this thesis results are the first ones relating *SOX1* with tumor cells proliferation promotion, even if this transcription factor has been related to neuronal progenitors' proliferation before (Elkouris et al., 2011; Kan et al., 2007).

Furthermore, we wanted to find the pathway through which *SOX1* was acting to develop the oncogenic phenotype. It has been previously shown that *SOX1* is a negative regulator of WNT/β-catenin signaling in several cancer types justifying its tumor suppressor activity. In GBM, however, we have not detected any remarkable effects of *SOX1* silencing in the expression of β-catenin and its downstream target MYC at cellular level *in vitro*, in tumors *in vivo*, as well as in clinical biopsies. Therefore, the SOX1 oncogenic functions in GBM seem to be β-catenin independent. Similar to these results, *SOX1* overexpression in the embryonal teratocarcinoma cell line, NT2/D1, did not affect WNT signaling activity (Mojsin et al., 2015). Regarding SOX1 modulation consequences, at molecular level, we detected that *SOX1* expression gain and silencing, in GSC and U251 cell, modulated SOX2 (stem cell marker), PML (Iwanami et al., 2013; Martin-Martin et al., 2016; Zhou et al., 2015) and cell cycle regulators (such as $p27^{KIP}$ and CYCLIN D1) expression (Buttitta and Edgar, 2007). These results suggest SOX2-PML and $p27^{KIP}$-CYCLIN D1 as downstream molecular effectors by which SOX1 functions in GBM governing self-renewal and proliferation programs. Additional studies have shown that *SOX1* alters *SOX2* expression in human laryngeal squamous cell carcinoma (Yang et al., 2015), regulates $p27^{KIP}$ levels in hepatocellular carcinoma (Tsao et al., 2012), and modulates CYCLIN D1 expression in hepatocellular and nasopharyngeal carcinoma as well as in breast cancer (Guan et al., 2014; Song et al., 2016; Tsao et al., 2012). Altogether, data presented reinforce the relevance of those genes underlying *SOX1* activity. However, further work is needed to define their interactions in GBM.

As a summary of the last chapter of this thesis, our work has identified that *SOX1* expression is highly enriched in the GSCs pool and its inactivation significantly impairs their malignant properties including proliferation, self-renewal ability, differentiation capacity as well as tumor initiation and progression. Based on our results, we postulate that SOX1 is a master developmental transcription factor, governing and maintaining cellular plasticity and heterogeneity associated with diverse regulatory programs. Moreover, we reveal that *SOX1* is overexpressed in a subset of GBM human biopsies and that its high levels are associated with shorter overall patient survival. Taken together, our data pointed out a previously unappreciated SOX1 role as a central player in GBM biology, prognosis, and therapy.

The prospective of this work is similar to the ones in previous chapters. The importance of *SOX1* as a prognostic biomarker may enable patients' stratification considering low and high *SOX1* expression tumors. Afterwards, our proposal is to apply a SOX1-targeted therapy in combination with the standard treatments, with the aim of eliminating both tumor bulk cells and GSCs, thus reducing tumor recurrence chances [Figure D1]. However, to achieve this objective safe SOX1-targeting drugs that can cross the brain blood barrier must be found.

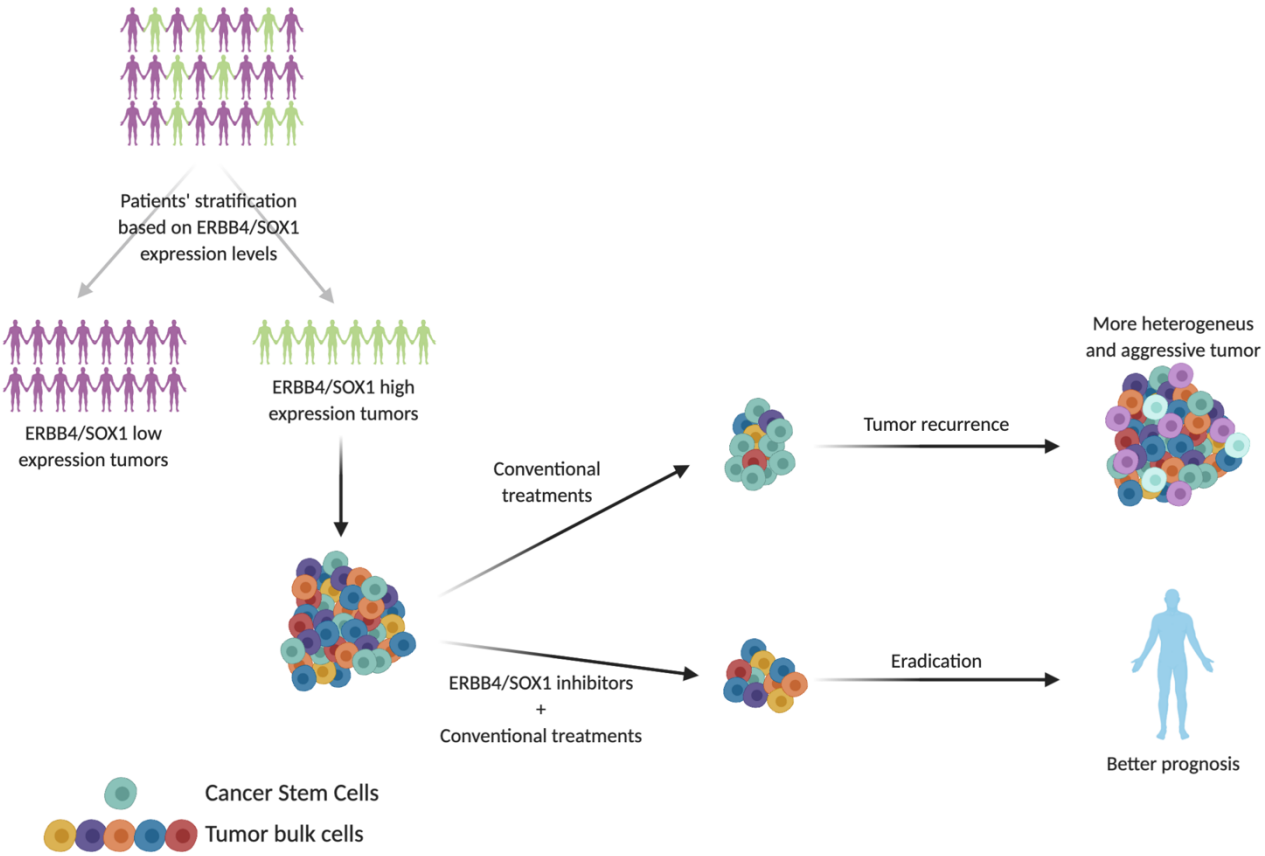

Figure D1. Schematic representation of this thesis prospective. The prospective of this thesis is the stratification of the patients based on ERBB4/SOX1 levels. Then, to treat the patients' tumors that present higher ERBB4/SOX1 levels there are two options: i) treat these patients with conventional treatments, which will target and eliminate tumor bulk cells, but not CSCs. Thus, this CSCs will proliferate and tumor recurrence will occur, normally generating a more heterogenous and aggressive tumor. ii) treat these patients with a combination of conventional treatments and ERBB4/SOX1 inhibitors. This combination will target both tumor bulk cells and CSCs, leading to the eradication of the tumor and a better prognosis for the patient. Created with BioRender.com.

Concluding remarks

1. ErbB4 is expressed in the inner EGL of the developing cerebellum, where and it is requiered for the correct organization of Purkinje cells and astrocytes, and, in consequence, to ensure the correct CGNPs migration to the IGL.
2. ErbB4 activation protects CGNPs and MB cells from apoptosis *in vitro* and *in vivo*.
3. ERBB4 presents a higher expression in Group 4 MBs, which correlates with poor prognosis. We therefore postulate ERBB4 as a good subgroup and prognostic biomarker for MB.
4. ERBB4 silencing inhibits cell viability and activates apoptosis in MB cells *in vitro*, and it is required for tumor progression *in vivo*.
5. ERBB4 plays an important role in the maintenance of MBSCs, where ERBB4 is highly expressed.
6. SHH MBs present higher levels of SOX1 expression, which correlates with poor prognosis.
7. SOX1 constitutes a better prognostic biomarker than genes of SHH signaling pathway in the case of SHH MBs.
8. SOX1 silencing inhibits MB proliferation *in vitro* and *in vivo*.
9. SOX1 is overexpressed in MBSCs, mediating their activity.
10. High SOX1 expression levels are associated with reduced survival in GBM patients, postulating it as a possible prognostic biomarker.
11. SOX1 is enriched in the GSC population and its knock-down inhibits their activity.
12. SOX1 promotes tumor formation and proliferation *in vitro* and *in vivo*, being its activity not mediated by the WNT/B-catenin signaling pathway in GBM.
13. SOX1-mediated tumor proliferation is regulated, in part, by PML and SOX2.

References

Abdullah, L.N., and Chow, E.K. (2013). Mechanisms of chemoresistance in cancer stem cells. Clin Transl Med 2, 3.

Agha, C.A., Ibrahim, S., Hassan, A., Elias, D.A., and Fathallah-Shaykh, H.M. (2010). Bevacizumab is active as a single agent against recurrent malignant gliomas. Anticancer Res 30, 609-611.

Ahlfeld, J., Favaro, R., Pagella, P., Kretzschmar, H.A., Nicolis, S., and Schuller, U. (2013). Sox2 requirement in sonic hedgehog-associated medulloblastoma. Cancer Res 73, 3796-3807.

Ahmad, Z., Jasnos, L., Gil, V., Howell, L., Hallsworth, A., Petrie, K., Sawado, T., and Chesler, L. (2015). Molecular and in vivo characterization of cancer-propagating cells derived from MYCN-dependent medulloblastoma. PLoS One 10, e0119834.

Ajani, J.A., Song, S., Hochster, H.S., and Steinberg, I.B. (2015). Cancer stem cells: the promise and the potential. Semin Oncol 42 Suppl 1, S3-17.

Al-Hajj, M., and Clarke, M.F. (2004). Self-renewal and solid tumor stem cells. Oncogene 23, 7274-7282.

Alcantara Llaguno, S., Chen, J., Kwon, C.H., Jackson, E.L., Li, Y., Burns, D.K., Alvarez-Buylla, A., and Parada, L.F. (2009). Malignant astrocytomas originate from neural stem/progenitor cells in a somatic tumor suppressor mouse model. Cancer Cell 15, 45-56.

Alcock, J., and Sottile, V. (2009). Dynamic distribution and stem cell characteristics of Sox1-expressing cells in the cerebellar cortex. Cell Res 19, 1324-1333.

Aldaregia, J., Odriozola, A., Matheu, A., and Garcia, I. (2018). Targeting mTOR as a Therapeutic Approach in Medulloblastoma. Int J Mol Sci 19.

Alder, J., Lee, K.J., Jessell, T.M., and Hatten, M.E. (1999). Generation of cerebellar granule neurons in vivo by transplantation of BMP-treated neural progenitor cells. Nat Neurosci 2, 535-540.

Alonso, M.M., Diez-Valle, R., Manterola, L., Rubio, A., Liu, D., Cortes-Santiago, N., Urquiza, L., Jauregi, P., Lopez de Munain, A., Sampron, N., et al. (2011). Genetic and epigenetic modifications of Sox2 contribute to the invasive phenotype of malignant gliomas. PLoS One 6, e26740.

An, Y., and Ongkeko, W.M. (2009). ABCG2: the key to chemoresistance in cancer stem cells? Expert Opin Drug Metab Toxicol 5, 1529-1542.

Arai, F., Hirao, A., Ohmura, M., Sato, H., Matsuoka, S., Takubo, K., Ito, K., Koh, G.Y., and Suda, T. (2004). Tie2/angiopoietin-1 signaling regulates hematopoietic stem cell quiescence in the bone marrow niche. Cell 118, 149-161.

Aubert, J., Stavridis, M.P., Tweedie, S., O'Reilly, M., Vierlinger, K., Li, M., Ghazal, P., Pratt, T., Mason, J.O., Roy, D., et al. (2003). Screening for mammalian neural genes via fluorescence-activated cell sorter purification of neural precursors from Sox1-gfp knock-in mice. Proc Natl Acad Sci U S A 100 Suppl 1, 11836-11841.

Auffinger, B., Tobias, A.L., Han, Y., Lee, G., Guo, D., Dey, M., Lesniak, M.S., and Ahmed, A.U. (2014). Conversion of differentiated cancer cells into cancer stem-like cells in a glioblastoma model after primary chemotherapy. Cell Death Differ 21, 1119-1131.

Ayrault, O., Zindy, F., Rehg, J., Sherr, C.J., and Roussel, M.F. (2009). Two tumor suppressors, p27Kip1 and patched-1, collaborate to prevent medulloblastoma. Mol Cancer Res 7, 33-40.

Azzarelli, R., Simons, B.D., and Philpott, A. (2018). The developmental origin of brain tumours: a cellular and molecular framework. Development 145.

Bachoo, R.M., Maher, E.A., Ligon, K.L., Sharpless, N.E., Chan, S.S., You, M.J., Tang, Y., DeFrances, J., Stover, E., Weissleder, R., et al. (2002). Epidermal growth factor receptor and Ink4a/Arf: convergent mechanisms governing terminal differentiation and transformation along the neural stem cell to astrocyte axis. Cancer Cell 1, 269-277.

Bal, M.M., Das Radotra, B., Srinivasan, R., and Sharma, S.C. (2006). Expression of c-erbB-4 in medulloblastoma and its correlation with prognosis. Histopathology 49, 92-93.

Bao, S., Wu, Q., McLendon, R.E., Hao, Y., Shi, Q., Hjelmeland, A.B., Dewhirst, M.W., Bigner, D.D., and Rich, J.N. (2006). Glioma stem cells promote radioresistance by preferential activation of the DNA damage response. Nature 444, 756-760.

Bartlett, F., Kortmann, R., and Saran, F. (2013). Medulloblastoma. Clin Oncol (R Coll Radiol) 25, 36-45.

Bass, A.J., Watanabe, H., Mermel, C.H., Yu, S., Perner, S., Verhaak, R.G., Kim, S.Y., Wardwell, L., Tamayo, P., Gat-Viks, I., et al. (2009). SOX2 is an amplified lineage-survival oncogene in lung and esophageal squamous cell carcinomas. Nat Genet 41, 1238-1242.

Batlle, E., and Clevers, H. (2017). Cancer stem cells revisited. Nat Med 23, 1124-1134.

Bernard, P., and Harley, V.R. (2010). Acquisition of SOX transcription factor specificity through protein-protein interaction, modulation of Wnt signalling and post-translational modification. Int J Biochem Cell Biol 42, 400-410.

Bernstein, J.J., and Woodard, C.A. (1995). Glioblastoma cells do not intravasate into blood vessels. Neurosurgery 36, 124-132; discussion 132.

Bhat, K.P.L., Balasubramaniyan, V., Vaillant, B., Ezhilarasan, R., Hummelink, K., Hollingsworth, F., Wani, K., Heathcock, L., James, J.D., Goodman, L.D., et al. (2013). Mesenchymal differentiation mediated by NF-kappaB promotes radiation resistance in glioblastoma. Cancer Cell 24, 331-346.

Bielecka-Wajdman, A.M., Lesiak, M., Ludyga, T., Sieron, A., and Obuchowicz, E. (2017). Reversing glioma malignancy: a new look at the role of antidepressant drugs as adjuvant therapy for glioblastoma multiforme. Cancer Chemother Pharmacol 79, 1249-1256.

Birchmeier, C. (2009). ErbB receptors and the development of the nervous system. Exp Cell Res 315, 611-618.

Blanpain, C. (2013). Tracing the cellular origin of cancer. Nat Cell Biol 15, 126-134.

Blanpain, C., and Fuchs, E. (2014). Stem cell plasticity. Plasticity of epithelial stem cells in tissue regeneration. Science 344, 1242281.

Blazek, E.R., Foutch, J.L., and Maki, G. (2007). Daoy medulloblastoma cells that express CD133 are radioresistant relative to CD133- cells, and the CD133+ sector is enlarged by hypoxia. Int J Radiat Oncol Biol Phys 67, 1-5.

Bleau, A.M., Hambardzumyan, D., Ozawa, T., Fomchenko, E.I., Huse, J.T., Brennan, C.W., and Holland, E.C. (2009). PTEN/PI3K/Akt pathway regulates the side population phenotype and ABCG2 activity in glioma tumor stem-like cells. Cell Stem Cell 4, 226-235.

Bonnet, D., and Dick, J.E. (1997). Human acute myeloid leukemia is organized as a hierarchy that originates from a primitive hematopoietic cell. Nat Med 3, 730-737.

Borah, A., Raveendran, S., Rochani, A., Maekawa, T., and Kumar, D.S. (2015). Targeting self-renewal pathways in cancer stem cells: clinical implications for cancer therapy. Oncogenesis 4, e177.

Borovski, T., De Sousa, E.M.F., Vermeulen, L., and Medema, J.P. (2011). Cancer stem cell niche: the place to be. Cancer Res 71, 634-639.

Bozdag, S.C., Yuksel, M.K., and Demirer, T. (2018). Adult Stem Cells and Medicine. Adv Exp Med Biol 1079, 17-36.

Brada, M., Judson, I., Beale, P., Moore, S., Reidenberg, P., Statkevich, P., Dugan, M., Batra, V., and Cutler, D. (1999). Phase I dose-escalation and pharmacokinetic study of temozolomide (SCH 52365) for refractory or relapsing malignancies. Br J Cancer 81, 1022-1030.

Brennan, C.W., Verhaak, R.G., McKenna, A., Campos, B., Noushmehr, H., Salama, S.R., Zheng, S., Chakravarty, D., Sanborn, J.Z., Berman, S.H., et al. (2013). The somatic genomic landscape of glioblastoma. Cell 155, 462-477.

Brown, A.L., Lupo, P.J., Okcu, M.F., Lau, C.C., Rednam, S., and Scheurer, M.E. (2015). SOD2 genetic variant associated with treatment-related ototoxicity in cisplatin-treated pediatric medulloblastoma. Cancer Med 4, 1679-1686.

Buonanno, A., and Fischbach, G.D. (2001). Neuregulin and ErbB receptor signaling pathways in the nervous system. Curr Opin Neurobiol 11, 287-296.

Burrell, R.A., McGranahan, N., Bartek, J., and Swanton, C. (2013). The causes and consequences of genetic heterogeneity in cancer evolution. Nature 501, 338-345.

Buttitta, L.A., and Edgar, B.A. (2007). Mechanisms controlling cell cycle exit upon terminal differentiation. Curr Opin Cell Biol 19, 697-704.

Butts, T., Green, M.J., and Wingate, R.J. (2014a). Development of the cerebellum: simple steps to make a 'little brain'. Development 141, 4031-4041.

Butts, T., Hanzel, M., and Wingate, R.J. (2014b). Transit amplification in the amniote cerebellum evolved via a heterochronic shift in NeuroD1 expression. Development 141, 2791-2795.

Bylund, M., Andersson, E., Novitch, B.G., and Muhr, J. (2003). Vertebrate neurogenesis is counteracted by Sox1-3 activity. Nat Neurosci 6, 1162-1168.

Cai, J., Wu, Y., Mirua, T., Pierce, J.L., Lucero, M.T., Albertine, K.H., Spangrude, G.J., and Rao, M.S. (2002). Properties of a fetal multipotent neural stem cell (NEP cell). Dev Biol 251, 221-240.

Calabrese, C., Poppleton, H., Kocak, M., Hogg, T.L., Fuller, C., Hamner, B., Oh, E.Y., Gaber, M.W., Finklestein, D., Allen, M., et al. (2007). A perivascular niche for brain tumor stem cells. Cancer Cell 11, 69-82.

Calgani, A., Vignaroli, G., Zamperini, C., Coniglio, F., Festuccia, C., Di Cesare, E., Gravina, G.L., Mattei, C., Vitale, F., Schenone, S., et al. (2016). Suppression of SRC Signaling Is Effective in Reducing Synergy between Glioblastoma and Stromal Cells. Mol Cancer Ther 15, 1535-1544.

Cancer Genome Atlas Research, N. (2008). Comprehensive genomic characterization defines human glioblastoma genes and core pathways. Nature 455, 1061-1068.

Cantone, I., and Fisher, A.G. (2013). Epigenetic programming and reprogramming during development. Nat Struct Mol Biol 20, 282-289.

Capper, D., Gaiser, T., Hartmann, C., Habel, A., Mueller, W., Herold-Mende, C., von Deimling, A., and Siegelin, M.D. (2009). Stem-cell-like glioma cells are resistant to TRAIL/Apo2L and exhibit down-regulation of caspase-8 by promoter methylation. Acta Neuropathol 117, 445-456.

Caren, H., Stricker, S.H., Bulstrode, H., Gagrica, S., Johnstone, E., Bartlett, T.E., Feber, A., Wilson, G., Teschendorff, A.E., Bertone, P., et al. (2015). Glioblastoma Stem Cells Respond to Differentiation Cues but Fail to Undergo Commitment and Terminal Cell-Cycle Arrest. Stem Cell Reports 5, 829-842.

Carrasco-Garcia, E., Lopez, L., Aldaz, P., Arevalo, S., Aldaregia, J., Egana, L., Bujanda, L., Cheung, M., Sampron, N., Garcia, I., et al. (2016). SOX9-regulated cell plasticity in colorectal metastasis is attenuated by rapamycin. Sci Rep 6, 32350.

Carrasco-Garcia, E., Sampron, N., Aldaz, P., Arrizabalaga, O., Villanua, J., Barrena, C., Ruiz, I., Arrazola, M., Lawrie, C., and Matheu, A. (2013). Therapeutic strategies targeting glioblastoma stem cells. Recent Pat Anticancer Drug Discov 8, 216-227.

Carraway, K.L., 3rd, Weber, J.L., Unger, M.J., Ledesma, J., Yu, N., Gassmann, M., and Lai, C. (1997). Neuregulin-2, a new ligand of ErbB3/ErbB4-receptor tyrosine kinases. Nature 387, 512-516.

Castillo, S.D., Matheu, A., Mariani, N., Carretero, J., Lopez-Rios, F., Lovell-Badge, R., and Sanchez-Cespedes, M. (2012). Novel transcriptional targets of the SRY-HMG box transcription factor SOX4 link its expression to the development of small cell lung cancer. Cancer Res 72, 176-186.

Castillo, S.D., and Sanchez-Cespedes, M. (2012). The SOX family of genes in cancer development: biological relevance and opportunities for therapy. Expert Opin Ther Targets 16, 903-919.

Cavalli, F.M.G., Remke, M., Rampasek, L., Peacock, J., Shih, D.J.H., Luu, B., Garzia, L., Torchia, J., Nor, C., Morrissy, A.S., et al. (2017). Intertumoral Heterogeneity within Medulloblastoma Subgroups. Cancer Cell 31, 737-754 e736.

Chaffer, C.L., Brueckmann, I., Scheel, C., Kaestli, A.J., Wiggins, P.A., Rodrigues, L.O., Brooks, M., Reinhardt, F., Su, Y., Polyak, K., et al. (2011). Normal and neoplastic nonstem cells can spontaneously convert to a stem-like state. Proc Natl Acad Sci U S A 108, 7950-7955.

Chedotal, A. (2010). Should I stay or should I go? Becoming a granule cell. Trends Neurosci 33, 163-172.

Chen, X., Wei, J., Li, C., Pierson, C.R., Finlay, J.L., and Lin, J. (2018). Blocking interleukin-6 signaling inhibits cell viability/proliferation, glycolysis, and colony forming activity of human medulloblastoma cells. Int J Oncol 52, 571-578.

Cheng, L., Huang, Z., Zhou, W., Wu, Q., Donnola, S., Liu, J.K., Fang, X., Sloan, A.E., Mao, Y., Lathia, J.D., et al. (2013). Glioblastoma stem cells generate vascular pericytes to support vessel function and tumor growth. Cell 153, 139-152.

Cheng, L., Wu, Q., Huang, Z., Guryanova, O.A., Huang, Q., Shou, W., Rich, J.N., and Bao, S. (2011). L1CAM regulates DNA damage checkpoint response of glioblastoma stem cells through NBS1. EMBO J 30, 800-813.

Clarke, M.F., Dick, J.E., Dirks, P.B., Eaves, C.J., Jamieson, C.H., Jones, D.L., Visvader, J., Weissman, I.L., and Wahl, G.M. (2006). Cancer stem cells--perspectives on current status and future directions: AACR Workshop on cancer stem cells. Cancer Res 66, 9339-9344.

Clifford, S.C., Lusher, M.E., Lindsey, J.C., Langdon, J.A., Gilbertson, R.J., Straughton, D., and Ellison, D.W. (2006). Wnt/Wingless pathway activation and chromosome 6 loss characterize a distinct molecular sub-group of medulloblastomas associated with a favorable prognosis. Cell Cycle 5, 2666-2670.

Cojoc, M., Mabert, K., Muders, M.H., and Dubrovska, A. (2015). A role for cancer stem cells in therapy resistance: cellular and molecular mechanisms. Semin Cancer Biol 31, 16-27.

Coluccia, D., Figuereido, C., Isik, S., Smith, C., and Rutka, J.T. (2016). Medulloblastoma: Tumor Biology and Relevance to Treatment and Prognosis Paradigm. Curr Neurol Neurosci Rep 16, 43.

Cordeiro, B.M., Oliveira, I.D., Alves, M.T., Saba-Silva, N., Capellano, A.M., Cavalheiro, S., Dastoli, P., and Toledo, S.R. (2014). SHH, WNT, and NOTCH pathways in medulloblastoma: when cancer stem cells maintain self-renewal and differentiation properties. Childs Nerv Syst 30, 1165-1172.

D'Aguanno, S., Valentini, E., Tupone, M.G., Desideri, M., Di Martile, M., Spagnuolo, M., Buglioni, S., Ercolani, C., Falcone, I., De Dominici, M., et al. (2018). Semaphorin 5A drives melanoma progression: role of Bcl-2, miR-204 and c-Myb. J Exp Clin Cancer Res 37, 278.

Dahan, P., Martinez Gala, J., Delmas, C., Monferran, S., Malric, L., Zentkowski, D., Lubrano, V., Toulas, C., Cohen-Jonathan Moyal, E., and Lemarie, A. (2014). Ionizing radiations sustain glioblastoma cell dedifferentiation to a stem-like phenotype through survivin: possible involvement in radioresistance. Cell Death Dis 5, e1543.

Dahlstrand, J., Lardelli, M., and Lendahl, U. (1995). Nestin mRNA expression correlates with the central nervous system progenitor cell state in many, but not all, regions of developing central nervous system. Brain Res Dev Brain Res 84, 109-129.

Dahmane, N., and Ruiz i Altaba, A. (1999). Sonic hedgehog regulates the growth and patterning of the cerebellum. Development 126, 3089-3100.

Dawson, M.A., and Kouzarides, T. (2012). Cancer epigenetics: from mechanism to therapy. Cell 150, 12-27.

de la Rocha, A.M., Sampron, N., Alonso, M.M., and Matheu, A. (2014). Role of SOX family of transcription factors in central nervous system tumors. Am J Cancer Res 4, 312-324.

de la Rosa, J., Saenz Antonanzas, A., Shahi, M.H., Melendez, B., Rey, J.A., and Castresana, J.S. (2016). Laminin-adherent versus suspension-non-adherent cell culture conditions for the isolation of cancer stem cells in the DAOY medulloblastoma cell line. Tumour Biol 37, 12359-12370.

Dean, M., Fojo, T., and Bates, S. (2005). Tumour stem cells and drug resistance. Nat Rev Cancer 5, 275-284.

Deheeger, M., Lesniak, M.S., and Ahmed, A.U. (2014). Cellular plasticity regulated cancer stem cell niche: a possible new mechanism of chemoresistance. Cancer Cell Microenviron 1.

Demirkol, S., Gomceli, I., Isbilen, M., Dayanc, B.E., Tez, M., Bostanci, E.B., Turhan, N., Akoglu, M., Ozyerli, E., Durdu, S., et al. (2017). A Combined ULBP2 and SEMA5A Expression Signature as a Prognostic and Predictive Biomarker for Colon Cancer. J Cancer 8, 1113-1122.

Deng, S., Yang, X., Lassus, H., Liang, S., Kaur, S., Ye, Q., Li, C., Wang, L.P., Roby, K.F., Orsulic, S., et al. (2010). Distinct expression levels and patterns of stem cell marker, aldehyde dehydrogenase isoform 1 (ALDH1), in human epithelial cancers. PLoS One 5, e10277.

Dey, J., Ditzler, S., Knoblaugh, S.E., Hatton, B.A., Schelter, J.M., Cleary, M.A., Mecham, B., Rorke-Adams, L.B., and Olson, J.M. (2012). A distinct Smoothened mutation causes severe cerebellar developmental defects and medulloblastoma in a novel transgenic mouse model. Mol Cell Biol 32, 4104-4115.

Di, C., and Zhao, Y. (2015). Multiple drug resistance due to resistance to stem cells and stem cell treatment progress in cancer (Review). Exp Ther Med 9, 289-293.

Ding, L., Ellis, M.J., Li, S., Larson, D.E., Chen, K., Wallis, J.W., Harris, C.C., McLellan, M.D., Fulton, R.S., Fulton, L.L., et al. (2010). Genome remodelling in a basal-like breast cancer metastasis and xenograft. Nature 464, 999-1005.

Dingli, D., Traulsen, A., and Pacheco, J.M. (2007). Stochastic dynamics of hematopoietic tumor stem cells. Cell Cycle 6, 461-466.

Doetsch, F., Garcia-Verdugo, J.M., and Alvarez-Buylla, A. (1997). Cellular composition and three-dimensional organization of the subventricular germinal zone in the adult mammalian brain. J Neurosci 17, 5046-5061.

Dolle, L., Boulter, L., Leclercq, I.A., and van Grunsven, L.A. (2015). Next generation of ALDH substrates and their potential to study maturational lineage biology in stem and progenitor cells. Am J Physiol Gastrointest Liver Physiol 308, G573-578.

Du, Y.C., Oshima, H., Oguma, K., Kitamura, T., Itadani, H., Fujimura, T., Piao, Y.S., Yoshimoto, T., Minamoto, T., Kotani, H., et al. (2009). Induction and down-regulation of Sox17 and its possible roles during the course of gastrointestinal tumorigenesis. Gastroenterology 137, 1346-1357.

Dubrovska, A., Kim, S., Salamone, R.J., Walker, J.R., Maira, S.M., Garcia-Echeverria, C., Schultz, P.G., and Reddy, V.A. (2009). The role of PTEN/Akt/PI3K signaling in the maintenance and viability of prostate cancer stem-like cell populations. Proc Natl Acad Sci U S A 106, 268-273.

Ekonomou, A., Kazanis, I., Malas, S., Wood, H., Alifragis, P., Denaxa, M., Karagogeos, D., Constanti, A., Lovell-Badge, R., and Episkopou, V. (2005). Neuronal migration and ventral subtype identity in the telencephalon depend on SOX1. PLoS Biol 3, e186.

Elenius, K., Choi, C.J., Paul, S., Santiestevan, E., Nishi, E., and Klagsbrun, M. (1999). Characterization of a naturally occurring ErbB4 isoform that does not bind or activate phosphatidyl inositol 3-kinase. Oncogene 18, 2607-2615.

Elenius, K., Corfas, G., Paul, S., Choi, C.J., Rio, C., Plowman, G.D., and Klagsbrun, M. (1997a). A novel juxtamembrane domain isoform of HER4/ErbB4. Isoform-specific tissue distribution and differential processing in response to phorbol ester. J Biol Chem 272, 26761-26768.

Elenius, K., Paul, S., Allison, G., Sun, J., and Klagsbrun, M. (1997b). Activation of HER4 by heparin-binding EGF-like growth factor stimulates chemotaxis but not proliferation. EMBO J 16, 1268-1278.

Elkouris, M., Balaskas, N., Poulou, M., Politis, P.K., Panayiotou, E., Malas, S., Thomaidou, D., and Remboutsika, E. (2011). Sox1 maintains the undifferentiated state of cortical neural progenitor cells via the suppression of Prox1-mediated cell cycle exit and neurogenesis. Stem Cells 29, 89-98.

Enguita-German, M., Schiapparelli, P., Rey, J.A., and Castresana, J.S. (2010). CD133+ cells from medulloblastoma and PNET cell lines are more resistant to cyclopamine inhibition of the sonic hedgehog signaling pathway than CD133- cells. Tumour Biol 31, 381-390.

Erlich, S., Goldshmit, Y., Lupowitz, Z., and Pinkas-Kramarski, R. (2001). ErbB-4 activation inhibits apoptosis in PC12 cells. Neuroscience 107, 353-362.

Espinosa, J.S., and Luo, L. (2008). Timing neurogenesis and differentiation: insights from quantitative clonal analyses of cerebellar granule cells. J Neurosci 28, 2301-2312.

Fan, X., and Eberhart, C.G. (2008). Medulloblastoma stem cells. J Clin Oncol 26, 2821-2827.

Fang, X., Yoon, J.G., Li, L., Yu, W., Shao, J., Hua, D., Zheng, S., Hood, L., Goodlett, D.R., Foltz, G., et al. (2011). The SOX2 response program in glioblastoma multiforme: an integrated ChIP-seq, expression microarray, and microRNA analysis. BMC Genomics 12, 11.

Ferlay, J., Colombet, M., Soerjomataram, I., Mathers, C., Parkin, D.M., Pineros, M., Znaor, A., and Bray, F. (2019). Estimating the global cancer incidence and mortality in 2018: GLOBOCAN sources and methods. Int J Cancer 144, 1941-1953.

Ferlay, J., Soerjomataram, I., Dikshit, R., Eser, S., Mathers, C., Rebelo, M., Parkin, D.M., Forman, D., and Bray, F. (2015). Cancer incidence and mortality worldwide: sources, methods and major patterns in GLOBOCAN 2012. Int J Cancer 136, E359-386.

Ferretti, E., Di Marcotullio, L., Gessi, M., Mattei, T., Greco, A., Po, A., De Smaele, E., Giangaspero, F., Riccardi, R., Di Rocco, C., et al. (2006). Alternative splicing of the ErbB-4 cytoplasmic domain and its regulation by hedgehog signaling identify distinct medulloblastoma subsets. Oncogene 25, 7267-7273.

Flames, N., Long, J.E., Garratt, A.N., Fischer, T.M., Gassmann, M., Birchmeier, C., Lai, C., Rubenstein, J.L., and Marin, O. (2004). Short- and long-range attraction of cortical GABAergic interneurons by neuregulin-1. Neuron 44, 251-261.

Fletcher, J.I., Haber, M., Henderson, M.J., and Norris, M.D. (2010). ABC transporters in cancer: more than just drug efflux pumps. Nat Rev Cancer 10, 147-156.

Forget, A., Martignetti, L., Puget, S., Calzone, L., Brabetz, S., Picard, D., Montagud, A., Liva, S., Sta, A., Dingli, F., et al. (2018). Aberrant ERBB4-SRC Signaling as a Hallmark of Group 4 Medulloblastoma Revealed by Integrative Phosphoproteomic Profiling. Cancer Cell 34, 379-395 e377.

Fornasari, B.E., El Soury, M., De Marchis, S., Perroteau, I., Geuna, S., and Gambarotta, G. (2016). Neuregulin1 alpha activates migration of neuronal progenitors expressing ErbB4. Mol Cell Neurosci 77, 87-94.

Forster, N., Saladi, S.V., van Bragt, M., Sfondouris, M.E., Jones, F.E., Li, Z., and Ellisen, L.W. (2014). Basal cell signaling by p63 controls luminal progenitor function and lactation via NRG1. Dev Cell 28, 147-160.

Frasson, C., Rampazzo, E., Accordi, B., Beggio, G., Pistollato, F., Basso, G., and Persano, L. (2015). Inhibition of PI3K Signalling Selectively Affects Medulloblastoma Cancer Stem Cells. Biomed Res Int 2015, 973912.

Friedmann-Morvinski, D., Bushong, E.A., Ke, E., Soda, Y., Marumoto, T., Singer, O., Ellisman, M.H., and Verma, I.M. (2012). Dedifferentiation of neurons and astrocytes by oncogenes can induce gliomas in mice. Science 338, 1080-1084.

Fujita, S. (1967). Quantitative analysis of cell proliferation and differentiation in the cortex of the postnatal mouse cerebellum. J Cell Biol 32, 277-287.

Fukazawa, R., Miller, T.A., Kuramochi, Y., Frantz, S., Kim, Y.D., Marchionni, M.A., Kelly, R.A., and Sawyer, D.B. (2003). Neuregulin-1 protects ventricular myocytes from anthracycline-induced apoptosis via erbB4-dependent activation of PI3-kinase/Akt. J Mol Cell Cardiol 35, 1473-1479.

Furnari, F.B., Fenton, T., Bachoo, R.M., Mukasa, A., Stommel, J.M., Stegh, A., Hahn, W.C., Ligon, K.L., Louis, D.N., Brennan, C., et al. (2007). Malignant astrocytic glioma: genetics, biology, and paths to treatment. Genes Dev 21, 2683-2710.

Gajjar, A., Chintagumpala, M., Ashley, D., Kellie, S., Kun, L.E., Merchant, T.E., Woo, S., Wheeler, G., Ahern, V., Krasin, M.J., et al. (2006). Risk-adapted craniospinal radiotherapy followed by high-dose chemotherapy and stem-cell rescue in children with newly diagnosed medulloblastoma (St Jude Medulloblastoma-96): long-term results from a prospective, multicentre trial. Lancet Oncol 7, 813-820.

Galli, R., Binda, E., Orfanelli, U., Cipelletti, B., Gritti, A., De Vitis, S., Fiocco, R., Foroni, C., Dimeco, F., and Vescovi, A. (2004). Isolation and characterization of tumorigenic, stem-like neural precursors from human glioblastoma. Cancer Res 64, 7011-7021.

Galoczova, M., Coates, P., and Vojtesek, B. (2018). STAT3, stem cells, cancer stem cells and p63. Cell Mol Biol Lett 23, 12.

Gandola, L., Massimino, M., Cefalo, G., Solero, C., Spreafico, F., Pecori, E., Riva, D., Collini, P., Pignoli, E., Giangaspero, F., et al. (2009). Hyperfractionated accelerated radiotherapy in the Milan strategy for metastatic medulloblastoma. J Clin Oncol 27, 566-571.

Gangemi, R.M., Griffero, F., Marubbi, D., Perera, M., Capra, M.C., Malatesta, P., Ravetti, G.L., Zona, G.L., Daga, A., and Corte, G. (2009). SOX2 silencing in glioblastoma tumor-initiating cells causes stop of proliferation and loss of tumorigenicity. Stem Cells 27, 40-48.

Garcia, I., Aldaregia, J., Marjanovic Vicentic, J., Aldaz, P., Moreno-Cugnon, L., Torres-Bayona, S., Carrasco-Garcia, E., Garros-Regulez, L., Egana, L., Rubio, A., et al. (2017). Oncogenic activity of SOX1 in glioblastoma. Sci Rep 7, 46575.

Garros-Regulez, L., Aldaz, P., Arrizabalaga, O., Moncho-Amor, V., Carrasco-Garcia, E., Manterola, L., Moreno-Cugnon, L., Barrena, C., Villanua, J., Ruiz, I., et al. (2016a). mTOR inhibition decreases SOX2-SOX9 mediated glioma stem cell activity and temozolomide resistance. Expert Opin Ther Targets 20, 393-405.

Garros-Regulez, L., Garcia, I., Carrasco-Garcia, E., Lantero, A., Aldaz, P., Moreno-Cugnon, L., Arrizabalaga, O., Undabeitia, J., Torres-Bayona, S., Villanua, J., et al. (2016b). Targeting SOX2 as a Therapeutic Strategy in Glioblastoma. Front Oncol 6, 222.

Gassmann, M., Casagranda, F., Orioli, D., Simon, H., Lai, C., Klein, R., and Lemke, G. (1995). Aberrant neural and cardiac development in mice lacking the ErbB4 neuregulin receptor. Nature 378, 390-394.

Gerecke, K.M., Wyss, J.M., and Carroll, S.L. (2004). Neuregulin-1beta induces neurite extension and arborization in cultured hippocampal neurons. Mol Cell Neurosci 27, 379-393.

Ghashghaei, H.T., Weber, J., Pevny, L., Schmid, R., Schwab, M.H., Lloyd, K.C., Eisenstat, D.D., Lai, C., and Anton, E.S. (2006). The role of neuregulin-ErbB4 interactions on the proliferation and organization of cells in the subventricular zone. Proc Natl Acad Sci U S A 103, 1930-1935.

Gibson, P., Tong, Y., Robinson, G., Thompson, M.C., Currle, D.S., Eden, C., Kranenburg, T.A., Hogg, T., Poppleton, H., Martin, J., et al. (2010). Subtypes of medulloblastoma have distinct developmental origins. Nature 468, 1095-1099.

Gilbertson, R., Hernan, R., Pietsch, T., Pinto, L., Scotting, P., Allibone, R., Ellison, D., Perry, R., Pearson, A., and Lunec, J. (2001). Novel ERBB4 juxtamembrane splice variants are frequently expressed in childhood medulloblastoma. Genes Chromosomes Cancer 31, 288-294.

Gilbertson, R.J., Clifford, S.C., MacMeekin, W., Meekin, W., Wright, C., Perry, R.H., Kelly, P., Pearson, A.D., and Lunec, J. (1998). Expression of the ErbB-neuregulin signaling network during human cerebellar development: implications for the biology of medulloblastoma. Cancer Res 58, 3932-3941.

Gilbertson, R.J., Perry, R.H., Kelly, P.J., Pearson, A.D., and Lunec, J. (1997). Prognostic significance of HER2 and HER4 coexpression in childhood medulloblastoma. Cancer Res 57, 3272-3280.

Golding, J.P., Trainor, P., Krumlauf, R., and Gassmann, M. (2000). Defects in pathfinding by cranial neural crest cells in mice lacking the neuregulin receptor ErbB4. Nat Cell Biol 2, 103-109.

Golub, M.S., Germann, S.L., and Lloyd, K.C. (2004). Behavioral characteristics of a nervous system-specific erbB4 knock-out mouse. Behav Brain Res 153, 159-170.

Gong, C., Valduga, J., Chateau, A., Richard, M., Pellegrini-Moise, N., Barberi-Heyob, M., Chastagner, P., and Boura, C. (2018). Stimulation of medulloblastoma stem cells differentiation by a peptidomimetic targeting neuropilin-1. Oncotarget 9, 15312-15325.

Goodell, M.A., Brose, K., Paradis, G., Conner, A.S., and Mulligan, R.C. (1996). Isolation and functional properties of murine hematopoietic stem cells that are replicating in vivo. J Exp Med 183, 1797-1806.

Goodrich, L.V., Milenkovic, L., Higgins, K.M., and Scott, M.P. (1997). Altered neural cell fates and medulloblastoma in mouse patched mutants. Science 277, 1109-1113.

Grammel, D., Warmuth-Metz, M., von Bueren, A.O., Kool, M., Pietsch, T., Kretzschmar, H.A., Rowitch, D.H., Rutkowski, S., Pfister, S.M., and Schuller, U. (2012). Sonic hedgehog-associated medulloblastoma arising from the cochlear nuclei of the brainstem. Acta Neuropathol 123, 601-614.

Greaves, M., and Maley, C.C. (2012). Clonal evolution in cancer. Nature 481, 306-313.

Green, M.J., Myat, A.M., Emmenegger, B.A., Wechsler-Reya, R.J., Wilson, L.J., and Wingate, R.J. (2014). Independently specified Atoh1 domains define novel developmental compartments in rhombomere 1. Development 141, 389-398.

Grimmer, M.R., and Weiss, W.A. (2006). Childhood tumors of the nervous system as disorders of normal development. Curr Opin Pediatr 18, 634-638.

Guan, Z., Zhang, J., Wang, J., Wang, H., Zheng, F., Peng, J., Xu, Y., Yan, M., Liu, B., Cui, B., et al. (2014). SOX1 down-regulates beta-catenin and reverses malignant phenotype in nasopharyngeal carcinoma. Mol Cancer 13, 257.

Guessous, F., Li, Y., and Abounader, R. (2008). Signaling pathways in medulloblastoma. J Cell Physiol 217, 577-583.

Hadjimichael, C., Chanoumidou, K., Papadopoulou, N., Arampatzi, P., Papamatheakis, J., and Kretsovali, A. (2015). Common stemness regulators of embryonic and cancer stem cells. World J Stem Cells 7, 1150-1184.

Haegele, L., Ingold, B., Naumann, H., Tabatabai, G., Ledermann, B., and Brandner, S. (2003). Wnt signalling inhibits neural differentiation of embryonic stem cells by controlling bone morphogenetic protein expression. Mol Cell Neurosci 24, 696-708.

Hambardzumyan, D., Becher, O.J., Rosenblum, M.K., Pandolfi, P.P., Manova-Todorova, K., and Holland, E.C. (2008). PI3K pathway regulates survival of cancer stem cells residing in the perivascular niche following radiation in medulloblastoma in vivo. Genes Dev 22, 436-448.

Hanahan, D., and Weinberg, R.A. (2000). The hallmarks of cancer. Cell 100, 57-70.

Hanahan, D., and Weinberg, R.A. (2011). Hallmarks of cancer: the next generation. Cell 144, 646-674.

Harari, D., Tzahar, E., Romano, J., Shelly, M., Pierce, J.H., Andrews, G.C., and Yarden, Y. (1999). Neuregulin-4: a novel growth factor that acts through the ErbB-4 receptor tyrosine kinase. Oncogene 18, 2681-2689.

Hayase, Y., Higashiyama, S., Sasahara, M., Amano, S., Nakagawa, T., Taniguchi, N., and Hazama, F. (1998). Expression of heparin-binding epidermal growth factor-like growth factor in rat brain. Brain Res 784, 163-178.

He, S., Nakada, D., and Morrison, S.J. (2009). Mechanisms of stem cell self-renewal. Annu Rev Cell Dev Biol 25, 377-406.

Heddleston, J.M., Hitomi, M., Venere, M., Flavahan, W.A., Yang, K., Kim, Y., Minhas, S., Rich, J.N., and Hjelmeland, A.B. (2011). Glioma stem cell maintenance: the role of the microenvironment. Curr Pharm Des 17, 2386-2401.

Hemmati, H.D., Nakano, I., Lazareff, J.A., Masterman-Smith, M., Geschwind, D.H., Bronner-Fraser, M., and Kornblum, H.I. (2003). Cancerous stem cells can arise from pediatric brain tumors. Proc Natl Acad Sci U S A 100, 15178-15183.

Holland, E.C., Celestino, J., Dai, C., Schaefer, L., Sawaya, R.E., and Fuller, G.N. (2000). Combined activation of Ras and Akt in neural progenitors induces glioblastoma formation in mice. Nat Genet 25, 55-57.

Hou, L.C., Veeravagu, A., Hsu, A.R., and Tse, V.C. (2006). Recurrent glioblastoma multiforme: a review of natural history and management options. Neurosurg Focus 20, E5.

Huang, E.H., Hynes, M.J., Zhang, T., Ginestier, C., Dontu, G., Appelman, H., Fields, J.Z., Wicha, M.S., and Boman, B.M. (2009). Aldehyde dehydrogenase 1 is a marker for normal and malignant human colonic stem cells (SC) and tracks SC overpopulation during colon tumorigenesis. Cancer Res 69, 3382-3389.

Huse, J.T., and Holland, E.C. (2009). Genetically engineered mouse models of brain cancer and the promise of preclinical testing. Brain Pathol 19, 132-143.

Hyman, D.M., Piha-Paul, S.A., Won, H., Rodon, J., Saura, C., Shapiro, G.I., Juric, D., Quinn, D.I., Moreno, V., Doger, B., et al. (2018). HER kinase inhibition in patients with HER2- and HER3-mutant cancers. Nature 554, 189-194.

Hynes, N.E., and Lane, H.A. (2005). ERBB receptors and cancer: the complexity of targeted inhibitors. Nat Rev Cancer 5, 341-354.

Ikushima, H., Todo, T., Ino, Y., Takahashi, M., Miyazawa, K., and Miyazono, K. (2009). Autocrine TGF-beta signaling maintains tumorigenicity of glioma-initiating cells through Sry-related HMG-box factors. Cell Stem Cell 5, 504-514.

Ito, K., Bernardi, R., Morotti, A., Matsuoka, S., Saglio, G., Ikeda, Y., Rosenblatt, J., Avigan, D.E., Teruya-Feldstein, J., and Pandolfi, P.P. (2008). PML targeting eradicates quiescent leukaemia-initiating cells. Nature 453, 1072-1078.

Ito, M. (2008). Control of mental activities by internal models in the cerebellum. Nat Rev Neurosci 9, 304-313.

Iulianella, A., Wingate, R.J., Moens, C.B., and Capaldo, E. (2019). The generation of granule cells during the development and evolution of the cerebellum. Dev Dyn 248, 506-513.

Iwakura, Y., and Nawa, H. (2013). ErbB1-4-dependent EGF/neuregulin signals and their cross talk in the central nervous system: pathological implications in schizophrenia and Parkinson's disease. Front Cell Neurosci 7, 4.

Iwanami, A., Gini, B., Zanca, C., Matsutani, T., Assuncao, A., Nael, A., Dang, J., Yang, H., Zhu, S., Kohyama, J., et al. (2013). PML mediates glioblastoma resistance to mammalian target of rapamycin (mTOR)-targeted therapies. Proc Natl Acad Sci U S A 110, 4339-4344.

Jakacki, R.I., Burger, P.C., Zhou, T., Holmes, E.J., Kocak, M., Onar, A., Goldwein, J., Mehta, M., Packer, R.J., Tarbell, N., et al. (2012). Outcome of children with metastatic medulloblastoma treated with carboplatin during craniospinal radiotherapy: a Children's Oncology Group Phase I/II study. J Clin Oncol 30, 2648-2653.

Jiang, T., Zhang, Y., Wang, J., Du, J., Raynald, Qiu, X., Wang, Y., and Li, C. (2017). A Retrospective Study of Progression-Free and Overall Survival in Pediatric Medulloblastoma Based on Molecular Subgroup Classification: A Single-Institution Experience. Front Neurol 8, 198.

Jimenez, A.P., Traum, A., Boettger, T., Hackstein, H., Richter, A.M., and Dammann, R.H. (2017). The tumor suppressor RASSF1A induces the YAP1 target gene ANKRD1 that is epigenetically inactivated in human cancers and inhibits tumor growth. Oncotarget 8, 88437-88452.

John, J.P., Pollak, A., and Lubec, G. (2009). Complete sequencing and oxidative modification of manganese superoxide dismutase in medulloblastoma cells. Electrophoresis 30, 3006-3016.

Jones, R.J., Collector, M.I., Barber, J.P., Vala, M.S., Fackler, M.J., May, W.S., Griffin, C.A., Hawkins, A.L., Zehnbauer, B.A., Hilton, J., et al. (1996). Characterization of mouse lymphohematopoietic stem cells lacking spleen colony-forming activity. Blood 88, 487-491.

Junttila, M.R., and de Sauvage, F.J. (2013). Influence of tumour micro-environment heterogeneity on therapeutic response. Nature 501, 346-354.

Kadin, M.E., Rubinstein, L.J., and Nelson, J.S. (1970). Neonatal cerebellar medulloblastoma originating from the fetal external granular layer. J Neuropathol Exp Neurol 29, 583-600.

Kadota, R.P., Mahoney, D.H., Doyle, J., Duerst, R., Friedman, H., Holmes, E., Kun, L., Zhou, T., and Pollack, I.F. (2008). Dose intensive melphalan and cyclophosphamide with autologous hematopoietic stem cells for recurrent medulloblastoma or germinoma. Pediatr Blood Cancer 51, 675-678.

Kainulainen, V., Sundvall, M., Maatta, J.A., Santiestevan, E., Klagsbrun, M., and Elenius, K. (2000). A natural ErbB4 isoform that does not activate phosphoinositide 3-kinase mediates proliferation but not survival or chemotaxis. J Biol Chem 275, 8641-8649.

Kamachi, Y., and Kondoh, H. (2013). Sox proteins: regulators of cell fate specification and differentiation. Development 140, 4129-4144.

Kan, L., Israsena, N., Zhang, Z., Hu, M., Zhao, L.R., Jalali, A., Sahni, V., and Kessler, J.A. (2004). Sox1 acts through multiple independent pathways to promote neurogenesis. Dev Biol 269, 580-594.

Kan, L., Jalali, A., Zhao, L.R., Zhou, X., McGuire, T., Kazanis, I., Episkopou, V., Bassuk, A.G., and Kessler, J.A. (2007). Dual function of Sox1 in telencephalic progenitor cells. Dev Biol 310, 85-98.

Kaneko, Y., Sakakibara, S., Imai, T., Suzuki, A., Nakamura, Y., Sawamoto, K., Ogawa, Y., Toyama, Y., Miyata, T., and Okano, H. (2000). Musashi1: an evolutionally conserved marker for CNS progenitor cells including neural stem cells. Dev Neurosci 22, 139-153.

Karamboulas, C., and Ailles, L. (2013). Developmental signaling pathways in cancer stem cells of solid tumors. Biochim Biophys Acta 1830, 2481-2495.

Katoh, Y., and Katoh, M. (2009). Hedgehog target genes: mechanisms of carcinogenesis induced by aberrant hedgehog signaling activation. Curr Mol Med 9, 873-886.

Kawauchi, D., Robinson, G., Uziel, T., Gibson, P., Rehg, J., Gao, C., Finkelstein, D., Qu, C., Pounds, S., Ellison, D.W., et al. (2012). A mouse model of the most aggressive subgroup of human medulloblastoma. Cancer Cell 21, 168-180.

Kelleher, M., Singh, R., O'Driscoll, C.M., and Melgar, S. (2019). Carcinoembryonic antigen (CEACAM) family members and Inflammatory Bowel Disease. Cytokine Growth Factor Rev 47, 21-31.

King, H.O., Brend, T., Payne, H.L., Wright, A., Ward, T.A., Patel, K., Egnuni, T., Stead, L.F., Patel, A., Wurdak, H., et al. (2017). RAD51 Is a Selective DNA Repair Target to Radiosensitize Glioma Stem Cells. Stem Cell Reports 8, 125-139.

Kirsch, L., Liscovitch, N., and Chechik, G. (2012). Localizing genes to cerebellar layers by classifying ISH images. PLoS Comput Biol 8, e1002790.

Ko, P.H., Lenka, G., Chen, Y.A., Chuang, E.Y., Tsai, M.H., Sher, Y.P., and Lai, L.C. (2020). Semaphorin 5A suppresses the proliferation and migration of lung adenocarcinoma cells. Int J Oncol 56, 165-177.

Komurasaki, T., Toyoda, H., Uchida, D., and Morimoto, S. (1997). Epiregulin binds to epidermal growth factor receptor and ErbB-4 and induces tyrosine phosphorylation of epidermal growth factor receptor, ErbB-2, ErbB-3 and ErbB-4. Oncogene 15, 2841-2848.

Komuro, H., and Rakic, P. (1998). Distinct modes of neuronal migration in different domains of developing cerebellar cortex. J Neurosci 18, 1478-1490.

Kornblum, H.I., Zurcher, S.D., Werb, Z., Derynck, R., and Seroogy, K.B. (1999). Multiple trophic actions of heparin-binding epidermal growth factor (HB-EGF) in the central nervous system. Eur J Neurosci 11, 3236-3246.

Korpal, M., Ell, B.J., Buffa, F.M., Ibrahim, T., Blanco, M.A., Celia-Terrassa, T., Mercatali, L., Khan, Z., Goodarzi, H., Hua, Y., et al. (2011). Direct targeting of Sec23a by miR-200s influences cancer cell secretome and promotes metastatic colonization. Nat Med 17, 1101-1108.

Kuhar, S.G., Feng, L., Vidan, S., Ross, M.E., Hatten, M.E., and Heintz, N. (1993). Changing patterns of gene expression define four stages of cerebellar granule neuron differentiation. Development 117, 97-104.

Kumar, V., Kumar, V., McGuire, T., Coulter, D.W., Sharp, J.G., and Mahato, R.I. (2017). Challenges and Recent Advances in Medulloblastoma Therapy. Trends Pharmacol Sci 38, 1061-1084.

Kuo, I.Y., Chang, J.M., Jiang, S.S., Chen, C.H., Chang, I.S., Sheu, B.S., Lu, P.J., Chang, W.L., Lai, W.W., and Wang, Y.C. (2014). Prognostic CpG methylation biomarkers identified by methylation array in esophageal squamous cell carcinoma patients. Int J Med Sci 11, 779-787.

Kuo, P.Y., Leshchenko, V.V., Fazzari, M.J., Perumal, D., Gellen, T., He, T., Iqbal, J., Baumgartner-Wennerholm, S., Nygren, L., Zhang, F., et al. (2015). High-resolution chromatin immunoprecipitation (ChIP) sequencing reveals novel binding targets and prognostic role for SOX11 in mantle cell lymphoma. Oncogene 34, 1231-1240.

Kwon, C.H., Zhao, D., Chen, J., Alcantara, S., Li, Y., Burns, D.K., Mason, R.P., Lee, E.Y., Wu, H., and Parada, L.F. (2008). Pten haploinsufficiency accelerates formation of high-grade astrocytomas. Cancer Res 68, 3286-3294.

Lapidot, T., Sirard, C., Vormoor, J., Murdoch, B., Hoang, T., Caceres-Cortes, J., Minden, M., Paterson, B., Caligiuri, M.A., and Dick, J.E. (1994). A cell initiating human acute myeloid leukaemia after transplantation into SCID mice. Nature 367, 645-648.

Lathia, J.D., Mack, S.C., Mulkearns-Hubert, E.E., Valentim, C.L., and Rich, J.N. (2015). Cancer stem cells in glioblastoma. Genes Dev 29, 1203-1217.

Lee, G., Auffinger, B., Guo, D., Hasan, T., Deheeger, M., Tobias, A.L., Kim, J.Y., Atashi, F., Zhang, L., Lesniak, M.S., et al. (2016). Dedifferentiation of Glioma Cells to Glioma Stem-like Cells By Therapeutic Stress-induced HIF Signaling in the Recurrent GBM Model. Mol Cancer Ther 15, 3064-3076.

Lee, J.S., Gil, J.E., Kim, J.H., Kim, T.K., Jin, X., Oh, S.Y., Sohn, Y.W., Jeon, H.M., Park, H.J., Park, J.W., et al. (2008). Brain cancer stem-like cell genesis from p53-deficient mouse astrocytes by oncogenic Ras. Biochem Biophys Res Commun 365, 496-502.

Leemhuis, T., Yoder, M.C., Grigsby, S., Aguero, B., Eder, P., and Srour, E.F. (1996). Isolation of primitive human bone marrow hematopoietic progenitor cells using Hoechst 33342 and Rhodamine 123. Exp Hematol 24, 1215-1224.

Lessard, J., and Sauvageau, G. (2003). Bmi-1 determines the proliferative capacity of normal and leukaemic stem cells. Nature 423, 255-260.

Leto, K., Arancillo, M., Becker, E.B., Buffo, A., Chiang, C., Ding, B., Dobyns, W.B., Dusart, I., Haldipur, P., Hatten, M.E., et al. (2016). Consensus Paper: Cerebellar Development. Cerebellum 15, 789-828.

Li, N., and Li, S. (2015). Epigenetic inactivation of SOX1 promotes cell migration in lung cancer. Tumour Biol 36, 4603-4610.

Li, Q., Rycaj, K., Chen, X., and Tang, D.G. (2015a). Cancer stem cells and cell size: A causal link? Semin Cancer Biol 35, 191-199.

Li, Y., Lv, Z., He, G., Wang, J., Zhang, X., Lu, G., Ren, X., Wang, F., Zhu, X., Ding, Y., et al. (2015b). The SOX17/miR-371-5p/SOX2 axis inhibits EMT, stem cell properties and metastasis in colorectal cancer. Oncotarget 6, 9099-9112.

Liang, L., Aiken, C., McClelland, R., Morrison, L.C., Tatari, N., Remke, M., Ramaswamy, V., Issaivanan, M., Ryken, T., Del Bigio, M.R., et al. (2015). Characterization of novel biomarkers in selecting for subtype specific medulloblastoma phenotypes. Oncotarget 6, 38881-38900.

Lin, Y.W., Tsao, C.M., Yu, P.N., Shih, Y.L., Lin, C.H., and Yan, M.D. (2013). SOX1 suppresses cell growth and invasion in cervical cancer. Gynecol Oncol 131, 174-181.

Liu, A., Yu, X., and Liu, S. (2013). Pluripotency transcription factors and cancer stem cells: small genes make a big difference. Chin J Cancer 32, 483-487.

Liu, G., Yuan, X., Zeng, Z., Tunici, P., Ng, H., Abdulkadir, I.R., Lu, L., Irvin, D., Black, K.L., and Yu, J.S. (2006). Analysis of gene expression and chemoresistance of CD133+ cancer stem cells in glioblastoma. Mol Cancer 5, 67.

Liu, Y., Song, L., Ni, H., Sun, L., Jiao, W., Chen, L., Zhou, Q., Shen, T., Cui, H., Gao, T., et al. (2017). ERBB4 acts as a suppressor in the development of hepatocellular carcinoma. Carcinogenesis 38, 465-473.

Lobo, N.A., Shimono, Y., Qian, D., and Clarke, M.F. (2007). The biology of cancer stem cells. Annu Rev Cell Dev Biol 23, 675-699.

Lou, J., Zhang, K., Chen, J., Gao, Y., Wang, R., and Chen, L.B. (2015). Prognostic significance of SOX-1 expression in human hepatocelluar cancer. Int J Clin Exp Pathol 8, 5411-5418.

Louis, D.N., Ohgaki, H., Wiestler, O.D., Cavenee, W.K., Burger, P.C., Jouvet, A., Scheithauer, B.W., and Kleihues, P. (2007). The 2007 WHO classification of tumours of the central nervous system. Acta Neuropathol 114, 97-109.

Louis, D.N., Perry, A., Reifenberger, G., von Deimling, A., Figarella-Branger, D., Cavenee, W.K., Ohgaki, H., Wiestler, O.D., Kleihues, P., and Ellison, D.W. (2016). The 2016 World Health Organization Classification of Tumors of the Central Nervous System: a summary. Acta Neuropathol 131, 803-820.

Ludwig, K., and Kornblum, H.I. (2017). Molecular markers in glioma. J Neurooncol 134, 505-512.

Ma, I., and Allan, A.L. (2011). The role of human aldehyde dehydrogenase in normal and cancer stem cells. Stem Cell Rev Rep 7, 292-306.

Machold, R., and Fishell, G. (2005). Math1 is expressed in temporally discrete pools of cerebellar rhombic-lip neural progenitors. Neuron 48, 17-24.

Mainwaring, L.A., and Kenney, A.M. (2011). Divergent functions for eIF4E and S6 kinase by sonic hedgehog mitogenic signaling in the developing cerebellum. Oncogene 30, 1784-1797.

Maji, S., Panda, S., Samal, S.K., Shriwas, O., Rath, R., Pellecchia, M., Emdad, L., Das, S.K., Fisher, P.B., and Dash, R. (2018). Bcl-2 Antiapoptotic Family Proteins and Chemoresistance in Cancer. Adv Cancer Res 137, 37-75.

Mak, A.B., Nixon, A.M., Kittanakom, S., Stewart, J.M., Chen, G.I., Curak, J., Gingras, A.C., Mazitschek, R., Neel, B.G., Stagljar, I., et al. (2012). Regulation of CD133 by HDAC6 promotes beta-catenin signaling to suppress cancer cell differentiation. Cell Rep 2, 951-963.

Malas, S., Postlethwaite, M., Ekonomou, A., Whalley, B., Nishiguchi, S., Wood, H., Meldrum, B., Constanti, A., and Episkopou, V. (2003). Sox1-deficient mice suffer from epilepsy associated with abnormal ventral forebrain development and olfactory cortex hyperexcitability. Neuroscience 119, 421-432.

Malki, S., Boizet-Bonhoure, B., and Poulat, F. (2010). Shuttling of SOX proteins. Int J Biochem Cell Biol 42, 411-416.

Mani, S.A., Guo, W., Liao, M.J., Eaton, E.N., Ayyanan, A., Zhou, A.Y., Brooks, M., Reinhard, F., Zhang, C.C., Shipitsin, M., et al. (2008). The epithelial-mesenchymal transition generates cells with properties of stem cells. Cell 133, 704-715.

Manoranjan, B., Venugopal, C., McFarlane, N., Doble, B.W., Dunn, S.E., Scheinemann, K., and Singh, S.K. (2012). Medulloblastoma stem cells: where development and cancer cross pathways. Pediatr Res 71, 516-522.

Mao, J., Ligon, K.L., Rakhlin, E.Y., Thayer, S.P., Bronson, R.T., Rowitch, D., and McMahon, A.P. (2006). A novel somatic mouse model to survey tumorigenic potential applied to the Hedgehog pathway. Cancer Res 66, 10171-10178.

Mao, P., Joshi, K., Li, J., Kim, S.H., Li, P., Santana-Santos, L., Luthra, S., Chandran, U.R., Benos, P.V., Smith, L., et al. (2013). Mesenchymal glioma stem cells are maintained by activated glycolytic metabolism involving aldehyde dehydrogenase 1A3. Proc Natl Acad Sci U S A 110, 8644-8649.

Marcato, P., Dean, C.A., Pan, D., Araslanova, R., Gillis, M., Joshi, M., Helyer, L., Pan, L., Leidal, A., Gujar, S., et al. (2011). Aldehyde dehydrogenase activity of breast cancer stem cells is primarily due to isoform ALDH1A3 and its expression is predictive of metastasis. Stem Cells 29, 32-45.

Marino, S. (2005). Medulloblastoma: developmental mechanisms out of control. Trends Mol Med 11, 17-22.

Martin-Martin, N., Piva, M., Urosevic, J., Aldaz, P., Sutherland, J.D., Fernandez-Ruiz, S., Arreal, L., Torrano, V., Cortazar, A.R., Planet, E., et al. (2016). Stratification and therapeutic potential of PML in metastatic breast cancer. Nat Commun 7, 12595.

Marusyk, A., Almendro, V., and Polyak, K. (2012). Intra-tumour heterogeneity: a looking glass for cancer? Nat Rev Cancer 12, 323-334.

Marusyk, A., and Polyak, K. (2010). Tumor heterogeneity: causes and consequences. Biochim Biophys Acta 1805, 105-117.

Matheu, A., Collado, M., Wise, C., Manterola, L., Cekaite, L., Tye, A.J., Canamero, M., Bujanda, L., Schedl, A., Cheah, K.S., et al. (2012). Oncogenicity of the developmental transcription factor Sox9. Cancer Res 72, 1301-1315.

Mathews, L.A., Hurt, E.M., Zhang, X., and Farrar, W.L. (2010). Epigenetic regulation of CpG promoter methylation in invasive prostate cancer cells. Mol Cancer 9, 267.

McGranahan, N., and Swanton, C. (2017). Clonal Heterogeneity and Tumor Evolution: Past, Present, and the Future. Cell 168, 613-628.

McNeill, K.A. (2016). Epidemiology of Brain Tumors. Neurol Clin 34, 981-998.

Medema, J.P. (2013). Cancer stem cells: the challenges ahead. Nat Cell Biol 15, 338-344.

Mei, L., and Xiong, W.C. (2008). Neuregulin 1 in neural development, synaptic plasticity and schizophrenia. Nat Rev Neurosci 9, 437-452.

Merino-Azpitarte, M., Lozano, E., Perugorria, M.J., Esparza-Baquer, A., Erice, O., Santos-Laso, A., O'Rourke, C.J., Andersen, J.B., Jimenez-Aguero, R., Lacasta, A., et al. (2017). SOX17 regulates cholangiocyte differentiation and acts as a tumor suppressor in cholangiocarcinoma. J Hepatol 67, 72-83.

Mille, F., Tamayo-Orrego, L., Levesque, M., Remke, M., Korshunov, A., Cardin, J., Bouchard, N., Izzi, L., Kool, M., Northcott, P.A., et al. (2014). The Shh receptor Boc promotes progression of early medulloblastoma to advanced tumors. Dev Cell 31, 34-47.

Min, S.S., An, J., Lee, J.H., Seol, G.H., Im, J.H., Kim, H.S., Baik, T.K., and Woo, R.S. (2011). Neuregulin-1 prevents amyloid beta-induced impairment of long-term potentiation in hippocampal slices via ErbB4. Neurosci Lett 505, 6-9.

Mojsin, M., Topalovic, V., Vicentic, J.M., Schwirtlich, M., Stanisavljevic, D., Drakulic, D., and Stevanovic, M. (2015). Crosstalk between SOXB1 proteins and WNT/beta-catenin signaling in NT2/D1 cells. Histochem Cell Biol 144, 429-441.

Moon, J.H., Kwon, S., Jun, E.K., Kim, A., Whang, K.Y., Kim, H., Oh, S., Yoon, B.S., and You, S. (2011). Nanog-induced dedifferentiation of p53-deficient mouse astrocytes into brain cancer stem-like cells. Biochem Biophys Res Commun 412, 175-181.

Morel, A.P., Lievre, M., Thomas, C., Hinkal, G., Ansieau, S., and Puisieux, A. (2008). Generation of breast cancer stem cells through epithelial-mesenchymal transition. PLoS One 3, e2888.

Morokoff, A., Ng, W., Gogos, A., and Kaye, A.H. (2015). Molecular subtypes, stem cells and heterogeneity: Implications for personalised therapy in glioma. J Clin Neurosci 22, 1219-1226.

Mullen, R.J., Buck, C.R., and Smith, A.M. (1992). NeuN, a neuronal specific nuclear protein in vertebrates. Development 116, 201-211.

Muraoka-Cook, R.S., Caskey, L.S., Sandahl, M.A., Hunter, D.M., Husted, C., Strunk, K.E., Sartor, C.I., Rearick, W.A., Jr., McCall, W., Sgagias, M.K., et al. (2006). Heregulin-dependent delay in mitotic progression requires HER4 and BRCA1. Mol Cell Biol 26, 6412-6424.

Muraoka-Cook, R.S., Feng, S.M., Strunk, K.E., and Earp, H.S., 3rd (2008). ErbB4/HER4: role in mammary gland development, differentiation and growth inhibition. J Mammary Gland Biol Neoplasia 13, 235-246.

Musial-Bright, L., Fengler, R., Henze, G., and Hernaiz Driever, P. (2011). Carboplatin and ototoxicity: hearing loss rates among survivors of childhood medulloblastoma. Childs Nerv Syst 27, 407-413.

Najafi, M., Mortezaee, K., and Ahadi, R. (2019). Cancer stem cell (a)symmetry & plasticity: Tumorigenesis and therapy relevance. Life Sci 231, 116520.

Nakagawa, T., Sasahara, M., Hayase, Y., Haneda, M., Yasuda, H., Kikkawa, R., Higashiyama, S., and Hazama, F. (1998). Neuronal and glial expression of heparin-binding EGF-like growth factor in central nervous system of prenatal and early-postnatal rat. Brain Res Dev Brain Res 108, 263-272.

Nakahata, T., Gross, A.J., and Ogawa, M. (1982). A stochastic model of self-renewal and commitment to differentiation of the primitive hemopoietic stem cells in culture. J Cell Physiol 113, 455-458.

Nakano, I. (2015). Stem cell signature in glioblastoma: therapeutic development for a moving target. J Neurosurg 122, 324-330.

Naresh, A., Long, W., Vidal, G.A., Wimley, W.C., Marrero, L., Sartor, C.I., Tovey, S., Cooke, T.G., Bartlett, J.M., and Jones, F.E. (2006). The ERBB4/HER4 intracellular domain 4ICD is a BH3-only protein promoting apoptosis of breast cancer cells. Cancer Res 66, 6412-6420.

Nekulova, M., Holcakova, J., Coates, P., and Vojtesek, B. (2011). The role of p63 in cancer, stem cells and cancer stem cells. Cell Mol Biol Lett 16, 296-327.

Ni, C.Y., Murphy, M.P., Golde, T.E., and Carpenter, G. (2001). gamma -Secretase cleavage and nuclear localization of ErbB-4 receptor tyrosine kinase. Science 294, 2179-2181.

Ni, C.Y., Yuan, H., and Carpenter, G. (2003). Role of the ErbB-4 carboxyl terminus in gamma-secretase cleavage. J Biol Chem 278, 4561-4565.

Nieto, M.A., Huang, R.Y., Jackson, R.A., and Thiery, J.P. (2016). Emt: 2016. Cell 166, 21-45.

Noguchi, K.K., Cabrera, O.H., Swiney, B.S., Salinas-Contreras, P., Smith, J.K., and Farber, N.B. (2015). Hedgehog regulates cerebellar progenitor cell and medulloblastoma apoptosis. Neurobiol Dis 83, 35-43.

Norden, A.D., Young, G.S., Setayesh, K., Muzikansky, A., Klufas, R., Ross, G.L., Ciampa, A.S., Ebbeling, L.G., Levy, B., Drappatz, J., et al. (2008). Bevacizumab for recurrent malignant gliomas: efficacy, toxicity, and patterns of recurrence. Neurology 70, 779-787.

Northcott, P.A., Buchhalter, I., Morrissy, A.S., Hovestadt, V., Weischenfeldt, J., Ehrenberger, T., Grobner, S., Segura-Wang, M., Zichner, T., Rudneva, V.A., et al. (2017). The whole-genome landscape of medulloblastoma subtypes. Nature 547, 311-317.

Northcott, P.A., Korshunov, A., Witt, H., Hielscher, T., Eberhart, C.G., Mack, S., Bouffet, E., Clifford, S.C., Hawkins, C.E., French, P., et al. (2011). Medulloblastoma comprises four distinct molecular variants. J Clin Oncol 29, 1408-1414.

Northcott, P.A., Robinson, G.W., Kratz, C.P., Mabbott, D.J., Pomeroy, S.L., Clifford, S.C., Rutkowski, S., Ellison, D.W., Malkin, D., Taylor, M.D., et al. (2019). Medulloblastoma. Nat Rev Dis Primers 5, 11.

Nowell, P.C. (1976). The clonal evolution of tumor cell populations. Science 194, 23-28.

Ocana, O.H., Corcoles, R., Fabra, A., Moreno-Bueno, G., Acloque, H., Vega, S., Barrallo-Gimeno, A., Cano, A., and Nieto, M.A. (2012). Metastatic colonization requires the repression of the epithelial-mesenchymal transition inducer Prrx1. Cancer Cell 22, 709-724.

Ohgaki, H., and Kleihues, P. (2013). The definition of primary and secondary glioblastoma. Clin Cancer Res 19, 764-772.

Oosterveen, T., Kurdija, S., Alekseenko, Z., Uhde, C.W., Bergsland, M., Sandberg, M., Andersson, E., Dias, J.M., Muhr, J., and Ericson, J. (2012). Mechanistic differences in the transcriptional interpretation of local and long-range Shh morphogen signaling. Dev Cell 23, 1006-1019.

Opanashuk, L.A., Mark, R.J., Porter, J., Damm, D., Mattson, M.P., and Seroogy, K.B. (1999). Heparin-binding epidermal growth factor-like growth factor in hippocampus: modulation of expression by seizures and anti-excitotoxic action. J Neurosci 19, 133-146.

Ortega, M.C., Bribian, A., Peregrin, S., Gil, M.T., Marin, O., and de Castro, F. (2012). Neuregulin-1/ErbB4 signaling controls the migration of oligodendrocyte precursor cells during development. Exp Neurol 235, 610-620.

Orzol, P., Holcakova, J., Nekulova, M., Nenutil, R., Vojtesek, B., and Coates, P.J. (2015). The diverse oncogenic and tumour suppressor roles of p63 and p73 in cancer: a review by cancer site. Histol Histopathol 30, 503-521.

Ostermann, S., Csajka, C., Buclin, T., Leyvraz, S., Lejeune, F., Decosterd, L.A., and Stupp, R. (2004). Plasma and cerebrospinal fluid population pharmacokinetics of temozolomide in malignant glioma patients. Clin Cancer Res 10, 3728-3736.

Ostrom, Q.T., Bauchet, L., Davis, F.G., Deltour, I., Fisher, J.L., Langer, C.E., Pekmezci, M., Schwartzbaum, J.A., Turner, M.C., Walsh, K.M., et al. (2014). The epidemiology of glioma in adults: a "state of the science" review. Neuro Oncol 16, 896-913.

Ostrom, Q.T., Gittleman, H., Truitt, G., Boscia, A., Kruchko, C., and Barnholtz-Sloan, J.S. (2018). CBTRUS Statistical Report: Primary Brain and Other Central Nervous System Tumors Diagnosed in the United States in 2011-2015. Neuro Oncol 20, iv1-iv86.

Oyharcabal-Bourden, V., Kalifa, C., Gentet, J.C., Frappaz, D., Edan, C., Chastagner, P., Sariban, E., Pagnier, A., Babin, A., Pichon, F., et al. (2005). Standard-risk medulloblastoma treated by adjuvant chemotherapy followed by reduced-dose craniospinal radiation therapy: a French Society of Pediatric Oncology Study. J Clin Oncol 23, 4726-4734.

Packer, R.J., Gajjar, A., Vezina, G., Rorke-Adams, L., Burger, P.C., Robertson, P.L., Bayer, L., LaFond, D., Donahue, B.R., Marymont, M.H., et al. (2006). Phase III study of craniospinal radiation therapy followed by adjuvant chemotherapy for newly diagnosed average-risk medulloblastoma. J Clin Oncol 24, 4202-4208.

Park, I.K., Qian, D., Kiel, M., Becker, M.W., Pihalja, M., Weissman, I.L., Morrison, S.J., and Clarke, M.F. (2003). Bmi-1 is required for maintenance of adult self-renewing haematopoietic stem cells. Nature 423, 302-305.

Park, T.S., Hoffman, H.J., Hendrick, E.B., Humphreys, R.P., and Becker, L.E. (1983). Medulloblastoma: clinical presentation and management. Experience at the hospital for sick children, toronto, 1950-1980. J Neurosurg 58, 543-552.

Pei, Y., Moore, C.E., Wang, J., Tewari, A.K., Eroshkin, A., Cho, Y.J., Witt, H., Korshunov, A., Read, T.A., Sun, J.L., et al. (2012). An animal model of MYC-driven medulloblastoma. Cancer Cell 21, 155-167.

Peitzsch, C., Kurth, I., Kunz-Schughart, L., Baumann, M., and Dubrovska, A. (2013). Discovery of the cancer stem cell related determinants of radioresistance. Radiother Oncol 108, 378-387.

Perez-Garcia, C.G. (2015). ErbB4 in Laminated Brain Structures: A Neurodevelopmental Approach to Schizophrenia. Front Cell Neurosci 9, 472.

Perez-Losada, J., and Balmain, A. (2003). Stem-cell hierarchy in skin cancer. Nat Rev Cancer 3, 434-443.

Pevny, L., and Placzek, M. (2005). SOX genes and neural progenitor identity. Curr Opin Neurobiol 15, 7-13.

Pevny, L.H., Sockanathan, S., Placzek, M., and Lovell-Badge, R. (1998). A role for SOX1 in neural determination. Development 125, 1967-1978.

Phillips, H.S., Kharbanda, S., Chen, R., Forrest, W.F., Soriano, R.H., Wu, T.D., Misra, A., Nigro, J.M., Colman, H., Soroceanu, L., et al. (2006). Molecular subclasses of high-grade glioma predict prognosis, delineate a pattern of disease progression, and resemble stages in neurogenesis. Cancer Cell 9, 157-173.

Piao, Y.S., Iwakura, Y., Takei, N., and Nawa, H. (2005). Differential distributions of peptides in the epidermal growth factor family and phosphorylation of ErbB 1 receptor in adult rat brain. Neurosci Lett 390, 21-24.

Pierfelice, T.J., Schreck, K.C., Eberhart, C.G., and Gaiano, N. (2008). Notch, neural stem cells, and brain tumors. Cold Spring Harb Symp Quant Biol 73, 367-375.

Pietsch, T., Waha, A., Koch, A., Kraus, J., Albrecht, S., Tonn, J., Sorensen, N., Berthold, F., Henk, B., Schmandt, N., et al. (1997). Medulloblastomas of the desmoplastic variant carry mutations of the human homologue of Drosophila patched. Cancer Res 57, 2085-2088.

Pinkas-Kramarski, R., Eilam, R., Alroy, I., Levkowitz, G., Lonai, P., and Yarden, Y. (1997). Differential expression of NDF/neuregulin receptors ErbB-3 and ErbB-4 and involvement in inhibition of neuronal differentiation. Oncogene 15, 2803-2815.

Plaks, V., Kong, N., and Werb, Z. (2015). The cancer stem cell niche: how essential is the niche in regulating stemness of tumor cells? Cell Stem Cell 16, 225-238.

Plowman, G.D., Green, J.M., Culouscou, J.M., Carlton, G.W., Rothwell, V.M., and Buckley, S. (1993). Heregulin induces tyrosine phosphorylation of HER4/p180erbB4. Nature 366, 473-475.

Pollard, S.M., Yoshikawa, K., Clarke, I.D., Danovi, D., Stricker, S., Russell, R., Bayani, J., Head, R., Lee, M., Bernstein, M., et al. (2009). Glioma stem cell lines expanded in adherent culture have tumor-specific phenotypes and are suitable for chemical and genetic screens. Cell Stem Cell 4, 568-580.

Prickett, T.D., Agrawal, N.S., Wei, X., Yates, K.E., Lin, J.C., Wunderlich, J.R., Cronin, J.C., Cruz, P., Rosenberg, S.A., and Samuels, Y. (2009). Analysis of the tyrosine kinome in melanoma reveals recurrent mutations in ERBB4. Nat Genet 41, 1127-1132.

Qi, L., Ren, K., Fang, F., Zhao, D.H., Yang, N.J., and Li, Y. (2015). Over Expression of BCL2 and Low Expression of Caspase 8 Related to TRAIL Resistance in Brain Cancer Stem Cells. Asian Pac J Cancer Prev 16, 4849-4852.

Qiu, Z.K., Shen, D., Chen, Y.S., Yang, Q.Y., Guo, C.C., Feng, B.H., and Chen, Z.P. (2014). Enhanced MGMT expression contributes to temozolomide resistance in glioma stem-like cells. Chin J Cancer 33, 115-122.

Rad, A., Esmaeili Dizghandi, S., Abbaszadegan, M.R., Taghechian, N., Najafi, M., and Forghanifard, M.M. (2016). SOX1 is correlated to stemness state regulator SALL4 through progression and invasiveness of esophageal squamous cell carcinoma. Gene 594, 171-175.

Raffel, C., Jenkins, R.B., Frederick, L., Hebrink, D., Alderete, B., Fults, D.W., and James, C.D. (1997). Sporadic medulloblastomas contain PTCH mutations. Cancer Res 57, 842-845.

Rakic, P. (1971). Neuron-glia relationship during granule cell migration in developing cerebellar cortex. A Golgi and electronmicroscopic study in Macacus Rhesus. J Comp Neurol 141, 283-312.

Read, T.A., Fogarty, M.P., Markant, S.L., McLendon, R.E., Wei, Z., Ellison, D.W., Febbo, P.G., and Wechsler-Reya, R.J. (2009). Identification of CD15 as a marker for tumor-propagating cells in a mouse model of medulloblastoma. Cancer Cell 15, 135-147.

Recasens, A., and Munoz, L. (2019). Targeting Cancer Cell Dormancy. Trends Pharmacol Sci 40, 128-141.

Reifenberger, J., Wolter, M., Weber, R.G., Megahed, M., Ruzicka, T., Lichter, P., and Reifenberger, G. (1998). Missense mutations in SMOH in sporadic basal cell carcinomas of the skin and primitive neuroectodermal tumors of the central nervous system. Cancer Res 58, 1798-1803.

Reya, T., Morrison, S.J., Clarke, M.F., and Weissman, I.L. (2001). Stem cells, cancer, and cancer stem cells. Nature 414, 105-111.

Ricci-Vitiani, L., Pallini, R., Larocca, L.M., Lombardi, D.G., Signore, M., Pierconti, F., Petrucci, G., Montano, N., Maira, G., and De Maria, R. (2008). Mesenchymal differentiation of glioblastoma stem cells. Cell Death Differ 15, 1491-1498.

Rieff, H.I., Raetzman, L.T., Sapp, D.W., Yeh, H.H., Siegel, R.E., and Corfas, G. (1999). Neuregulin induces GABA(A) receptor subunit expression and neurite outgrowth in cerebellar granule cells. J Neurosci 19, 10757-10766.

Riese, D.J., 2nd, Bermingham, Y., van Raaij, T.M., Buckley, S., Plowman, G.D., and Stern, D.F. (1996a). Betacellulin activates the epidermal growth factor receptor and erbB-4, and induces cellular response patterns distinct from those stimulated by epidermal growth factor or neuregulin-beta. Oncogene 12, 345-353.

Riese, D.J., Kim, E.D., Elenius, K., Buckley, S., Klagsbrun, M., Plowman, G.D., and Stern, D.F. (1996b). The epidermal growth factor receptor couples transforming growth factor-alpha, heparin-binding epidermal growth factor-like factor, and amphiregulin to Neu, ErbB-3, and ErbB-4. J Biol Chem 271, 20047-20052.

Rio, C., Buxbaum, J.D., Peschon, J.J., and Corfas, G. (2000). Tumor necrosis factor-alpha-converting enzyme is required for cleavage of erbB4/HER4. J Biol Chem 275, 10379-10387.

Rio, C., Rieff, H.I., Qi, P., Khurana, T.S., and Corfas, G. (1997). Neuregulin and erbB receptors play a critical role in neuronal migration. Neuron 19, 39-50.

Rochkind, S., Blatt, I., Sadeh, M., and Goldhammer, Y. (1991). Extracranial metastases of medulloblastoma in adults: literature review. J Neurol Neurosurg Psychiatry 54, 80-86.

Ropolo, M., Daga, A., Griffero, F., Foresta, M., Casartelli, G., Zunino, A., Poggi, A., Cappelli, E., Zona, G., Spaziante, R., et al. (2009). Comparative analysis of DNA repair in stem and nonstem glioma cell cultures. Mol Cancer Res 7, 383-392.

Roskoski, R., Jr. (2014). The ErbB/HER family of protein-tyrosine kinases and cancer. Pharmacol Res 79, 34-74.

Safa, A.R., Saadatzadeh, M.R., Cohen-Gadol, A.A., Pollok, K.E., and Bijangi-Vishehsaraei, K. (2015). Glioblastoma stem cells (GSCs) epigenetic plasticity and interconversion between differentiated non-GSCs and GSCs. Genes Dis 2, 152-163.

Santos, J.C., Carrasco-Garcia, E., Garcia-Puga, M., Aldaz, P., Montes, M., Fernandez-Reyes, M., de Oliveira, C.C., Lawrie, C.H., Arauzo-Bravo, M.J., Ribeiro, M.L., et al. (2016). SOX9 Elevation Acts with Canonical WNT Signaling to Drive Gastric Cancer Progression. Cancer Res 76, 6735-6746.

Sarkar, A., and Hochedlinger, K. (2013). The sox family of transcription factors: versatile regulators of stem and progenitor cell fate. Cell Stem Cell 12, 15-30.

Saury, J.M., and Emanuelson, I. (2011). Cognitive consequences of the treatment of medulloblastoma among children. Pediatr Neurol 44, 21-30.

Saxena, S., Hayashi, Y., Wu, L., Awaji, M., Atri, P., Varney, M.L., Purohit, A., Rachagani, S., Batra, S.K., and Singh, R.K. (2018a). Pathological and functional significance of Semaphorin-5A in pancreatic cancer progression and metastasis. Oncotarget 9, 5931-5943.

Saxena, S., Purohit, A., Varney, M.L., Hayashi, Y., and Singh, R.K. (2018b). Semaphorin-5A maintains epithelial phenotype of malignant pancreatic cancer cells. BMC Cancer 18, 1283.

Schepers, G.E., Teasdale, R.D., and Koopman, P. (2002). Twenty pairs of sox: extent, homology, and nomenclature of the mouse and human sox transcription factor gene families. Dev Cell 3, 167-170.

Schmahmann, J.D. (2004). Disorders of the cerebellum: ataxia, dysmetria of thought, and the cerebellar cognitive affective syndrome. J Neuropsychiatry Clin Neurosci 16, 367-378.

Schmahmann, J.D., and Caplan, D. (2006). Cognition, emotion and the cerebellum. Brain 129, 290-292.

Schoenhals, M., Kassambara, A., De Vos, J., Hose, D., Moreaux, J., and Klein, B. (2009). Embryonic stem cell markers expression in cancers. Biochem Biophys Res Commun 383, 157-162.

Schuller, U., Heine, V.M., Mao, J., Kho, A.T., Dillon, A.K., Han, Y.G., Huillard, E., Sun, T., Ligon, A.H., Qian, Y., et al. (2008). Acquisition of granule neuron precursor identity is a critical determinant of progenitor cell competence to form Shh-induced medulloblastoma. Cancer Cell 14, 123-134.

Segers, V.F.M., Dugaucquier, L., Feyen, E., Shakeri, H., and De Keulenaer, G.W. (2020). The role of ErbB4 in cancer. Cell Oncol (Dordr) 43, 335-352.

Shankar, G.M., Balaj, L., Stott, S.L., Nahed, B., and Carter, B.S. (2017). Liquid biopsy for brain tumors. Expert Rev Mol Diagn 17, 943-947.

Short, S.C., Giampieri, S., Worku, M., Alcaide-German, M., Sioftanos, G., Bourne, S., Lio, K.I., Shaked-Rabi, M., and Martindale, C. (2011). Rad51 inhibition is an effective means of targeting DNA repair in glioma models and CD133+ tumor-derived cells. Neuro Oncol 13, 487-499.

Singer, E., Judkins, J., Salomonis, N., Matlaf, L., Soteropoulos, P., McAllister, S., and Soroceanu, L. (2015). Reactive oxygen species-mediated therapeutic response and resistance in glioblastoma. Cell Death Dis 6, e1601.

Singh, A., and Settleman, J. (2010). EMT, cancer stem cells and drug resistance: an emerging axis of evil in the war on cancer. Oncogene 29, 4741-4751.

Singh, S.K., Clarke, I.D., Hide, T., and Dirks, P.B. (2004a). Cancer stem cells in nervous system tumors. Oncogene 23, 7267-7273.

Singh, S.K., Clarke, I.D., Terasaki, M., Bonn, V.E., Hawkins, C., Squire, J., and Dirks, P.B. (2003). Identification of a cancer stem cell in human brain tumors. Cancer Res 63, 5821-5828.

Singh, S.K., Hawkins, C., Clarke, I.D., Squire, J.A., Bayani, J., Hide, T., Henkelman, R.M., Cusimano, M.D., and Dirks, P.B. (2004b). Identification of human brain tumour initiating cells. Nature 432, 396-401.

Song, L., Liu, D., He, J., Wang, X., Dai, Z., Zhao, Y., Kang, H., and Wang, B. (2016). SOX1 inhibits breast cancer cell growth and invasion through suppressing the Wnt/beta-catenin signaling pathway. APMIS 124, 547-555.

Sottile, V., Li, M., and Scotting, P.J. (2006). Stem cell marker expression in the Bergmann glia population of the adult mouse brain. Brain Res 1099, 8-17.

Steinbichler, T.B., Dudas, J., Skvortsov, S., Ganswindt, U., Riechelmann, H., and Skvortsova, II (2018). Therapy resistance mediated by cancer stem cells. Semin Cancer Biol 53, 156-167.

Sterling, J.A., Oyajobi, B.O., Grubbs, B., Padalecki, S.S., Munoz, S.A., Gupta, A., Story, B., Zhao, M., and Mundy, G.R. (2006). The hedgehog signaling molecule Gli2 induces parathyroid hormone-related

peptide expression and osteolysis in metastatic human breast cancer cells. Cancer Res 66, 7548-7553.

Strick, P.L., Dum, R.P., and Fiez, J.A. (2009). Cerebellum and nonmotor function. Annu Rev Neurosci 32, 413-434.

Stupp, R., Dietrich, P.Y., Ostermann Kraljevic, S., Pica, A., Maillard, I., Maeder, P., Meuli, R., Janzer, R., Pizzolato, G., Miralbell, R., et al. (2002). Promising survival for patients with newly diagnosed glioblastoma multiforme treated with concomitant radiation plus temozolomide followed by adjuvant temozolomide. J Clin Oncol 20, 1375-1382.

Stupp, R., Hegi, M.E., Mason, W.P., van den Bent, M.J., Taphoorn, M.J., Janzer, R.C., Ludwin, S.K., Allgeier, A., Fisher, B., Belanger, K., et al. (2009). Effects of radiotherapy with concomitant and adjuvant temozolomide versus radiotherapy alone on survival in glioblastoma in a randomised phase III study: 5-year analysis of the EORTC-NCIC trial. Lancet Oncol 10, 459-466.

Stupp, R., Mason, W.P., van den Bent, M.J., Weller, M., Fisher, B., Taphoorn, M.J., Belanger, K., Brandes, A.A., Marosi, C., Bogdahn, U., et al. (2005). Radiotherapy plus concomitant and adjuvant temozolomide for glioblastoma. N Engl J Med 352, 987-996.

Su, H.Y., Lai, H.C., Lin, Y.W., Chou, Y.C., Liu, C.Y., and Yu, M.H. (2009). An epigenetic marker panel for screening and prognostic prediction of ovarian cancer. Int J Cancer 124, 387-393.

Sun, C., Wang, L., Huang, S., Heynen, G.J., Prahallad, A., Robert, C., Haanen, J., Blank, C., Wesseling, J., Willems, S.M., et al. (2014). Reversible and adaptive resistance to BRAF(V600E) inhibition in melanoma. Nature 508, 118-122.

Sundvall, M., Korhonen, A., Paatero, I., Gaudio, E., Melino, G., Croce, C.M., Aqeilan, R.I., and Elenius, K. (2008). Isoform-specific monoubiquitination, endocytosis, and degradation of alternatively spliced ErbB4 isoforms. Proc Natl Acad Sci U S A 105, 4162-4167.

Sundvall, M., Veikkolainen, V., Kurppa, K., Salah, Z., Tvorogov, D., van Zoelen, E.J., Aqeilan, R., and Elenius, K. (2010). Cell death or survival promoted by alternative isoforms of ErbB4. Mol Biol Cell 21, 4275-4286.

Suva, M.L., Rheinbay, E., Gillespie, S.M., Patel, A.P., Wakimoto, H., Rabkin, S.D., Riggi, N., Chi, A.S., Cahill, D.P., Nahed, B.V., et al. (2014). Reconstructing and reprogramming the tumor-propagating potential of glioblastoma stem-like cells. Cell 157, 580-594.

Suva, M.L., Riggi, N., and Bernstein, B.E. (2013). Epigenetic reprogramming in cancer. Science 339, 1567-1570.

Svalina, M.N., Kikuchi, K., Abraham, J., Lal, S., Davare, M.A., Settelmeyer, T.P., Young, M.C., Peckham, J.L., Cho, Y.J., Michalek, J.E., et al. (2016). IGF1R as a Key Target in High Risk, Metastatic Medulloblastoma. Sci Rep 6, 27012.

Swartling, F.J., Savov, V., Persson, A.I., Chen, J., Hackett, C.S., Northcott, P.A., Grimmer, M.R., Lau, J., Chesler, L., Perry, A., et al. (2012). Distinct neural stem cell populations give rise to disparate brain tumors in response to N-MYC. Cancer Cell 21, 601-613.

Sweeney, C., Lai, C., Riese, D.J., 2nd, Diamonti, A.J., Cantley, L.C., and Carraway, K.L., 3rd (2000). Ligand discrimination in signaling through an ErbB4 receptor homodimer. J Biol Chem 275, 19803-19807.

Tagscherer, K.E., Fassl, A., Campos, B., Farhadi, M., Kraemer, A., Bock, B.C., Macher-Goeppinger, S., Radlwimmer, B., Wiestler, O.D., Herold-Mende, C., et al. (2008). Apoptosis-based treatment of

glioblastomas with ABT-737, a novel small molecule inhibitor of Bcl-2 family proteins. Oncogene 27, 6646-6656.

Takahashi, K., and Yamanaka, S. (2006). Induction of pluripotent stem cells from mouse embryonic and adult fibroblast cultures by defined factors. Cell 126, 663-676.

Taylor, M.D., Liu, L., Raffel, C., Hui, C.C., Mainprize, T.G., Zhang, X., Agatep, R., Chiappa, S., Gao, L., Lowrance, A., et al. (2002). Mutations in SUFU predispose to medulloblastoma. Nat Genet 31, 306-310.

Taylor, M.D., Northcott, P.A., Korshunov, A., Remke, M., Cho, Y.J., Clifford, S.C., Eberhart, C.G., Parsons, D.W., Rutkowski, S., Gajjar, A., et al. (2012). Molecular subgroups of medulloblastoma: the current consensus. Acta Neuropathol 123, 465-472.

Temple, S. (2001). The development of neural stem cells. Nature 414, 112-117.

Tidcombe, H., Jackson-Fisher, A., Mathers, K., Stern, D.F., Gassmann, M., and Golding, J.P. (2003). Neural and mammary gland defects in ErbB4 knockout mice genetically rescued from embryonic lethality. Proc Natl Acad Sci U S A 100, 8281-8286.

Timmann, D., Drepper, J., Frings, M., Maschke, M., Richter, S., Gerwig, M., and Kolb, F.P. (2010). The human cerebellum contributes to motor, emotional and cognitive associative learning. A review. Cortex 46, 845-857.

Tlsty, T.D., and Coussens, L.M. (2006). Tumor stroma and regulation of cancer development. Annu Rev Pathol 1, 119-150.

Tran, T.H., Utama, F.E., Sato, T., Peck, A.R., Langenheim, J.F., Udhane, S.S., Sun, Y., Liu, C., Girondo, M.A., Kovatich, A.J., et al. (2018). Loss of Nuclear Localized Parathyroid Hormone-Related Protein in Primary Breast Cancer Predicts Poor Clinical Outcome and Correlates with Suppressed Stat5 Signaling. Clin Cancer Res 24, 6355-6366.

Treisman, D.M., Li, Y., Pierce, B.R., Li, C., Chervenak, A.P., Tomasek, G.J., Lozano, G., Zheng, X., Kool, M., and Zhu, Y. (2019). Sox2(+) cells in Sonic Hedgehog-subtype medulloblastoma resist p53-mediated cell-cycle arrest response and drive therapy-induced recurrence. Neurooncol Adv 1, vdz027.

Tsai, J.H., Donaher, J.L., Murphy, D.A., Chau, S., and Yang, J. (2012). Spatiotemporal regulation of epithelial-mesenchymal transition is essential for squamous cell carcinoma metastasis. Cancer Cell 22, 725-736.

Tsao, C.M., Yan, M.D., Shih, Y.L., Yu, P.N., Kuo, C.C., Lin, W.C., Li, H.J., and Lin, Y.W. (2012). SOX1 functions as a tumor suppressor by antagonizing the WNT/beta-catenin signaling pathway in hepatocellular carcinoma. Hepatology 56, 2277-2287.

Uchida, N., Buck, D.W., He, D., Reitsma, M.J., Masek, M., Phan, T.V., Tsukamoto, A.S., Gage, F.H., and Weissman, I.L. (2000). Direct isolation of human central nervous system stem cells. Proc Natl Acad Sci U S A 97, 14720-14725.

Ulasov, I.V., Nandi, S., Dey, M., Sonabend, A.M., and Lesniak, M.S. (2011). Inhibition of Sonic hedgehog and Notch pathways enhances sensitivity of CD133(+) glioma stem cells to temozolomide therapy. Mol Med 17, 103-112.

Van Meir, E.G., Hadjipanayis, C.G., Norden, A.D., Shu, H.K., Wen, P.Y., and Olson, J.J. (2010). Exciting new advances in neuro-oncology: the avenue to a cure for malignant glioma. CA Cancer J Clin 60, 166-193.

Vanner, R.J., Remke, M., Gallo, M., Selvadurai, H.J., Coutinho, F., Lee, L., Kushida, M., Head, R., Morrissy, S., Zhu, X., et al. (2014). Quiescent sox2(+) cells drive hierarchical growth and relapse in sonic hedgehog subgroup medulloblastoma. Cancer Cell 26, 33-47.

Vaskovsky, A., Lupowitz, Z., Erlich, S., and Pinkas-Kramarski, R. (2000). ErbB-4 activation promotes neurite outgrowth in PC12 cells. J Neurochem 74, 979-987.

Veikkolainen, V., Vaparanta, K., Halkilahti, K., Iljin, K., Sundvall, M., and Elenius, K. (2011). Function of ERBB4 is determined by alternative splicing. Cell Cycle 10, 2647-2657.

Venere, M., Han, Y.G., Bell, R., Song, J.S., Alvarez-Buylla, A., and Blelloch, R. (2012). Sox1 marks an activated neural stem/progenitor cell in the hippocampus. Development 139, 3938-3949.

Verhaak, R.G., Hoadley, K.A., Purdom, E., Wang, V., Qi, Y., Wilkerson, M.D., Miller, C.R., Ding, L., Golub, T., Mesirov, J.P., et al. (2010). Integrated genomic analysis identifies clinically relevant subtypes of glioblastoma characterized by abnormalities in PDGFRA, IDH1, EGFR, and NF1. Cancer Cell 17, 98-110.

Vermeulen, Z., Segers, V.F., and De Keulenaer, G.W. (2016). ErbB2 signaling at the crossing between heart failure and cancer. Basic Res Cardiol 111, 60.

Vidal, G.A., Naresh, A., Marrero, L., and Jones, F.E. (2005). Presenilin-dependent gamma-secretase processing regulates multiple ERBB4/HER4 activities. J Biol Chem 280, 19777-19783.

Vignot, S., Frampton, G.M., Soria, J.C., Yelensky, R., Commo, F., Brambilla, C., Palmer, G., Moro-Sibilot, D., Ross, J.S., Cronin, M.T., et al. (2013). Next-generation sequencing reveals high concordance of recurrent somatic alterations between primary tumor and metastases from patients with non-small-cell lung cancer. J Clin Oncol 31, 2167-2172.

Visvader, J.E. (2011). Cells of origin in cancer. Nature 469, 314-322.

Vullhorst, D., Neddens, J., Karavanova, I., Tricoire, L., Petralia, R.S., McBain, C.J., and Buonanno, A. (2009). Selective expression of ErbB4 in interneurons, but not pyramidal cells, of the rodent hippocampus. J Neurosci 29, 12255-12264.

Wang, X.Q., Lo, C.M., Chen, L., Ngan, E.S., Xu, A., and Poon, R.Y. (2017a). CDK1-PDK1-PI3K/Akt signaling pathway regulates embryonic and induced pluripotency. Cell Death Differ 24, 38-48.

Wang, Y., Wang, Y., Chen, H., and Liang, Q. (2017b). Endothelial Cells Promote Formation of Medulloblastoma Stem-Like Cells via Notch Pathway Activation. J Mol Neurosci 63, 152-158.

Wang, Z. (2017). ErbB Receptors and Cancer. Methods Mol Biol 1652, 3-35.

Wechsler-Reya, R., and Scott, M.P. (2001). The developmental biology of brain tumors. Annu Rev Neurosci 24, 385-428.

Wei, Y., Jiang, Y., Zou, F., Liu, Y., Wang, S., Xu, N., Xu, W., Cui, C., Xing, Y., Liu, Y., et al. (2013). Activation of PI3K/Akt pathway by CD133-p85 interaction promotes tumorigenic capacity of glioma stem cells. Proc Natl Acad Sci U S A 110, 6829-6834.

Williams, C.S., Bernard, J.K., Demory Beckler, M., Almohazey, D., Washington, M.K., Smith, J.J., and Frey, M.R. (2015). ERBB4 is over-expressed in human colon cancer and enhances cellular transformation. Carcinogenesis 36, 710-718.

Wingate, R.J., and Hatten, M.E. (1999). The role of the rhombic lip in avian cerebellum development. Development 126, 4395-4404.

Wojcinski, A., Lawton, A.K., Bayin, N.S., Lao, Z., Stephen, D.N., and Joyner, A.L. (2017). Cerebellar granule cell replenishment postinjury by adaptive reprogramming of Nestin(+) progenitors. Nat Neurosci 20, 1361-1370.

Wolter, M., Reifenberger, J., Sommer, C., Ruzicka, T., and Reifenberger, G. (1997). Mutations in the human homologue of the Drosophila segment polarity gene patched (PTCH) in sporadic basal cell carcinomas of the skin and primitive neuroectodermal tumors of the central nervous system. Cancer Res 57, 2581-2585.

Wood, H.B., and Episkopou, V. (1999). Comparative expression of the mouse Sox1, Sox2 and Sox3 genes from pre-gastrulation to early somite stages. Mech Dev 86, 197-201.

Wright, M.H., Calcagno, A.M., Salcido, C.D., Carlson, M.D., Ambudkar, S.V., and Varticovski, L. (2008). Brca1 breast tumors contain distinct CD44+/CD24- and CD133+ cells with cancer stem cell characteristics. Breast Cancer Res 10, R10.

Wu, S.M., Choo, A.B., Yap, M.G., and Chan, K.K. (2010). Role of Sonic hedgehog signaling and the expression of its components in human embryonic stem cells. Stem Cell Res 4, 38-49.

Xu, J., Gong, L., Qian, Z., Song, G., and Liu, J. (2018). ERBB4 promotes the proliferation of gastric cancer cells via the PI3K/Akt signaling pathway. Oncol Rep 39, 2892-2898.

Yamanaka, R. (2008). Cell- and peptide-based immunotherapeutic approaches for glioma. Trends Mol Med 14, 228-235.

Yan, F., Tan, X., Wan, W., Dixon, B.J., Fan, R., Enkhjargal, B., Li, Q., Zhang, J., Chen, G., and Zhang, J.H. (2017). ErbB4 protects against neuronal apoptosis via activation of YAP/PIK3CB signaling pathway in a rat model of subarachnoid hemorrhage. Exp Neurol 297, 92-100.

Yang, N., Wang, Y., Hui, L., Li, X., and Jiang, X. (2015). SOX 1, contrary to SOX 2, suppresses proliferation, migration, and invasion in human laryngeal squamous cell carcinoma by inhibiting the Wnt/beta-catenin pathway. Tumour Biol 36, 8625-8635.

Yang, Z.J., Ellis, T., Markant, S.L., Read, T.A., Kessler, J.D., Bourboulas, M., Schuller, U., Machold, R., Fishell, G., Rowitch, D.H., et al. (2008). Medulloblastoma can be initiated by deletion of Patched in lineage-restricted progenitors or stem cells. Cancer Cell 14, 135-145.

Yao, B., Wang, J., Qu, S., Liu, Y., Jin, Y., Lu, J., Bao, Q., Li, L., Yuan, H., and Ma, C. (2019). Upregulated osterix promotes invasion and bone metastasis and predicts for a poor prognosis in breast cancer. Cell Death Dis 10, 28.

Yao, J.J., Sun, J., Zhao, Q.R., Wang, C.Y., and Mei, Y.A. (2013). Neuregulin-1/ErbB4 signaling regulates Kv4.2-mediated transient outward K+ current through the Akt/mTOR pathway. Am J Physiol Cell Physiol 305, C197-206.

You, J.S., and Jones, P.A. (2012). Cancer genetics and epigenetics: two sides of the same coin? Cancer Cell 22, 9-20.

Zappone, M.V., Galli, R., Catena, R., Meani, N., De Biasi, S., Mattei, E., Tiveron, C., Vescovi, A.L., Lovell-Badge, R., Ottolenghi, S., et al. (2000). Sox2 regulatory sequences direct expression of a (beta)-geo transgene to telencephalic neural stem cells and precursors of the mouse embryo, revealing regionalization of gene expression in CNS stem cells. Development 127, 2367-2382.

Zeng, N., Liu, L., McCabe, M.G., Jones, D.T., Ichimura, K., and Collins, V.P. (2009). Real-time quantitative polymerase chain reaction (qPCR) analysis with fluorescence resonance energy transfer (FRET) probes reveals differential expression of the four ERBB4 juxtamembrane region variants between medulloblastoma and pilocytic astrocytoma. Neuropathol Appl Neurobiol 35, 353-366.

Zhang, D., Sliwkowski, M.X., Mark, M., Frantz, G., Akita, R., Sun, Y., Hillan, K., Crowley, C., Brush, J., and Godowski, P.J. (1997). Neuregulin-3 (NRG3): a novel neural tissue-enriched protein that binds and activates ErbB4. Proc Natl Acad Sci U S A 94, 9562-9567.

Zhou, J., Wulfkuhle, J., Zhang, H., Gu, P., Yang, Y., Deng, J., Margolick, J.B., Liotta, L.A., Petricoin, E., 3rd, and Zhang, Y. (2007). Activation of the PTEN/mTOR/STAT3 pathway in breast cancer stem-like cells is required for viability and maintenance. Proc Natl Acad Sci U S A 104, 16158-16163.

Zhou, L., Picard, D., Ra, Y.S., Li, M., Northcott, P.A., Hu, Y., Stearns, D., Hawkins, C., Taylor, M.D., Rutka, J., et al. (2010). Silencing of thrombospondin-1 is critical for myc-induced metastatic phenotypes in medulloblastoma. Cancer Res 70, 8199-8210.

Zhou, W., Cheng, L., Shi, Y., Ke, S.Q., Huang, Z., Fang, X., Chu, C.W., Xie, Q., Bian, X.W., Rich, J.N., et al. (2015). Arsenic trioxide disrupts glioma stem cells via promoting PML degradation to inhibit tumor growth. Oncotarget 6, 37300-37315.

Zhu, M., Zhang, C., Chen, D., Chen, S., and Zheng, H. (2019). MicroRNA-98-HMGA2-POSTN signal pathway reverses epithelial-to-mesenchymal transition in laryngeal squamous cell carcinoma. Biomed Pharmacother 117, 108998.

Zhu, Y., Guignard, F., Zhao, D., Liu, L., Burns, D.K., Mason, R.P., Messing, A., and Parada, L.F. (2005). Early inactivation of p53 tumor suppressor gene cooperating with NF1 loss induces malignant astrocytoma. Cancer Cell 8, 119-130.

Zhuo, L., Theis, M., Alvarez-Maya, I., Brenner, M., Willecke, K., and Messing, A. (2001). hGFAP-cre transgenic mice for manipulation of glial and neuronal function in vivo. Genesis 31, 85-94.

Zurawel, R.H., Chiappa, S.A., Allen, C., and Raffel, C. (1998). Sporadic medulloblastomas contain oncogenic beta-catenin mutations. Cancer Res 58, 896-899.

Publications within the PhD

Auzmendi-Iriarte J, **Aldaregia J**, Garcia I, Andermatten JA, Elortza F, Azkargorta M, Cuervo AM, Matheu A. Chaperone-mediated autophagy activates different proteomic and transcriptomic pathways to maintain glioma stem cell activity. **In preparation**.

Aldaregia J, Braza S, Odriozola A, Errarte P, Uriz JJ, Garcia I, Matheu A. High SOX1 expression is a hallmark of SHH medulloblastomas and its inhibition depletes tumor malignancy. **In preparation**.

Aldaregia J, Errarte P, Olazagoitia-Garmendia A, Gimeno M, Uriz JJ, Gershon TR, Garcia I, Matheu A. Erbb4 Is Required for Cerebellar Developmentand Malignant Phenotype of Medulloblastoma. **Cancers.** 2020 Apr 17;12(4):997.

Garcia I, **Aldaregia J**, Marjanovic Vicentic J, Aldaz P, Moreno-Cugnon L, Torres-Bayona S, Carrasco-Garcia E, Garros-Regulez L, Egaña L, Rubio A, Pollard S, Stevanovic M, Sampron N, Matheu A. Oncogenic activity of SOX1 in glioblastoma. **Scientific Reports**. 2017 Apr 20;7:46575.

Aldaregia J, Odriozola A, Matheu A, Garcia I. Targeting mTOR as a Therapeutic Approach in Medulloblastoma. **International Journal of Molecular Science**. 2018 Jun 22;19(7):1838.

Garcia I, **Aldaregia J**, Matheu A. Diffuse intrinsic pontine gliomas: the future of combination therapy with mTORC1/2 inhibitors and radiation. **Tralational Cancer Research**. 2017 Jul 17; 6(S6):S1098-S1100.

Carrasco-Garcia E, Lopez L, Aldaz P, Arevalo S, **Aldaregia J**, Egaña L, Bujanda L, Cheung M, Sampron N, Garcia I, Matheu A. SOX9-regulated cell plasticity in colorectal metastasis is attenuated by rapamycin. **Scientific Reports**. 2016 Aug 30;6:32350.